DEVELOPMENT OF POLYMERIC NANOCARRIERS FOR DRUG DELIVERY TO CANCER CELLS

by

ABHISHEK SAHU

In Partial Fulfillment of the Requirements

for the Degree of

DOCTOR OF PHILOSOPHY

DEPARTMENT OF BIOTECHNOLOGY

INDIAN INSTITUTE OF TECHNOLOGY GUWAHATI

APRIL 2009

INDIAN INSTITUTE OF TECHNOLOGY GUWAHATI

DEPARTMENT OF BIOTECHNOLOGY

CERTIFICATE

It is to certify that the matter embodied in this thesis entitled "***Development of Polymeric Nanocarriers for Drug Delivery to Cancer Cells***" is the results of investigations carried out by me under the supervision of Dr. Utpal Bora and Dr. Pranab Goswami, Department of Biotechnology, Indian Institute of Technology Guwahati, Guwahati, India for the award of degree of Doctor of Philosophy. This work has not been submitted elsewhere for any degree, diploma, associateship or membership etc. of any institute or university to the best of my knowledge and belief.

Abhishek Sahu
01/04/09

Abhishek Sahu
(Candidate)
Roll No: 05610606

CERTIFIED

1 April 2009

9.04.09

Dr. Utpal Bora

(Supervisor)

Associate Professor
Department of Biotechnology
IIT Guwahati
Guwahati -781039, Assam
INDIA

Dr. Pranab Goswami

(Co-supervisor)

Associate Professor
Department of Biotechnology
IIT Guwahati
Guwahati – 781039, Assam
INDIA

Acknowledgements

I would like to express my sincere appreciation to my research supervisors Dr. Utpal Bora and Dr. Pranab Goswami for their continuous support and guidance throughout this work. Dr. Bora's investment of discussions, comments and suggestions contributed significantly to the quality of this work. His examples and the things he has taught me will certainly help me in my future career. I must acknowledge the freedom that I was given in every step of my research work.

I am grateful to Prof. G. Barua, Director, IIT Guwahati for providing all the necessary facilities and a conducive academic environment. Appreciation is expressed to the members of my doctoral committee members Dr. A. Ramesh, Dr. V. V. Dasu and Dr.V. K. Dubey for their precious suggestions in completing this work. . I owe my gratitude to the Department of Biotechnology and CIF, IIT Guwahati for providing me all the supports and necessary facilities and thanks to all staff members in the department for their help during my PhD studies. I sincerely appreciate the financial support from MHRD, DBT and DST in the form of fellowship and research grants.

My great thanks to our research group members Naresh, Ratul, Debajeet and Shahin for providing me a healthy and enjoyable environment for the research and being wonderful juniors. I am thankful to my senior scholars for their valuable suggestions and Vijay for his help with AFM.

I am immensely pleased to express my heartiest thanks to my friends Mahantyda, Subhamda, Pallab, Beda, Sanjay, Majumder, Achlesh, Kaushikda, Shadab, Sukhi, Abhijitda, Anirbanda and Shampadi for their moral support. Their presence made my four years stay at IITG memorable.

Lastly, and also most importantly, I would like to thank my parents, my brother, my sister and friends of college days for their endless love, unlimited support and enormous encouragement when I encountered difficulties, felt depressed and lost strength. Without them, none of my achievements would have been possible.

CONTENTS

भारतीय प्रौद्योगिकी संस्थान गुवाहाटी
Indian Institute of Technology Guwahati

SYNOPSIS

Designing of nanosystems that are able to deliver therapeutic molecules to the right place, at a desired dose, at the appropriate time in a controlled manner is currently an important area of research. Pharmaceutical nanocarriers have evolved as one of the major means for drug delivery in cancer chemotherapy due to their unique advantages over conventional dosage. The present research work deals with the development of polymeric nanocarriers for delivery of curcumin, a potential anticancer molecule. Curcumin has showed great promises in the last decade for cancer therapy but the clinical progress of this compound has been slow due to its poor water solubility and low bioavailability. Nanocarrier based delivery of curcumin could provide an opportunity to expand the clinical repertoire of this efficacious agent by enabling aqueous dispersion. Based on these considerations, the objectives of the present research work were fixed as follows:

1. Development of a synthetic nanocarrier and its application in curcumin delivery.
    i. Synthesis and characterization of synthetic mPEG-PA nanocarrier.
    ii. Evaluation of the nanocarrier for drug encapsulation.
    iii. Delivery of the nanocarrier encapsulated drug to *in vitro* cultured cancer cells.
2. Formulation of curcumin in Pluronic nanocarriers.
    i. Encapsulation of curcumin in Pluronic nanocarriers by self assembly.
    ii. Study of drug release and stability of the Pluronic based formulations.
    iii. Delivery of Pluronic encapsulated curcumin to *in vitro* cultured cancer cells.
3. Natural food protein based nanoparticle for curcumin delivery.
    i. Purification and characterization of casein micellar nanoparticles from milk.
    ii. Fluorescence study of curcumin binding to casein micelle nanoparticles.

iii. Effect of curcumin complexed casein micelles on *in vitro* cultured cancer cells.

Chapter One starts with a brief historical development of the concept of drug delivery and moves onto describe the fundamental understanding of drug delivery systems with an emphasis on nanosystems. A review of different types of nanocarriers used in drug delivery and their advantages has been discussed with a focus on cancer therapy. Detailed discussions on the use of inorganic, lipid and polymer based nanocarrier systems are presented along with information about the various commercialized drug delivery products based on nanosystems. The chapter also discusses about the chemistry and multi-therapeutic potential of curcumin. The clinical progress of curcumin, recent advances in the area of its delivery and its promising future as a chemotherapeutic drug against cancer are also reviewed.

Chapter Two describes the synthesis of a novel synthetic nanocarrier for curcumin delivery. An amphiphilic polymer, mPEG-PA was synthesized by conjugating mPEG with palmitate by an ester linkage in a single step reaction. The conjugate forms micelle based nanocarriers by self-assembly in aqueous solution. mPEG-PA was characterized through ^{1}HNMR and FT-IR spectroscopy. The size and morphology of the micelle nanostructures were characterized by DLS and AFM. The mPEG-PA based micelle nanocarriers were able to encapsulate curcumin in its hydrophobic core and also efficiently delivers it to the cancer cells.

Chapter Three deals with use of Pluronics for curcumin delivery. Pluronics are commercially available FDA approved tri-block copolymers for pharmaceutical applications. Pluronic based micelle nanocarriers have been used for the encapsulation of many hydrophobic drugs but no attempt has been made for its use in curcumin

encapsulation. We thought the use of a commercially available, low cost, biocompatible and pharmaceutically acceptable material for curcumin formulation may help to reduce the clinical problems with the drug. We used two varieties of Pluronics (F127 and F68) used for the formulation of curcumin. The drug encapsulation, stability and *in vitro* release and delivery to cervical cancer (HeLa) cells were studied.

In **Chapter Four** we present the application of food protein based nanoparticles for drug delivery to cancer cells. The inspiration behind this work was the traditional use of milk in administering herbal medications. We exploited natural nanostructures of casein micelles, isolated from bovine milk as a carrier of curcumin. Our study showed that curcumin molecules form complexes with casein micelles by binding to its hydrophobic regions. Observation in fluorescence microscope showed that Curcumin-CM complex was also effectively internalized by cancer cells and induced cytotoxic effects.

Our work has been peer reviewed and resulted in the following international journal publications:

1. **A. Sahu**, U. Bora, N. Kasoju and P. Goswami. Synthesis of novel biodegradable and self-assembling methoxy poly(ethylene glycol) – palmitate nanocarrier for curcumin delivery to cancer cells. ***Acta Biomaterialia*** 4 (6): 1752-1761, 2008.
2. **A. Sahu**, N. Kasoju and U. Bora. Fluorescence study of curcumin-casein micelle complexation and its application as drug nanocarrier to cancer cells. ***Biomacromolecules*** 9 (10): 2905-2912, 2008.
3. **A. Sahu,** N. Kasoju, R.R. Bhonde and U. Bora. Pluronic nanoparticles for curcumin delivery to cancer cells. (Submitted for publication).

Apart from the thesis work, my involvement in other research activities in the group resulted in the following peer reviewed articles in international journals:

1. **A. Sahu**, P. Goswami and U. Bora. Microwave mediated rapid synthesis of chitosan. ***Journal of Materials Science: Materials in Medicine*** 20 (1): 171-175, 2009.
2. S.S. Ali, N. Kasoju, A. Luthra, A. Singh, H. Sharanabasava, **A. Sahu** and U. Bora. Indian medicinal herbs as sources of antioxidants. ***Food Research International*** 41 (1): 1-15, 2008.
3. U. Bora, **A. Sahu**, A.P. Saikia, V.K. Ryakala, P. Goswami. Medicinal plants used by the people of Northeast India for curing malaria. ***Phytotherapy Research*** 21 (8): 800-804, 2007.

ABBREVIATIONS

AFM	Atomic Force Microscopy
CLSM	Confocal Laser Scanning Microscopy
CMC	Critical Micelle Concentration
DDS	Drug Delivery System
DLS	Dynamic Light Scattering
DMEM	Dulbecco's Modified Eagle's Medium
EMEM	Eagle's Minimal Essential Medium
EPR	Enhanced Permeation and Retention
FDA	Food and Drug Administration
K_b	Binding Constant
K_{SV}	Stern-Volmer Quenching Constant
k_q	Fluorescence quenching rate constant
mPEG	Methoxy Poly (ethylene glycol)
mPEG-PA	Methoxy Poly (ethylene glycol)-palmitate
MPS	Mononuclear Phagosytosis System
MTT	3 (4, 5 Dimethylthiazol-2-yl) 2, 5 diphenyltetrazolium bromide
nm	Nanometer
NP(s)	Nanoparticle(s)
PBS	Phosphate Buffer Saline
PCL	Poly (ε-caprolactone)
PEG	Poly (ethylene glycol)
PGA	Poly (glycolic acid)
PLA	Poly (lactic acid)
PLGA	Poly (lactic acid-co-glycolic acid)
RES	Reticuloendothelial System
SEM	Scanning Electron Microscopy
τ_0	Fluorophore lifetime in the absence of quencher
µg	Microgram
µl	Microliter
µM	Micromolar

SCHEMES

LIST OF TABLES

LIST OF FIGURES

Figure 2.4: Plot of intensity ratio ($I_{335/332}$) from pyrene excitation spectra as function of log (concentration) for mPEG-PA (solid line) and mPEG (broken line). The CMC value of mPEG-PA conjugate was calculated from the crossover point of $I_{335/332}$.

Figure 2.5: DLS and AFM study of free mPEG-Palmitate micelle and Curcumin loaded mPEG-Palmitate micelle. (A1, A2) Size distribution of mPEG-PA self-assembled micelles in PBS (pH 7.4) measured by dynamic light scattering. (B1, C1) Atomic force microscopy (AFM) images of self-assembled micelles of mPEG-PA. (B2, C2) AFM image of drug loaded micelles. The micelles are spherical in shape as seen in topographic image (B1, B2). C represents the 3D view of B.

Figure 2.6: Increased solubility of micelle encapsulated curcumin (B) compare to free curcumin (A) in water. It can be clearly visualized that free curcumin (without the aid of any organic solvent) is insoluble in water.

Figure 2.7: UV-visible absorbance spectra of curcumin in different type of solutions. (a) Curcumin in aqueous solution containing 10% methanol, (b) Curcumin loaded in mPEG-PA micelle and (c) Methanolic solution of curcumin.

Figure 2.8: Fluorescence emission spectra of curcumin in different type of solutions. (a) Curcumin in aqueous solution containing 10% methanol, (b) Curcumin loaded in mPEG-PA micelle and (c) Methanolic solution of curcumin. Excitation wavelength (λ_{ex}) was 420 nm.

Figure 2.9: In vitro stability of curcumin loaded mPEG-PA micelle in PBS (pH 7.4), simulated gastric fluid (pH 1.2) and simulated intestinal fluid (pH 6.8) at 37ºC.

Figure 2.10: ^{1}HNMR spectrum of the palmitic acid obtained after lipase catalyzed cleavage of the ester bond in mPEG-PA.

Figure 2.11: Lipase catalyzed release of drug (curcumin) from micelle nanoparticle in PBS (pH 7.4) at 37ºC. More than 90% of drug has been released within 48 hours because of enzymatic degradation of micelles.

Figure 2.12: Drug release from micelle nanoparticle by HeLa cell lysate. Drug release was greater in presence of cell lysate with respect to control.

Figure 2.13: Differential interference contrast (DIC) and fluorescence images of internalization of free and micelle loaded curcumin by HeLa cells. The green fluorescence of curcumin inside the cells can be observed clearly. Cells were visualized at 2h after treatment.

Figure 2.14: Effect of empty mPEG-PA nanocarriers on cultured HeLa cells. Only minimal toxicity of the nanocarriers can be seen in this concentration range.

Figure 2.15: Cell viability of HeLa cells exposed to free curcumin and mPEG-PA micelle encapsulated curcumin, doses ranging from 1 to 30 μM for 48 hours. The percentage of viable cells was quantified using MTT assay.

Figure 2.16: The morphological change in HeLa cells after 24h of treatment with (A) empty mPEG-PA and (B) curcumin encapsulated mPEG-PA. Cells were of regular flattened morphology when treated with empty micelles of mPEG-PA (A1) and no fluorescence was observed (A2). After treatment with curcumin encapsulated mPEG-PA micelles significant change in cellular morphology (B1) and strong green fluorescence (B2) was observed under the microscope.

Figure 3.1: AFM images of drug encapsulated micelle nanocarriers (A) Curcumin loaded Pluronic F127 micelles and (B) Curcumin loaded Pluronic F68 micelles. A1 and B1 represents topograph images of the nanocarriers whereas, A2 and B2 represents 3D

view of A1 and B1. The micellar nanoparticles are nearly spherical in shape with size less than 100 nm.

Figure 3.2: UV-visible absorption spectra of free curcumin (control, solubilized with 1% DMSO) and curcumin encapsulated Pluronic micelles.

Figure 3.3: Fluorescence emission spectra of free curcumin (control, solubilized with 1% DMSO) and curcumin encapsulated Pluronic micelles. Excitation wavelength was 420 nm.

Figure 3.4: *In vitro* release of curcumin from Pluronic micelles at physiological condition (pH 7.4, 37ºC).

Figure 3.5: Storage stability of curcumin encapsulated Pluronic micelles in aqueous solution form at 25ºC and 4ºC.

Figure 3.6: Storage stability of lyophilized curcumin encapsulated Pluronic micelle formulation at 4ºC.

Figure 3.7: *In vitro* cytotoxicity of empty Pluronic micelles against HeLa cells. The cell viability was determined by MTT assay after treatment for 48h. Both the copolymers showed good cytocompatibility upto concentrations of 5 mg/ml.

Figure 3.8: *In vitro* cytotoxicity assay of free curcumin and curcumin encapsulated in Pluronic micelles against HeLa cells.

Figure 3.9: Fluorescence microscope images of HeLa cells incubated with curcumin encapsulated in Pluronic F127 and F68 micelle nanocarriers at 37 ºC for 4h. Intracellular green fluorescence of curcumin can be observed clearly, which confirms the uptake of drug loaded micelle nanocarriers by the cancer cells.

Figure 3.10: The morphological change in HeLa cells after treatment with drug encapsulated Pluronic micelles. The cells (3×10^5) were seeded in 35 mm culture dish treated with 20 μM of curcumin encapsulated in Pluronic for 48h. The cells were photographed in culture condition using 40X objective. (A) Control cells, (B) Cells treated with curcumin encapsulated in Pluronic F127, (C) Cells treated with curcumin encapsulated in Pluronic F68.

Figure 4.1: SDS-PAGE of molecular weight marker (Lane M); skimmed milk (Lane 1) and purified casein micelle (Lane 2): the 4 distinct bands with molecular weight ranging from 37 to 26 kDa belongs to αs1-casein, αs2-casein, β-casein and κ-casein respectively.

Figure 4.2: Stability of casein micelle (CM) suspensions in Tris buffer (pH 7.4) containing 10 mM $CaCl_2$. (A) Turbidity (τ) of purified CM suspension at wavelength of 400 nm (▲) and 600 nm (■) showing a linear change with different CM concentrations. (B) Change of α (wavelength dependence of turbidity) with different CM concentrations. The α value remained nearly constant.

Figure 4.3: Size distribution of CM suspension measured by DLS. The average diameter of the CM particles was found to be 166.3 nm.

Figure 4.4: Observation of CM particles under scanning electron microscope (SEM).

Figure 4.5: Morphology analysis of CM particles by AFM. Particles were almost spherical in shape with average size distribution of 200 nm.

Figure 4.6: (A) Absorption spectra of CM suspension (broken line) and CM-curcumin complex (solid line). Difference spectra (B) revealed that the curcumin bound to CM shows absorption maxima at 424 nm.

Figure 4.7: Fluorescence emission spectra of 5 μM curcumin in buffer solution (pH 7.4) in presence of CM at different concentrations (a) 0 (b) 0.5 (c) 1.0 (d) 1.5 (e) 2.0 (f) 2.5 (g) 3.0 (h) 4.0 (i) 5.0 (j) 10.0 (k) 12.5 (l) 15.0 (m) 17.5 and (n) 20.0 μM respectively. Excitation wavelength was 420 nm.

Figure 4.8: Change of curcumin fluorescence intensity at 500 nm in the presence of increasing concentrations of CM. It showed that 17 μM CM is required for saturation of 5 μM curcumin binding.

Figure 4.9: Double reciprocal plot of [CM] vs change in curcumin fluorescence intensity (ΔFI). Binding constant (K_b) was estimated to be 1.48 X 10^4 M^{-1} between curcumin and CM from the plot.

Figure 4.10: Quenching of CM intrinsic fluorescence by curcumin. Fluorescence emission spectra of CM suspension at excitation wavelengths of 280 nm in presence of (i) 0 (ii) 1 (iii) 1.5 (iv) 2.0 (v) 2.5 (vi) 3.0 (vii) 3.5 (viii) 4.0 (ix) 4.5 and (x) 5.0 μM curcumin respectively.

Figure 4.11: Stern-Volmer plot of protein fluorescence quenching when excitation wavelength was 280 nm.

Figure 4.12: Fluorescence emission spectra of CM suspension at excitation wavelengths of and 295 nm in presence of (i) 0 (ii) 1 (iii) 1.5 (iv) 2.0 (v) 2.5 (vi) 3.0 (vii) 3.5 (viii) 4.0 (ix) 4.5 (x) 5.0 μM curcumin respectively.

Figure 4.13: Stern-Volmer plot of protein fluorescence quenching when excitation wavelength was 295 nm.

Figure 4.14: Fluorescence emission spectra of curcumin in presence of undissociated CM and dissociated CM showed high fluorescence intensity due to complexation by hydrophobic interactions and the same with casein hydrolysate showed poor fluorescence intensity due to lack of hydrophobic domains.

Figure 4.15: Cytotoxicity assay of free curcumin (□) and CM-curcumin complex (■) on *in vitro* cultured HeLa cells. CM-curcumin complex showed comparable cytotoxic effect to free curcumin.

Figure 4.16: Cellular uptake study of CM-curcumin complex (■) and free curcumin (□) on *in vitro* cultured HeLa cells.

Figure 4.17: Microscopic observation of CM-curcumin complex induced morphological changes with time in HeLa cells. (A1-A4) Control cells treated with CM without drug showed no change of morphology with time. (B1-B4) Cells treated with CM-curcumin complex containing 30 μM curcumin exhibited marked morphological changes due to apoptosis. (C1-C4) Intracellular green fluorescence of curcumin revealed that the complex was efficiently internalized into the cells.

CHAPTER 1

Introduction
&
Review of Literature

1.1 Introduction

The effort of mankind to confront disease dates back to early civilization. Substances taken from nature were used to treat dysfunctions of life processes and with the advancement of science the active compounds or drugs were identified and isolated. Since then the field of pharmaceutical science has been developing steadily over the years, and has today become invaluable in helping us staying healthy and prevent disease. Initially these drugs could only be administered in limited manner through reactive environments in the body which reduced the effectiveness of administered drugs. The recent history of drug-delivery technology began in the 1950s with the introduction of the first microencapsulated drug particles and then research in the 1960s provided an initial understanding of pharmacokinetics and therapeutic drug monitoring (Rosen and Abribat, 2005). In the 1960s, polymers began to be used to deliver drugs, and scientists formulated a systematic approach to product development that combined an understanding of pharmacokinetics, the biological interface and biocompatibility. This approach has been extremely important in the development of systems in which pharmacokinetic or pharmacodynamic effects provide feedback that allows a device to monitor and regulate dosing. Progress came with the development of biomaterial carriers which could encapsulate or immobilize drugs and increase efficacy. These carriers allowed the release of drug in sites which were previously inaccessible. The nature of these carriers progressed over the years from ceramics, to natural, to synthetic materials. Despite these progresses cancer remained one of the deadliest diseases over the years and the clinical use of most conventional chemotherapeutics is often limited due to inadequate delivery of therapeutic drug concentrations to the tumor target tissue or due to severe and harmful toxic effects on normal organs. It is therefore important to find out new drug which can effectively kill cancer cells without showing toxicity to normal cells and

develop novel technologies that can be used for tumor specific drug delivery to improve the therapeutic index. In recent years, nanotechnology has shown tremendous potential in cancer prevention, detection, diagnosis, imaging and treatment. Most prominently polymers have emerged as a desired material for the site specific delivery of anticancer drugs and are increasingly being explored in the form of micro and nanocarriers.

1.2 Drug Delivery Systems (DDS)

The activity of a drug is determined by the net biological effects produced by its interaction with the cells at its site of action in the body. Unless the drug can be delivered to its site of action at a rate and concentration that minimize side-effects and maximize therapeutic effects, the efficacy of the therapy is compromised. So, it is necessary for the drug to reach the site of action somehow following administration at adequate concentrations. The purpose of drug delivery system (DDS) is to enhance or facilitate the action of therapeutic compounds, making the administration of complex new drugs feasible, as well as adding critical value to the drugs that are currently in the market. In a DDS the drug is associated with a carrier which is designed to alter the release profile, absorption, biodistribution, metabolism and elimination of drugs *in vivo* to attain the desired therapeutic response (Allen and Cullis, 2004). Furthermore, obstacles arising from low drug solubility, fast clearance rates, drug degradation, non-specific toxicity or inability to cross biological barriers can be tackled by proper design and engineering of the DDS, in a case-to-case manner (Langer, 1990; Kostarelos 2003). Initially the usual carriers developed for drug delivery purposes were polymer beads, microspheres, microcapsules, hydrogels etc. But with the advancement of research, nanocarriers were prepared and showed enormous potential as DDS. Nanocarriers are submicron size colloidal particles with size range in 10 to 1000 nm. These

small sizes of the nanocarriers enable them to pass through certain biological barriers and use of materials in nanoscale provided unparallel freedom to modify fundamental properties such as solubility, diffusivity, blood circulation half-life, drug release characteristics and immunogenecity (Zhang and Gu et al., 2008). They are also better suited for intravenous (i.v.) delivery compared to conventional microcarriers. As the smallest capillaries in the body are only 5 to 6 μm in diameter, so the size of particles being distributed into the bloodstream must be significantly smaller than 5 μm, without forming aggregates, to ensure that the particles do not form an embolism (Hans and Lowman, 2002). A wide variety of drugs can be delivered using nanoparticulate carriers via different routes such as oral, intravenous, trasdermal, nasal, vaginal etc.(Moghimi et al., 2006). They can be used to deliver hydrophilic drugs, hydrophobic drugs, proteins, vaccines, other biological macromolecules, etc. Nanocarriers can improve the therapeutic index of currently available drugs by increasing drug solubility and drug stability, allowing the development of potentially effective new chemical entities that have been stalled during the preclinical or clinical development because of suboptimal pharmacokinetic or biochemical properties (Cho et al., 2008). They can also be formulated for targeted delivery to the lymphatic system, brain, arterial walls, lungs, liver, spleen, or made for long-term systemic circulation. A different variety of nanocarriers have been developed for DDS and they are not limited to only polymers but metals, inorganic, ceramic materials can also be used. Therefore, numerous protocols exist for synthesizing nanoparticles based on the type of drug used, the desired delivery route and the materials used for the DDS. Once a protocol is chosen, the parameters must be tailored to create the best possible characteristics for the nanoparticles. The most important characteristics of nanoparticles for a DDS are their size, encapsulation efficiency, zeta potential (surface charge) and release characteristics (Kostarelos, 2003;

Gronenberg et al., 2006). In last decade, nanocarriers have showed potential to provide more effective and more convenient routes of administration, lower therapeutic toxicity, extend the drug life cycle and ultimately reduce healthcare costs (Zhang and Gu et al., 2008). A number of nanocarriers based therapeutic products have been developed and marketed for the treatment of cancer, pain, infections, influenza, allergy, cancer etc. (Table 1.1) (Kawasaki and Player, 2005; Couvreur and Vauthier, 2006).

1.3 Nanocarriers in cancer therapy

Cancer is a leading cause of death worldwide which accounted for 7.9 million deaths (around 13% of all deaths) in 2004 and is projected to rise continuously with an estimated 12 million deaths in 2030 (WHO). Its treatment normally involves surgery, radiation therapy, chemotherapy or some combination of these. Out of these methods chemotherapy is more patient friendly and the only hope of treatment against metastasized tumors. Systemically administered chemotherapy can be curative for some tumors but the complex biology of tumors i.e. size, heterogeneity, location and vascularization often limits the effectiveness of chemotherapy (Fung and Saltzman, 1997; Jain, 1990). Current cancer chemotherapy has also a number of limitations that lead to poor therapeutic results. Chemotherapeutic treatments normally involve use of drugs which are highly cytotoxic in nature and cannot differentiate between normal cells and tumor cells. Due to this lack specificity, conventionally administrated chemotherapy drugs lead to the damage of healthy tissue, especially of the normally dividing cells of the bone marrow, skin, and gastro-intestinal mucosa, among other tissues. In addition, most of the drugs used against cancer are hydrophobic in nature shows poor bioavailability which leads to insufficient concentration of the drug in circulation to kill the cancer cells As a result of which most of

the cancers become drug resistance, which is a big concern. So, one of the ways to overcome the deficiencies of current treatment methods is to hunt for new drug which are less prone to damage normal cells and develop delivery systems that significantly improve the pharmacological characteristics of the drug *in vivo* and specifically target them to tumor cells. Use of different types of nanocarriers (Figure 1.1) have showed greater advantages like – they improves the solubility of poorly soluble drugs, prolongs the half-life of drug in systemic circulation by reducing uptake by mononuclear phagocyte system (MPS), release drugs at a sustained rate and predictive manner thus lowers the frequency of administration (Ferrari, 2005; Peer et al., 2007). Another unique advantage of using nanocarriers is that they can deliver the drugs in a targeted manner to reduce the systemic side effects (Maeda, 2001; Brannon-Peppas and Blanchette et al., 2004). Generally two types of targeting modalities are used with nanocarriers – (i) passive targeting and (ii) active targeting. Passive targeting of nanocarriers uses the general features of tumor tissues i.e. leaky vasculature and poor lymphatic drainage. The increased permeability of the blood vessels (defective endothelial cell architecture) in tumors is characteristic of rapid and defective vascularization during angiogenesis which allows nanocarriers to extravasate into the tumor tissues whereas; free drugs can diffuse nonspecifically to any tissues. Furthermore, the dysfunctional lymphatic drainage in tumors retains the accumulated nanocarriers and allows them to release drugs in the vicinity of tumor cells (Matsumara and Maeda, 1986). This total process of extravasation and accumulation is termed as enhanced permeation and retention (EPR) effect (Figure 1.2) (Maeda et al., 2000). So, the passive targeting of tumor tissues through EPR effect is the unique feature which is only achievable with nanocarriers and for such a passive targeting mechanism to work the average size of the carrier should be below 400 nm and its surface properties must be controlled to avoid uptake by the

reticuloendothelial (RES) system (Yuan F et al., 1995; Brannon-Peppas and Blanchette et al., 2004). Active targeting schemes have been designed based on the specific interaction of ligands and receptors. Actively targeted nanocarriers were prepared by conjugating tumor cell specific ligands to the surface of nanocarriers. The ligand helps the nanocarrier to bind specifically to the cancer cells and then get internalized by receptor mediated endocytosis (Ferrari, 2005; Gu et al., 2007; Peer et al., 2007).

Table 1.1 Nanotechnology based DDS products in market for different diseases

Trade Name	Drug	Formulation	Indication	Company
Ambisome	Amphotericin B	Liposome	Fungal Infections	Giled Sciences, NeXstar Pharma
Amphocil	Amphotericin B	Lipocomplex	Fungal Infections	Sequss Pharma
Abelcet	Amphotericin B	Lipid Complex	Fungal Infections	Enzon Pharma
Amphotec	Amphotericin B	Lipid dispersion	Fungal Infections	InterMune
DaunoXome	Daunorubicine	Liposome	Kaposi's sarcoma	Giled Sciences
Myocet	Doxorubicin	Liposome	Brest Cancer	Zeneus Pharma
Doxil/Caelyx	Doxorubicin	PEGylated Liposome	Kaposi's sarcoma, Ovarian cancer	Ortho Biotech, Schering-Plough
Depocyt	Cytarabine	Liposome	Cancer	SkyePharma
Onco TCS	Vincristine	Liposome	Non-Hodgkin's lymphoma	Inex Pharma, Enzon Pharma

Visudyne	Vertiporfin	Liposome	Age related macular degeneration	QLT, Novartis
Inflexal V	Influenza vacine	Virosome	Influenza	Berna Biotech
Epaxal	Hepatitis vaccine	Virosome	Hepatitis A	Berna Biotech
Estrasorb	Estradiol	Micellar Nanoparticle	Menopausal therapy	Novavax
Eestrin	Estradiol	Calcium phosphate nanoparticle	Menopausal therapy	BioSante
Rapamune	Sirolimus	Nanocrystal	Immunosppresant in kidney transplant patient	Wyeth, Elan
MegaceES	Megesterol acetate	Nanocrystal	Eating disorders	Elan, Par Pharma
Emend	Aprepitant	Nanocrystal	Antiemetic	Elan, Merck
Tricor	Fenofibrate	Nanocrystal	Lipid regulation	Elan, Abbott
Triglide	Fenofibrate	Nanocrystal	Lipid regulation	SkyePharma, First Horizon Pharma
Abraxane	Paclitaxel	Albumin nanoparticle	Cancer	Abraxis BioScience

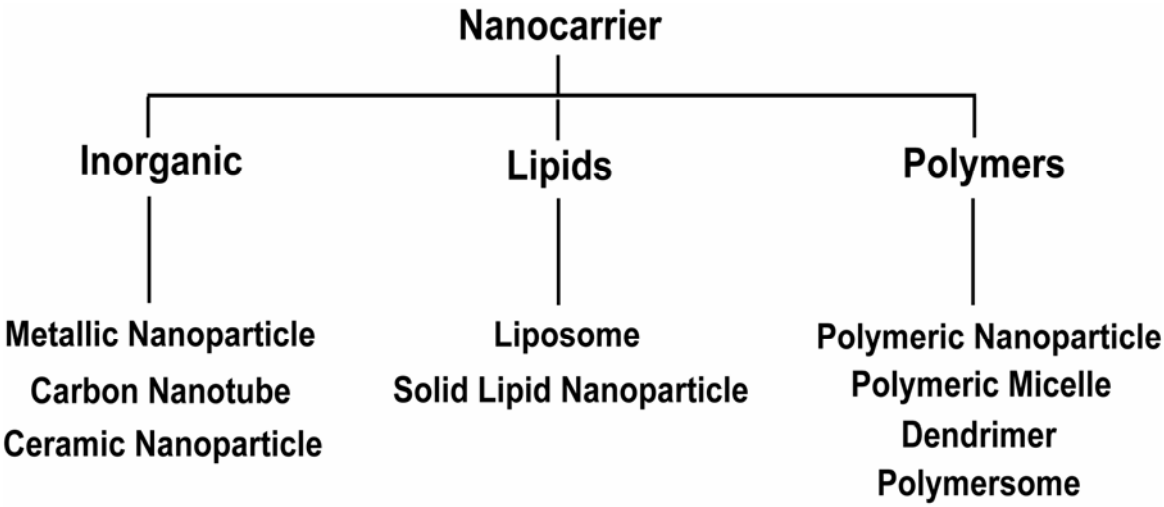

Figure1.1: Different types of nanocarriers used as DDS in cancer therapy.

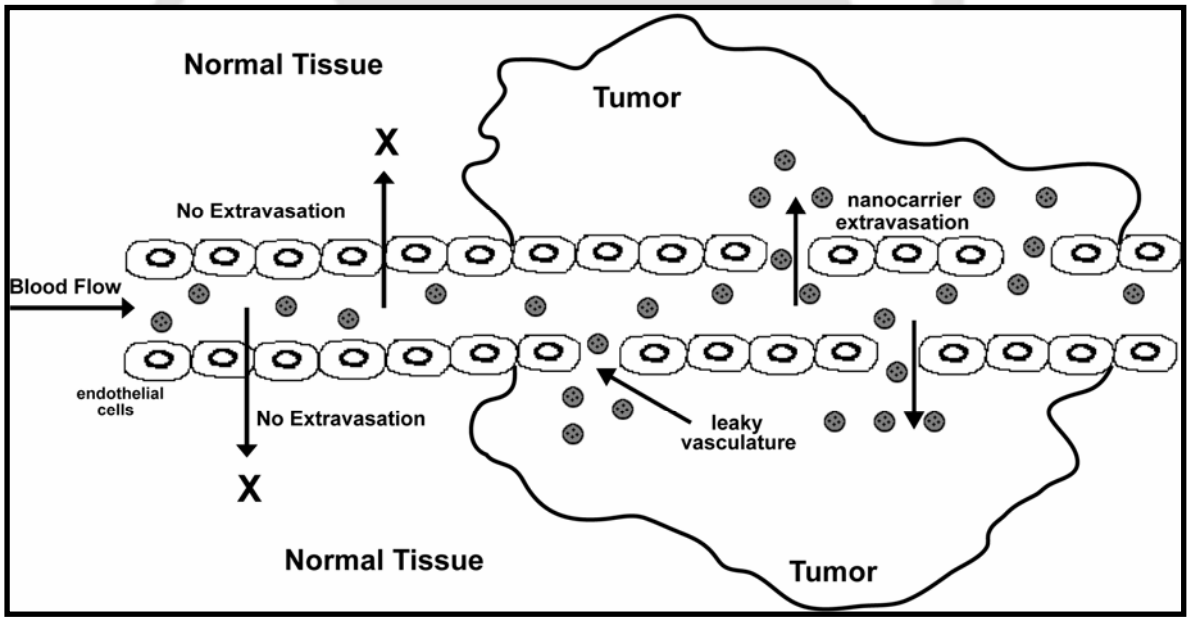

Figure1.2: Passive tumor targeting by EPR effect.

1.4 Metallic Nanoparticles

1.4.1 Gold Nanoparticle

Michael Faraday first described the generation of colloidal gold nanoparticles in 1857 and since then, it has been used to meet a variety of needs in science and even in medicine. Recently, gold nanoparticles have emerged as attractive candidate for delivery of various therapeutic molecules into their targets due to their unique chemical and physical properties. Colloidal gold particles are relatively inert and biologically compatible non-toxic carriers. It can be synthesized easily with sizes ranging from 1 nm to 150 nm and functionalized with organic monolayer to provide required functionality (Grabar et al., 1995). Studies across the world have shown that different types of therapeutics such as small drug molecules, proteins, DNA and RNA can be delivered through colloidal gold nanoparticles (Ghosh et al., 2008). Small molecule drugs such as methotrexate, kahalalide F etc. were conjugated over the gold NP surface through electrostatic interaction or thiol functionalization and shown to act as drug carrier (Chen et al., 2007; Hosta et al., 2009). Paciotti et al., (2004) carried out *in vivo* study to investigate the therapeutic effect of PEGylated gold colloids with adsorbed tumor necrosis factor (cAu-PEG-TNF). When cAu-PEG-TNF was injected intravenously into mice, they were largely accumulated in MC-38 colon carcinoma tumors compared to liver, spleen, or other healthy organs. TNF provided both targeting and therapeutic action via killing the targeted cells. Importantly, the particles were more effective at diminishing tumor mass than free TNF. Recent studies by this group have demonstrated enhanced tumor therapy by grafting paclitaxel, an anticancer drug, onto cAu-PEG-TNF. In another approach to generate a multifunctional gold nanoparticle, a vector named CYT-21001, is designed to target the delivery of both TNF and paclitaxel to solid tumors (Paciotti et al., 2006). Gold NPs can also be modified and conjugated with suitable proteins/peptides to be target the cell

nucleus. Tkachenko et al (2004) combined a cell-targeting peptide and a nucleus-targeting peptide from adenovirus into a long peptide and loaded them onto gold NPs which were already modified with a shell of BSA and used for target the nucleus of human hepatocarcinoma HepG2 cells. The resulting cellular trajectories indicated that the NP uptake and nucleus translocation strongly depends on the peptide sequence and cell type. In addition to the surface chemistry of gold NPs, their physical properties can be exploited for cancer treatment. Gold NPs cause local heating when they are irradiated with light in the "water window" (800 nm – 1200 nm). Huang et al. (2007) have reported about potential use of gold NPs in photothermal destruction of tumors.

1.4.2 Magnetic Nanoparticle

Magnetic NPs have been investigated for biomedical applications for more than 30 years. Up to now, magnetic NPs have been used in medicine as contrast agents in magnetic resonance imaging (MRI), for local hyperthermia and as targetable carriers for drug delivery systems. The concept of using magnetic micro and nanoparticles for drug delivery was originally proposed by Widder, Senyi and colleagues (Senyi et al., 1978; Widder et al., 1979) and in recent years it has gained prominence for targeted delivery of therapeutics in cancer chemotherapy (Gupta and Gupta, 2005; Dobson 2006). In these systems, therapeutic compounds are attached to biocompatible magnetic nanoparticles and magnetic fields generated outside the body are focused on specific targets in vivo. The fields capture the particle complex resulting in enhanced delivery to the target site.

There are many magnetic materials available with a wide range of magnetic properties. However, many of these materials, such as cobalt and chromium are not suitable for the use as biomedical agents in vivo due to their high toxic nature. The iron oxide based

nanoparticles such as magnetite (Fe_3O_4) and maghemite (γ-Fe_2O_3) are relatively safe and the most commonly used materials suitable for drug targeting *in vivo*. They are commonly prepared by co-precipitation of Fe^{2+} and Fe^{3+} aqueous salt solutions by addition of a base. The overall chemical reaction of Fe_3O_4 precipitation can be given as (Lu et al., 2007a):

$$Fe^{2+} + 2\ Fe^{3+} + 8\ OH^- = Fe_3O_4 + 4\ H_2O$$

The control of size, shape and composition of nanoparticles depends on the type of salts used (e.g. chlorides, sulphates, nitrates, perchlorates, etc.), Fe^{2+} and Fe^{3+} ratio, pH and ionic strength of the media (Lu et al., 2007a). The other established method of magnetic NP synthesis includes thermal decomposition and microemulsion (Lu et al., 2007a). Biocompatible magnetic particles are prepared by coating the magnetic cores with a metal or polymer (Mandal et al., 2005; Gupta and Gupta, 2005). By functionalizing the polymer or metal coating it is possible to attach or encapsulate the anticancer agents for targeted cancer chemotherapy. This coating also prevents the leaching of potentially toxic components into the body during *in vivo* applications. After encapsulating or attaching the drug molecules into the particle, the complex is injected into the blood stream, often using a catheter to position the injection site near the target. High magnetic fields are focused over the target tumor site which forces the injected particles to extravasate into the tumor tissue. While this may be effective for the tumors close to the body's surface, as the magnetic field strength falls off rapidly with distance, tumors deeper into the body become more difficult to target. The key parameters in the behavior of magnetic NPs are related to surface chemistry, size (magnetic core, hydrodynamic volume, and size distribution), and magnetic properties (magnetic moment, remanence, coercivity). The surface chemistry is especially important to avoid the action of the reticuloendothelial system (RES) to increase the half-life in the blood stream. Coating the NPs with a neutral and hydrophilic polymer i.e. polyethylene glycol

(PEG), polysaccharides, serum albumin etc. increases the circulatory half-life from minutes to hours or days. The main advantages of magnetic (organic or inorganic) NPs are that they can be: (i) visualized (superparamagnetic NPs are used in MRI), (ii) guided or held in place by means of a magnetic field and (iii) heated in a magnetic field to trigger drug release or to produce hyperthermia/ablation of tissue. Magnetic particles were first applied by Widder et al (1983) to deliver cytotoxic drugs into sarcoma tumors implanted in rat tail and directed by an external magnetic field. Their results showed a total remission of the sarcomas. In contrast, there was no remission in the control group without magnetic directing even with 10 times higher dose of the drug. Alexiou et al (2000) have used mitoxantrone (MTX) bound to starch stabilized magnetic ferrofluids (FFs) for the treatment of locoregional cancer. Mitoxantrone bound to magnetic ferrofluids (FF-MTX) was injected intraarterially (femoral artery) into the New Zealand white rabbits, previously implanted with VX-2 squamous cell carcinoma. Targeting of MTX-FF into the tumor site with an external magnetic field resulted in significant remission of the tumor compared with the control group (no treatment) without systemic toxicity. A preclinical study in Sprague-Dawley rats with anticancer drug attached magnetic NPs showed no intolerance and good efficiency in tumor regression (Lubbe et al., 1996a). The first phase I clinical trial of magnetically targeted drug delivery in human patients with advanced solid tumors was performed by Lubbe et al (1996b). In that study, epirubicine was complexed to magnetic NPs on the basis of electrostatic interactions between phosphate group bound to the surface of the particle and amino sugar present within the drug. Out of 14 patients studied, epirubicin was effectively targeted to the tumor site in 6 patients. A second clinical trial was performed by Koda et al (2002) on 32 patients with hepatocellular carcinoma, in which doxorubicin hydrochloride was coupled to magnetic particles and delivered by sub selective hepatic artery

catheterization. The particle-drug complex was targeted to the tumor site using an external magnetic field and particle localization examined with MRI. The results showed that out of 32 patients studied, tumors were targeted effectively in the 30 patients. Although progress in clinical applications of magnetically targeted carriers has been slow but the results have been promising and with further development it may provide another tool for the effective treatment of cancers.

1.5 Carbon Nanotube

The discovery Carbon nanotube (CNT) in 1991 has opened a new era in materials science and nanotechnology research (Ijima, 1991). CNT consist exclusively of carbon atoms arranged in a series of condensed benzene rings rolled-up into a tubular structure. This novel nanomaterial belongs to the family of fullerenes, the third allotropic form of carbon along with graphite and diamond. CNT can be classified in two general categories, based on their structure: single-walled (SWNT), which consist of one layer of cylinder graphene and multi-walled (MWNT), which contain several concentric graphene sheets (Figure 1.3). CNT have nanometric dimensions: SWNT have diameters from 0.4 to 2.0 nm and lengths in the range of 20–1000 nm, while MWNT are bigger objects with diameters in the range of 1.4–100 nm and lengths from 1 to several μm. CNTs have very interesting physicochemical properties such as: ordered structure with high aspect ratio, ultralight weight, high mechanical strength, high electrical conductivity, high thermal conductivity, metallic or semi-metallic behaviour and high surface area (Rao and Cheetham, 2001). The combination of these characteristics makes CNT a unique material with the potential for diverse applications including drug delivery (Bianco et al., 2005). The CNT commonly carries the drug one of three ways: the drug can be attached to the outer sidewall of nanotubes by specific interaction or by covalent

attachment or the drug can be placed inside the nanotube (Figure 1.4). Both of these methods are effective for the delivery and distribution of drugs inside the body. Feazell et al. (2007) used SWNT as longboat delivery system for platinum (IV) anticancer drugs. They prepared amine functionalized PEG tethered soluble SWNTs and conjugated platinum (IV) drug through amide linkage by carbodiimide chemistry. Results from atomic absorption spectroscopy (AAS) study suggested that one nanotube contains ~ 65 platinum (IV) drug and subsequent analysis showed effective delivery of the drug inside the testicular carcinoma cell line NTera-2. The functionalized SWNT also have been used for the formulation of doxorubicin (Liu et al. 2007). Pre-PEGylated SWNT was synthesized and doxorubicin loading was achieved by simple non-covalent binding via Π-stacking. DOX loaded SWNTs induced significant U87 cancer cell death through apoptosis, similar to free DOX. The supramolecular system was also applied for targeted drug delivery by conjugating cyclic RGD peptide on the terminal groups of PEG on SWNTs. RGD functionalized SWNTs showed enhanced doxorubicin delivery to integrin $\alpha_v\beta_3$ positive U87MG cells but not to integrin $\alpha_v\beta_3$ negative MCF-7 cells. In a recent study, Liu et al. (2008) have showed in vivo potential of SWNT drug delivery for tumor suppression in mice. They conjugated paclitaxel (PTX) to branched polyethylene glycol chains on SWNTs via a cleavable ester bond to obtain a water-soluble SWNT-PTX conjugate, which resulted higher efficacy in suppressing tumor growth than clinical Taxol in a murine 4T1 breast cancer model, owing to prolonged blood circulation and 10-fold higher tumor PTX uptake by SWNT delivery. Thus, nanotube drug delivery is promising for high treatment efficacy and minimum side effects for future cancer therapy with low drug doses. An important characteristic of CNT is their high propensity to cross cell membranes. CNT labeled with a fluorescent agent were easily internalized and could be tracked into the cytoplasm or the

nucleus of fibroblasts using epifluorescence and confocal microscopy. The mechanism of uptake of this type of CNT appears to be passive and endocytosis-independent. Incubation with cells in the presence of endocytosis inhibitors did not influence the cell penetration ability of CNT. Furthermore, CNT showed similar behaviors when incubation with the cells was carried out at lower temperatures (Shi and Dai, 2005).

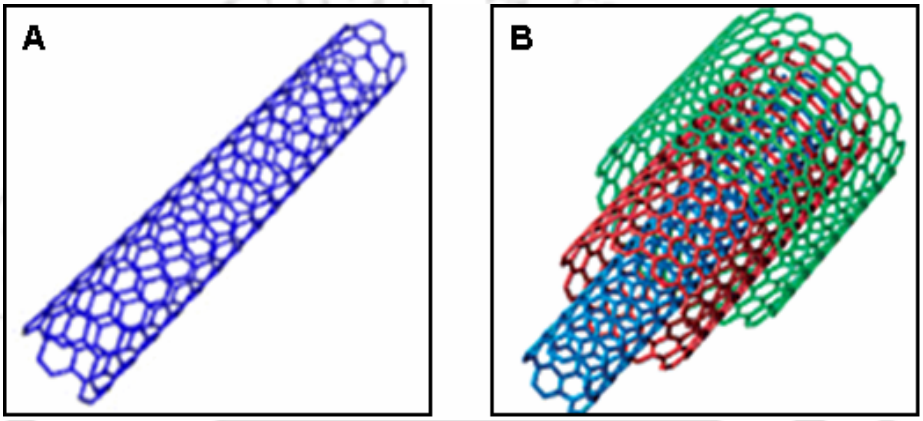

Figure 1.3: Carbon Nanotubes: (A) Single wall carbon nanotube (SWNT) and (B) Multiwall carbon nanotube (MWNT).

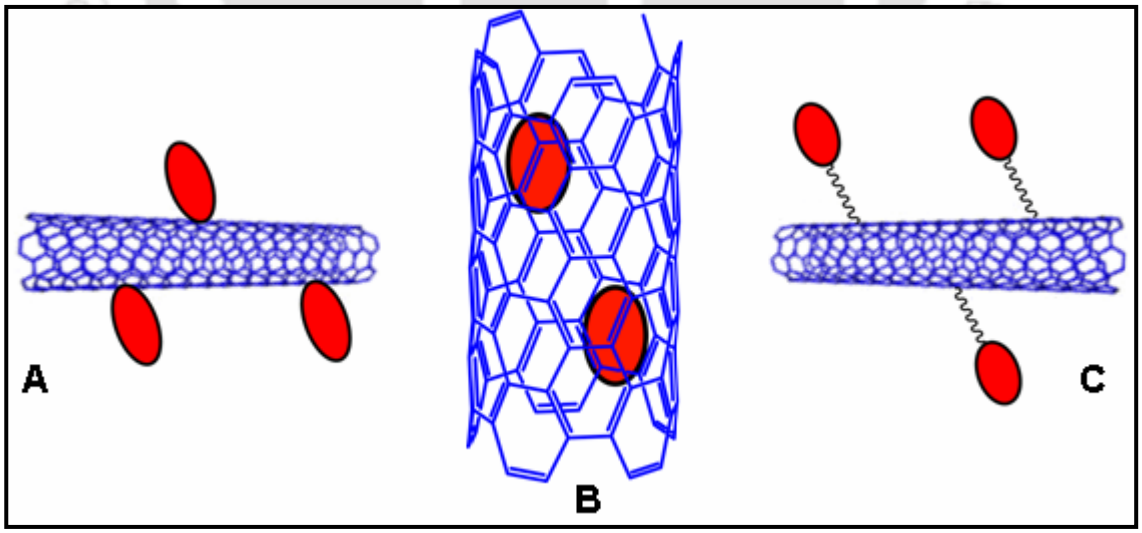

Figure 1.4: Different approaches of drug loading in carbon nanotube. The drugs can be (A) bound over the nanotube sidewall through specific interactions, (B) entrapped inside the nanotube and (C) covalently conjugated with the nanotube sidewall.

1.6 Ceramic Nanoparticles

Ceramic compounds are inorganic systems with porous characteristics and can be easily engineered with the desired size and porosity. In recent years, growing interest has emerged to utilize ceramic nanoparticles as drug vehicles and most of this research has been done using typical biocompatible ceramic materials such as silica, calcium carbonate, calcium phosphate and hydroxyapatite (Paul and Sharma 2003).

1.6.1 Silica

Silica NPs are the most widely and extensively used inorganic/ceramic system in drug delivery applications due to their ease of preparation, good biocompatibility and excellent stability (Chen et al., 2004; Trewyn et al., 2007a). Mesoporous silica NPs were prepared by sol-gel process, in which the polymerization of anionic orthosilisic acid occurs in the presence of cationic surfactant CTAB (Trewyn et al., 2007c). The pore size and environment can be tailored to selectively store different molecules of interest and while the size and shape of the particles can be tuned to maximize cellular uptake (Slowing et al., 2008; Lu et al., 2007c; Trewyn et al., 2007b). A study by Roy et al. (2003) reveals that silica-based doped nanoparticles can be an achievable drug delivery tactic in the photodynamic therapy to fight cancer. In a recent study Lu et al (2007b) successfully loaded hydrophobic anticancer drug camptothecin into mesoporous silica nanoparticles and delivered them into pancreatic (PANC-1, AsPC-1, Capan-1), gastric (MKN 45) and colon (SW 480) human cancer cells to induce apoptosis. In another study, nanoformulation of hydrophobic photosensitizer was prepared by incorporating them into organically modified silica nanoparticles for photodynamic therapy of cancer (Ohulchanskyy et al., 2007). Active targeting of these NPs also achieved through the conjugation of folic acid over the particle surface (Rosenholm et al., 2009).

1.6.2 Calcium Phosphate

Calcium phosphate is biocompatible and biodegradable and is native to the body as the principle mineral component of teeth and bones. This natural occurrence of CP is one of the primary advantages over other synthetic drug delivery systems. Encapsulation of drugs in calcium phosphate NPs has potential as a nontoxic, bioresorbable vehicle for drug delivery to cells and tumors. Schmidt et al (2004) prepared aqueous cored calcium phosphate nanoshells as a potential candidate for hydrophilic drug delivery system. Barroug et al (2006) prepared calcium phosphate/cisplatin formulation which exhibited cytotoxic effects in a dose dependent manner. Recently, Kester et al (2008) have used these NPs for delivery of the anticancer drug ceramide. They found that ceramide loaded calcium phosphate NPs were highly effective for inducing apoptosis in melanoma and breast cancer cell lines.

1.6.3 Hydroxyapatite

Hydroxyapatite is a naturally occurring form of calcium apatite and it is part of bones and teeths in human body. In an investigation of ceramic NPs as DDS, insulin has been entrapped in hydroxyapatite NPs. The insulin release profile shows promising results for orally administered insulin instead of repeatable injections (Paul and Sharma, 2001). Porous hydroxyapatite ceramics have been used for encapsulation of chemotherapeutic agent methotrexate and cis-platinum for local chemotherapy of cancer (Itokazu et al., 1998; Uchida et al., 2005).

1.6.4 Calcium Carbonate

Calcium carbonate is also a biocompatible and biodegradable inorganic material which is utilized for biomedical applications (Sukhorukov et al., 2004). Hydrophilic drugs erythropoietin, betamethasone phosphate and bioactive protein granulocyte-colony

stimulating factor (G-CSF) was efficiently entrapped into the calcium carbonate particles and sustained release of drugs from particles were confirmed by both *in vitro* and *in vivo* experiments (Ueno et al., 2005).

1.7 Lipid Based Nanocarriers

1.7.1 Liposome

Liposomes are vesicles with an aqueous interior surrounded by one or more concentric bilayers of lipids with a diameter ranging from a minimal of ~30 nm to several microns. Liposomes are spontaneously formed through self-assembly when amphiphilic lipids such as phospholipids are dispersed in water in certain concentrations and whether the drug is encapsulated in the aqueous core or in the surrounding bilayer of the liposome is dependent on the characteristics of the drug and the encapsulation process. In general, water-soluble drugs are encapsulated within the central aqueous core, whereas lipid-soluble drugs are incorporated directly into the lipid membrane. They were first proposed as carriers of biologically active substances in 1971 and since it has been comprehensively used, principally for cancer (Gregoriadis et al., 1971; Gregoriadis et al., 1974). They can be classified as large multilamellar liposomes (MLV), small unilamellar vesicles (SUV) or large unilamellar vesicles (LUV), depending on their size and the number of lipid bilayers (Lasic and Papahadjopoulos, 1998). However, for injectable clinical applications, practically all liposome formulations are prepared in the submicron range (<200 nm size) and considered as nano particulate systems (Schiffelers and Storm 2008). The early liposome work was mostly based on formulations composed of neutral egg lecithin (PC), often in combination with negatively or positively charged lipids. These liposomes were found to rapidly release a large fraction their encapsulated contents in circulation and were quickly

removed from circulation by macrophages of the RES residing in liver and spleen (Torchilin, 2005). From there, liposomes have moved a long way to become a pharmaceutical carrier of choice for numerous practical applications. Current liposomal drugs evolved through a number of design strategies for improved biodistribution over free drugs. Sterically stabilized (stealth) liposomes, are designed to reduce the uptake by RES and prolong the duration of exposure of the drug encapsulated liposome in the systemic circulation (Papahadjopoulos et al., 1991). So, stealth liposomes can circulate for days as stable constructs and slowly extravasate in neoangiogenic vessels in tumors to provide effective passive targeting of drugs to tumor tissue (Woodle 1995). True molecular targeting can be achieved using immunoliposomes, in which the liposome is linked to ligands such as monoclonal antibody fragments directed against cancer-associated antigens (Park et al., 1997; Kontermann 2006). Immunoliposomes combine antibody-mediated tumor recognition with liposomal delivery and target cell internalization, provide intracellular drug release. Other ligands such as RGD peptide or folic acid also have been conjugated over liposome surface for active tumor targeting (Dubey et al., 2004; Gabizon et al., 2004). So, these new generations of liposomes offers improved chemical stability of encapsulated drug, enhanced accumulation and prolonged drug exposure in tumors which ultimately helps in to increase the therapeutic index of chemotherapy. The real breakthrough developments in the area during the past 20 years have resulted in the approval of several liposomal drugs, and the appearance of many unique biomedical products and technologies involving liposomes (Torchilin 2005, Schiffelers and Storm 2008). Liposome based delivery systems, particularly liposomal anthracyclines, have had the greatest impact in oncology to date. Liposomal doxorubicin formulations have been commercialized more than 10 years ago and they are the most routinely used chemotherapeutic drug formulation against cancer today (Lasic,

1996; Markman et al., 2004). Future liposome therapeutics is building on these validated designs as well as on pharmacologic insights into their mechanisms of delivery. For example, camptothecin analogues, anti-angiogenesis agents, and antisense oligonucleotides each represent rational candidates for delivery in highly stabilized and long-circulating liposomes (Park et al., 2004). Some other liposomal anticancer agents that are currently in development are SN-38 (LE-SN38), lurtotecan (OSI-211), 9NC, irinotecan, CKD-602 (S-CKD602, paclitaxel and doxorubicin (LEP-ETU) (Zamboni 2005). An immunoliposome consisting of novel anti-HER2 scFv F5 conjugated to PLD, selectively binds to and internalizes in HER2-overexpressing tumor cells is currently in development (Hong et al., 2006).

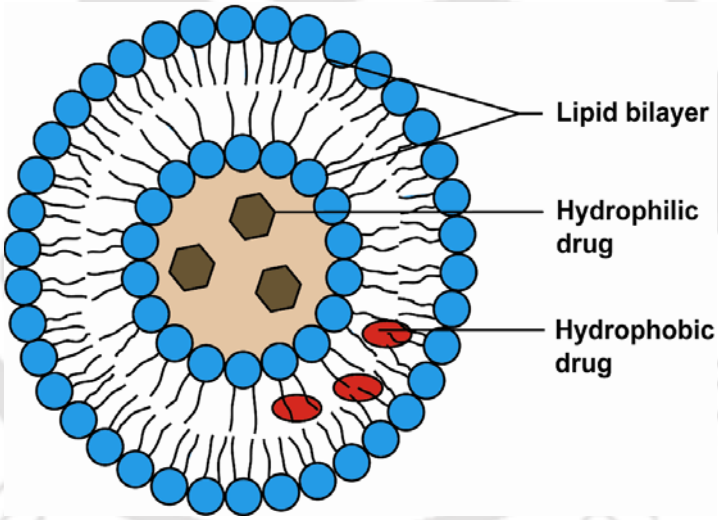

Figure 1.5: Drug encapsulation in liposome. Hydrophilic drugs are encapsulated in the inner aqueous core whereas hydrophobic drugs are solubilized in lipid bilayer.

1.7.2 Solid lipid nanoparticles (SLN)

SLNs are submicron particulate drug delivery system which is made from lipids which are solid at room temperature and body temperature. The natural or artificial synthetic lipids which are biocompatible and biodegradable (e.g. tristearin, tripalmitin, trilaurin, glyceryl

behenate, cetylpalmitate, stearic acid, plamitic acid etc.) are used for preparation of SLN as carriers for the delivery of drugs enveloped or dispersed in the solid colloidal particles (Muller et al., 2000). The particle diameters are in the range of approximately 50 to 1000 nm. The main advantages of the SLN with regard to drug delivery are high biocompatibility, high bioavailability, controlled drug release, excellent physical stability, protection of incorporated labile drugs from degradation, low systemic toxicity and no problems with multiple routs of administration, such as oral, intravenous, pulmonary and transdermal administration. This versatility of SLN as a drug carrier makes SLN a potential generic platform for the delivery of diverse anticancer cytotoxic agents. Since their discovery, a number of SLN based systems have been utilized for the delivery of many cytotoxic anticancer drugs such as, doxorubicin, paclitaxel, camptothecin, etoposide, fluorodoxouridine, idarubicin, all trans-retinoic acid etc (Wong et al., 2007). Serpe et al (2004) evaluated the cytotoxicity of SLN formulations carrying cholesterol butyrate, doxorubicin or paclitaxel on the human colorectal cancer cell line HT-29 and found that drug encapsulated in SLN showed more cytotoxicity compared to the equivalent amount of drug in the free solution. To find out whether SLN can lead to increased tumor drug concentrations via EPR effect, Reddy et al (2005) used Dalton's lymphoma tumor bearing mice to compare the biodistribution of free etoposide and radio-labeled etoposide loaded into SLN. Their result shows that the tumor concentration of SLN after subcutaneous injection was 59 folds higher than that obtained after intravenous and 8 folds higher than after intraperitoneal route at 24 h post-injection which is promising in terms of cancer chemotherapy. Several biodistribution studies have demonstrated significant alterations in drug distribution when the tested anticancer agent was delivered using SLN. It was also found that the biodistribution of an anticancer drug delivered by SLN may be further

manipulated by route of injection to achieve the desired therapeutic goal. Another interesting and significant finding of several biodistrobution studies is that SLN can overcome the blood-brain barrier to deliver the drug into the brain (Kaur et al., 2008). The results in the preclinical studies using cell culture systems or animal models have so far been very promising but there is still lack of clinical studies for the use of SLN for cancer therapy. The few disadvantages observed with SLN are, insufficient loading capacity, drug expulsion after polymorphic transition during storage and releatively high water content of the dispersions (70–99.9%) (Westesen et al., 1997). The drug loading capacity of conventional SLN is limited by the solubility of drug in the lipid melt, the structure of the lipid matrix and the polymorphic state of the lipid matrix (Freitas and Müller, 1999). To overcome these problems, many modifications were made with the conventional SLN system and at the turn of the millennium, the new generation of the lipid nanoparticles, the nanostructured lipid carriers (NLC) and lipid drug conjugate (LDC) have been developed (Radtke and Müller, 2001; Olbrich et al., 2000).

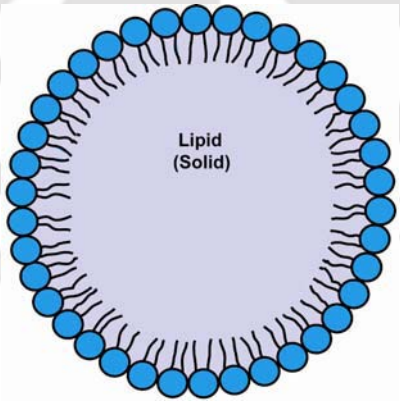

Figure 1.6: Schematic of a solid lipid nanoparticle. The inner matrix is of solid lipid where the drugs are dispersed or encapsulated.

1.8 Polymer based DDS

Polymers occupy the major portion of materials used for DDS and they are predominantly favored over other materials because –

(i) Polymers present seemingly endless diversity in topology and chemistry, which is a crucial advantage over other classes of materials to meet the ever-increasing requirements of new designs of drug delivery formulations.

(ii) The chemical composition and architecture of polymers can be readily tailored to accommodate drugs with varying hydrophobicity, molecular weight, pI, etc.

(iii) The surface properties, morphologies, and compositions of polymer matrices can be easily optimized to achieve the desired biocompatibility, controlled polymer degradation and drug release kinetics.

(iv) Through chemical modification, the polymer carrier can possess specific delivery information.

A polymer used in controlled drug delivery formulations, must be chemically inert, non-toxic, biocompatible, free of leachable impurities and be readily processable. Despite that, several other physicochemical considerations are critical in the application of polymer-based systems for drug delivery. First, drugs need to be efficiently loaded into the polymer-based delivery system at an appropriate amount in order to achieve therapeutic effects over a certain time period. The drug loading is largely dependent on the properties of the polymer-based delivery system, the properties of the drug, and the method of preparation of the delivery system. Secondly, the integrity of the drug should be retained during the process of loading, storing, and in the circulation system after the administration. The ability to maintain drug stability is closely related to the physicochemical properties of the microenvironment in the polymer-based delivery systems and to the interactions between the

drug and the polymer. Thirdly, the drug-loaded delivery system requires proper surface properties, which strongly affect the stability of the colloidal system as well as the biocompatibility and biodistribution of the drug-carrier conjugate. Finally, the kinetics and the mechanism of the drug release from the carrier into the biological system need also to be fully understood in order to get optimal drug release profiles. To achieve these goals various different classes of polymers have been utilized in DDS. But on the basis of their origin they can be divided into two major categories: (i) Synthetic Polymer and (ii) Natural Polymer.

Table1.2: Different types of polymers used in preparation of nanocarriers

Classification		Polymer
Natural Polymers	**Protein**	Albumin, , Gelatin, Collagen, Casein, Whey, Gliadin, Vicilin, Legumin, Zein etc.
	Polysaccharide	Alginate, Chitosan, Cyclodextrins, Dextran, Hyaluronic acid, Pullulan etc.
	Nucleic Acid	Single and double stranded DNA, Oligonucelotides etc.
Synthetic Polymers	**Polyesters**	Poly(lactic acid), Poly(glycolic acid), Poly lactic-co-glycolic acid, Poly(hydroxy butyrate), Poly(ε-caprolactone), Poly(β-malic acid) & Poly(dioxanones)
	Polyanhydrides	Poly(sebacic acid), Poly(adipic acid), Poly(terphthalic acid) and various copolymers
	Polyamides	Poly (imino carbonates), Polyamino acids
	Acrylic Polymers	Polymethacrylates, Poly(methyl methacrylate), Poly hydro(ethylmethacrylate) etc.
	Phosphorous Based Polymers	Polyphosphates, Polyphosphonates, Polyphosphazenes
	Others	Poly(cyano acrylates), Polyurethanes, Polyortho esters, Polydihydropyrans, Polyacetals, Polyvinyl pyrrolidone, Ethyl vinyl acetate, Poloxamers, Poloxamines etc.

1.9 Synthetic polymers used in drug delivery

These are man made materials i.e. synthesized in laboratory through chemical reaction. As these polymers are synthesized in laboratory with controlled environment, so they can be tailored to achieve required functionalities which can improve the efficacy of the drug used (Uhrich et al., 1999). But the problem with synthetic polymers is the present of unwanted monomers which can be toxic for in vivo applications (Pillai and Panchagnula, 2001). From a polymer chemistry perspective, it is important to appreciate that different mechanisms of controlled release require polymers with a variety of physicochemical properties. Some of the unique characteristics of synthetic polymers that make them versatile in drug delivery systems include (Kost and Langer, 1991; Angelova and Hunkeler, 1999; Langer, 2000):

- Wide molecular weight distribution
- Variety of visco-elastic properties
- Special characteristics associated with phase transitions
- Variety of dissolution time
- Specialized chemical reactivity
- A variety of manufacturing methods

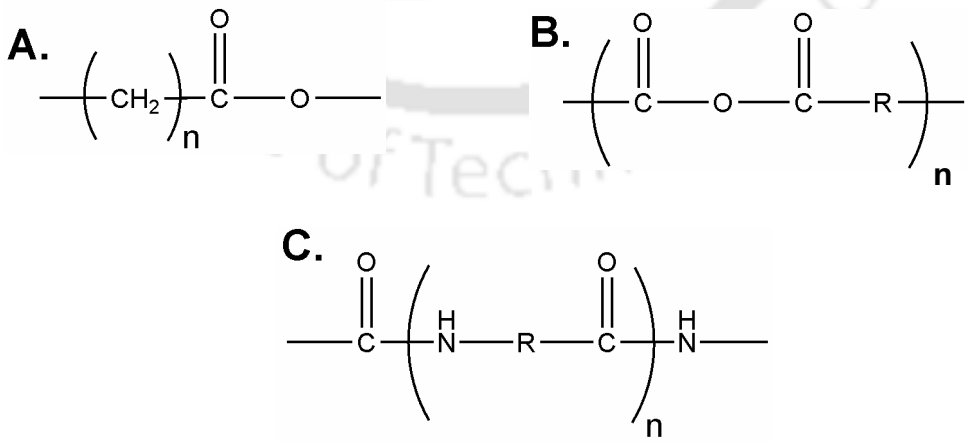

Figure 1.7: Basic chemical structure of commonly used synthetic polymers in DDS. (A) Polyester, (B) Polyanhydride and (C) Polyamide.

1.9.1 Poly(esters)

Poly(esters) are the best characterized, most widely studied synthetic, biodegradable polymer system and extensively employed in drug delivery applications. Poly(esters) based on poly(lactic acid) (PLA), poly-(glycolic acid) (PGA) and their copolymers, poly(lactic acid-*co*-glycolic acid) (PLGA), are some of the best defined biomaterials with regard to design and performance and are approved by FDA for human use (Lemoine et al., 1996). They are synthesized through ring opening polymerization of cyclic lactones and degradation of these polymers yields the corresponding hydroxy acid, which are natural metabolites of the body, making them safe for *in vivo* use. In aqueous media, these polymers degrade by bulk degradation with random hydrolysis of ester bonds of the polymer backbone to form lactic and glycolic acids (Jain et al., 2000). The factors that affect the rate of hydrolytic degradation include type and composition of the polymer backbone, nature of pendent groups, molecular weight, pH, enzymes, and geometry of the particles. The preparation of PLA and PLGA nanoparticles included various techniques such as nanoprecipitation, simple and multiple emulsions, salting out, spray drying and supercritical fluid technology (Jain et al., 2000; Bala et al., 2004; Niwa et al., 1993). The experimental variables for each protocol can be altered to influence the physicochemical properties, such as particle size, particle size distribution, morphology, and zeta potential. The release of encapsulated drug from PLA and PLGA nanoparticles may occur by a combination of diffusion and polymer degradation at a rate that is influenced by properties of the polymer and nanoparticles and the environment (Astete and Sabliov, 2006). Another FDA approved poly(ester) which is widely used is poly(ε-caprolactone) or PCL. It is a semicrystalline polymer synthesized by anionic, cationic, free radical or ring opening polymerization and available in a range of molecular weights (Lemoine et al., 1996). It degrades by bulk

hydrolysis of ester bonds autocatalyzed by the carboxylic acid end groups and the presence of enzymes such as protease, amylase, and pancreatic lipase accelerates polymer degradation (Seppala et al., 2004). The various methods of preparation of poly(ε-caprolactone) NPs include emulsion polymerization, interfacial deposition, emulsion–solvent evaporation, desolvation, and dialysis (Sinha et al., 2004).

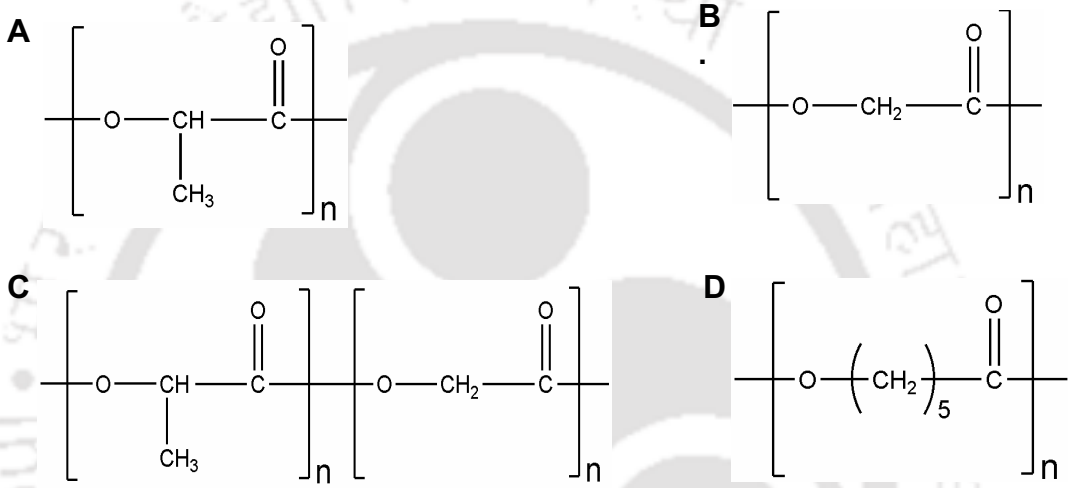

Figure 1.8: Chemical structures of commonly used polyesters in drug delivery applications. (A) Poly (lactic acid), (B) Poly (glycolic acid), (C) Poly (lactic-co-glycolic acid) and (D) Poly (ε-caprolactone).

1.9.2 Polyanhydrides

Polyanhydrides are an important class of synthetic biomaterials used for more than two decades as carriers of drugs to various organs of the human body such as brain, bone, blood vessels, and eyes (Kumar and Langer et al., 2002). Polyanhydrides are biocompatible and degrade in vivo into non-toxic counterparts that are eliminated from the body as metabolites. Some polyanhydride-based formulations are also clinically available for treating glioblastoma multiforme, a universally fatal form of brain cancer (Dang et al., 1996). These polymers have a hydrophobic backbone with a hydrolytically labile anhydride linkage. High

hydrolytic reactivity of the anhydride linkage provides an intrinsic advantage in versatility and control of degradation rates. These polymers vary in chemical composition widely and include aliphatic, aromatic and fatty acid based polyanhydrides. The majority of polyanhydrides studied are based on sebacic acid (SA), p- (carboxyphenoxy) propane (CPP) and p-(carboxyphenoxy) hexane (CPH). The rate of degradation depends on the chemical composition of the polymer. In general, aliphatic polyanhydrides degrade more rapidly than the aromatic polymer. Hence, copolymer blends with varying ratios of aliphatic-to-aromatic polyanhydrides can be synthesized to suit specific applications. Polyanhydride nanospheres are commonly prepared by the emulsion–solvent evaporation method using PVA as a stabilizer (Lee and Chu, 2007). However, as polyanhydrides are hydrolabile, they need to be flash frozen in liquid nitrogen and lyophilized immediately. An example of their use to deliver drugs is entrapment of bovine zinc insulin by phase inversion nanoencapsulation (Cheng et al., 2004).

1.9.3 Polyamides

Polyamides form another important class of polymers particularly as drug delivery matrices. Polyamides with a structural resemblance to polypeptides are used as matrices for the transport of drugs. Examples include different types of poly (amino acids) such as poly (L-glutamic acid), poly (aspartic acid) are derived from the corresponding natural amino acids (General and Thunemann, 2002). Nakanishi and co-workers have developed a polymeric micelle carrier system consisting of PEG-conjugated doxorubicin: poly (aspartic acid) for the transport of doxorubicin. This carrier system has a highly hydrophobic inner core, and therefore, it can also entrap a useful amount of doxorubicin in addition to the conjugated doxorubicin. The entrapped doxorubicin was released from the inner core by diffusion and

expressed stronger activity than free doxorubicin against all the tumour lines tested (Nakanishi et al., 2001). Li and co-workers have synthesised a novel biodegradable poly (ester amide) derived from 3-morpholine and ε-caprolactone. Increase in morpholine content enhanced water absorption of the polymers. In vitro degradation data and release profiles of 5-fluorouracil showed that both the degradation rate and drug release rate increased with an enhanced morpholine content in the polymers (Li et al., 2002).

1.10 Natural polymers used in drug delivery

In spite of development of various synthetic and semi synthetic polymers, natural polymers are still widely used in DDS due to their biodegradability and easy availability. Proteins and polysaccharides are the two main classes of natural polymers which are regularly used in DDS. The potential problems of natural polymers are that they can cause immunoreaction, especially protein based systems and to achieve desired property often chemical modifications are required. Natural polymers may vary widely in their composition and therefore physicochemical properties. Such variability in properties may result in poor reproducibility in delivery characteristics, such as drug loading and release kinetics. Also, the natural polymers extracted and purified from plant and animal sources often vary significantly in their purity.

1.10.1 Chitosan

Chitosan is a nontoxic, biodegradable polymer obtained by deacetylation of chitin, a natural polysaccharide that is a component of the crustacean exoskeleton. Chitosan is known to have various biological activities including immuno-enhancing effects, antifungal and antimicrobial activities (Sudarshan et al., 1992). Unmodified chitosan is soluble in acidic media and has significant mucoadhesive properties. The physicochemical properties of

chitosan are determined by the solution pH and ionic strength. Chitosan nanoparticles may be prepared using various methods, including emulsion crosslinking, coacervation, spray drying, emulsion droplet coalescence, ionic gelation, and reverse micellar microemulsuion method (Agnihotri et al., 2004; Bodnar et al., 2005). The size of nanoparticles will depend on the molecular weight of chitosan, its concentration, and its surface charge (Lopez-Leon et al., 2005). Over the years chitosan is the most abundantly used biopolymer for drug delivery. Drugs ranging from small organic molecules to proteins and nucleic acids have been successfully delivered using chitosan nanoparticles. Chitosan nanoparticles when used as drug carrier against cancer have shown potent cytotoxic effects on various tumor cell lines *in vitro* and *in vivo*. Hydrophilic water soluble drugs can be incorporated easily into chitosan nanoparticles without the modification of chitosan itself. Cationic anthracycline drug doxorubicin hydrochloride forms complex with anionic chitosan, showed anti-proliferative activity against human melanoma A375 cells, C26 murine colorectal carcinoma cells in vitro and good in vivo therapeutic efficacy against J774A.1 macrophage tumor cells implanted Balb/c mice (Janes et al., 2001; Maitra et al., 2001). The nucleotide analogue 5-fluorouracil when capsulated in chitosan nanoparticle prepared by ionic gelation with polyaspartic acid, proved useful for the treatment of human gastric carcinoma model in vivo (Zhang et al., 2008). To encapsulate hydrophobic anticancer drugs, chitosan nanoparticles were prepared by modifying with hydrophobic moieties such as, cholic acid, 5β-cholanic acid and cholesterol (Lee et al., 1998; Wang et al., 2007). These modified chitosan nanoparticles were used for the delivery of poorly soluble anticancer drugs such as paclitaxel, cisplatin, docetaxel etc (Kim et al., 2006; Min et al., 2008). A recent study showed that hydrophobically modified chitosan nanoparticles can also be used for the delivery of small peptide drugs in cancer therapy (Kim et al., 2008). The conjugates of

anticancer agents with chitosan and its derivatives display good anticancer effects with a decrease in the adverse effects of the original drug due to a predominant distribution into the cancer and a gradual release of free drug from the conjugates (Kato et al., 2005). For instance, doxifluridine and 1-beta-D-arabinofuranosylcytosine (Ara-C) were conjugated with chitosan via glutaric spacer, and the conjugates of Ara-C with chitosan, in particular, showed a good antitumour effect against P388-bearing leukemia model mice. Glycol-chitosan (G-Chi) was distributed mainly in the systemic circulation and the kidney after i.v. administration into normal mice, and retained long in the kidney. The therapeutic effect of the conjugates of mitomycin C (MMC) with G-Chi was not necessarily improved in comparison with that of the free drug, but toxic side-effects appeared to decrease with the conjugates. The conjugates of MMC with 6-O-carboxymethyl-chitin showed almost complete suppression of tumor growth at 10 mg equivalent MMC/kg, though a lethal adverse effect was also observed. The conjugates of MMC with N-succinyl-chitosan showed good antitumour activities against various tumor models due to their predominant distribution into the tumor tissue and sustained-release characteristics, irrespective of water-insoluble and soluble formulations (Kato et al., 2005).

1.10.2 Alginate

Alginate is an anionic biopolymer produced by marine brown algae consists of linear chains of α-l-guluronic acid (G) and β-d-mannuronic acid (M) residues joined by 1,4-glycosidic linkages and is of interest as a polymer to prepare nanocarriers owing to its good water solubility, biocompatibility, biodegradability, non-toxicity, mucoadhesion and gelation properties. In the body, the alginates degrade by acidic hydrolysis of the guluronic and mannuronic segments. Further, in addition to being biodegradable, alginates are

nonimmunogenic. Alginate nanoparticles have been widely studied for particle formation in the size range of 100 nm to 2 mm for drug delivery (Rajaonarivony et al., 1993; Sarmento et al, 2006). In vivo, alginate nanoparticles accumulate in the Kupffer cells, parenchymal cells of liver, and phagocytes of spleen and lungs (Ahmad et al., 2006). Alginate nanoparticles have also been reported to be absorbed into Peyer's patches, suggesting that they may enhance targeting to the intestinal mucosa (Borges et al., 2006). Because they are prepared in an aqueous environment under mild conditions, alginate nanoparticles are particularly suitable for formulating proteins, peptides, and oligonucleotides (George and Abraham, 2006; Lambert et al., 2001). Alginate-surfactant nanoparticles can be prepared by emulsification-crosslinking technology which can significantly enhance and sustain the cellular delivery of water-soluble drugs such as doxorubicin, resulting in enhanced therapeutic efficacy in tumor cells (Chavanpatil et al., 2007a). Fluorescence microscopy studies demonstrated that alginate nanoparticles encapsulated doxorubicin was predominantly localized in the perinuclear vesicles and to a lesser extent in the nucleus, whereas free doxorubicin accumulated mainly in peripheral endocytic vesicles. These surfactant-biopolymer nanoparticles also inhibit P-gp-mediated drug efflux in drug resistant tumor cells, which make them ideal carrier of therapeutic agents to drug resistant cancer cells (Chavanpatil et al., 2007b). In a novel study antineoplastic drug cisplatin was first complexed with alginate and then transformed into nanoparticles by ionic crosslinking with chitosan (Cafaggi et al., 2007). Preliminary pharmacological experiments on cytotoxicity *in vitro* indicated that the cisplatin entrapped nanoparticles had a similar or slightly less activity compared to free cisplatin on P388 and A2780 cell lines. Recently alginate was used to prepare biocompatible nanocapsules which can load lipophilic oily compounds in the core (Lertsutthiwong et al., 2008).

1.10.3 Cyclodextrin

Cyclodextrins are cyclic oligosaccharides consisting of six, seven or eight glucopyranose units, namely α- ,β-, γ-cyclodextrin, linked by α-1,4-glycosidic bonds to form macrocycle (Szejtli, 1998) (Figure 1.9). They have bucket shaped structure with hollow lipophilic interior and a hydrophilic exterior, they are biocompatible and they do not elicit immune response (Martin del Valle, 2004). Throughout the years cyclodextrins have gained increasing interest as drug delivery systems because of their capacity to form soluble inclusion complexes with many hydrophobic drugs and to prevent degradation of labile molecules (Hirayama and Uekama, 1999; Davis and Brewster, 2004). Horvath et al. (2008) proved that higher water solubility and anticancer activity of hydrophobic platinum compounds can be attained by nanoencapsulation with cyclodextrin. Many other different anticancer drugs such as doxorubicin, paclitaxel, tamoxifen etc. have been shown to form inclusion complexes with cyclodextrin nanoparticles and are efficient system for the delivery of drugs (Memisoglu et al., 2005; Hamada et al., 2006).

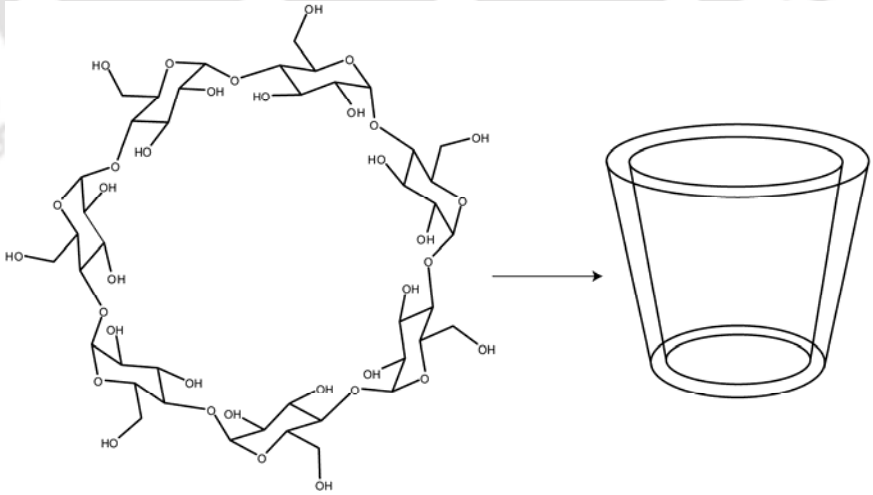

Figure 1.9: Chemical structure of β-cyclodextrin (left side) and its bucket shaped 3-D structure (right side). The inner region of the bucket is used for drug complextation through hydrophobic interactions.

1.10.4 Other Polysaccharides

The other macromolecular polysaccharides which are commonly used in DDS include pullulan and dextran. Pullulan is a nonimmunogenic, nontoxic, water soluble, linear, nonionic polysaccharide with α(1–4) and α(1–6) linkages with free hydroxyl groups which are intracellularly synthesized and secreted by a fungus, *Aureobasidium pullulans*. To make pullulan nanoparticles, the polymer must first be made hydrophobic, typically by conjugating alkyl groups, cholesterol groups or succinyl groups which uiltimately self-assembles to form stable hydrogel nanoparticles (Akiyoshi et al., 1993; Na et al., 2003). Alternately, pullulan nanoparticles can be formed by cross - linking reverse micelles of the polymer with glutaraldehyde (Gupta and Gupta, 2004). Pullulan nanoparticles successfully delivered HER2 oncoprotein to induce humoral and cellular immune responses against HER2 expressing murine sarcomas (Gu et al., 1998). Na and Bae, (2002) developed pH sensitive self-assembled nanoparticles of succinylated pullulan acetate/sulfonamide (PA/SDM) conjugates which provided some advantages for targeted anti-cancer drug delivery due to the particle self-aggregation and enhanced drug release rates at tumor pH. Folate-modified cholesterol-bearing pullulan NPs were synthesized for targeted delivery of doxorubicin to cancer cells over expressing folic acid receptors (Sunamoto and Ushio, 2006).

On the other hand, dextrans are glucose polymers derived from sucrose with α(1–6) glucosidic linkage. Clinically this natural polysaccharide has been used for plasma volume expansion, peripheral flow promotion and as antithrombolytic agents (Thoren, 1981). Dextran is commonly conjugated to other polymers, such as PLGA, PCL, polystyrene, and poly(methyl methacrylate) for preparation of NPs (Mehvar, 2000; Bajgai et al., 2008). Covalent grafting of these polymers on the dextran side chain helped to form the NPs by

self-assembly in which the polysaccharide chain act as shell (Qiu et al., 2009). Dextran based particles have been developed as a carrier of anticancer drug mitomycin C, to reduce the side effects of the drug and enhance its efficiency (Cheung et al., 2005). Hydrophobically modified dextran, in which the polymer was chemically modified by covalent conjugation of hydrocarbon chains, was used for the preparation of NPs by solvent-diffusion or o/w emulsion method (Aumelas et al., 2007). In another approach nonionic dextran was first modified to anionic dextran sulfate and then NPs were prepared by ionic gelation with cationic chitosan or polyethyleneimine (PEI). This ionically crosslinked dextran based hydrophilic NPs were effective carrier of insulin and amphotericin B (Tiyaboonchai et al., 2003; Tiyaboonchai and Limpeanchob, 2007).

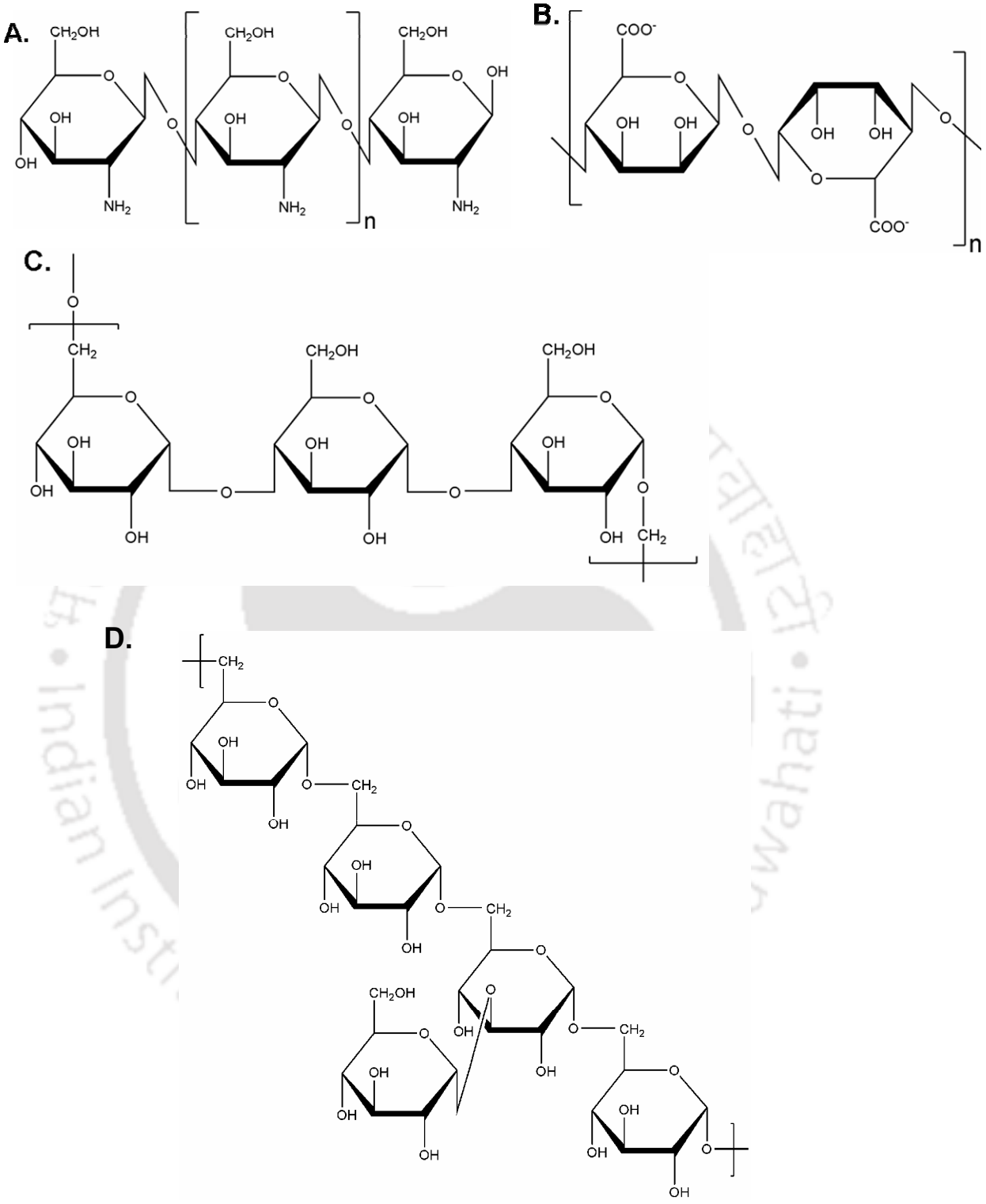

Figure 1.10: Commonly used polysaccharides for the preparation of polymeric nanocarriers. (A) Chitosan, (B) Alginate, (C) Pullulan and (D) Dextran.

1.10.5 Albumin

Serum albumins are widely used as a material for drug carrier since they are considered to be biodegradable and safe. Both bovine serum albumin (BSA) and human serum albumin (HSA) have been used in drug delivery applications but ultimately HSA is preferred over BSA due to its nonimmunogenicity. HSA is the major soluble protein in blood, globular in nature, contains approximately 585 amino acids in α-helical tertiary structure. It is a positively charged, multifunctional protein and involved in transport, ligand binding and enzymatic activities. Albumin nanoparticles can be prepared by controlled desolvation, pH induced coacervation, and/or chemical cross-linking with glutaraldehyde (Langer et al., 2003). Doxorubicin was loaded to the HSA nanoparticles either by adsorption to the nanoparticle surfaces or by incorporation into the particle matrix. The anti-cancer effects of the drug-loaded nanoparticles were increased in comparison to doxorubicin solution in several neuroblastoma cell lines (Dreis et al., 2007). The coupling of the antibody trastuzumab to HSA nanoparticles showed a specific targeting to HER2-overexpressing cells with cellular uptake by receptor-mediated endocytosis (Steinhauser et al., 2006).

The HSA-based nanoparticle formulation of paclitaxel, ABI-007 (Abraxane®) was approved by the FDA in 2005 (Hawkins et al., 2008). This drug loaded NPs were average 130 nm in size and prepared by high pressure homogenization without any harmful solvent. The drug incorporation in nanoparticles follows a new concept to improve drug solubility, with a variety of advantages conferred to the standard paclitaxel therapy (Desai et al, 2006). To further improve the efficacy of Abraxane®, this nanoparticle was modified with tumor homing peptides to selectively target them into extravascular tumor tissue. This targeted Abraxane® produced a statistically highly significant inhibition of tumor growth compared with untargeted Abraxane® (Karmali et al., 2009).

1.10.6 Collagen and Gelatin

Collagens are the main protein of connective tissue in animals and the most abundant protein in mammals, making up about 25% to 35% of the whole-body protein content (Lee et al., 2001). Collagens are centrally involved in the formation of fibrillar and microfibrillar networks of the extracellular matrix, basement membranes as well as other structures of the extracellular matrix. This family of proteins has been used extensively in tissue engineering applications but very limited reports are available for DDS (Freiss, 1998; Ruszczak et al., 2003). Collagen microspheres were used for delivery of hydrophobic peptide drug cyclosporine, protein drug glial cell line-derived neurotrophic factor (GDNF) and small organic molecule retinol (Gebhardt et al., 1995; Lee et al., 2009; Rossler et al., 1995).

Gelatin is a protein which is obtained by either alkaline or acidic hydrolysis of collagen. It has been widely used in cosmetics, in many different types of food products as well as in pharmaceutical formulations and approved by FDA for extravascular administration. The physicochemical properties of gelatin depend on the method of extraction and the extent of thermal denaturation that occurs during the purification. Gelatin nanoparticles can be prepared by various methods, including chemical crosslinking, water-in-oil (w/o) emulsification and desolvation (Azarmi et al., 2006). The nanoparticulate carriers of gelatin have been used for efficient intracellular delivery of the encapsulated payload (Young et al., 2005). Doxorubicin conjugated Gelatin NP was prepared by glutaraldehyde crosslinking showed 42% drug loading, which was released only after NP digestion by proteolytic enzymes (Leo et al., 1997). Paclitaxel loaded gelatin NPs have been used for intravesical bladder cancer therapy (Lu et al., 2004). Surface medication of gelatin NPs was done to reduce the uptake by RES. When administered in the systemic circulation, PEG-modified nanoparticles are preferentially distributed to solid tumor due to the hyperpermeability of the

angiogenic blood vessels by the EPR effect (Kaul and Amiji, 2002). They also showed the biodistribution and tumor targeting results of gelatin and PEG-modified gelatin nanoparticles, labeled with iodine-125, upon intravenous administration in mice bearing Lewis lung carcinoma (LLC) (Kaul and Amiji, 2002). The plasma and the tumor half-lives, the mean residence time, and the area-under-the-curve of the PEGylated gelatin nanoparticles were significantly higher than those for the gelatin nanoparticles. In another study, gelatin NPs were grafted with NeutrAvidin in the partcle surface and then conjugated with biotinylated anti CD-3 antibodies for specific drug targeting to T lymphocytes (Balthasar et al., 2005). In a similar process biotinylated EGFR molecules were conjugated with avidin modified gelatin NPs to target lung cancer cells (Tseng et al., 2007).

1.10.7 Milk Proteins

Food biopolymers, specifically milk proteins, are widely used in pharmaceutical formulations and formulated foods because they have high nutritional value and are generally recognized as safe (GRAS). The protein content of milk is broadly subdivided into two major groups, casein and whey and both types can be used for drug delivery purposes (Chen et al., 2006). There are very few studies involved with casein nanoparticles. Earlier well-defined, core-shell poly(methyl methacrylate) (PMMA)/casein nanoparticles, ranging from 80 to 130 nm in diameter, were prepared via a direct graft copolymerization of methyl methacrylate (MMA) from casein (Zhu et al., 2003). In a recent study, dextran was grafted to casein through the Amadori rearrangement of the Maillard reaction and the resulting casein-graft-dextran was shown to produce nanoparticle and simultaneously encapsulate model drug β-carotene by hydrophobic interaction (Pan et al., 2007). Whey proteins can be used as hydrogel and/or nanoparticle systems for controlled release of bioactive compounds

(Gunasekaran et al., 2007). Recently acquired knowledge of whey protein physical chemistry has allowed us to build protein nanoparticles using the bottom-up approach. A monodisperse suspension of 40 nm whey protein nanospheres was obtained by modulating parameters affecting the thermal aggregation process (Leclerc et al., 2005). Aggregates of submicron size can be obtained at relatively low calcium and protein concentrations and at a temperature around 55 °C, which is well below the denaturation temperature of β-lactoglobulin (about 74 °C). The most probable mechanism leading to the formation of these nanoaggregates involves electrostatic interactions between protein and calcium, hydrophobic interactions between proteins and the consolidation of the structure by intermolecular disulfide bonds (Leclerc et al., 2005). Further in vitro experiments with Caco-2 cells suggest that whey protein nanoparticles could be internalized by cells and degraded therein to release the nutraceutical compounds, significantly improving nutraceutical compound bioavailability while avoiding undesired toxic side effects of the free compounds (Leclerc et al., 2005).

1.10.8 Other Proteins

Plant proteins isolated from vegetal food sources are also attractive candidate for drug carriers. In this regard gliadin, a glycoprotein derived from wheat gluten, has been used as a matrix for the preparation of drug loaded nanospheres. Gliadin nanoparticles are prepared by the desolvation method by first pouring an organic solution of polymer into an aqueous phase such as physiological saline containing a surfactant stabilizer and then evaporating the organic solvent (Ezpeleta et al., 1996a). Duclairoir et al (1999) have used gliadin NPs for entrapment of all-trans-retinoic acid which is an attractive agent against a range of human malignancies. Furthermore this protein NPs was also used in encapsulation of lipophilic vitamin E to prevent the degradation of this labile molecule (Duclairoir et al., 2003). A

limitation on the use of gliadins is that patient sensitivity causes an autoimmune disorder called celiac disease. Other plant based proteins which have been used in nanoparticle preparation and drug delivery are pea seed storage proteins vicilin and legumin, wheat protein zein and plant lipid transfer proteins (Mirshahi et al., 1996; Ezpeleta et al., 1996b; Pato et al., 2001).

1.10.9 Nucleic Acid

Nucleic acid, mainly DNA is also used for preparation of drug carriers. Inherent self-assembly properties of DNA have been used to prepare nanostructures or nanogel particles (Aldaye et al., 2008; Lin et al., 2009). The main ways to create DNA hydrogel structures include enzyme-catalyzed assembly of branched DNA and chemical cross-linking of DNA (Um et al., 2006; Horkay and Basser, 2004). Very recently, the interactions between negatively charged DNA and positively charged surfactants have been used to form DNA gel particles by interfacial diffusion (Moran et al., 2007). These DNA hydrogels were biocompatible, biodegradable, inexpensive to fabricate and easily moulded into desired shapes and sizes. These DNA based hydrogels have been shown as potential drug carriers by encapsulating model fluorescent compounds (Tang et al., 2009). The self-assembly property of DNA has been used to construct cage like structure for encapsulation of enzymes (Erben et al., 2006). Moreover, researchers have prepared DNA buckyballs by DNA-polystyrene hybrid polymer. The hybrid molecules spontaneously self-assemble into hollow balls of nearly 400 nm in diameter and the open spaces in the structure allow molecules to enter or go out. Drugs could be encapsulated in buckyballs to be carried into cells, where natural enzymes would break down the DNA, releasing the drug. DNA based drug delivery systems are promising but still in their infancy and no report of drug delivery against cancer so far.

1.11 Polymer based nanocarriers

1.11.1 Polymer nanoparticle

The application of polymer made particles (micro and nano) as means for drug delivery was one of the most broadly investigated strategies during the last decades. Polymer NPs are solid, colloidal particles made of synthetic or natural polymeric substances and vary in size from 10 nm to 1000 nm (Hans and Lowman, 2002). The drug of interest is dissolved, entrapped, adsorbed, attached and/or encapsulated into or onto the nano-matrix for effective delivery. Depending on the production methodology, two types of nanoparticles can be constructed i.e. nanospheres and nanocapsules, to acheive different properties and release characteristics for the best delivery or encapsulation of the therapeutic agent (Soppimath et al., 2001; Panyam and Labhasetwar, 2003). Nanospheres are matrix systems in which the drug is physically and uniformly dispersed whereas, nanocapsules are vesicular systems in which a drug is confined to a cavity surrounded by the polymer (Soppimath et al., 2001). Polymeric NPs displayed interesting features related to the protection/stabilization of sensitive active compounds and their delivery profiles. Due to the higher surface area leading to faster solubilization rates, nano-sized structures usually show higher plasma concentrations and AUC values. The most broadly investigated polymers include the natural chitosan, alginate, gelatin, albumin and the synthetic polylactic acid (PLA), poly(lactic-co-glycolic) acid (PLGA), polycaprolactone (PCL), poly(cyanoacrylate) (PCA) etc. However, unmodified polymer NPs prepared from hydrophobic synthetic polymers was removed from the body by opsonization and phagocytosis. The modification of the NP surface with highly hydrophilic chains (e.g., polyethylene glycol) resulted in lower recognition by the host and longer circulation times for NPs was obtained (Leroux et al., 1996). The interaction of synthetic polymeric nanoparticles with cells was promoted by coating them with chitosan,

which is naturally muchoadhesive (Lemarchand et al., 2004). Oral administration of peptides or proteins has been performed effectively by encapsulating them in polymer nanospheres which provides improved stability, less degradation and greater absorption in GI tract (Vila et al., 2002). Similarly oral delivery of vaccines and anticancer drugs were also showed promise for patient friendly formulations (Win and Feng, 2005; Rieux et al., 2006). The cellular uptake of polymer NPs depends on the surface coating, charge and concentration of particles (Davda and Labhasetwar, 2002; Win and Feng, 2005). Nanoencapsulation enhanced the transfer of drugs across the brain blood barrier (BBB) for delivery into brain. Drugs that have successfully been transported into the brain using polymeric nanocarriers include hexapeptide dalargin, dipeptide kytorphin, loperamide, tubocurarine, the NMDA receptor antagonist MRZ 2/576 and doxorubicin. (Kreuter, 2001). Polymeric nanoparticles also have been used very extensively against cancer (Pridgen et al., 2007). The surface of polymer nanoparticles can be modified easily to target cancer cells by conjugation with ligands such as antibody, folate, transferrin, peptides and aptamers (Byrne et al., 2008).

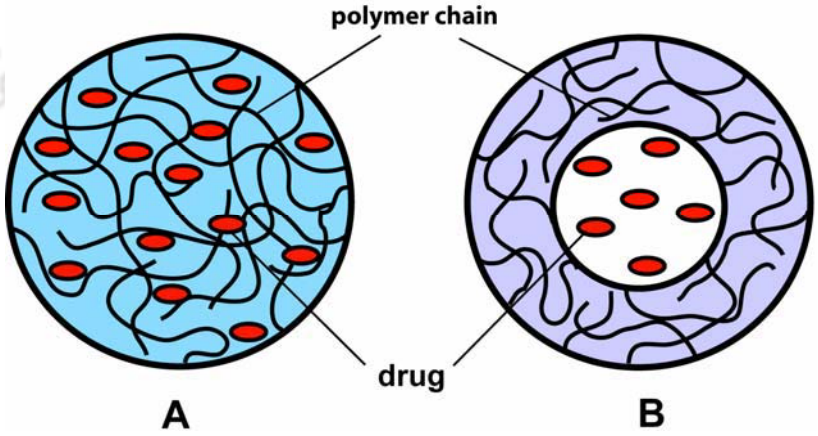

Figure 1.11: Drug encapsulated polymer nanoparticles: A. Nanosphere: drug molecules are dispersed in the solid polymer matrix, B. Nanocapsule: drug molecules are present in the core covered with the polymer shell.

1.11.2 Polymeric Micelle

Polymeric micelles represent a separate class of nanocarriers which are formed by self-assembly from copolymers consisting of both hydrophilic and hydrophobic units. These are nanoscopic (~100 nm) spherical structures with a core-shell architecture where the hydrophobic units of the polymer form the core and hydrophilic units form the shell. They were first proposed as drug carriers in 1984 and in recent years they have emerged as potential nanocarrier of anticancer drugs for cancer therapy (Bader et al., 1984; Nishiyama and Kataoka, 2006). Thermodynamic phenomenon underlying micelle formation from amphiphilic polymers are the same as for micellization of any low molecular weight surfactants i.e. the formation of micelles is driven by the decrease of free energy in the system because of the removal of hydrophobic fragments from the aqueous environment and the reestablishing of hydrogen bond network in water. Additional energy gain results from formation of Van der Waals bonds between hydrophobic blocks in the core of the formed micelles (Jones and Leroux, 1998). The key parameter for micellization process is the critical micelle concentration (CMC) of amphiphile. At very low concentrations amphiphilic copolymers exist as single chains (unimers) in solution but as concentration increases to reach the CMC, polymer chains start to associate to form micelle nanostructures (Hernandez et al., 2005). Polymeric micelles generally exhibit a CMC value much lower than that of low molecular weight surfactants which renders them to be more suitable for drug delivery applications (Wilhelm et al., 1991). Hydrophobic core of polymeric micelles provides an excellent cargo space for the incorporation and stabilization of hydrophobic drugs whereas the shell is responsible for micelle stabilization and interactions with plasmatic proteins and cell membranes. The biodistribution of the micellar carrier is also dictated by the nature of the hydrophilic shell (Gaucher et al., 2005). It usually consists of hydrophilic, nonionic,

biocompatible polymers such as poly(ethylene glycol), poly(N-vinyl-pyrrolidone) and poly(vinyl alcohol) (Elbert and Hubbell, 1996). The nanoscopic dimension as well as unique properties offered by separated core and shell domains in the structure of polymeric micelles has made them one of the most promising carriers for passive or active drug targeting in cancer. The small size of polymeric micelles makes the carrier unrecognizable by the phagocytic cells of RES, elongating their blood circulation, and facilitating the carrier's extravasation from tumor vasculature (Allen et al., 1999). The small size of polymeric micelles is also expected to ease penetration of the carrier within the tumor tissue and further internalization of polymeric micelles into the tumor cells (Kwon, 1998; Allen et al., 1999). To date, two of the drugs that have been most commonly formulated in block copolymer micelles are doxorubicin and paclitaxel. Doxorubicin has been successfully loaded into micelles formed from PEG-b-poly(3-caprolactone) (PEG-b-PCL), PEG-b-poly(D,L-lactide-co-glycolide) (PEG-b-PLGA), PEO-b-poly(propylene oxide)-b-PEO (Pluronic), and PEG-b-poly (aspartic acid) (PEG-b-PAsp) whereas, paclitaxel has been successfully loaded into PEG-b-poly(D,L-lactide) (PEG-b- PDLLA), poly(N-vinyl-pyrrolidone)-b-PDLLA (PVP-b-PDLLA), PEG-b-PCL and PEG-b-poly(d-valerolactone) (PEG-b-PVL) micelles (Shuai et al., 2004; Yoo and Park, 2001; Kwon et al., 1994; Liggins et al., 2002). Cisplatin and camptothecin were other drugs which have been formulated in micellear nanocarriers (Uchino et al., 2005; Watanabe et al., 2006).

Many preclinical fundamental studies have evaluated the relationships between the composition of the copolymers and the physico-chemical properties of the micelles. The properties of the micelles such as polymer–drug compatibility, thermodynamic and kinetic stability, and the drug release profiles have been shown to influence the in vivo performance and therapeutic effectiveness of the micelle-formulated drugs (Torchilin, 2007). These

studies serve as guidelines for the optimization of polymeric micelles for clinical applications. In order to design an effective micellar drug delivery system, several key physico-chemical properties of the micelles should be considered as a means to optimize performance. These include micelle size and size distribution, morphology, and stability (Nishiyama and Kataoka, 2006; Torchilin, 2007). In the past two decades, four polymeric micelle formulations loaded with chemotherapeutic drugs (NK911, SP1049C, Genexol-PM, and NK105) have entered clinical trial development (Matsumura et al., 2004; Danson et al., 2004; Kim et al., 2004). The results from the clinical studies have indicated that the polymeric micelle formulations reduce the toxicity associated with conventional formulations of these drugs that, in turn, results in a higher therapeutic index (Rapoport et al., 2003; Hamaguchi et al., 2005).

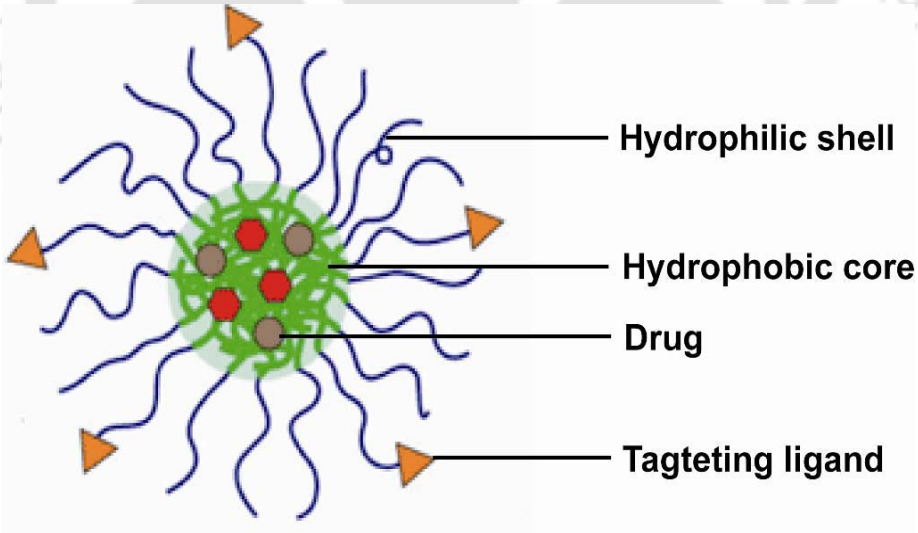

Figure 1.12: Schematic illustration of a polymeric micelle encapsulating drugs in its hydrophobic core.

Table 1.3: Polymeric micelle formulation of anticancer drugs currently in clinical trials.

Trade Name	Drug	Polymer Used	Indication	Phase	Company
SP1049C	Doxorubicin	Poloxamer	Metastatic Adenocarcinoma of the Upper Gastrointestinal Tract	Phase III	Supratek Pharma Ltd. Canada
NK911	Doxorubicin	PEG –*b*– poly(aspartic acid)	Metastatic or Recurrent Solid Tumors	Phase II	Nippon Kayaku Co. Ltd., Japan
Genexol-PM	Paclitaxel	Methoxy poly(ethylene glycol)-b-poly (lactide)	Lung and Brest Cancer	Phase II	Samyang Co., South Korea
NK105	Paclitaxel	Modified PEG –*b* – poly(aspartic acid)	Stomach Cancer	Phase II	NanoCarrier Co. Ltd., Japan

1.11.3 Dendrimer

Dendrimers are synthetic macromolecules with tree-like structures. The word *dendrimer* originates from the Greek *dendron*, meaning "tree" and *meros*, meaning "part". They are hyperbranched and monodisperse three-dimensional macromolecules, characterized by layers from a core focal point called generations and multivalent end group functionalities with defined molecular weights and host–guest entrapment properties (Figure 1.13). Dendrimers are synthesized from branched monomer units in a step-wise manner, thus it is possible to precisely control their molecular properties, such as size, shape, dimension, density, polarity, flexibility, and solubility, by choosing different building/branching units and surface functional groups (Lee et al., 2005). These nanosized structures can host a

variety of carrier molecules, both hydrophobic and hydrophilic, and are useful delivery agents for genes and drugs. Recently, dendrimers have emerged as new alternatives and efficient tools for delivery of anticancer therapeutics (Wolinsky and Grinstaff, 2008).

There are mainly two strategies to synthesize dendrimers, (i) divergent method, in which the branching units are grown outwards from a central core (Tomalia et al., 1985) and (ii) convergent method, in which the dendrimer is synthesized from the periphery and terminate at the core (Hawker and Fréchet, 1990). The branching units are described by generation, starting with the central core molecule as generation 0 (G0) and increasing with each successive addition of branching points (i.e. G1, G2 etc.) and adopt a more globular shape with increasing generation. Dendrimers are often characterized by their terminal generation, such that a G5 dendrimer refers to a polymer with four generations of branch points emanating from a central branched core. In general, dendrimers possess empty internal cavities and can encapsulate hydrophobic drug molecules. In addition, they have a much higher surface functional group density when compared with conventional macromolecules, giving rise to their applications for enhancing the solubility of many drugs. Furthermore, the large numbers of surface functional groups on dendrimer's outer shell can be modified or conjugated with a variety of interesting guest molecules. So, broadly there are three methods for using dendrimers in drug delivery: (*a*) the drug is covalently attached to the periphery of the dendrimer to form dendrimer prodrugs, (*b*) the drug is coordinated to the outer functional groups via ionic interactions, or (*c*) the dendrimer acts as a unimolecular micelle by encapsulating a pharmaceutical through the formation of a dendrimer-drug (i.e., host–guest) supramolecular assembly. Over the last few years many dendritic molecules have been developed for effective anticancer therapy and the majority of studies have been performed with polyamidoamine (PAMAM) dendrimer. Various anticancer drugs have been

solubilized by conjugation to the dendrimer surface or simple non covalent interaction with dendrtic core for efficient delivery of these therapeutic molecules to tumor cells. Ooya et al. (2004) have reported the hydrotopic solubilization of paclitaxel in aqueous solution by poly (glycerol) dendrimer formulations whereas Neerman et al. (2004) used melamine based dendrimers to solubilize methotrexate and 6-mercaptopurine, two FDA approved anticancer drugs. Their study also showed that the solubilization in dendrimer reduces drug toxicity in C3H mice models. In another study, Morgan et al. (2006) have used fourth generation Poly (glycerol succinic acid) (G4-PGLSA) dendrimers with carboxylate peripheral groups to encapsulate 10-hydroxycamptothecin (10-HCPT) and 7-butyl-10-aminocamptothecin (BACPT) for delivery to cancer cells. The encapsulation in dendrimer increased overall water solubility of the hydrophobic drug molecules and also showed significant anticancer activity as evaluated with HT-29 colon carcinoma, MCF-7 breast carcinoma, non–small cell lung carcinoma (NCI-H460), and glioblastoma (SF-268) cell lines. In a recent study Lee et al. (2006) prepared an asymmetric doxorubicin functionalized bow-tie dendrimer by PEGylation of one side of a 2,2-bis (hydroxyl methyl) propionic acid dendrimer (G3) and attachment of the drug via an acyl hydrazone linkage (pH sensitive linkage) to the other side (G4) resulting in overall doxorubicin content of 8-10% and following intravenous administration to BALB/c mice with C-26 colon carcinoma tumors showed approximately 9 fold higher tumor uptake compared to free doxorubicin. A single injection of doxorubicin-conjugated dendrimer caused complete tumor regression and 100% survival of mice over two months, while no cures were observed by free drug treatment. It is well established that the conjugation of special targeting moieties (sugar, folic acid, peptide, antibody etc.) to dendrimers can lead to preferential distribution of the cargo in the targeted tissue or cells (Yang et al., 2009). Researchers have shown that folic acid conjugated dendrimers

demonastrated a dramatic enhancement of binding avidity with target tumor cells that overexpress folic acid receptors (Quintana et al., 2002). In several studies folic acid conjugated PAMAM dendrimers were synthesized and further conjugated to anticancer drug methotrexate or paclitaxel. These drug conjugated dendrimers were shown to deliver the drug preferentially in KB cells (overexpressing folic acid receptors) in a targeted manner (Kono et al., 1999; Majoros et al., 2006). Shukla et al. (2005) conjugated a double cyclized RGD (RGD-4C) peptide to partially acetylated G5-PAMAM dendrimer and used for the targeting of tumor neovasculature via uniquely expressed integrins in human umbilical vein endothelial cells (HUVEC). Several research groups have explored monoclonal antibody conjugation to dendrimers for specific targeting of tumor cells that overexpress certain antigens. Anti-prostate specific membrane antigen (PSMA), J591, conjugated G5-PAMAM dendrimer was found to specifically bind to PMSA-positive LNCaP.FGC cells but not to PMSA-negative PC-3 cells (Patri et al., 2004; Thomas et al., 2004). A similar type of study showed that dendrimer conjugated to human growth factor receptor-2 (HER-2) monoclonal antibody (often overexpressed in breast and ovarian cancer) targets HER-2 expressing tumors in animals (Shukla et al. 2006). Wu et al. (2006) achieved targeted delivery of methotrexate to epidermal growth factor receptor–positive brain tumors by means of cetuximab (IMC-C225) dendrimer bioconjugates.

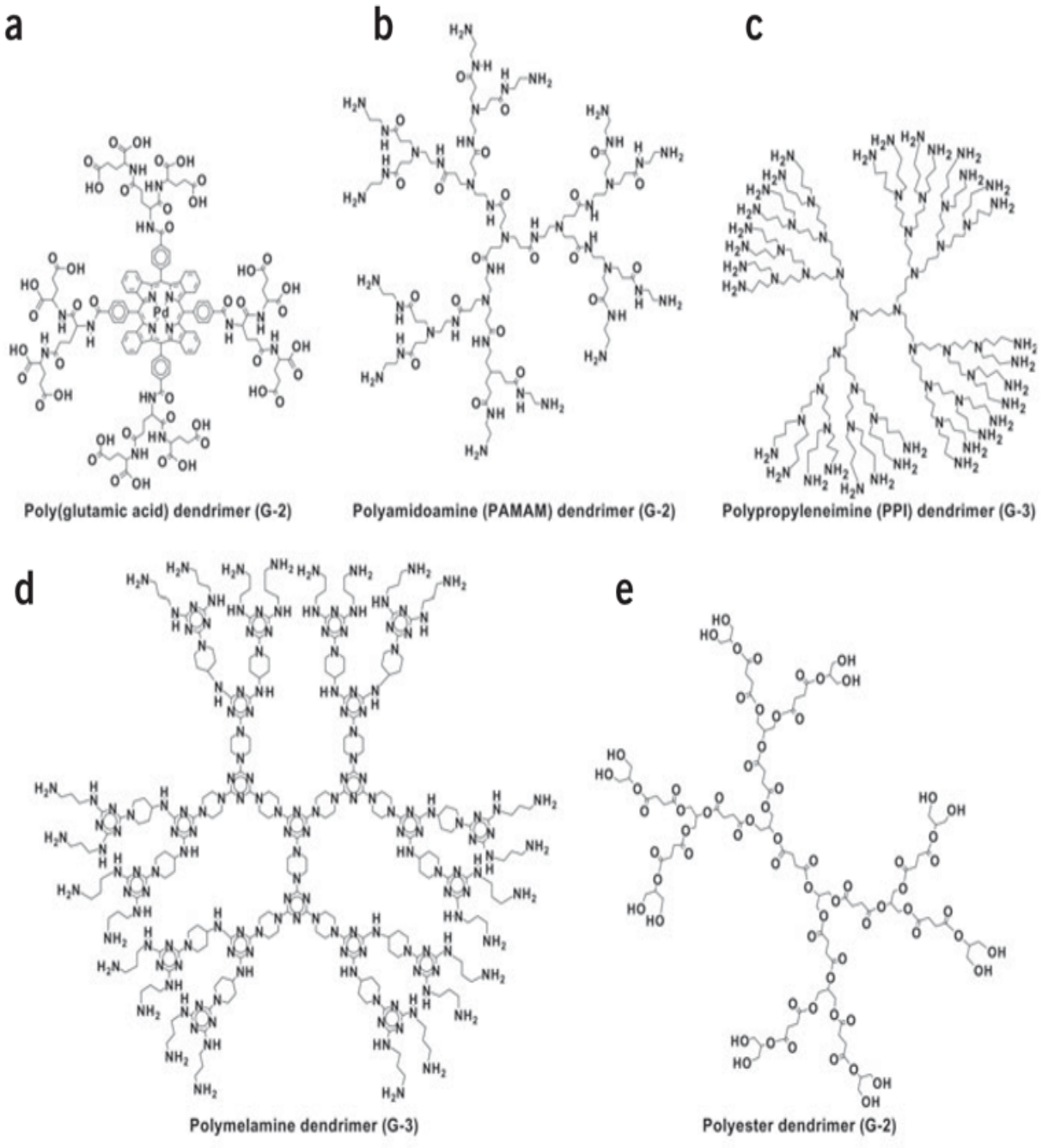

Figure 1.13: Structures of different dendrimers used for delivery of therapeutic molecules (Lee et al., 2005). The G value indicates the generation numbers of each dendrimer.

1.11.4 Polymersome

Polymersomes are bilayered vesicles of amphiphilic synthetic polymers which are similar to liposomes (Figure 1.14) (Discher and Eisenberg, 2002). These polymeric vesicles can accommodate lipophilic drugs across the bilayer membrane and water-soluble ones within the core. The formation of these vesicles is constrained to a very narrow hydrophilic/ hydrophobic ratio of the block copolymers and preparations are similar to that of liposomes. These vesicles are tougher and less permeable than phospholipid vesicles, and thus offer advantages for encapsulation and drug delivery. Polymersomes generally possess a greater PEG surface density and longer circulation times compared to PEGylated liposomes. Furthermore, the use of synthetic polymers enables designers to manipulate the characteristics of these vesicles. Initially these polymer vesicles are prepared from the diblock copolymers PEG-b-PBD (polybutadiene) and PEG-b-PEE (polyethylethylene), which have significant limitation for *in vivo* therapeutics as they are not biodegradable and likely not fully biocompatible. So, in an effort to create vesicles that degrade and release their contents the research investigations are now focused on the development of biodegradable polymersomes composed of PEGylated polyesters such as PEG-b-PLA, PEG-b-PDLLA and PEG-b-PCL (Meng et al., 2003). Polymersomes have been suggested as useful vehicles for the encapsulation of potent cancer drugs with narrow therapeutic indices and their high payload capacity further makes them ideal candidates for clinical use (Levine et al., 2008).

Ahmed et al (2006) combined two anticancer drugs with different solubility: doxorubicin (core) and taxol (membrane) in order to attain improved activity against solid tumors. A single systemic injection of the encapsulated dual drug combination cause two-fold higher cell death in tumors than free drug and show quantitatively similar increases in maximum

tolerated dose and drug accumulation within the tumors—suggesting promise for multi-drug delivery. To date most of the investigations about polymersomes have been focused on block copolymers although previously Lee and Yang et al (2006) and currently Zhengh et al (2009) showed that these nanovesicles can also be prepared from graft copolymers. They synthesized graft copolymers containing methoxy-poly(ethylene glycol) and ethyl-*p*-aminobenzoate side groups (PEG/EAB–PPPs) to fabricate biodegradable polymersomes for water-soluble anti-cancer drug delivery (Zheng et al., 2009). Recently, much effort has been directed to the development of intelligent polymersomes that respond to internal or external stimuli, in particular, pH, temperature, redox potential, light, magnetic field, and ultrasound either reversibly or nonreversibly. Stimuli-sensitive polymersomes have emerged as novel programmable delivery systems in which the release of the encapsulated contents can be readily modulated by the stimulus which may result in significantly enhanced therapeutic efficacy and minimized possible side effects (Meng et al., 2009). Initial successes in cancer treatment as well as a broad spectrum of functionality suggest this synthetic nanocarrier system offer a rather generic approach for drug delivery.

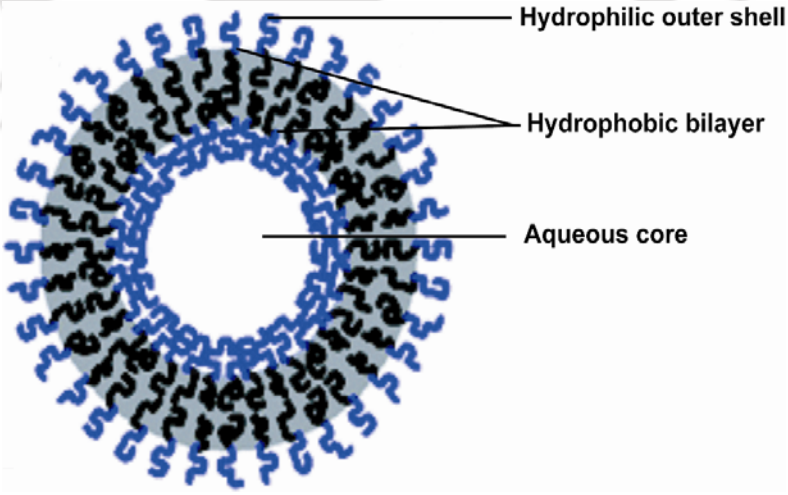

Figure 1.14: Polymersome – liposome like vesicles made with amphiphilic polymers.

1.12 Curcumin

1.12.1 Source, Molecular structure and Physicochemical Properties

Curcumin is the active ingredient of dietary spice turmeric (*Curcuma longa*). It is a polyphenolic compound isolated from rhizome of the plant. It was first purified in 1815, obtained in crystalline form in 1870 and ultimately identified as 1,6-heptadiene-3,5-dione-1,7-bis(4-hydroxy-3-methoxyphenyl)-(1E,6E) or diferuloylmethane. Lampe and Milobedeska (1913) confirmed and synthesized the feruloylmethane skeleton of curcumin. Curcumin is a yellow-orange powder with molecular formula of $C_{21}H_{20}O_6$, molecular weight of 368.38 Da and a melting point of 183 °C. It exhibits poor solubility in water but soluble in common organic solvents such as ethanol, methanol, acetone, dimethylsulfoxide (DMSO) and chloroform. It possesses three protons that are ionizable in water, the enolic proton with a pKa of approximately 8.5 and two phenolic protons with pKa of 10 to 10.5 (Shen and Ji, 2007). Curcumin exhibits keto-enol tautomerism having a predominant keto form in acidic and neytral solutions and enol form in alkaline solution (Figure 1.15). It is stable at acidic pH but unstable at neutral and basic pH, under which it get degraded to ferulic acid and feruloylmethane (Wang et al., 1997). The improved stability of curcumin at acidic pH condition was attributed to its conjugated diene structure. Spectrophotometrically, the maximum absorption (λ_{max}) of curcumin occurs in the range of 415 nm to 430 nm. It was found that nature of the solvent affects the absorption spectrum of curcumin only slightly, produces a small red shift on going from toluene to more polar solvents (Chignell et al., 1994). Curcumin also possess inherent fluorescence properties which strongly dependent on the environment. The fluorescence intensity and position of the peak maxima (λ_{max}), both were largely determined by the polarity of the solvent. In more nonpolar solvent the fluorescence intensity increased and the peak maxima (λ_{max}) showed a large blue shift

(Chignell et al., 1994; Khopde et al., 2000). A stokes shift of more than 100 nm was observed when curcumin was transferred from highly polar DMSO (λ_{max} 549 nm) to nonpolar cyclohexane (λ_{max} 446 nm) (Khopde et al., 2000).

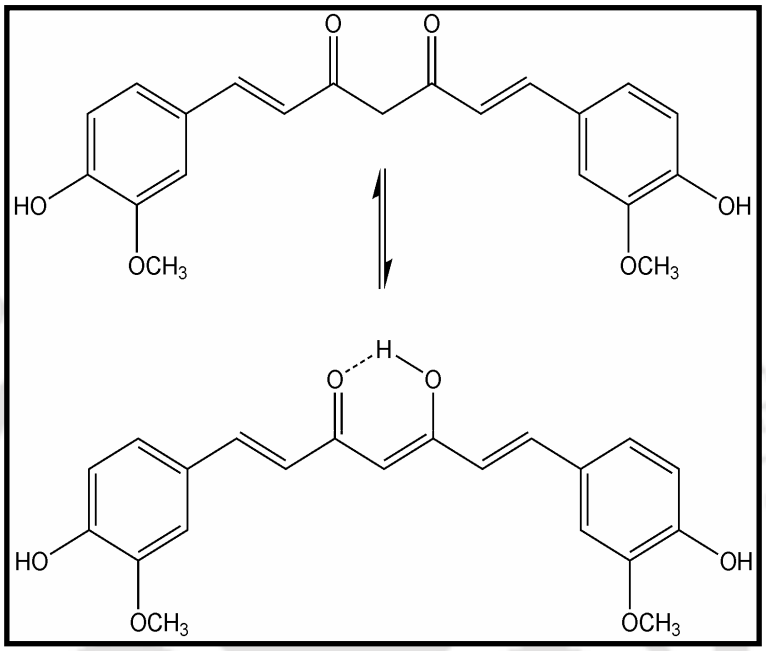

Figure 1.15: Chemical structure of curcumin showing keto-enol tautomerism.

1.12.2 Therapeutic potential of curcumin

Turmeric is widely consumed in India as a dietary spice but it has been also used for cenuries in traditional Indian folk medicine for the treatment of various illnesses such as biliary disorders, cough, hepatic disorders, rheumatism, sinusitis, anorexia etc. (Jain et al., 1991). Modern scientific research has proved that the most active molecule in turmeric which is responsible for the therapeutics is curcumin. Numerous studies indicated that curcumin has antioxidant, anti-inflammatory properties and bactericidal, fungicidal activity. It has wound healing capacity as punch wounds in curcumin treated animals healed faster than untreated animals (Sidhu et al., 1998). Curcumin's uses are well documented for treatment of various respiratory conditions e.g. asthama, bronchial hyperactivity and allergy

(Goel et al., 2008). Dietary curcumin suppressed the progression of experimentally induced diabetes in albino rat by reducing the blood sugar and hemoglobin levels (Babu and Srinivasan, 1995). Deodhar et al (1980) reported that rheumatoid arthritis patients treated with curcumin showed significant improvements in morning stiffness, walking time and joint swelling. Curcumin was also found to be a potent and selective inhibitor of HIV-1 LTR directed gene expressions and a modest inhibitor of HIV-1 and HIV-2 proteases (Sui et al., 1993). It was also found that curcumin reduced oxidative damage and amyloid pathology in an Alzeimer transgenic mouse model (Lim et al., 2001). The low dose (160 ppm) of curcumin was able to inhibit the formation of insoluble beta amyloid by 43 to 50%. In another study, Egan et al (2004) showed that oral administration of dietary curcumin corrects the cystic fibosis defects in mice bearing mutated CFTR gene. So, curcumin posses multiple medicinal values and offers potential benefits in several chronic illnesses including cardiovascular, neurodegenerative, pulmonary and autoimmune diseases (Aggarwal and Harikumar, 2009). But in this thesis our objective was to utilize curcumin as a potent chemotherapeutic drug. The most compelling and key rationale for the therapeutic use of curcumin is its extremely superior safety profile. No toxicity with curcumin was found in animal and human studies even at very high doses (Shankar et al., 1980; Lao et al., 2006).

1.12.3 Potential as a chemotherapeutic drug

Numerous research teams provided evidence that curcumin has chemopreventive and chemotherapeutic effects. Curcumin blocks the initiation of cancer by preventing carcinogen activation and also act as a suppressing agent to inhibit the proliferation of malignant cells during promotion and progression of cancer. The ability of curcumin to induce apoptosis in cancer cells without cytotoxic effects on healthy cells and its antiangiogenesis properties

makes it as a potent candidate as chemotherapeutic drug. In addition to a role as a chemopreventive and chemotherapeutic agent, curcumin also function as a chemosensitizer, enhancing the activity of other anti-neoplastic agents and radiosensitizer, enhancing the activity of radiation therapy. Evidences from research suggests that curcumin exerts its chemopreventive and chemotherapeutic activity by interacting with diverse range of molecular targets inside the cells such as transcription factors, growth factors and their receptors, cytokines, enzymes and genes regulating cell proliferation and apoptosis (Reuter et al., 2008).

1.12.4 *In vitro* studies against cancer

Curcumin has been shown to inhibit the proliferation of an extremely wide array of cancer cell types in vitro. This includes cells from cancers of the bladder, breast, lung, pancreas, prostate, cervix, head and neck, ovary, kidney, brain, osteosarcoma, leukemia and melanoma (Aggarwal et al., 2003). The suppression of cell proliferation by curcumin usually occurs through its effects on the cell cycle. Depending on the cell type, the inhibition of cell proliferation at different phases of the cell cycle has been reported. Curcumin also inhibits expression of growth and metastases promoting oncogenes and act as a chemopreventative agent. Several studies have shown that curcumin downregulates the expression of NF-κB, which is a nuclear transcription factor required for the expression of genes involved in cell proliferation, cell invasion, metastasis, angiogenesis and plays crucial role in signal transduction pathways of several cancers (Siebenlist et al., 1994). Curcumin also modulates the expression of NF-κB regulated gene products such as cyclooxygenase-2 (COX-2), cyclin D1, adhesion molecules, MMPs, inducible nitric oxide synthase, Bcl-2 and Bcl-XL (Shishodia et al., 2005). It is a potent inhibitor of various other transcription factors such as

activated protein-1 (AP-1), signal transducer and activator of transcription (STAT) proteins, peroxisome proliferation activated receptor-γ (PPAR-γ) and β-carenin (Shishodia et a., 2007) which regulate the expression of genes that contribute to tumorigenesis. Curcumin has been found to exert growth inhibitory effects on cancer cells by inhibiting the expression of some key signaling molecules such as, tumor necrosis factor-α (TNF-α), interlukin 1β (IL-1β), interlukin 6 (IL-6) etc. Curcumin's anticancer effects are also mediated through its ability to inhibit the activity of several protein kinases which are activated in human cancers including phosphorylase kinase, protein kinase C (PKC). Protamine kinase (cPK), autophosphorylation activated protein kinase (AK), pp60c-src tyrosine kinase (Shishodia et al., 2007). Woo et al. (2003) suggested that the induction of Caki (human kidney carcinoma cells) programmed cell death is activated by Akt dephosphorylation, Bcl-2, Bcl-XL and inhibitor of apoptosis (IAP) protein inhibition, as well as cytochrome *c* release and caspase 3 activation. Recently, Aoki et al (2007) showed that curcumin induces apoptosis in acute T cell leukemias by inhibiting the phosphatidylinositol 3 kinase/ AKT pathways and to induce G2/M arrest and autophagic cell death in malignant glioma cells by inhibition of Akt and Erk signaling pathways. Earlier Pan et al (2001) showed that induction of apoptosis in human leukemia HL-60 cells by curcumin is mediated through cytochrome *c* release and activation of caspases whereas Bush et al (2001) described that curcumin induces apoptosis in human melanoma cells through a Fas receptor/caspase-8 pathway independent of p53. Curcumin has been shown to induce apoptosis in human prostate cancer (PC-3) and colon cancer (HT-29) cell lines through activation of p53 and simultaneous downregulation of MDM2 oncogene expression and on the other hand, apoptosis in human multidrug-resistant Jurkat cells is described to be caspase 3 independent (Piwocka et al., 2002). In case of hepatocellular cancer cells, curcumin appears to alter the metastases potential of tumor cells

by inhibiting the activity of matrix metalloproteinase-9 (MMP-9) and MMP-2 (Mitra et al., 2006). Curcumin can also suppress tumor cell growth by effectively regulating the activity of several enzymes (e.g. hemoygenase-1, Ras protein etc.) that control tumor cell growth and proliferation (McNally et al., 2007).

1.12.5 *In vivo* studies against cancer

Besides the extensive in vitro demonstrations of curcumin's antiproliferative effects, numerous other studies have evaluated its efficacy in various animal models in vivo. The first animal studies of curcumin's antitumor effects – performed with ascitic lymphoma cells in mice (Kuttan et al., 1985). More recently, several animal studies have shown that curcumin has a dose-dependent chemopreventive effect in skin, mammary gland, stomach, oesophagus, intestine, colon, lung, liver, duodenal, esophageal and oral carcinogenesis (Maheswari et al. 2006). Curcumin significantly suppressed azoxymethane induced colonic preneoplastic lesions, tumor incidence and tumor multiplicity in rats. Other studies demonstrated that curcumin inhibits cancer development in rat stomach initiated by N-methyl-N'-nitro-N-nitrosoguanisine (MNNG) and reduces the multiplicity of esophageal tumors. In studies with mice, curcumin was able to inhibit skin tumor formation and promotion induced by benz[a]pyrene, 7,12-dimethylbenz[a]anthracene (DMBA) and promoted by phorbol esters, 12-*O*-tetradecanoylphorbol-13-acetate (TPA) (Singh et al. 1998; Azuine and Bhide, 1992; Huang et al. 1988). Curcumin also inhibits the mammary tumor-initiating activity of DMBA, in vivo formation of mammary DMBA–DNA adducts in female rats and exert chemopreventive activity when administered during the promotion/progression stage of colon carcinogenesis. Furthermore, one group has studied not only curcumin's chemopreventive effects but also its effects on the initiation or post-

initiation phase of *N*-nitrosomethylbenzylamine (NMBA)-induced esophageal carcinogenesis in male F344 rats. Using a slightly different approach, another group investigated curcumin's ability to prevent tumors in C57BL/6J-Min/+ (Min/+) mice that bear a germline mutation in the APC gene and spontaneously develop numerous intestinal adenomas by 15 weeks of age. At a dietary level of 0.15 % curcumin decreased tumor formation in Min/+ mice by 63% and detailed examination of intestinal tissues from the treated animals showed that tumor prevention was associated with decreased expression of the oncoprotein β-catenin and increased apoptosis of enterocytes (Mahmoud et al., 2000). In another study, the effects of curcumin administered at a daily dose of 100 mg/kg were investigated in an animal (Wistar rat) model of *N*-nitrosodiethylamine (DENA)-initiated and phenobarbital (PB)-induced hepatocarcinogenesis and investigators found that this daily dose of the drug prevented reduction of defensive hepatic glutathione antioxidant activity, decreased lipid peroxidation and minimized the histological alterations induced by DENA/PB (Sreepriya et al., 2006). In a study in rodents, curcumin was able to inhibit the development of *N*-methyl-*N*′-nitro-*N*-nitrosoguanidine (MNNG)-induced stomach cancer, an effect that may be mediated in part by an ability to suppress the proliferation of *Helicobacter pylori* (the major pathogen in human gastric cancer) (Mahady et al., 2002). In addition to its preventive activity against chemically induced tumors curcumin has been shown to be an effective cytotoxic agent against the UMUC human bladder tumor cell line and MBT2 mouse bladder tumor cell line and also effectively inhibited implantation and growth of bladder tumor cells in C3H mice (Sindhwani et al., 2001). Bosquests et al. showed that systemic administration of curcumin (20 µg/kg body weight) for 6 consecutive days inhibited tumor growth by 31% to rats bearing the AH-130 ascites hepatoma (Bosquets et al., 2001). Other studies in vivo have investigated the effects of curcumin on tumor

angiogenesis and the biomarkers COX-2 and VEGF in hepatocellular carcinoma cells implanted in nude mice (Yoysungnoen et al., 2006). Meanwhile, researchers have shown that curcumin can suppress the growth of head and neck carcinoma, modulate the growth of prostate cancer in rodents, and inhibit the growth of human pancreatic cancer in nude mice, partly by suppressing angiogenesis and inducing apoptosis (Dorai et al., 2001; LoTempio et al., 2005).

1.12.6 Clinical trials of curcumin against cancer

The positive results obtained from preclinical studies motivated the researchers for clinical trials of curcumin against human cancers. Considering the promising results obtained from different clinical trials (Table1.4) it is hoped that curcumin will soon be approved for cancer treatment.

Table 1.4: Clinical trials of curcumin against several human cancers (Aggarwal et al., 2003; Goel et al., 2008; Hatcher et al., 2008).

Type of Cancer	Study Type/ Design	No. of Patients	Starting Date/ Status	Trial Site
Colon cancer	Phase-I, randomized	24	Completed	University of Michigan, Ann Arbor, USA
Colon cancer	Phase-III, randomized	100	March 2006	Tel-Aviv Sourasky Medical Center, Tel-Aviv, Israel
Colorectal cancer, ACF	Phase-I, randomized	-	Suspended	Rockefeller University Hospital, New York, USA
Colorectal cancer, ACF	Phase-II, non-randomized	48	September 2006	University of Illinois, Chicago, USA
Pancreatic cancer	Phase-II, non-randomized	45	July 2004	Rambam Medcial Center, Haifa, Israel

Pancreatic cancer	Phase-II, non-randomized	50	November 2004	M.D. Anderson Cancer Center, Houston, USA
Pancreatic cancer	Phase II (8 g/day)	40	August 2007	Kyoto University, Japan
Cervical cancer (Stage IIb, IIIb)	Phase II/III DBRPC (2 g/day, bid, 1 year)	100	-	AIIMS, Delhi, India
HNSCC	Phase II/III DBRPC (3.6 g/day, bid)	300	-	AIIMS, Delhi, India
Advanced HNSCC	Phase II (1–8 g/day; 56 days)	40	-	Himalyan Institute of Medical Sciences, India
Gall bladder cancer	Phase II (2–8 g/day)	60	-	BHU, India
Oral leukoplakia	Phase II (curcumin gel, 3×/day, 6 month)	100	-	Regional Cancer Center, India
Oral premalignant lesions	Phase II/III DBRPC (4 g/day, bid × 28 days)	90	-	Tata Memorial Cancer Center, India
Oral premalignant lesions	Phase II/III DBRPC (3.6 g/day, bid)	96	November 2006	Amrita Institute, Kochi, India

***** ACF **-** Aberrant crypt foci; HNSCC – Head and neck squamus cell carcinoma

1.12.7 Problems with clinical development of curcumin

Curcumin have shown immense potential as a cancer chemopreventive agent but its clinical development has been quite slow so far. This was because the pharmacokinetic studies of curcumin indicated in general a low bioavailability following oral application. Ravindranath and Chandrasekhara (1980) showed that after oral administration of 400 mg of curcumin to

rats, no curcumin was found in heart blood, whereas, a trace amount (less than 5 μg/ml) was found in portal blood. In a clinical study, Shoba et al. (1998) showed that after oral administration of 2 g kg^{-1} of curcumin to rats a maximum serum concentration of 1.35 ± 0.23 μg ml^{-1} was observed at time 0.83 h, whereas in humans the same dose of curcumin resulted in extremely low (0.006 ± 0.005 μg ml^{-1} at 1 h) serum levels. This low systemic bioavailability of curcumin is mainly attributed to its poor water solubility and partly to its metabolism. It was found that after oral dosing curcumin undergoes extensive metabolic conjugation and reduction in liver and intestinal tract (Pan et al., 1999; Ireson et al., 2001). The major metabolites in suspensions of human or rat hepatocytes were identified as hexahydrocurcumin and hexahydrocurcuminol. The major products of curcumin biotransformation identified in rat plasma were curcumin glucuronide and curcumin sulfate, whereas hexahydrocurcumin, hexahydrocurcuminol, and hexahydrocurcumin glucuronide were present in small amounts (Figure 1.16). Further, it was confirmed that curcumin was sulfated by human phenol sulfotransferase isoenzymes SULT1A1 and SULT1A3 whereas; equine alcohol dehydrogenase catalyzed the reduction of curcumin to hexahydrocurcumin (Ireson et al., 2002). Despite the fact that curcumin gets rapidly metabolized in intestinal tract the major concern with this compound is its poor solubility in aqueous solution. Low solubility in physiological fluid leads to low absorption of curcumin in gut and thus its bioavailability become less. Solubility is also a concern for intravenous administration as formation of drug aggregate can cause embolism of blood capillary and high localized concentration at the site of deposition.

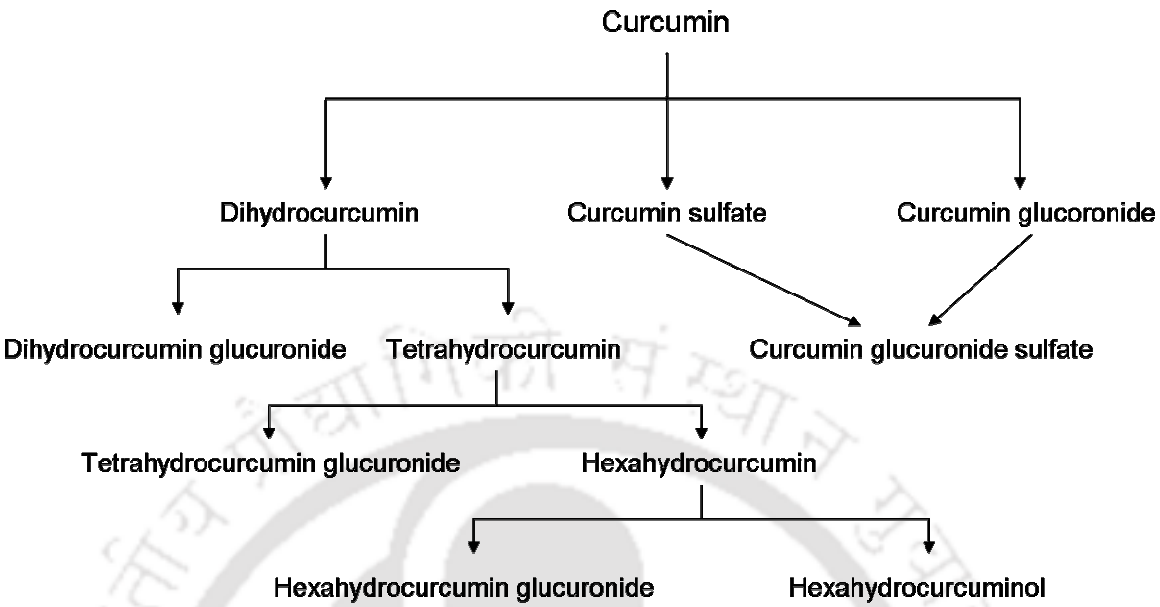

Figure 1.16: Curcumin metabolism products in liver and intestine after oral administration.

1.12.8 DDS for curcumin delivery

This low oral bioavailability of curcumin inevitably limited the application of this agent. Development of new formulations or analogues of curcumin with better bioavailability, as well as novel routes of administration, is critical for future development of curcumin. It requires a suitable carrier or delivery system to overcome the problems associated with it without compromising its activity. Although there has been only limited studies concerning about making a formulation or DDS for curcumin. The first delivery system of curcumin was developed by Kumar and Lewis et al. (2002) in which they formulated curcumin in biodegradable microspheres of chitosan and BSA. The microspheres were prepared by emulsion-solvent evaporation method coupled with chemical cross-linking of the natural polymers and curcumin was encapsulated into these carriers upto an extent of 79.49 and 39.66% respectively with albumin and chitosan. In vitro release studies indicated a biphasic

drug-release pattern, characterized by a typical burst effect followed by a slow release. It was evident from this study that these polymeric microspheres could be successfully employed as a prolonged-release drug delivery system for better therapeutic management of inflammation as compared with oral or subcutaneous administration of curcumin (Li et al., 2005). An intravenous formulation was developed by encapsulating curcumin in liposomes. This liposomal formulation has showed antiproliferative and proapoptotic effects equal to or greater than that of free curcumin against human pancreatic cancer cell lines *in vitro* and *in vivo*. The continuation of this study recently showed that the same liposomal formulation of curcumin is able to suppress the growth of head and neck squamus cell carcinoma *in vitro*. Nude mice xenograft tumors were suppressed after 3.5 weeks of treatment with i.v. liposomal curcumin, and there was no demonstrable toxicity of liposomal curcumin upon autopsy (Wang et al., 2008). In between, Bisht et al. (2007) prepared "nanocurcumin", a polymeric nanoparticle formulation of curcumin. In this report they have prepared ~50 nm nanoparticles utilizing the micellar aggregates of cross-linked and random copolymers of N-isopropylacrylamide (NIPAAM) withN-vinyl-2-pyrolidone (VP) and poly(ethylene glycol) monoacrylate (PEG-A). Nanocurcumin demonstrated comparable *in vitro* therapeutic efficacy against a panel of human pancreatic cancer cell lines and found that nanocurcumin's mechanisms of action on cancer cells is similar to that of free curcumin. Salamaso et al (2007) prepared a new cyclodextrin based carrier for active targeting of curcumin. The PEG and folic acid functionalized cyclodextrin was shown to increase the solubility and stability of the curcumin by forming inclusion complex. The in vitro studies also demonstrated that the carrier possesses potential selectivity for the folate receptor over expressing human nasopharyngeal tumor KB cell line. Ma et al (2008) used PEO-PCL block copolymer micelle for solubilization and delivery of curcumin. They prepared curcumin

loaded micelles by co-solvent evaporation technique and theses micelle encapsulated curcumin was stable in physiological solution and retained its cytotoxic activity in a mouse melanoma cell line (B16-F10) and human mantle cell lymphoma cell lines SP-53 and JeKo-1. In another study, a stable intravenous formulation of curcumin was prepared using lipid based nanoparticles. Curcumin was incorporated in nanosized lipid vesicles and nanospheres. Intravenous injection of these formulations in rats showed that, these systems are effective for delivery of the drug to tissue macrophages, specifically bone marrow and splenic macrophages. So this nanoformulation of curcumin could be a therapeutically beneficial for with oxidative injury and inflammation (Sou et al., 2008). In the most recent finding it was found that encapsulation of curcumin in PLGA nanoparticles improved its oral bioavailability by at least 9-fold compared to curcumin administered with piperine as absorption enhancer (Shaikh et al., 2009).

CHAPTER 1

Introduction
&
Review of Literature

CHAPTER 2

Synthetic mPEG-PA Polymeric Nanocarrier for Curcumin Delivery to Cancer Cells

CHAPTER 3

Formulation of Curcumin in Pluronic Nanocarriers for Cancer Chemotherapy

CHAPTER 4

Natural Food Protein Based Nanoparticle for Curcumin Delivery to Cancer Cells

Summary
&
Future Directions

Bibliography

Publications

Other Publications

2.1 Introduction

Interest in nanocarriers for cancer chemotherapy is growing (Peer et al., 2007). Polymeric micelles has gained attention as nanocarriers (Torchilin, 2007; Jones and Leroux, 1999; Kwon, 2003) due to several advantages like, i) their low toxicity, ii) high stability iii) their small size (< 200 nm) is ideal for passive targeting of solid tumor tissue sites by enhanced permeation and retention (EPR) effect (Maeda et al., 2000), iv) they can be prepared in large quantities easily and reproducibly. Several drugs formulated in polymeric micelles are in clinical trial development for the treatment of various cancers (Kim et al., 2004; Matsumura, 2004). Studies on polymeric micelles prepared from block copolymers have been carried out by many groups (Kataoka et al, 2001; Gaucher et al, 2005). But synthesis of block copolymers by polymerization reaction is a multistep and tedious process that requires expertise. Recently many studies have been conducted on self-aggregation behavior of hydrophobically modified water-soluble polymers, which can self-assemble to form micelle in aqueous phase (Torchilin, 2001; Lukyanov and Torchilin, 2004). Studies have shown that polymeric amphiphile consisting of hydrophilic PEG and hydrophobic low molecular weight natural components such as diacyllipid, fatty acid, and bile salts can form self-aggregated micelles and they can be used for the delivery of hydrophobic drugs (Kim et al., 2000; Kim et al., 2001).

In this chapter, we described a simple method of synthesis and characterization of a novel polymeric amphiphile based on mPEG as hydrophilic and palmitate as hydrophobic segment. PEG is a well-known biocompatible polymer with antifouling property and palmitate is a naturally occurring fatty acid in animals. The nonionic hydrophilic PEG shell can suppress opsonin adsorption and subsequent clearance by the mononuclear phagocyte system thereby prolonging circulation time and influences the pharmacokinetics and

biodistribution of the drug delivery system (Owens and Peppas, 2006; Vonarbourg et al., 2006) whereas the hydrophobic core of palmitate can solubilize curcumin. The conjugate was synthesized in a single step reaction. The PEG chain was conjugated with palmitate through an ester linkage that can be degraded inside the cells. The mPEG-PA conjugate forms self-assembled micelle nanoparticle with hydrophobic anticancer drug curcumin in the core. We also demonstrate enzyme-triggered release of drug by hydrolyzing the ester linkage of the amphiphilic conjugate by lipase.

2.2 Materials and Methods

2.2.1 Materials

mPEG (Mw 5000) and palmitoyl chloride was purchased from Fluka (Bangalore, India) and Aldrich (Bangalore, India) respectively. Curcumin was from Himedia laboratories (Mumbai, India). Porcine pancreatic lipase and pyrene was from Sigma (Bangalore, India). All the solvents used in the study were of analytical grade and obtained from Merck (Mumbai, India).

Human cervical cancer cell line (HeLa) was obtained from National Centre for Cell Science (Pune, India). Cells were maintained in EMEM containing 2 mM L-glutamine, 1.5 g/L sodium bicarbonate, 0.1 mM non essential amino acids and 1.0 mM sodium pyruvate supplemented with 10% FBS and 1% antibiotic antimycotic solution (1000 U/ml penicillin G, 10 mg/ml streptomycin sulfate, 5mg/ml gentamycin and 25 µg/ml amphotericin B). Cells were cultured at 37°C in a humidified atmosphere supplied with 5% CO_2.

2.2.2 Synthesis of mPEG-PA conjugate

The synthesis of mPEG-PA conjugate was carried out by reacting mPEG with palmitoyl chloride. mPEG (1mM) was dissolved in toluene and mixed with triethylamine (1mM). A

solution of palmitoyl chloride (1.1 mM) in toluene was added drop wise and stirred continuously for 3 h at 60ºC. The solution was then filtered through filter paper (Whatman, grade 1) to remove the precipitated triethylamine hydrochloride salt and clear filtrate was collected in a conical flask. The mPEG-PA conjugate was then precipitated from filtrate solution by adding cold diethyl ether. The precipitate was collected by filtration and dried under vacuum.

2.2.3 Characterization of mPEG-PA conjugate

The purified conjugate was characterized by nuclear magnetic resonance (NMR) spectroscopy and Fourier transformed infrared (FT-IR) spectroscopy. For NMR analysis, the dried conjugate was dissolved in $CDCl_3$ and the spectrum was recorded in ^1H NMR (Mercury Plus 400MHz, Varian). The FT-IR spectrum of the conjugate was recorded with a Spectrum One spectrophotometer (Perkin Elmer, USA). A 2% (w/w) mixture of dried conjugate and potassium bromide (KBr) was ground into a fine powder using an agate mortar, compressed into a disc, scanned at a resolution of 1 cm^{-1} over a frequency region of 450 to 4,000 cm^{-1} and the characteristic peaks of IR transmission spectra were recorded.

2.2.4 Measurement of critical micelle concentration (CMC) of mPEG-PA conjugate

The critical micelle concentration (CMC) of mPEG-PA was determined by using pyrene as a hydrophobic fluorescence probe. The CMC was determined based on the intensity of pyrene excitation spectra and shift of the spectra with increasing mPEG-PA concentrations. The pyrene solutions ($6X10^{-6}$ M) in acetone were added into the test tubes and evaporated to remove the solvent. Then, solutions of mPEG-PA micelles in PBS (0.01M, pH 7.4) were added to the above test tubes in concentrations ranging from 0.001 to 1 mg/ml, bringing the final concentration of pyrene to $6.0X10^{-7}$ M. The solutions were vortexed and kept overnight

at 37ºC to equilibrate pyrene with the micelles. Steady-state fluorescence excitation spectra (Fluoro Max-3, Jobin Yvon, Horiba, USA) of pyrene were recorded from 300 nm to 360 nm keeping emission wavelength fixed at 390 nm with slit width of 2.5 and 5.0 nm for excitation and emission respectively.

2.2.5 Encapsulation of curcumin in micellar nanoparticle

The encapsulation efficiency of curcumin was studied in different concentrations of mPEG-PA. Curcumin solution in methanol was added to the solution of mPEG-PA in chloroform to obtain different drug:polymer ratio ranging from 1:20 to 1:100. Methanol was evaporated under vacuum to produce a film consisting of mPEG-PA/curcumin mixture. Micelles were formed by extensive vortexing of the film in PBS. Nonencapsulated curcumin was separated by centrifugation of the micelle suspension at 5000 rpm (Sigma 4K-15 refrigerated centrifuge, India) for 10 min and quantified spectrophotometrically (Cary 100 BIO UV-VIS spectrophotometer, Varian, USA) at 425 nm. The entrapment efficiency was calculated by following equation:

$$\text{Encapsulation efficiency (\%)} = \frac{(\text{Total amount of curcumin - Free curcumin})}{\text{Total amount of curcumin}} \times 100$$

$$\text{Drug Loading (\%)} = \left(\frac{\text{amount of curcumin in nanocarrier}}{\text{amount of curcumin loaded nanocarrier}} \right) \text{X } 100$$

$$= \frac{\text{Curcumin}}{\text{Curcumin + mPEG-PA}} \text{ X } 100$$

2.2.6 Physical characterization of drug encapsulated micelle nanostructure

2.2.6.1 Dynamic light scattering (DLS)

Size distribution of empty and curcumin encapsulated mPEG-PA micelles (2.5 mg/ml in 0.01M PBS, pH 7.4) were analyzed by dynamic light scattering (Zetasizer NanoZS, Malvern Instruments, UK) using an argon laser beam at 633 nm and 90° scattering angle.

2.2.6.2 Atomic force microscopy (AFM)

The shape of the free micelle nanoparticles and drug loaded micelle nanoparticles was characterized by atomic force microscopy (Picoscan, Molecular Imaging, USA). A drop of micellar solution (2.5 mg/ml) was placed on freshly cleaved mica. After 1 min incubation the surface was gently rinsed with deionized water to remove unbound micelles. The dried nanoparticle sample was mounted on sample holder using double-sided adhesive tapes and scanned by the AFM maintained in a constant temperature and vibration free environment in non-contact mode.

2.2.6.3 UV-Visible and Fluorescence spectroscopy

The micelle-loaded curcumin was characterized by absorption and fluorescence spectra. UV-Visible spectra of aqueous solution of curcumin encapsulated in mPEG-PA micelles were recorded with Cary-100Bio spectrophotometer (Varian). The fluorescence emission spectra of curcumin in same micelle solutions were taken using excitation wavelength of 420 nm with FluoroMax-3 spectroflourimeter (Jobin Yvon, Horiba). The excitation and emission slit widths were 2 nm and 5 nm respectively and the scan rate was 1nm/sec.

2.2.7 *In vitro* stability of drug loaded micelle

100 mg of curcumin-loaded mPEG-PA was dispersed in 10 ml of physiological buffer (0.01M PBS, pH 7.4), simulated gastric fluid (0.2 g sodium chloride and 0.7 ml concentrated HCl in 100 ml water, pH 1.2) and simulated intestinal fluid (0.68 mg KH_2PO_4 and 7.7 ml of 0.2 M NaOH in 100 ml water, pH 6.8) separately and incubated at 37ºC under gentle agitation. Drug retention was studied at different time intervals ranging from 6 to 48 hours. The percentage of drug retained was determined with the following equation:

$$\text{Drug Retention (\%)} = \frac{(\text{Total curcumin encapsulated - Released curcumin})}{\text{Total curcumin encapsulated}} \times 100$$

2.2.8 Enzyme catalyzed degradation of micelle and *in vitro* drug release

To examine the degradation of micelle and site of action of enzyme, 50 mg of mPEG-PA was dissolved in 10 ml of 0.1 M PBS (pH 7.4) containing bovine pancreatic lipase (0.5 mg/ml) and kept at 37ºC. After 48 hr the precipitate was collected and washed several times with water and dried. Dried precipitate was recrystallized from chloroform and analyzed by ^{1}H NMR to confirm the cleavage site.

To estimate the drug release by enzyme catalyzed degradation of micelle, the lipase solution in PBS (0.01 M, pH 7.4) was added to the drug loaded micelle solution at a final concentration of 0.5 mg/ml and incubated at 37°C. Samples were collected at different time intervals ranging from 2 to 48 hours and release curcumin was estimated as described in section 2.2.5. The release was quantified as follows:

$$\text{Release (\%)} = \frac{\text{Released curcumin}}{\text{Total curcumin}} \times 100$$

To study the drug release by cellular enzymes, cell lysate was obtained from HeLa cells by mechanical lysis followed by centrifugation at 10000g for 10 min at 4°C. The supernatant containing intracellular enzymes was added to the drug loaded micelle solution and drug release was quantified as in section 2.2.5.

2.2.9 Cellular uptake and cytotoxicity studies

To visualize the cellular uptake of drug loaded micelle HeLa cells were grown in 35 mm culture plate up to 80% confluency. Cells were treated with 15 μM of free and micelle encapsulated curcumin. As curcumin is insoluble in aqueous solution the free curcumin was

dissolved with the aid of dimethyl sulfoxide (DMSO). The final concentration of DMSO in the culture medium was always < 1%. After 2 hour incubation at 37°C, cells were examined under confocal laser scanning microscope (LSM 510 Meta, Zeiss, Germany) for the intracellular curcumin fluorescence.

The cytotoxicity of empty mPEG-PA nanocariers, free curcumin and nanocarrier encapsulated curcumin was determined by methylthiazoletetrazolium dye (MTT) assay as described by Mosmann (1983). HeLa cells were seeded in 96-well cell culture plate at a density of 1×10^4 cells/well and grown for 24 hours before the assay. The cells were then exposed to a series of different concentrations of free and encapsulated curcumin (1 to 30 μM) for 48 hours. After incubation 100 μl of DMSO was added to each well and absorbance was measured at 570 nm using a microplate reader (Biorad Microplate Reader, Model 680, USA). The cell viability was expressed as a percentage compared to that of the control by following equation:

$$\text{Viability (\%)} = {}^{Nt}\!/_{Nc} \times 100$$

Where, *Nt* was the absorbance of the cells treated with free curcumin or curcumin loaded micelles and *Nc* was the absorbance of the untreated cells. Similarly, different concentrations of empty micelles were used to test the cytotoxicity of the nanocarrier.

2.3. Results

2.3.1 Synthesis of the conjugate

mPEG-PA conjugate was prepared in a single step reaction by reacting palmitoyl chloride with mPEG (Scheme 2.1). The synthesis of conjugate was confirmed by ^{1}H NMR and FT-IR spectra. ^{1}H NMR of the conjugate showed five signals at δ 0.83, 1.23, 2.18, 3.6 and 3.3 from the conjugate whereas the peak at 7.1 was due to $CDCl_3$ (Figure 2.1). The IR spectrum of mPEG-PA conjugate showed a sharp peak at 1734 cm^{-1} which was absent in the spectrum of unmodified mPEG (Figure 2.2).

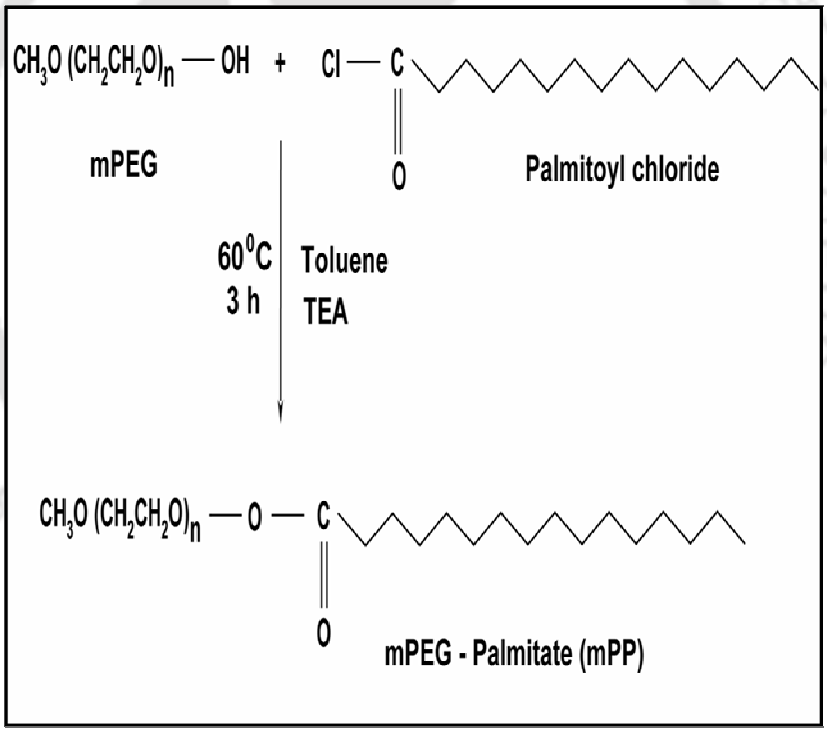

Scheme 2.1: Synthesis of methoxy poly(ethylene glycol) palmitate (mPEG-PA) conjugate. The hydrophilic mPEG was conjugated to hydrophobic palmitate through an ester linkage by reacting with palmitoyl chloride.

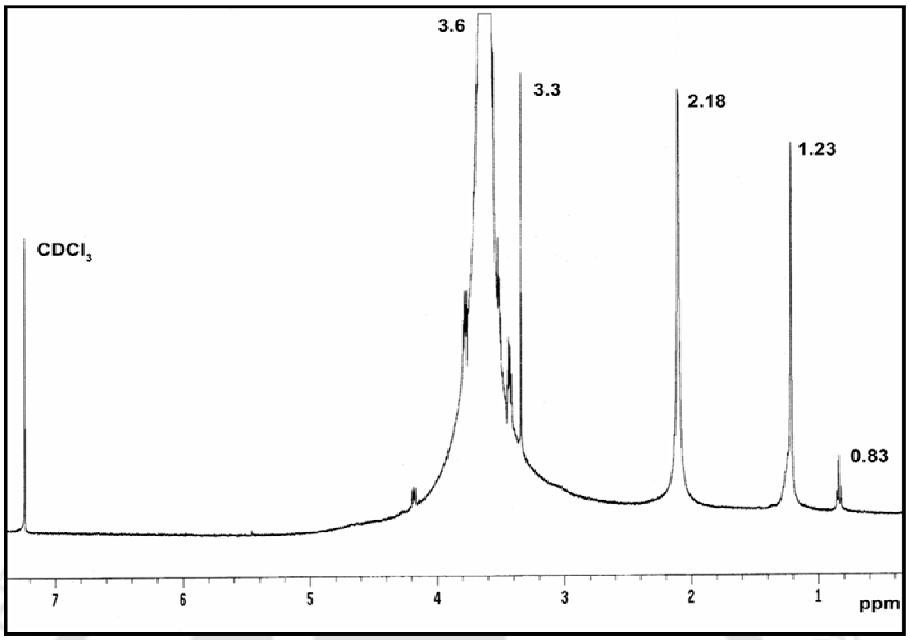

Figure 2.1: ^{1}H NMR spectrum of mPEG-PA in $CDCl_3$.

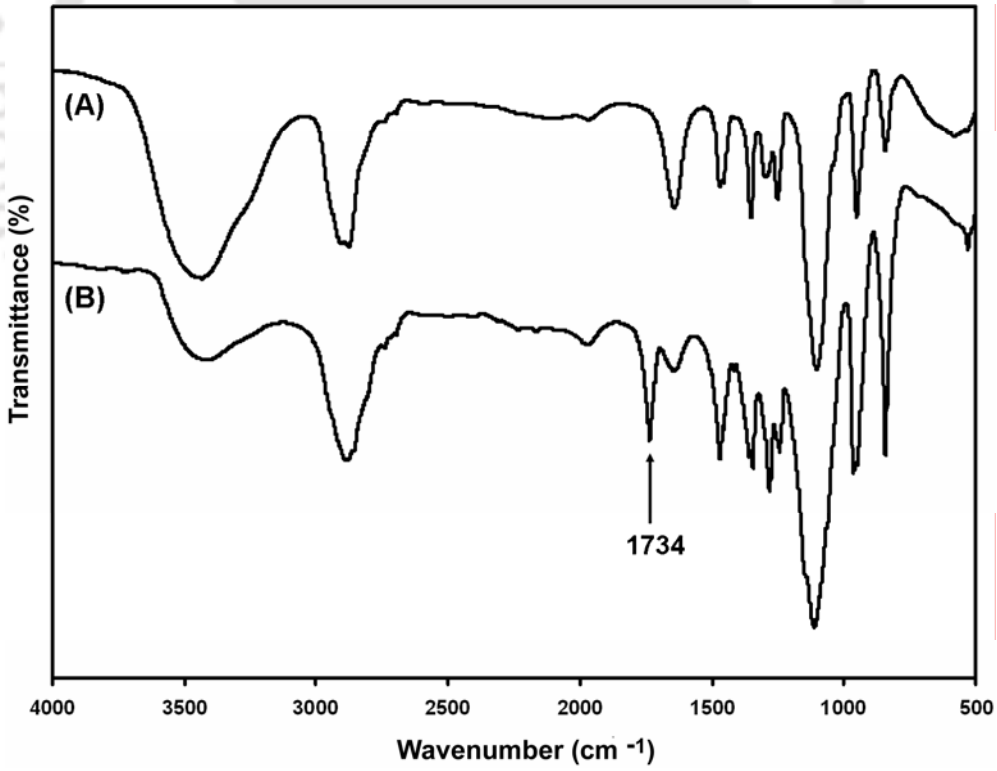

Figure 2.2: FT-IR spectrum of mPEG (A) and mPEG-PA (B) conjugate. The peak at 1734 cm^{-1} in the spectrum of mPEG-PA confirms the presence of ester linkage in the conjugate.

2.3.2 Self-aggregation of mPEG-PA and CMC

The formation of self-aggregates of mPEG-PA in aqueous solution was studied by fluorescence spectroscopy where pyrene was used as fluorescent probe. The fluorescence intensity of the pyrene increased with the increase in the concentration of mPEG-PA and its excitation peak shifted from 332 to 335 nm (Figure 2.3). The CMC of micelle was determined from the curve showing relationship between changes in intensity ($I_{335/332}$) of pyrene with the log (concentration) of mPEG-PA (Figure 2.4). The CMC was calculated from the crossover point and its value was found to be 0.12 g/L. However, in the control where only mPEG was used no appreciable change in pyrene fluorescent intensity was observed over all the concentrations.

2.3.3 Physical characterization of mPEG-PA micelle nanostructures

Size and morphology of the self-assembled micelle nanoparticles of mPEG-PA was determined by light scattering (DLS) measurements and AFM. The mean diameter of the blank micelles and drug loaded micelles were found to be 41.43 nm and 47.36 nm respectively, with a narrow size distribution in DLS experiment (Figure 2.5 A1, A2). The AFM image taken at non-contact mode showed that the micelles were spherical in shape before and after drug loading (Figure 2.5 B, C). The micelles were spherical in shape and the size observed in the AFM was in good agreement with that measured by dynamic light scattering (DLS).

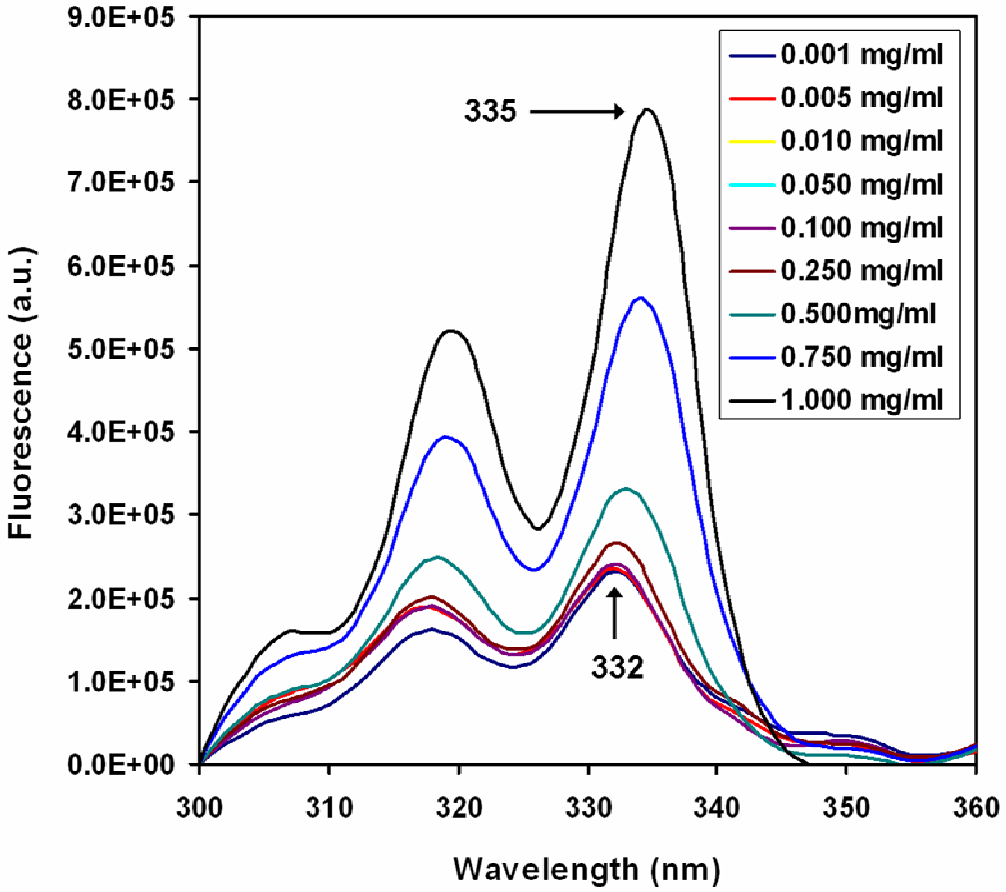

Figure 2.3: Fluorescence excitation spectra of pyrene ($6x10^{-7}$M) in mPEG-PA solution (0.01M PBS, pH 7.4) with concentrations of: (a) 0.001, (b) 0.005, (c) 0.01, (d) 0.05, (e) 0.1, (f) 0.25, (g) 0.5, (h) 0.75 and (i) 1.0 mg/ml.

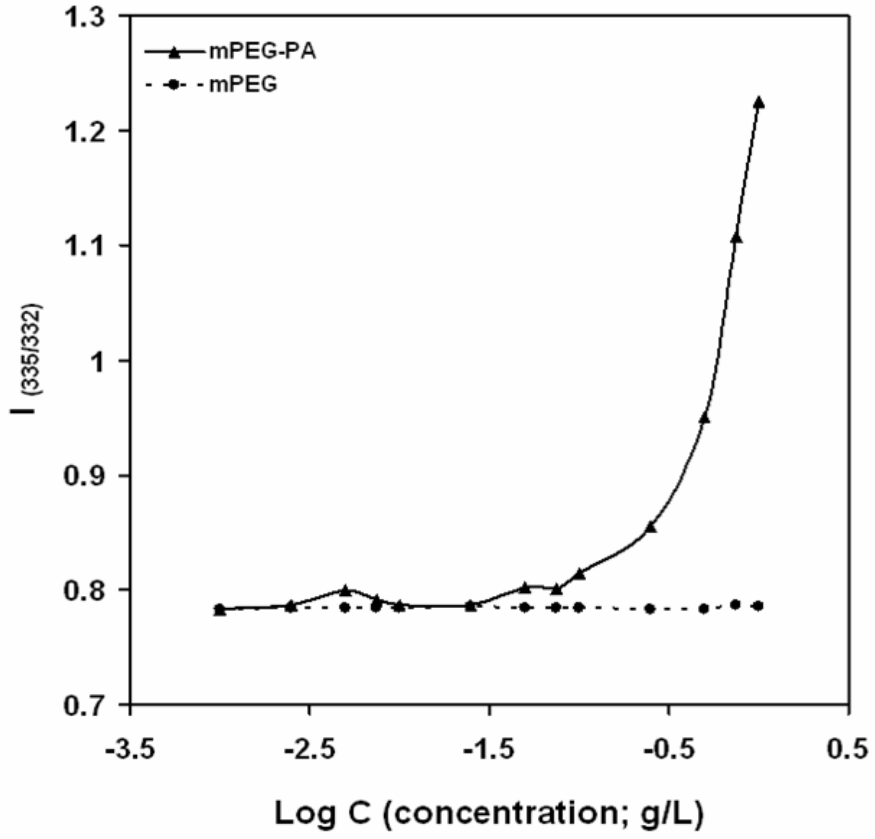

Figure 2.4: Plot of intensity ratio ($I_{335/332}$) from pyrene excitation spectra as function of log (concentration) for mPEG-PA (solid line) and mPEG (broken line). The CMC value of mPEG-PA conjugate was calculated from the crossover point of $I_{335/332}$.

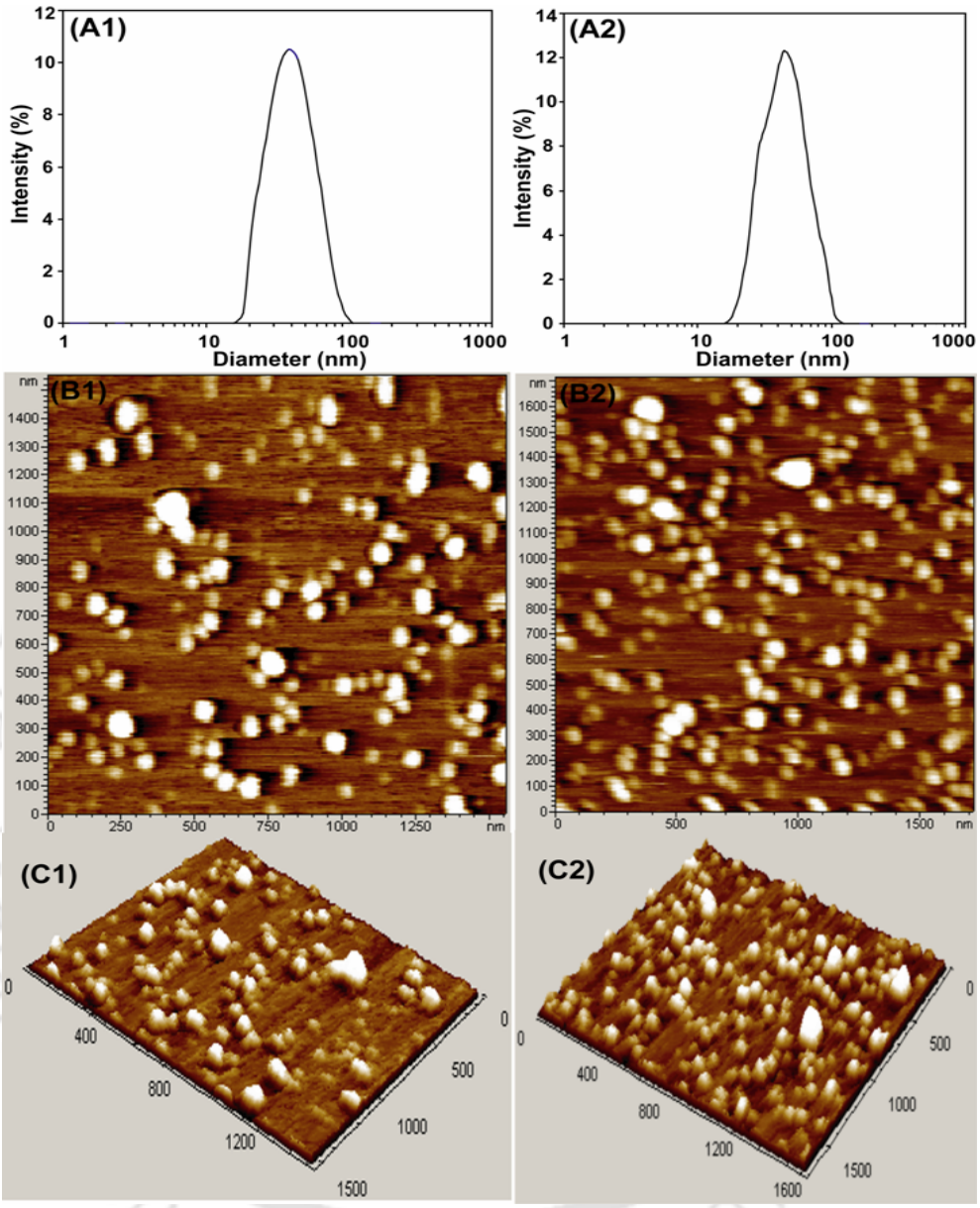

Figure 2.5: DLS and AFM study of free mPEG-Palmitate micelle and Curcumin loaded mPEG-Palmitate micelle. (A1, A2) Size distribution of mPEG-PA self-assembled micelles in PBS (pH 7.4) measured by dynamic light scattering. (B1, C1) Atomic force microscopy (AFM) images of self-assembled micelles of mPEG-PA. (B2, C2) AFM image of drug loaded micelles. The micelles are spherical in shape as seen in topographic image (B1, B2). C represents the 3D view of B.

2.3.4 Curcumin encapsulation in nanocarrier

The encapsulation efficiency of curcumin in mPEG-PA micelles was dependent on drug to polymer conjugate ratio (Table 3.1). Encapsulation efficiency was found to be 31% when drug to conjugate ratio (w/w) was 1:20. The encapsulation efficiency increases as we increased the amount of mPEG-PA and vice versa. At 1:100, drug to mPEG-PA ratio the encapsulation efficiency was close to 100%. So, when drug to polymer ratio was high the encapsulation was lower and it increased as the ratio decreased (Table 3.1). The drug loading content did not vary much with change in drug to polymer ratio. The drug loading varied between 1 to 1.5%.

Table 2.1: Drug loading: curcumin encapsulation with different ratio of drug to mPEG-PA.

Drug:mPEG-PA Ratio (w/w)	Drug Encapsulation (%)	Drug Loading (%) (w/w)
1:20	30.83 ± 2.99	1.47 ± 0.14
1:25	41.27 ± 3.07	1.41 ± 0.15
1:30	51.71 ± 2.57	1.39 ± 0.16
1:40	62.42 ± 2.61	1.30 ± 0.19
1:50	75.6 ± 4.23	1.48 ± 0.08
1:75	83.08 ± 4.50	1.10 ± 0.05
1:100	99.15 ± 0.51	0.99 ± 0.01

2.3.5 Photophysical properties of nanocarrier encapsulated curcumin

The micelle encapsulated curcumin was soluble in aqueous solution (Figure 2.6) and showed distinct photophysical properties. Curcumin in aqueous solution (1% methanol solution was used to solubilize curcumin which otherwise was insoluble in pure water) has weak absorption with a peak at around 425 nm (Figure 2.7). The absorption intensity of encapsulated curcumin increases sharply as that of curcumin dissolved in methanol alone (Figure 2.7). The fluorescence spectra also exhibited similar behavior. In aqueous solution it shows a weak broad peak at 550 nm whereas the micelle-loaded curcumin shows a well-defined blue shifted fluorescent peak at 500 nm with high intensity (Figure 2.8).

2.3.6 *In vitro* stability of drug loaded nanocarriers

Micelles can retain more than 95% of incorporated curcumin for the first 24 hours. Drug retention inside the micelles after 36 and 48 hours of incubation was more than 92% and 87% respectively (Figure 2.19). 80% drug was retained after 48 hours of incubation in simulated gastric fluid (pH 1.2) and in case of simulated intestinal fluid it was 84%.

2.3.7 Enzyme catalyzed degradation of mPEG-PA and *in vitro* drug release

The enzyme catalyzed biodegradation of the mPEG-PA conjugate was carried out by incubating empty micelles with lipase. ^{1}H NMR of the precipitate showed four peaks at δ 0.88, 1.3, 1.6 and 2.18 (Figure 2.10). In vitro lipase catalyzed release of curcumin from the micelle nanocarriers was observed for 48 hours. In first 12 hours 30% of curcumin was released from micelle, which increased up to 85% in 24 hours. Thereafter a drop in rate of release was observed and finally 92% of curcumin was released in total 48 hours (Figure 2.11). We also observed the in vitro degradation and drug release from the micelles by HeLa

cell lysate. After incubation with cell lysate with curcumin loaded nanocarriers, around 15% and 26% drug release was observed after 12 and 24 hour respectively (Figure 2.12).

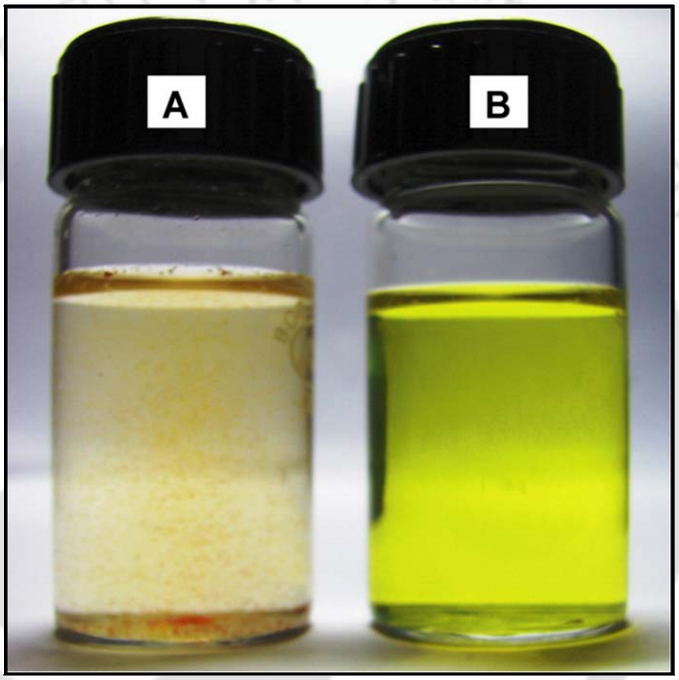

Figure 2.6: Increased solubility of micelle encapsulated curcumin (B) compare to free curcumin (A) in water. It can be clearly visualized that free curcumin (without the aid of any organic solvent) is insoluble in water.

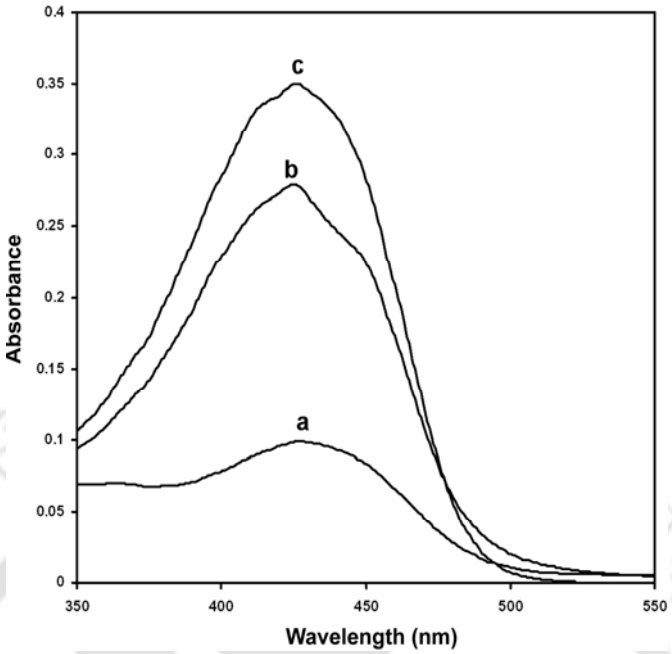

Figure 2.7: UV-visible absorbance spectra of curcumin in different type of solutions. (a) Curcumin in aqueous solution containing 10% methanol, (b) Curcumin loaded in mPEG-PA micelle and (c) Methanolic solution of curcumin.

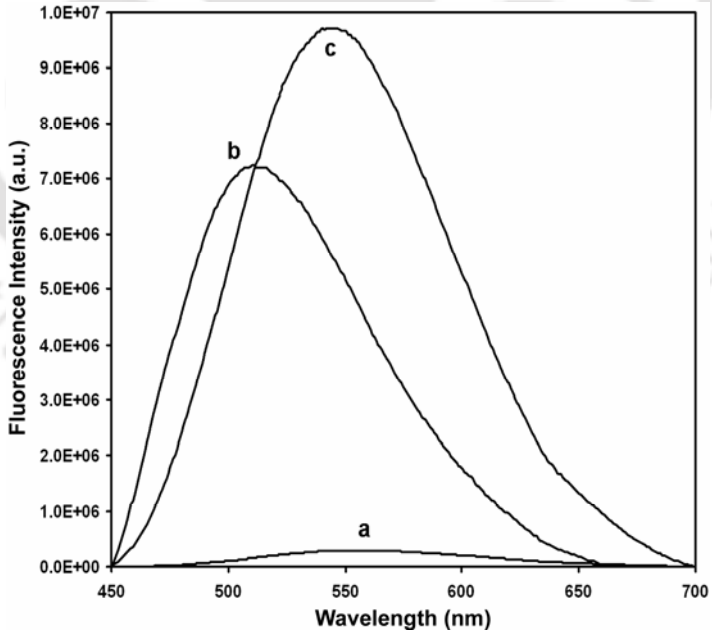

Figure 2.8: Fluorescence emission spectra of curcumin in different type of solutions. (a) Curcumin in aqueous solution containing 10% methanol, (b) Curcumin loaded in mPEG-PA micelle and (c) Methanolic solution of curcumin. Excitation wavelength (λ_{ex}) was 420 nm.

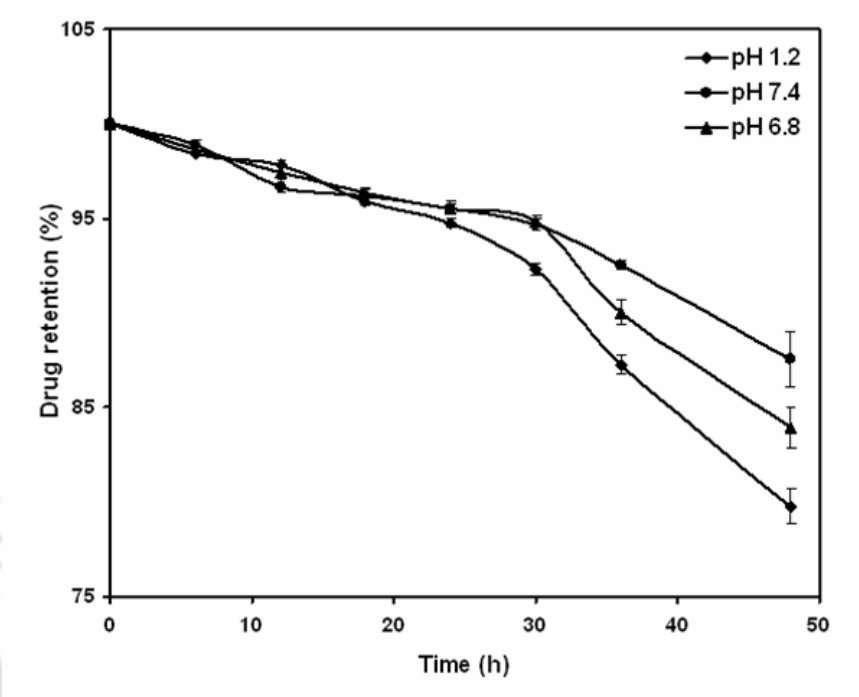

Figure 2.9: In vitro stability of curcumin loaded mPEG-PA micelle in PBS (pH 7.4), simulated gastric fluid (pH 1.2) and simulated intestinal fluid (pH 6.8) at 37ºC.

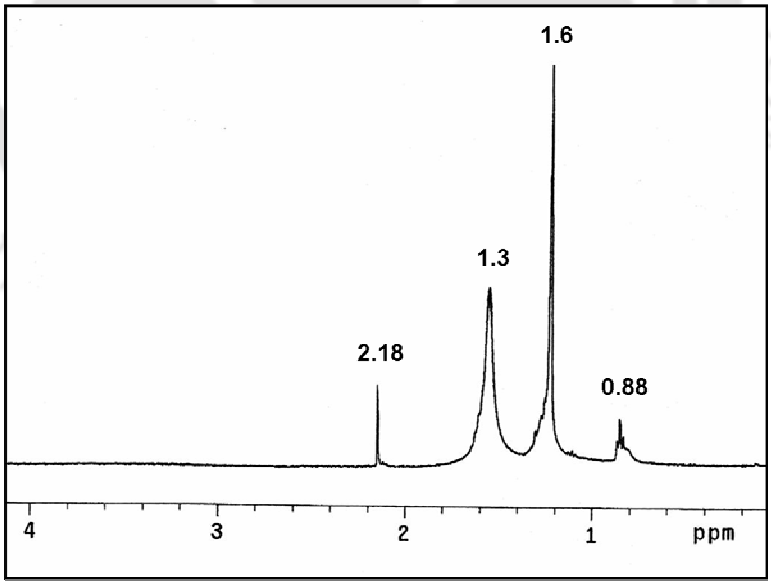

Figure 2.10: ^{1}HNMR spectrum of the palmitic acid obtained after lipase catalyzed cleavage of the ester bond in mPEG-PA.

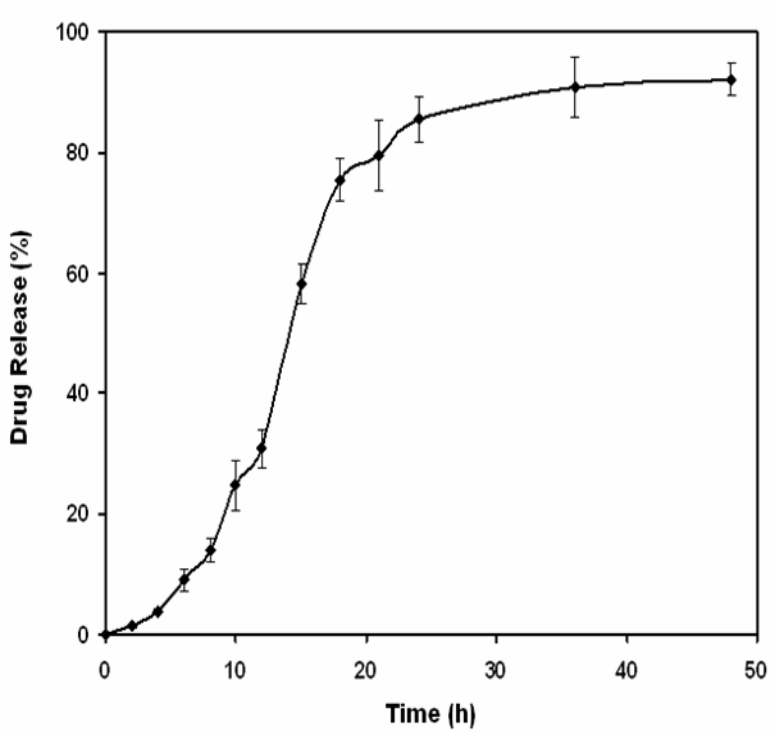

Figure 2.11: Lipase catalyzed release of drug (curcumin) from micelle nanoparticle in PBS (pH 7.4) at 37ºC. More than 90% of drug has been released within 48 hours because of enzymatic degradation of micelles.

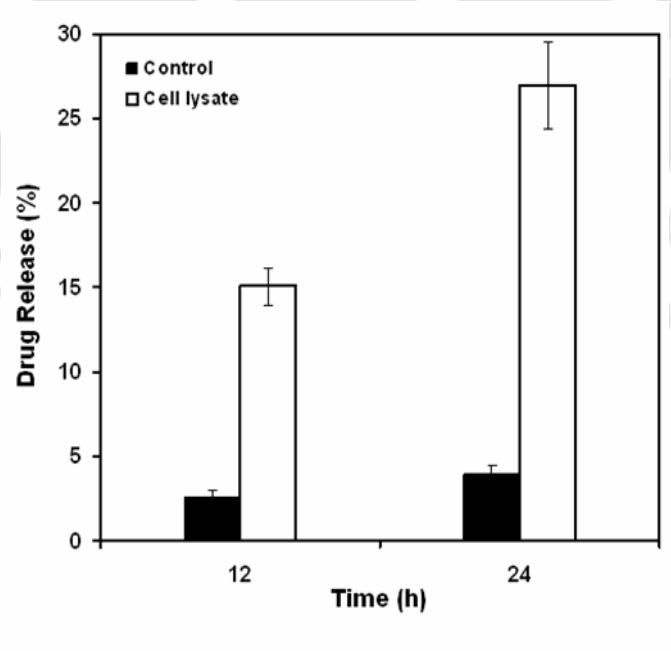

Figure 2.12: Drug release from micelle nanoparticle by HeLa cell lysate. Drug release was greater in presence of cell lysate with respect to control.

2.3.8 Cellular uptake and *in vitro* cytotoxicity studies

We studied the cellular uptake of free and encapsulated curcumin by confocal microscopy. The microscopic images of control cells without any drug exposure and cells incubated with empty mPEG-PA micelles did not show any fluorescence, where as the images of cells treated with encapsulated and free curcumin exhibited green fluorescence (Figure 2.13). The fluorescence was mainly observed in the cytoplasm of the cells.

In cytotoxicity study, when cells were incubated with the empty micelle nanocarriers, only minimal cell death was observed with increasing concentration (Figure 2.14). More than 90% cells were viable with treatment up to 5 mg/ml concentration of mPEG-PA, but when 10 mg/ml concentration of mPEG-PA was used the viability decreased to nearly 83%. As, more than 95% of cell viability was observed with 2.5 mg/ml of mPEG-PA concentration so, we have used it for further study. Free and nanocarrier encapsulated curcumin exhibited similar cytotoxic effect on HeLa cells. A dose dependent cytotoxicity was observed in both the cases (Figure 2.15). From this result the IC_{50} of free and nanocarrier encapsulated curcumin was calculated as 14.32 μM and 15.58 μM respectively. Under the microscope no loss in cellular morphology was found when cells were treated with empty nanocarriers but significant changes were found after treatment with curcumin loaded nanocarriers. Cells were shrinked, membrane structure was damaged and they have loosed there attachment from substratum (Figure 2.16). At the same time no fluorescence was observed with empty micelles but significant green fluorescence was observed for drug entrapped micelles (Figure 2.16).

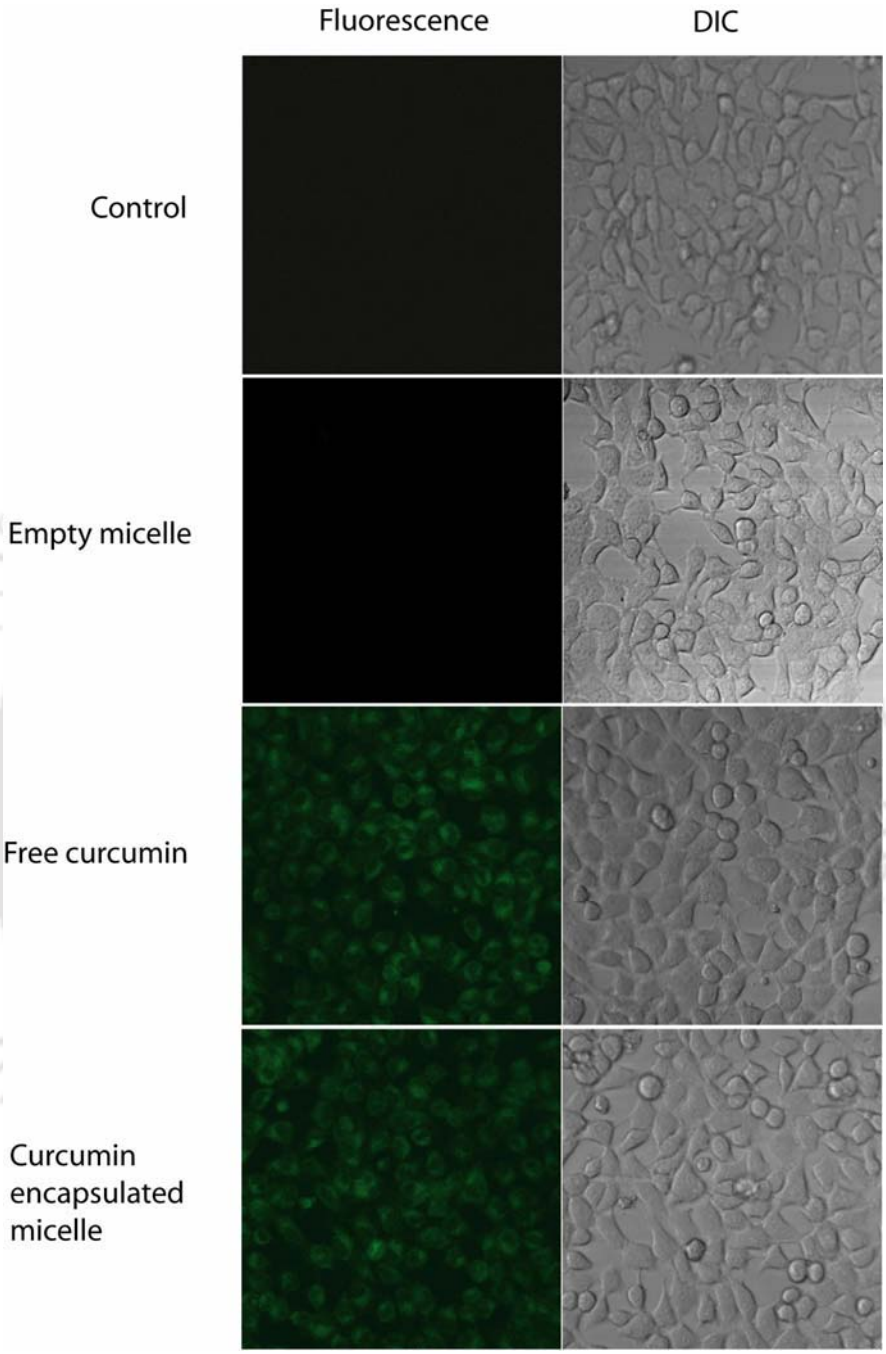

Figure 2.13: Differential interference contrast (DIC) and fluorescence images of internalization of free and micelle loaded curcumin by HeLa cells. The green fluorescence of curcumin inside the cells can be observed clearly. Cells were visualized at 2h after treatment.

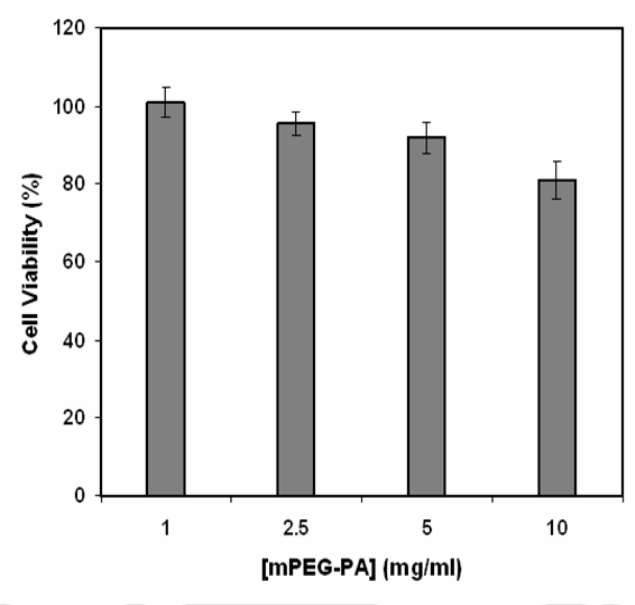

Figure 2.14: Effect of empty mPEG-PA nanocarriers on cultured HeLa cells. Only minimal toxicity of the nanocarriers can be seen in this concentration range.

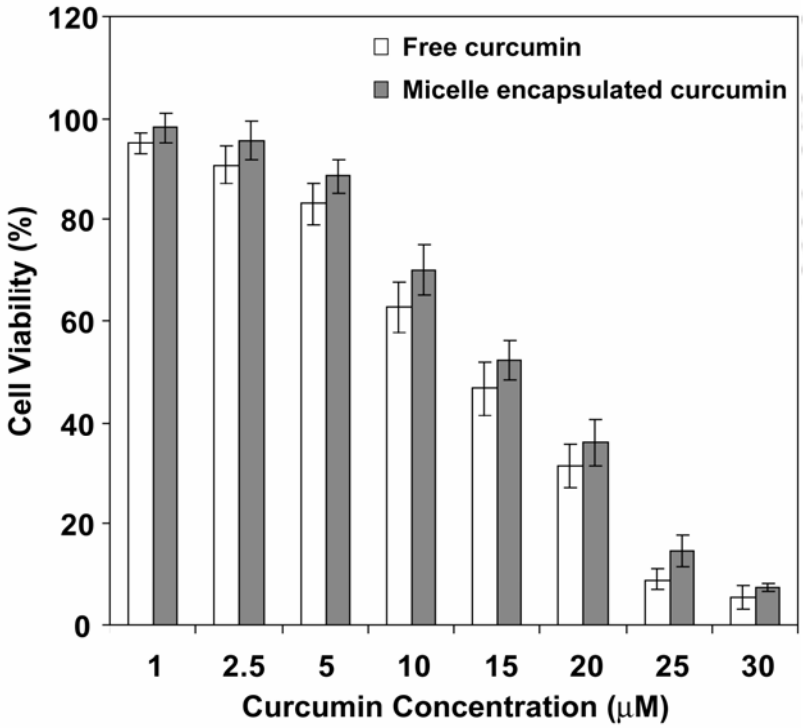

Figure 2.15: Cell viability of HeLa cells exposed to free curcumin and mPEG-PA micelle encapsulated curcumin, doses ranging from 1 to 30 μM for 48 hours. The percentage of viable cells was quantified using MTT assay.

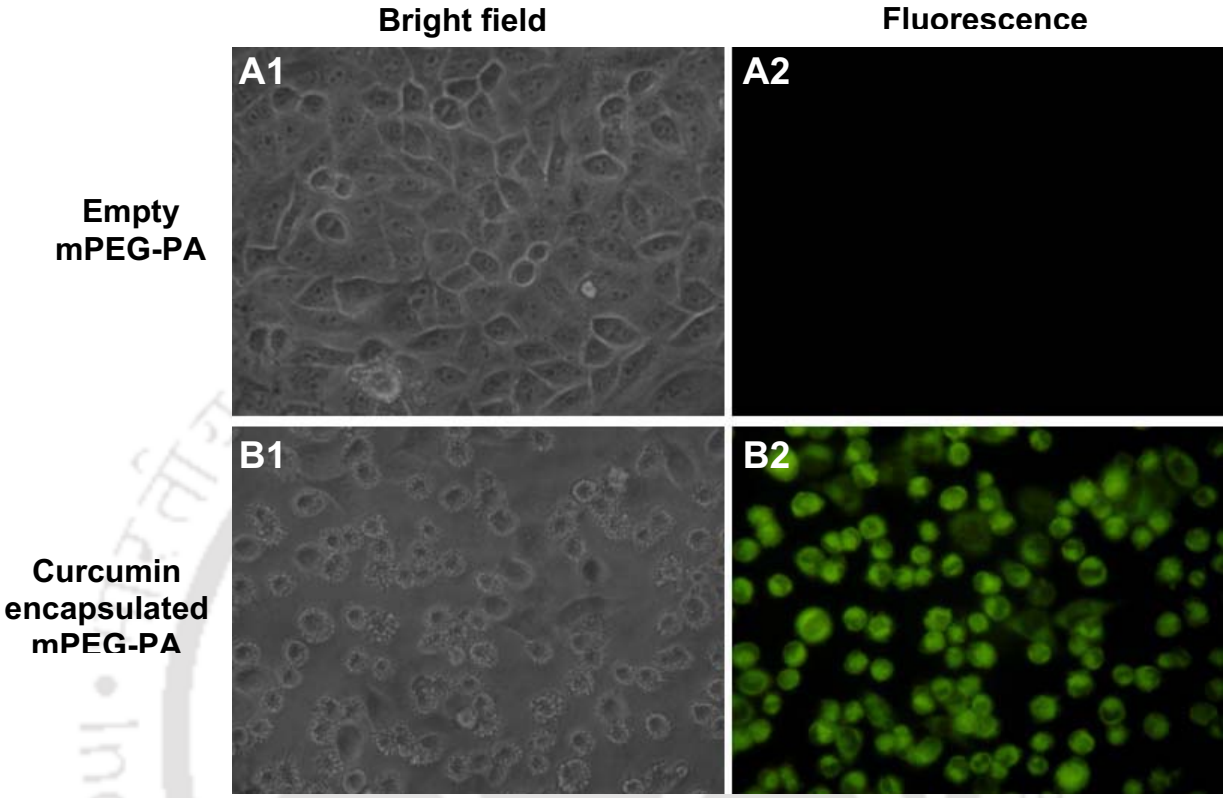

Figure 2.16: The morphological change in HeLa cells after 24h of treatment with (A) empty mPEG-PA and (B) curcumin encapsulated mPEG-PA. Cells were of regular flattened morphology when treated with empty micelles of mPEG-PA (A1) and no fluorescence was observed (A2). After treatment with curcumin encapsulated mPEG-PA micelles significant change in cellular morphology (B1) and strong green fluorescence (B2) was observed under the microscope.

2.4. Discussions

Hydrophobically modified PEGs have been explored in the preparation of micellar delivery systems for lipophilic drugs. In this regard, conjugates of PEG with diacyllipid such as pholphatidylethanolamine (PEG-PE) have been shown to form micelles and efficiently encapsulate hydrophobic drugs paclitaxel and tamoxifen for delivery to cancer cells (Gao et al., 2002). Similarly conjugation of PEG with fatty acids also can form micelle nanostructrures in aqueous solution (Lee et al., 2003).

The palmitoyl chloride was reacted with hydroxyl group of mPEG to form an ester linkage as shown in Scheme 2.1. In the ^{1}HNMR spectrum of the conjugate the signals at δ 3.6 and 3.3 were due to the methylene protons of PEG oxyethylene unit and protons of methoxy end group respectively. Coupling of the palmitate residue to mPEG was confirmed by the appearance of signals in the region δ 0.8 to δ 2.4 ppm. The sharp peak at 1734 cm^{-1} in the IR spectrum of mPEG-PA conjugate was due to the stretching vibration of ester bond. This peak was not present in the spectrum of mPEG, which confirmed the formation of mPEG-PA conjugate via ester linkage.

The self-aggregation phenomenon of mPEG-PA was studied using flurometric method. We observed strong fluorescence when mPEG-PA micelles were formed in presence of pyrene in an aqueous solution against control experiments carried out with pyrene in mPEG (Figure 2.4). This was because pyrene behaves as a self-quenching agent in polar environment and exhibits strong fluorescence when located inside or close to the hydrophobic domain of micelle. With the increase in the concentration of mPEG-PA the fluorescence intensity of pyrene increased indicating that the pyrene molecules was gradually transferred from aqueous solution to the less polar hydrophobic interior of self-aggregated mPEG-PA micelle. The partitioning of pyrene also brought the shift of its excitation peak from 332 to

335 nm (Wilhelm et al., 1991). Pyrene fluorescence intensity ($I_{335/332}$) values remain nearly unchanged at low concentrations of mPEG-PA but with further increase of concentration, intensity begin to increase significantly, implying the onset of self aggregation and formation of micelle nanostructures (Figure 2.3). No change in pyrene fluorescence was observed with mPEG which clearly indicated that mPEG cannot aggregate to form micelle like structure. It implies that the presence of hydrophobic palmitate chain was necessary for the micelle formation. The concentration of the mPEG-PA at which the micelles were started to form is known as CMC which is the most important parameter regarding the thermodynamic stability of the micelles. The micelle formation is a thermodynamic process and the relationship between CMC and the free energy of micellization (ΔG°_{M}) of an amphiphile in aqueous solution can be written as:

$$\Delta G^{0}_{M} = -RT \ln(CMC)$$

Where, R is universal gas constant and T is temperature.

So, the lower is the CMC value of a given amphiphilic polymer, the more stable are the micelles. This is specially important from the pharmacological point of view, since upon dilution with a large volume of the blood only micelles with low CMC value will able to exist, while micelles with high CMC value may dissociate into unimers and their content may precipitate in blood. The value of CMC obtained for mPEG-PA was much lower than low molecular weight surfactant (e.g. 2.3 g/L for sodium dodecyl sulfate in water). It indicates micelles formed from mPEG-PA conjugate were thermodynamically stable and could preserve stability without dissociation after dilution caused by intravenous injection.

The average size of the drug loaded micelles was found to be less than 50 nm, which was comparable to the other nanoformulations of curcumin. This size range of the nanocarriers is encouraging with regards to passive targeting of tumor tissues through EPR effect.

To investigate whether these micelle nano-carriers would be advantageously used for encapsulating highly hydrophobic drug curcumin for delivery to cancer cells, we studied the encapsulation of curcumin by the novel mPEG-PA conjugate. The encapsulation efficiency of curcumin increased as the amount of conjugate increased. This was because of the fact that, with the increase of conjugate, more micelles formed which solubilized more amount of curcumin in their core. The solubilization of curcumin in mPEG-PA made a clear yellowish solution whereas without the nanocarriers free curcumin was not able to solubilize in water (Figure 2.6). This clear solution was obtained due to the encapsulation of curcumin in core of the micelle nanocarriers (Scheme 2.2).

Curcumin has intrinsic fluorescence properties. The photophysical properties and fluorescence spectra of curcumin are highly sensitive to the polarity of the environment and showed significant solvent dependent shifts in emission maxima (Chignell et al., 1994). We found that, after encapsulation in micelles the absorption and fluorescence intensity of curcumin increased significantly. The fluorescence peak maxima of micellar curcumin exhibited a large blue shift. This increase of absorption and fluorescence intensity and blue shift of peak maxima suggests that curcumin in mPEG-PA is encapsulated in the hydrophobic core of the micelle where the environment is nonpolar.

For effective passive targeting of cancerous tissues drug loaded micelles should be able to retain the drug for prolonged time in circulation. We observed that mPEG-PA micelles were able to retain more than 80% of drug after 48 hours. Thus the micellar formulation was very stable under broad physiological pH conditions.

The mPEG-PA conjugate is biodegradable as evidenced by enzyme degradation studies. When lipase acts on mPEG-PA micelle we anticipated release of free mPEG in the solution and palmitic acid as an insoluble precipitate (Scheme 2.3). ^{1}H NMR of the precipitate

(Figure 2.10) confirmed that it was palmitic acid and micelle degradation occurred due to the cleavage of the ester bond of the conjugate as per proposed scheme (Scheme 2.3).

To verify that the ester linkage of mPEG-PA can be cleaved inside the cells to release the entrapped drug, we performed an in vitro experiment with HeLa cell lysate. The cell lysate successfully degraded the micelles to release curcumin (Figure 2.12). So, the conjugate is biodegradable and can be degraded in situ by the cells. Taking advantage of intrinsic fluorescence properties of curcumin we observed that cells can internalize micelle encapsulated curcumin as effectively as free curcumin. But the mPEG-PA encapsulated curcumin has the added advantage of enhanced solubility and can therefore be directly used without any organic solvent.

Since, mPEG is nontoxic and approved by FDA for pharmaceutical applications and palmitic acid is a natural fatty acid found in human body, we expect the mPEG-PA conjugate should be biocompatible, biodegradable and potentially safe as a drug carrier for clinical use. *In vitro* cytotoxicity assay proved that empty nanocarriers showed only minimal cytotoxicity and nanocarriers encapsulated drug was as effective as free curcumin. Also under the microscope we observed significant change in morphology of the cells after treatment with nanocarrier encapsulated curcumin. The green fluorescence of curcumin was observed all over the cells, earlier which were mainly in the cytoplasm (Figure 2.14). So, in the cell cytoplasm, the nanocarriers were degraded by the action of enzymes and released the drug which ultimately diffuses slowly into the nucleus and exerted its effect. It has been reported that curcumin induce cytotoxic effects in HeLa cells through apoptosis. Although we have not done any molecular assay to find out the mechanism of cell death but our microscopic study suggests that, nanocarrier entrapped curcumin also induced cell death

through apoptosis. These results demonstrated that this delivery system could be a promising choice for administering curcumin without loss of its therapeutic efficacy.

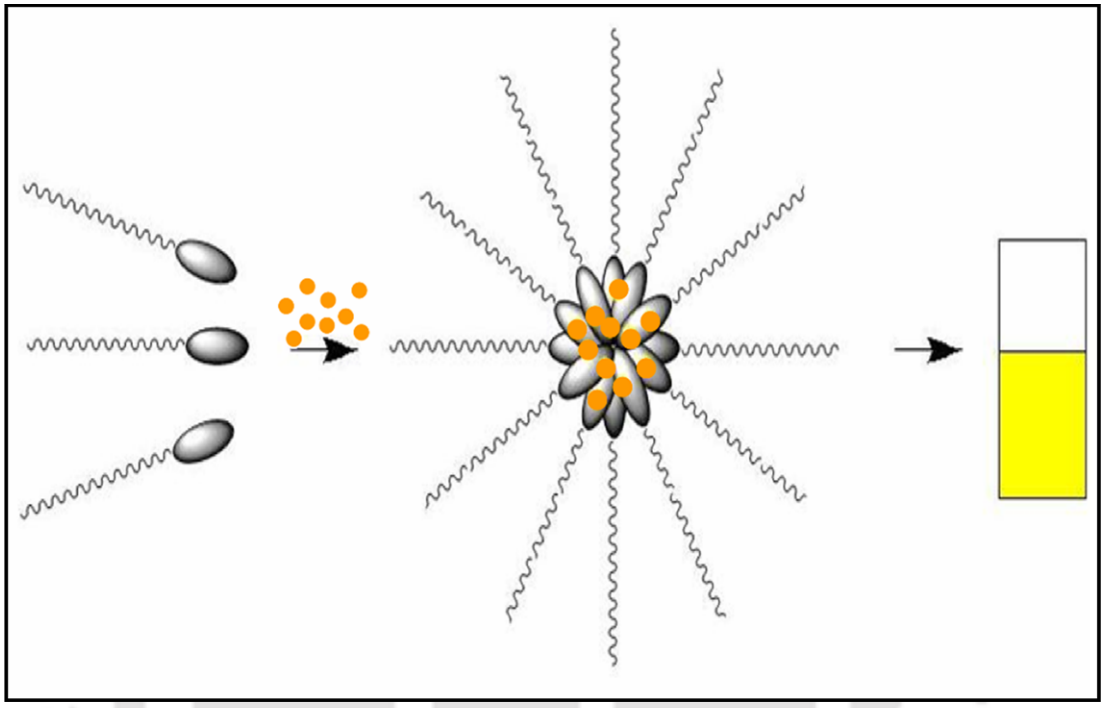

Scheme 2.2: Self-assembly of mPEG-PA in aqueous solution to form micelle nanocarriers and simultaneous encapsulation of curcumin in the core of nanocarriers.

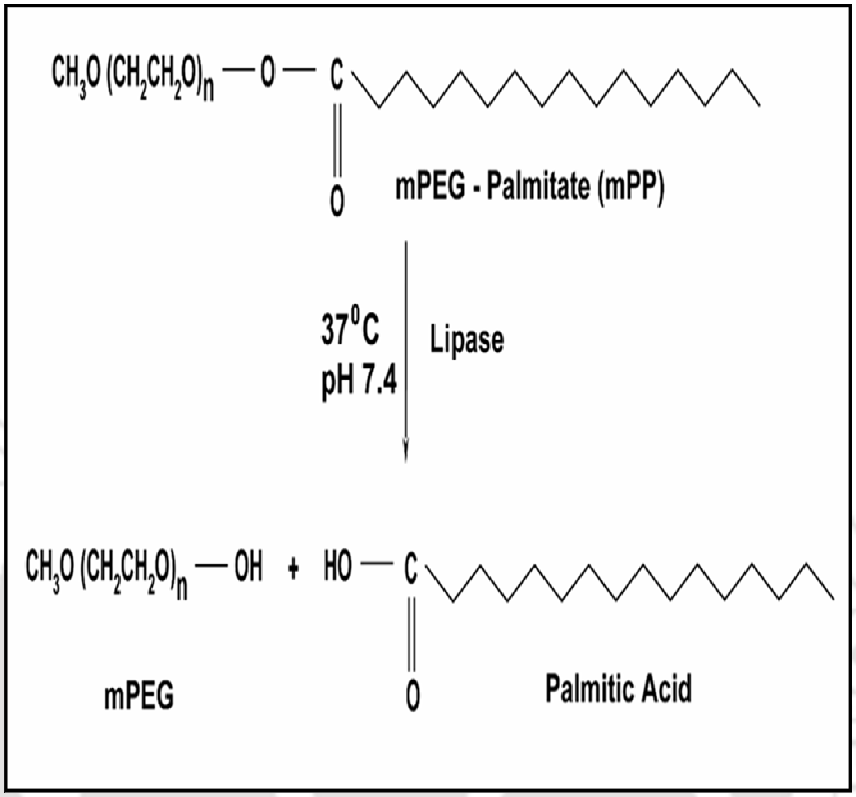

Scheme 2.3: Lipase catalyzed degradation of mPEG-PA. Lipase hydrolyzes the ester bond of mPEG-PA to yield mPEG and palmitic acid in physiological condition (37ºC, pH 7.4).

2.5 Conclusions

We have prepared a novel biodegradable polymeric mPEG palmitate amphiphilic conjugate in a single step reaction, which forms spherical micelles in aqueous solution through a process of self-assembly. The novel conjugate, which showed minimal toxicity on HeLa cells can successfully encapsulate hydrophobic drug as exhibited with studies involving chemo preventive agent curcumin. Encapsulation of curcumin in the core of the micelles increased the aqueous solubility of the drug. Drug loaded nanocarriers showed good stability over a wide pH range. Thus this novel micellar nanoencapsulation may improve the bioavailability of curcumin and will make this drug amenable to intravenous dosing without affecting its anticancer properties. This conjugate is a potential model system for encapsulating hydrophobic drugs and preparation of enzyme triggered release systems as demonstrated by *in vitro* studies for enzyme-mediated degradation and release of encapsulated drug with lipase and HeLa cell lysate.

CHAPTER 3

Formulation of Curcumin in Pluronic Nanocarriers for Cancer Chemotherapy

CHAPTER 4

Natural Food Protein Based Nanoparticle for Curcumin Delivery to Cancer Cells

3.1 Introduction

Nanoformulation of hydrophobic drugs in block copolymer micelles have been increasingly developed as preferred drug nanocarriers against cancer and showed immense potential for development of parenteral formulation as well as oral delivery of anticancer drugs (Kwon and Kataoka, 1995; Bromberg, 2008). Polymeric micelles made of Pluronic block copolymers have proved to be effective carrier of hydrophobic drugs with long-circulating characteristics through avoidance of trapping by the reticuloendothelial system (RES) (Batrakova and Kabanov, 2008). Pluronic block copolymers (also termed Poloxamer) are FDA approved for pharmaceutical and medical applications, including parenteral administration and listed in the US and British pharmacopoeia as pharmaceutical excipients and extensively used as emulsification, solubilization, dispersion, thickening, coating and wetting agents (Chowdhary et al., 2000). These block copolymers are consists of hydrophilic ethylene oxide (EO) and hydrophobic propylene oxide (PO) blocks arranged in a triblock structure EO_x–PO_y–EO_x (often abbreviated as PEO–PPO–PEO, Scheme 3.1), where *x* and *y* chain lengths vary from 2-130 and 16-70 units respectively. This arrangement results in amphiphilic copolymers, which self assemble into micelles in the aqueous solution with core-shell structure above their critical micelle concentrations (CMC). The core is formed by the hydrophobic interactions of the PO blocks and remains segregated from the aqueous exterior by the hydrophilic corona formed by EO blocks (Scheme 3.2). The hydrophobic core of such micelles serves as a cargo space for the incorporation of lipophilic therapeutic compounds, while the hydrophilic corona contributes greatly to the pharmaceutical behavior of block copolymer formulations by maintaining the micelles in a dispersed state, as well as by decreasing undesirable drug interactions with cells and proteins through steric-stabilization effects (Kabanov et al., 2002).

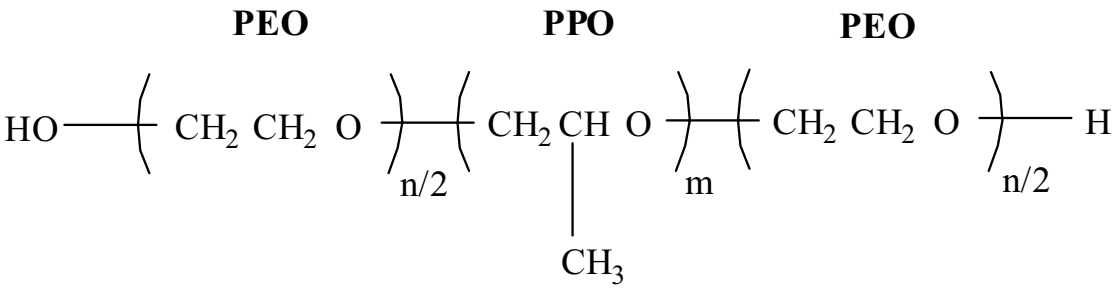

Scheme 3.1: Chemical structure of Pluronic tri-block copolymers. The central PPO block is hydrophobic in nature which is flanked by PEO hydrophilic blocks.

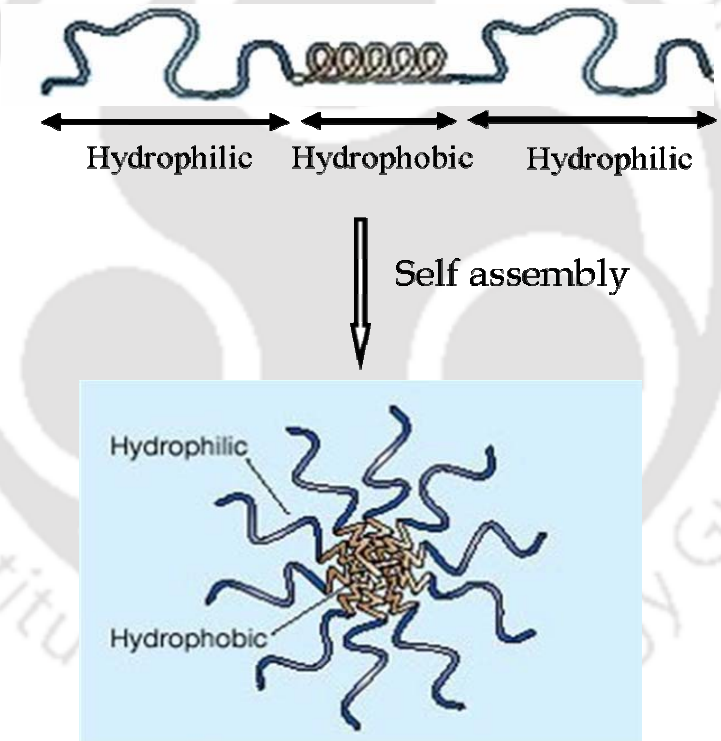

Scheme 3.2: Self-assembly of Pluronic block copolymer into micelle nanostructure with PPO hydrophobic core and PEO hydrophilic shell structure.

Therefore, the noncovalent incorporation of drugs into the hydrophobic PO core of the Pluronic micelles results in increased solubility, metabolic stability, bioavailability and circulation time (Chiappetta and Sosnik, 2007). Recent studies have proven several unique advantages of these biocompatible nanostructures as drug delivery carriers *in vivo*. Pluronic copolymers have been shown to enhance the therapeutic activity of anticancer agents in cancer cells and a formulation of doxorubicin with mixed micelles of Pluronic is in clinical trial for the treatment of multi drug resistant (MDR) tumors (Exner et al., 2005; Danson et al., 2004). The commercial availability, ease of preparation, well-studied physical properties and strong safety profile makes the Pluronics particularly appealing for drug delivery purposes. In this chapter, we aimed to develop nanoformulation of curcumin based on Pluronic micelles for cancer chemotherapy. Although a variety of substances has been solubilized in Pluronic micelles but the potential of these block copolymers for delivery of curcumin has not yet been studied.

3.2 Materials and Methods

3.2.1 Materials

Pluronic F68 and F127 were purchased from Aldrich (Bangalore, India). Curcumin was procured from Himedia (Mumbai, India). MTT was from SRL (Mumbail, India). All the salts and solvents used in the study were purchased from Merck (Mumbai, India). Cell culture plates were purchased from Corning (USA). All the cell culture media and reagents used in the study were purchased from Sigma (USA). HeLa, cancer cell line was obtained as gift from National Center for Cell Science (Pune, India). All other reagents and buffer solution components were analytical grade preparations. Distilled and deionized water was used in all experiments.

3.2.2 Preparation of drug loaded Pluronic micelles

Curcumin loaded Pluronic micelles was prepared by thin film rehydration method. Stock solutions of curcumin (1 mg/ml) and Pluronic copolymers (10 mg/ml) were prepared in methanol and chloroform respectively. Required amount of stock solutions were transferred to separate tubes to obtain different drug to polymer ratio and drug containing polymer films were prepared by evaporating organic solvent under vacuum. The films were rehydrated in PBS (0.01M, pH 7.4) by extensive vortexing to prepare drug encapsulated micelles. Amount of curcumin incorporated in micelles was estimated spectrophotometrically as reported earlier in Chapter 2. Drug encapsulation and loading in micelle nanocarriers was calculated as follows (Park et al., 2005):

$$\text{Drug Encapsulation (\%)} = \left(\frac{\text{amount of curcumin encapsulated}}{\text{amount of curcumin used}}\right) \text{X } 100$$

$$\text{Drug Loading (\%)} = \left(\frac{\text{amount of curcumin in nanocarrier}}{\text{amount of curcumin loaded nanocarrier}}\right) \text{X } 100$$

$$= \frac{\text{Curcumin}}{\text{Curcumin + Pluronic}} \text{ X } 100$$

3.2.3 Physicochemical characterization of micelles

UV-Visible spectra of aqueous solution of curcumin encapsulated in Pluronic F68 and F127 micelles were recorded with Cary-100Bio spectrophotometer (Varian). The fluorescence emission spectra of curcumin in same micelle solutions were taken using excitation wavelength of 420 nm with FluoroMax-3 spectroflourimeter (Jobin Yvon, Horiba). The excitation and emission slit widths were 2 nm and 5 nm respectively and the scan rate was 1nm/sec.

Atomic force microscopy (AFM, Picoscan, Molecular Imaging, USA) was used to determine the shape and morphology of the micellar nanocarriers. 10 µl of the sample solutions were placed on the freshly cleaved mica and dried under stream of nitrogen. The samples were dried under a stream of nitrogen and mounted on the microscope scanner. The micelle shape was observed and imaged at non-contact mode.

3.2.4 *In vitro* release of curcumin from Pluronic micelle

Release of curcumin from Pluronic micelles was studied at physiological condition (pH 7.4, 37º C). Curcumin (1 mg) loaded Pluronic (100 mg) was prepared in 50 ml physiological buffer (0.01M PBS, pH 7.4) by thin film rehydration method. Non-encapsulated curcumin was separated out by centrifugation. Curcumin loaded micelle solution was placed in incubator at 37º C under gentle agitation (120 rpm). Samples were withdrawn periodically and curcumin was quantified spectrophotometrically. The percentage of curcumin released from the micelles at various time points was calculated by following equation:

$$\text{Drug Release (\%)} = \left(\frac{\text{Released curcumin}}{\text{Total encapsulated curcumin}} \right) \text{X } 100$$

3.2.5 Stability studies

Stability of the curcumin encapsulated Pluronic micelles was evaluated for both in solution form and lyophilized form respectively. Curcumin loaded Pluronic aqueous dispersions were stored at 25º C and 4º C in the dark and characterized for drug retention at fixed time intervals up to 10 days after preparation. Lyophilized formulation was obtained by freeze-drying of curcumin encapsulated pluronic micelles in a freeze dryer (Christ, Germany). During freeze drying the chamber pressure was maintained at 0.035 mbar and temperature

was –55 ºC. Stability of the lyophilized formulations was checked similarly as above at the temperature 25 ºC.

3.2.6 *In vitro* cell viability and cellular uptake assay

The cytocompatibility of Pluronic copolymers and the activity of curcumin entrapped into Pluronic micelles for the proliferation inhibition of HeLa carcinoma cells was investigated by *in vitro* MTT assay and compared with that of free curcumin. Cells (1×10^4/well) were seeded in 96-well cell culture plates and after 24 h were treated with different concentrations of empty pluronics, free curcumin and Pluronic encapsulated curcumin. After 48h of treatment media were carefully removed, cells were washed twice with PBS and 100 µl fresh medium containing 0.5 mg/ml MTT was added to each well. The plates were incubated at 37 °C for 4 h. Then the medium was totally removed and 100 µl DMSO was added to each well to solubilize the insoluble formazan crystals. The absorbance, which was proportional to cell viability, was subsequently measured at 570 nm in each well using a 96 well plate-reader (Bio-Rad, USA). The percentage of cell viability was calculated as follows:

$$\text{Cell viability (\%)} = \frac{A_{sample}}{A_{control}} \times 100$$

Where, A_{sample} was the absorbance of the cells treated with free or nanocarrier encapsulated curcumin, while $A_{control}$ was the absorbance of the cells without curcumin treatment.

To visualize the uptake of drug encapsulated nanocarriers, HeLa cells were grown on 35mm cell culture plates up to ~80% confluency. After that, the growth medium was replaced with medium containing 20 µM curcumin encapsulated in Pluronic F127 and F68 micelles separately. Cells were incubated at 37 ºC for 4h to allow the uptake of nanocarriers and visualized under inverted fluorescence microscope (Nikon TS100, Japan). We also

visualized the cells after 48h of treatment with nanocarrier loaded curcumin to observe the change in cellular morphology.

3.3 Results

3.3.1 Drug Loading

The encapsulation efficiency and loading contents of curcumin into Pluronic micelles are summarized in Table 3.1. The drug loading (%) was calculated on weight/weight (w/w) and moles/moles (M/M) basis. Pluronic F127 showed higher encapsulation efficiency than Pluronic F68. The drug encapsulation efficiency by both the Pluronic copolymers increased with the increase in drug to polymer ratio and highest encapsulation was found when the ratio was 1:50. With this ratio the drug loading (w/w) was found to be 1.87% for Pluronic F127 and 1.38% for Pluronic F68. The molar drug loading (M/M) efficiency of Pluronic F127 was higher than that of Pluronic F68.

Table 3.1: Drug encapsulation and loading at different drug to Pluronic ratios.

Pluronic Type	Drug:Pluronic Ratio (w/w)	Drug Encapsulation (%)	Drug Loading (%) (w/w)	Drug Loading (%) (M/M)
Pluronic F68	1:5	25.72 ± 1.19	4.29 ± 0.19	21.08 ± 0.98
	1:10	34.53 ± 0.74	3.14 ± 0.07	23.98 ± 0.52
	1:25	55.01 ± 0.81	2.12 ± 0.05	26.23 ± 0.57
	1:50	70.24 ± 1.34	1.38 ± 0.04	21.99 ± 0.69
Pluronic F127	1:5	34.33 ± 1.24	5.72 ± 0.21	29.94 ± 1.07
	1:10	46.2 ± 1.40	4.2 ± 0.13	35.74 ± 1.08
	1:25	79.05 ± 1.52	3.04 ± 0.06	45.66 ± 0.88
	1:50	95.57 ± 1.65	1.87 ± 0.03	38.81 ± 0.67

3.3.2 Physicochemical characterization

3.3.2.1 Atomic Force Microscopy

Figure 3.1 represents the AFM image of curcumin encapsulated Pluronic F127 and F68 micelles. It can be observed that micelles were spherical in shape for both the formulations and sizes of the nanocarriers were below 100 nm.

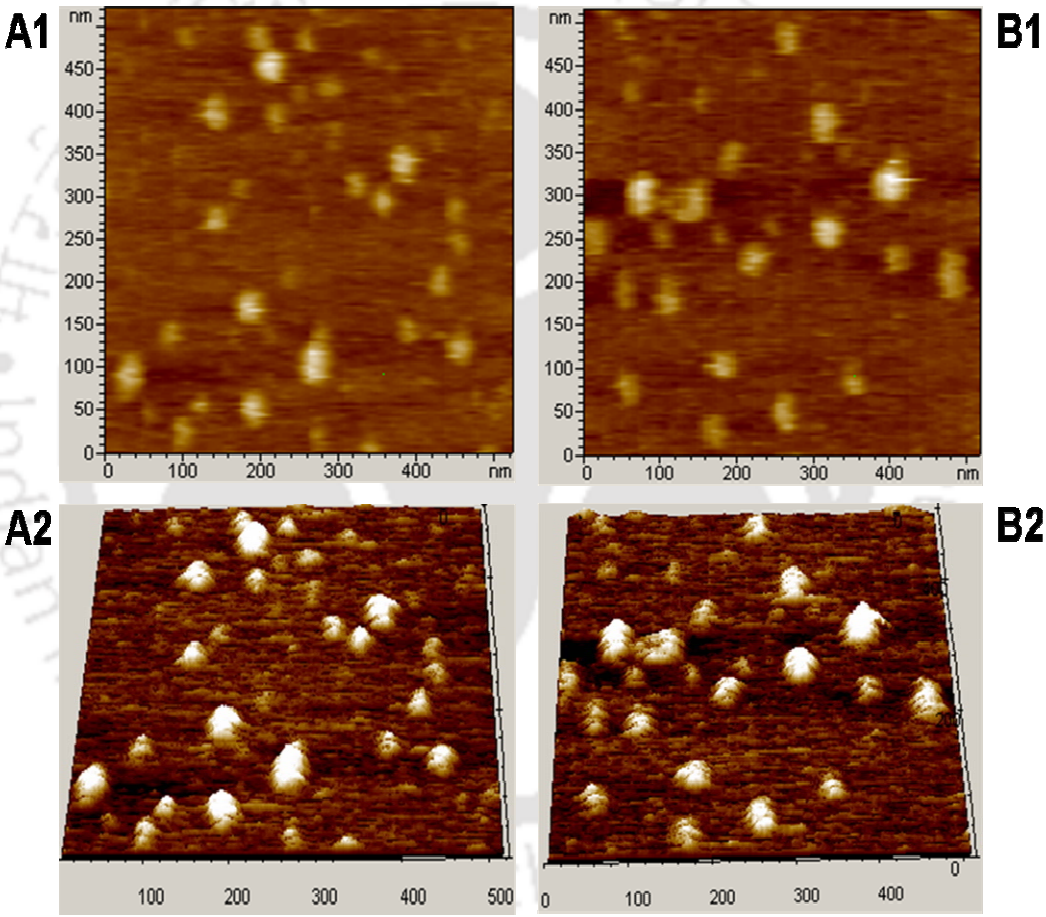

Figure 3.1: AFM images of drug encapsulated micelle nanocarriers (A) Curcumin loaded Pluronic F127 micelles and (B) Curcumin loaded Pluronic F68 micelles. A1 and B1 represents topograph images of the nanocarriers whereas, A2 and B2 represents 3D view of A1 and B1. The micellar nanoparticles are nearly spherical in shape with size less than 100 nm.

3.3.2.2 UV-visible and Fluorescence spectroscopy

Curcumin in aqueous solution (1% DMSO solution was used to solubilize curcumin, which was insoluble in pure water) has weak absorption, with a broad peak at 425 nm, whereas the absorption intensity of encapsulated curcumin increased sharply when encapsulated in Pluronic micelles (Figure 3.2). Curcumin encapsulated in Pluronic F127 micelles showed higher intensity than curcumin in F68 micelles. Free curcumin in aqueous solution showed a broad and weak fluorescence peak at 550 nm. The Pluronic encapsulated curcumin showed well-defined fluorescence maxima at 497 nm (Pluronic F127) and 507 nm (Pluronic F68) with high intensity (Figure 3.3).

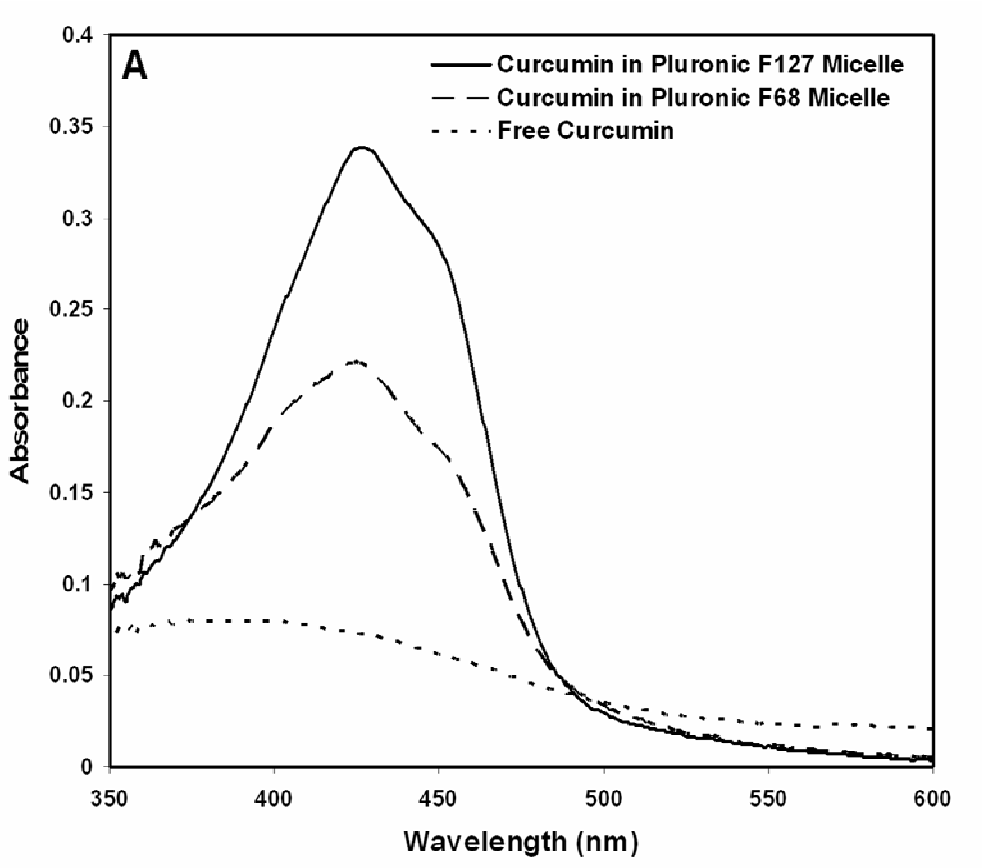

Figure 3.2: UV-visible absorption spectra of free curcumin (control, solubilized with 1% DMSO) and curcumin encapsulated Pluronic micelles.

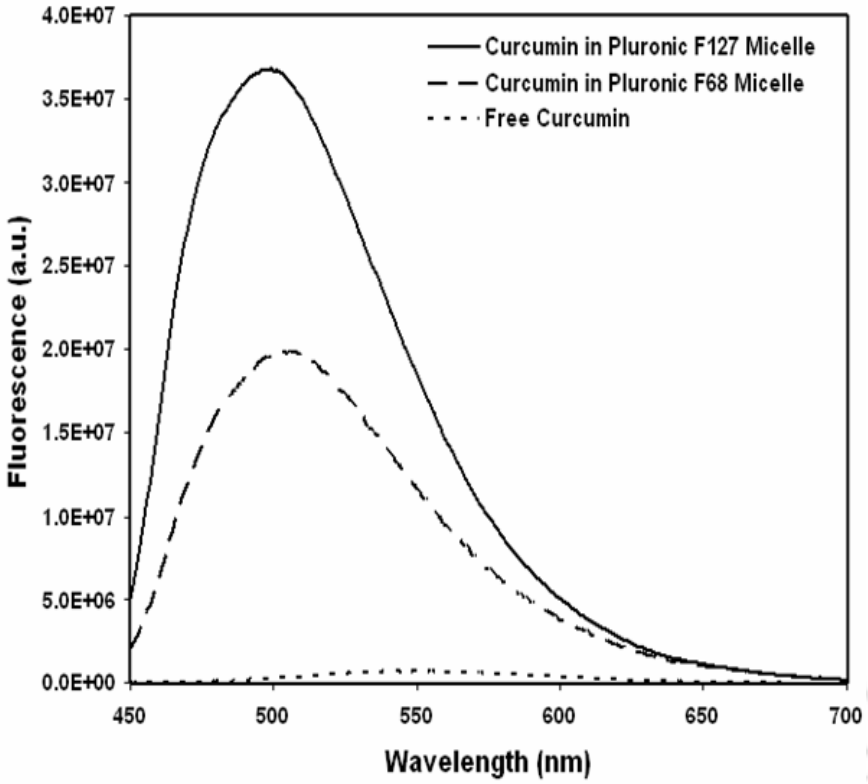

Figure 3.3: Fluorescence emission spectra of free curcumin (control, solubilized with 1% DMSO) and curcumin encapsulated Pluronic micelles. Excitation wavelength was 420 nm.

3.3.3 *In vitro* Release Study

The *in vitro* release behaviors of curcumin loaded Pluronic micelle formulations were studied in physiological conditions and representatively shown in Figure 3.4. In case of both the formulations, a typical two-phase release profile was observed. A relatively rapid release was in first stage followed by a sustained and slow release over a prolonged time up to 10 days. In comparison with the release from Pluronic F68 micelles, curcumin release from Pluronic F127 micelles was slower. In case of P-F68 micelles more than 20% of curcumin was released during the first 4h compared with 8% P-F127 micelles. After that, the release was slow and sustained from both type of micelles and finally at 240 h 80% of drug was released from F68 micelles whereas 63% drug was released from F127 micelles. The T_{50}

value (time required for release of 50% of the encapsulated drug) for curcumin release form Pluronic F68 and F127 formulations were 36 and 144h respectively.

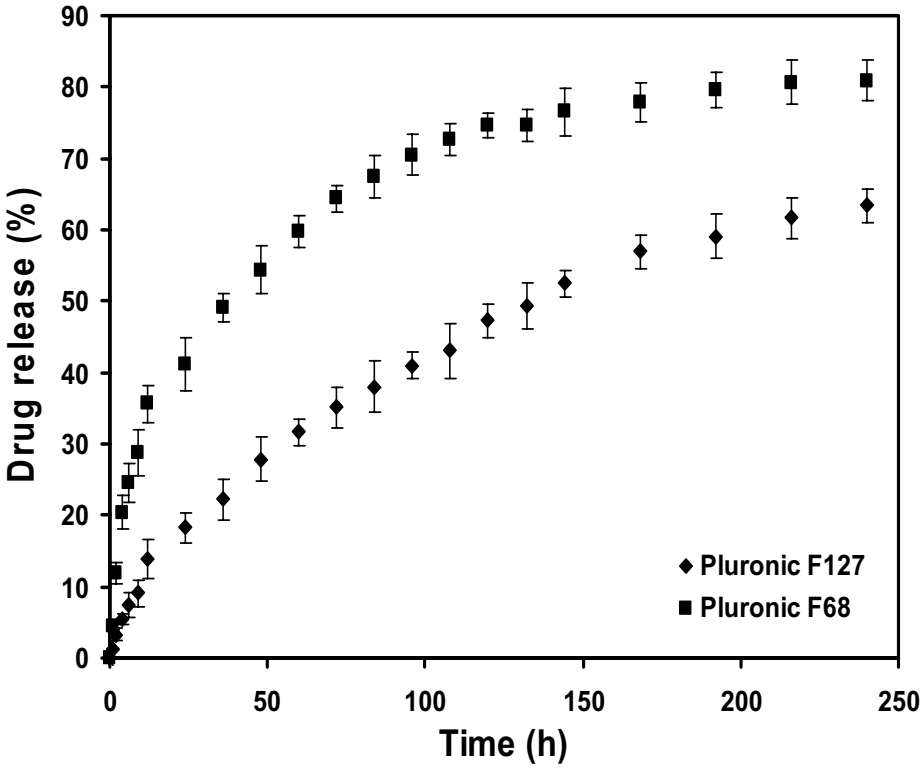

Figure 3.4: *In vitro* release of curcumin from Pluronic micelles at physiological condition (pH 7.4, 37ºC).

To analyze the drug release kinetics and mechanism, data were analyzed using the following four models (Ahuja et al., 2007):

1. Zero order

$$\frac{M_t}{M_\infty} = k_0 t$$

2. First Order

$$\frac{M_t}{M_\infty} = 1 - \exp(-k_1 t)$$

3. Higuchi Model (Higuchi, 1963)

$$\frac{M_t}{M_\infty} = k_H t^{1/2}$$

4. Power Law Model (Korsmeyer et al., 1983)

$$\frac{M_t}{M_\infty} = kt^n$$

Where, M_t/M_∞ represents the fractional drug release at time t and k_0, k_1, k_H, k represents zero order release constant, first order release constant, Higuchi constant and Korsemeyer-Peppas constant respectively. In the Power law model n is an exponent that characterizes the diffusional release kinetic mechanism. The data were analyzed for initial 60% release only. The values of k_0, k_1, k_H, k and n were determined by fitting the release data into respective equations and presented in Table 3.2 together with regression coefficients (R^2).

Table 3.2: Release parameters for curcumin formulations in Pluronic micelles obtained after fitting the *in vitro* drug release data to four different mathematical models of drug release kinetics.

Mathematical Models		Curcumin Formulation	
		Pluronic F68	Pluronic F127
Zero Order	k_0	0.0123	0.0038
	R^2	0.5596	0.885
1st Order	k_1	0.0076	0.0023
	R^2	0.7921	0.9673
Higuchi	k_H	0.0826	0.042
	R^2	0.9648	0.9898
Power Law	k	0.0731	0.0195
	n	0.5551	0.6724
	R^2	0.9133	0.9826

3.3.4 Stability study

The storage stability of the curcumin encapsulated Pluronic micelle solutions were investigated at 25ºC and 4ºC. At both the temperature the aqueous solution of formulations was not stable for long time, drug aggregation and precipitation was started to occur after three days (Figure 3.5). The stability of the freeze-dried formulation was tested for 3 months. The data shows no significant loss in drug retention by both types of Pluronic copolymers within this time period (Figure 3.6). The peak fluorescence emission wavelength was also not changed which indicated that curcumin remained in the same region of micelles after freeze-drying and reconstitution. Therefore, the curcumin loaded Pluronic could be stored as lyophilized powder form and reconstituted in aqueous solution just before use.

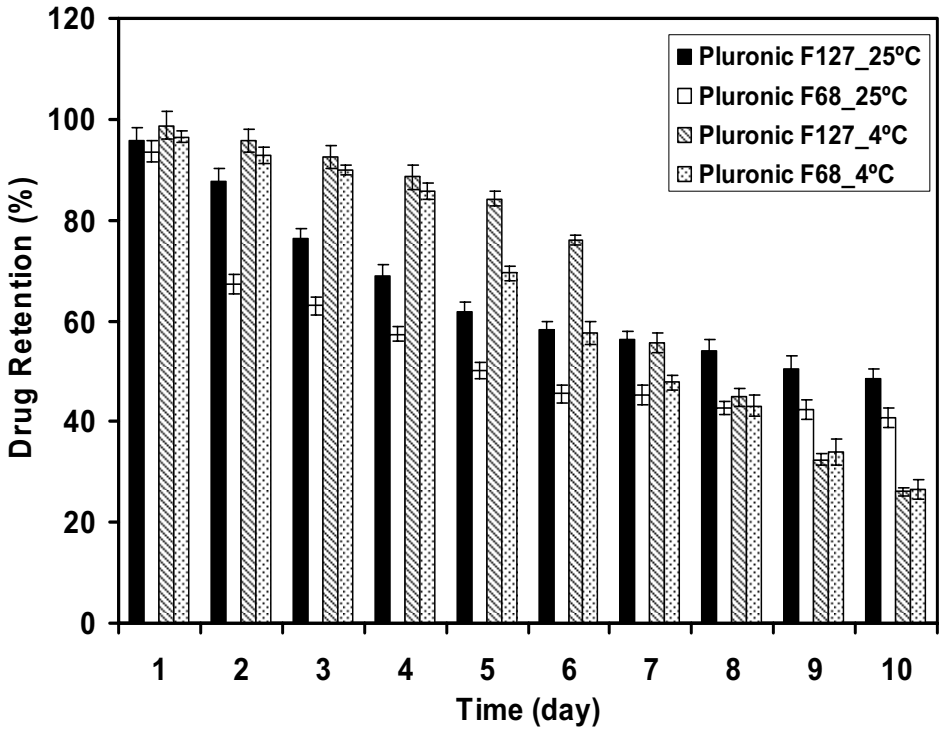

Figure 3.5: Storage stability of curcumin encapsulated Pluronic micelles in aqueous solution form at 25ºC and 4ºC.

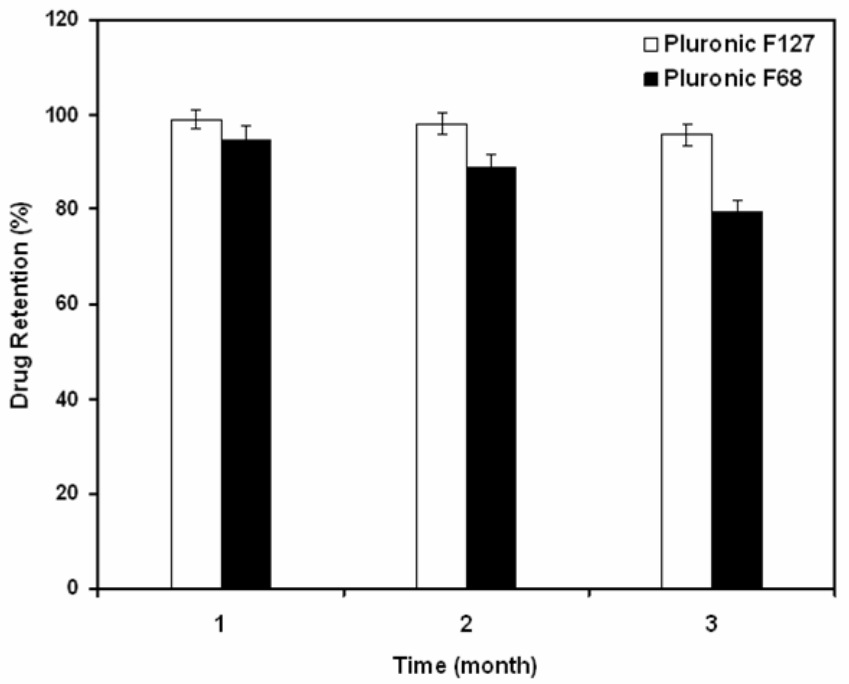

Figure 3.6: Storage stability of lyophilized curcumin encapsulated Pluronic micelle formulation at 4ºC.

3.3.5 *In vitro* cytotoxicity and cellular uptake studies

The pluronic copolymers did not showed cytotoxicity. Four different concentrations i.e. 1, 2.5, 5 and 10 mg/ml of both the copolymers were used to evaluate the cytotoxic activity of empty nanocarriers. Cell viability greater than 95% was observed for concentration of 1 and 2.5 mg/ml for both the polymers whereas in case of 5 mg/ml concentration the survival was more than 90%. But the cell viability reduced to near 85% when 10 mg/ml concentration of the polymers used (Figure 3.7). The *in vitro* cytotoxic activity of Pluronic based formulations of curcumin showed almost similar cytotoxicity when compared to free curcumin against HeLa cells. Dose dependant cytotoxicity of curcumin was observed in all the cases whether drug is in encapsulated form or in free form (Figure 3.8). The IC_{50} of free curcumin was found to be 14.32 μM whereas IC_{50} of Pluronic F127 and F68 micelle encapsulated curcumin was calculated to be 17.45 μM and 16.01 μM respectively.

Fluorescence microscopy was employed to visualize the cellular internalization of curcumin loaded Pluronic micelle nanocarriers using intrinsic green fluorescence of the drug molecules. In the microscopic images (taken after 4h of incubation) strong green fluorescence was observed inside the HeLa cells (Figure 3.9). After 48h of incubation the cellular morphology changed completely (Figure 3.10). Most of the cells were dead, fragmented and detached from the substratum. The green fluorescence from curcumin was still observed inside the floating dead cells. No fluorescence was observed in case of control cells treated with Pluronic micelles without curcumin.

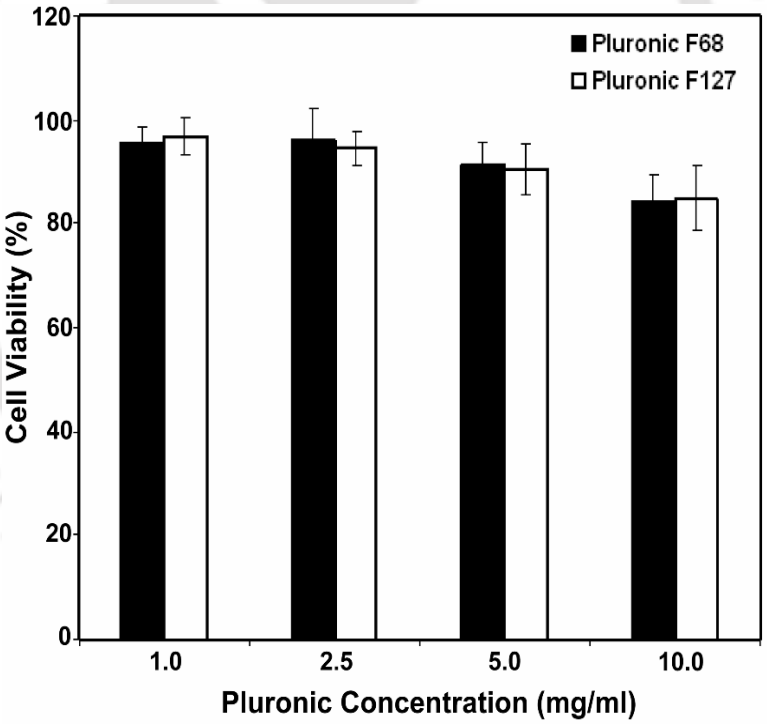

Figure 3.7: *In vitro* cytotoxicity of empty Pluronic micelles against HeLa cells. The cell viability was determined by MTT assay after treatment for 48h. Both the copolymers showed good cytocompatibility upto concentrations of 5 mg/ml.

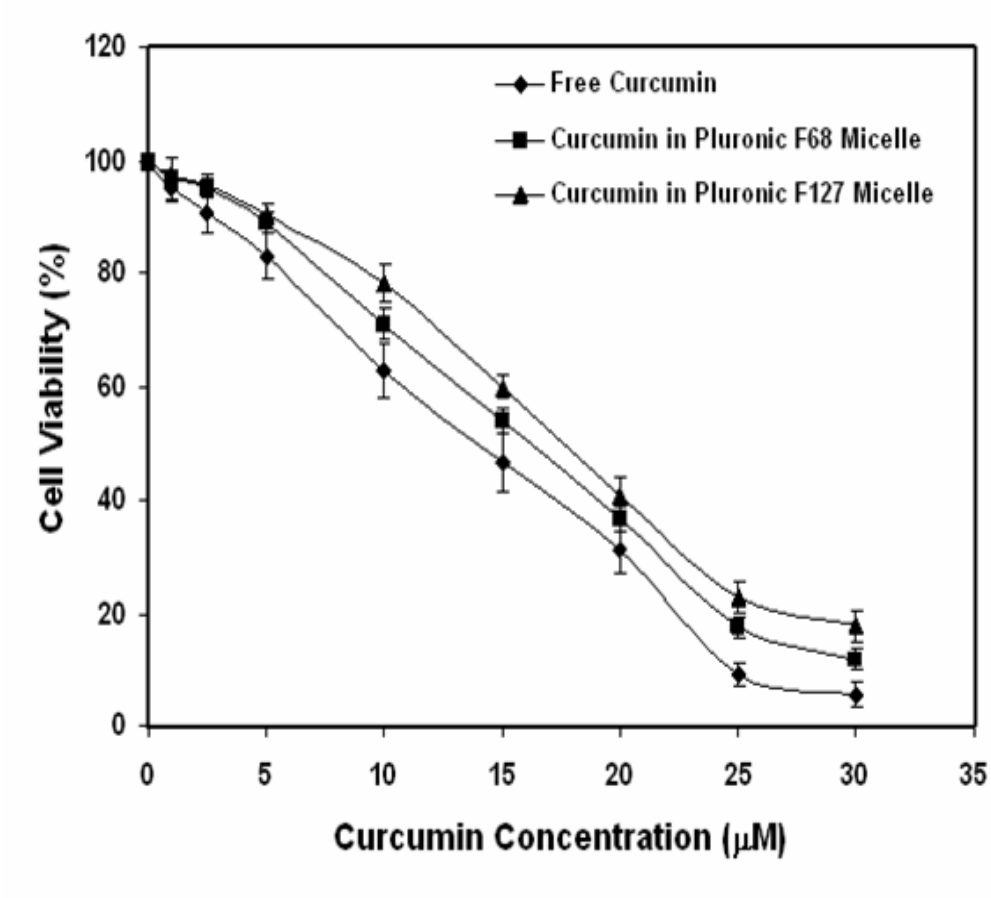

Figure 3.8: *In vitro* cytotoxicity assay of free curcumin and curcumin encapsulated in Pluronic micelles against HeLa cells.

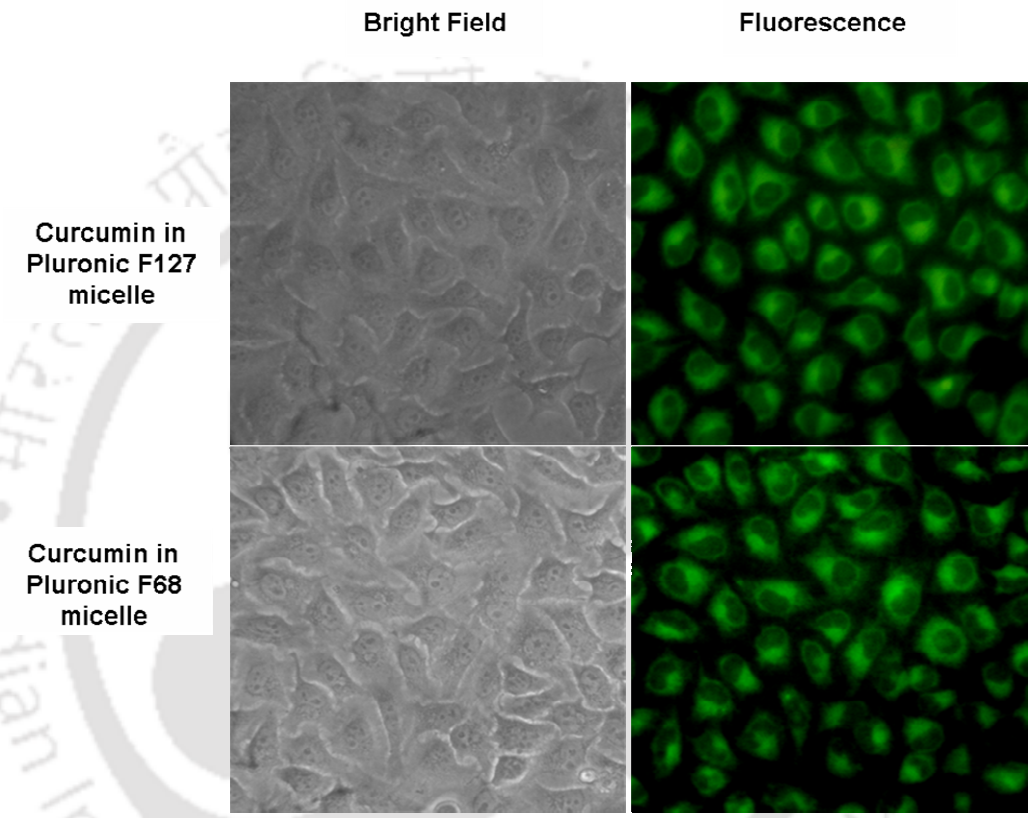

Figure 3.9: Fluorescence microscope images of HeLa cells incubated with curcumin encapsulated in Pluronic F127 and F68 micelle nanocarriers at 37 ºC for 4h. Intracellular green fluorescence of curcumin can be observed clearly, which confirms the uptake of drug loaded micelle nanocarriers by the cancer cells.

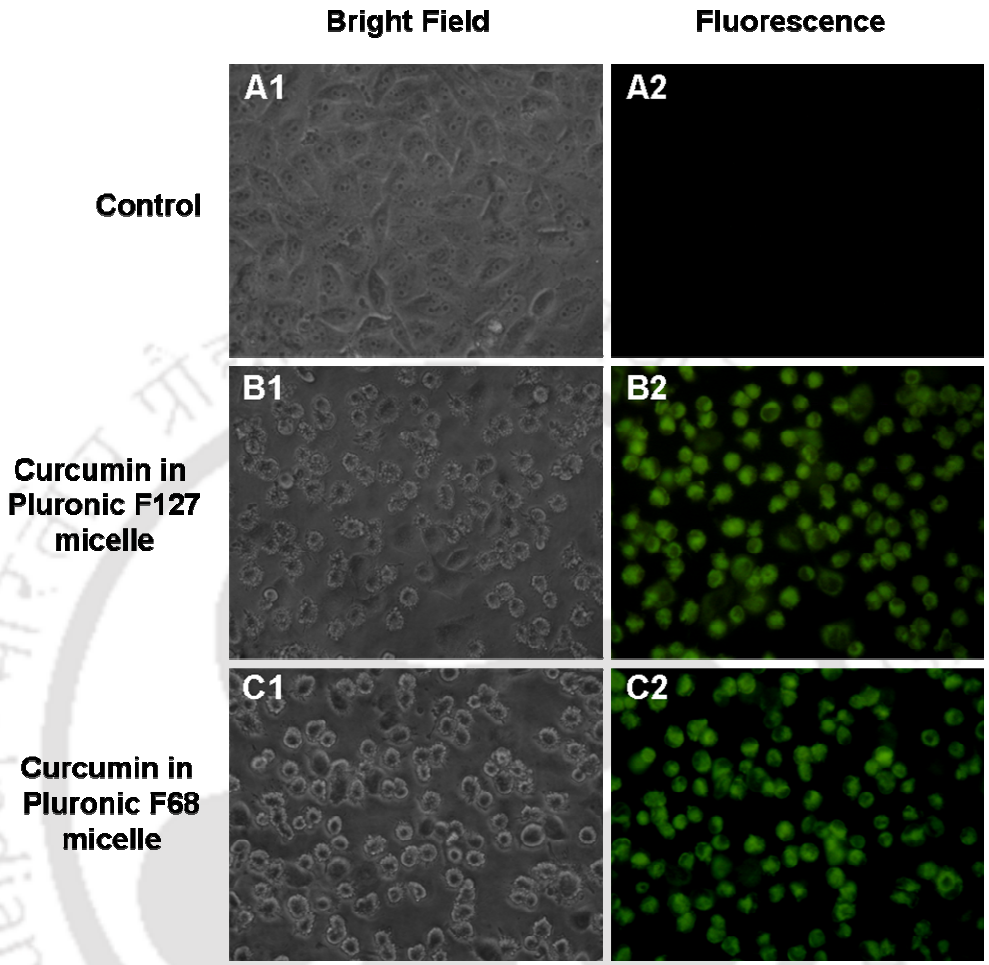

Figure 3.10: The morphological change in HeLa cells after treatment with drug encapsulated Pluronic micelles. The cells were seeded in 35 mm culture dish treated with 20 μM of curcumin encapsulated in Pluronic for 48h. The cells were photographed in culture condition using 40X objective. (A) Control cells, (B) Cells treated with curcumin encapsulated in Pluronic F127, (C) Cells treated with curcumin encapsulated in Pluronic F68.

3.4 Discussions

Curcumin is a potential anticancer drug but the lack of solubility has hindered its progression into clinical trials and this has been a major limitation in developing patient friendly formulations of this molecule for clinical applications. Development of new effective drug delivery system (DDS) for curcumin is one of the most important goals in present-day chemotherapy. Encapsulation of curcumin in commercially available and pharmaceutically acceptable Pluronic block copolymers may provide a formulation of this potential drug for chemotherapy.

The curcumin loading into the Pluronic micelles occurred through the partitioning of the hydrophobic drug within the core of the micelles formed by self-assembly of the tri-block copolymers in aqueous solution. Curcumin loaded into Pluronic micelle core by hydrophobic interactions. Our results showed that Pluronic F127 showed better encapsulation efficiency and higher loading percentage than Pluronic F68. Several of the major factors which influence the loading capacity and loading efficiency of block copolymer micelles are nature of the core forming block, core block length and total copolymer weight. The physical properties of both the pluronic copolymers used in the study are summarized in the Table 3.3. It shows that Pluronic F127 contains more number of hydrophobic PO units than Pluronic F68 and the ratio of hydrophobic PO to hydrophilic EO units are also higher in case of Pluronic F127. In the hydrophobic PO chain of Pluronic block copolymers, there is one $–CH_3$ group present per monomer, which is the main interaction site between a hydrophobic drug and micelle core. As, Pluronic F127 contains more hydrophobic sites than Pluronic F68 in its micelle core-forming block, so it acts as a better solubilizing agent for hydrophobic curcumin molecules. Physical properties of nanocarriers such as shape and size are important parameters for their *in vivo* fate and utility

as drug carrier. Curcumin loaded micelle nanostructures formed by self-assembly of Pluronic F127 and F68 were spherical with diameter below 100 nm, which were consistent with the results reported by others. The small size of the curcumin loaded Pluronic micelles allow more extravasation from circulation and distribution of drug into the tumor mass, which make these nanocarriers ideal candidate for passive targeting of solid tumors tissue sites by enhanced permeation and retention (EPR) effect (Maeda, 2001).

Table 3.3: Physical properties of Pluronic F68 and F127 block co-polymers.

	Pluronic F68	**Pluronic F127**
Mw (Da)	8400	12600
Average no. of EO units	152.7	200.5
Average no. of PO units	29.0	65.2
Total weight of EO units (Da)	6720	8820
Total weight of PO units (Da)	1680	3780
Ratio of PO:EO	0.25	0.43

The micelle-encapsulated curcumin shows distinct photophysical properties. The visible absorption spectra of encapsulated curcumin show slight differences from that of free curcumin. After encapsulation in micelle nanostuctures curcumin molecules showed enhanced absorbance but only marginal change in peak maxima. The evidence for the hydrophobic character of drug encapsulation in Pluronic core was achieved by fluorescence studies. Fluorescence properties of curcumin are strongly depends on the polarity of its

surrounding environment. Generally, the fluorescence peak maxima (λ_{max}) of curcumin molecules shifts to a shorter wavelength and fluorescence intensity increases as the polarity of surrounding environment decreases. The fluorescence intensity of curcumin in Pluronic F127 was higher than Pluronic F68 and also the blue shift was more in case of Pluronic F127. This blue shift in curcumin peak fluorescence emission toward lower wavelength is indicative of partitioning of curcumin molecules from the aqueous medium into the more hydrophobic, low polarity environment. The difference in the peak position and intensity suggests that the curcumin molecules feels different non polar environment in the micelle cores. Although the micelle-forming block is same for both Pluronic F127 and F68 but their molecular weight varies. Also the CMC of Pluronic F127 is lower than Pluronic F68. These are the probable reasons for the difference in core polarity of the micelles.

The release of a lipophilic compound from core-shell micelle nanocarriers is largely dependent on the hydrophobic properties of the inner core and hydrophobic interaction between the drug and inner core. The stronger the interaction between the drug and the core-forming block, the slower the release of drug from micelle (Gao et al., 2008; Allen et al., 2000). The slow and sustained release of curcumin from Pluronic F127 micellar nanocarriers in compared to Pluronic F68 can be explained by the fact that curcumin molecules show greater interaction in case of Pluronic F127 micelles. This slow and sustained release profile of curcumin from Pluronic F127 micelles is advantageous because efficient chemotherapy requires that the anticancer drug concentration in the blood be maintained between the minimum effective therapeutic level and the maximum tolerable level for long enough periods. Based on regression coefficient analysis we concluded that the models of Higuchi and Power law were best fitted with drug release kinetics data for both type of micelles. This

analysis suggests that the predominant mechanism behind the drug release from the micelles was diffusion.

Storage stability of the drug formulations is important factor for commercial development of pharmaceutical products. We have evaluated the storage stability of curcumin formulation with two different Pluronic copolymers in aqueous as well as lyophilized form. In aqueous solution the formulation showed unsatisfactory results for long-term storage. This unstable nature of the aqueous solution of drug loaded Pluronic micelles can be explained by the unique nature of micellization of Pluronic block copolymers. Micellization of Pluronic copolymers are not only dependent on CMC but also strongly dependent on temperature because the hydrophobicity of PPO blocks changes with temperature (Bohorquez et al., 1999). It has been shown that the critical temperature range for Pluronic micelle formation is 25ºC to 40ºC. The CMC of Pluronic F127 and F68 become almost 100 times greater when temperature falls from 37ºC to 25ºC (Croy and Kwon, 2004) (Table 3.4). These higher CMC values of Pluronic block copolymers leads to lower stability of the formulations at 25ºC. At 4ºC the PPO block of Pluronic molecules becomes completely soluble in water and micelle disintegration occurs. So, when curcumin loaded micelle solutions were stored at 4ºC, micelles lost their intact structure due to solubilization of hydrophobic PPO blocks and drug precipitated.

Table 3.4: Critical micelle concentrations (CMC) of Pluronic F68 and F127 block co-polymers at different temperatures (25°C and 37°C).

	Pluronic F68	Pluronic F127
CMC at 25°C (M)	1.33×10^{-2}	7.19×10^{-5}
CMC at 37°C (M)	1.23×10^{-4}	8.73×10^{-7}

A freeze-drying process is a useful process to obtain a dry powder form for long-term stability and preserving the original properties of pharmaceutical and biological products. Formulation of curcumin in both the Pluronic copolymer was lyophilized without any addition of cryoprotectants and found to be more stable for long-term storage than aqueous form. The presence of long PEO chains in Pluronic micelles can act as cryoprotectants during lyophilization. So, the formulation can be freeze-dried easily and stored for months in the lyophilized form, with restoration of the original properties upon reconstitution in aqueous solution.

The pharmacological activity of drug molecules loaded physically or chemically in polymeric nanocarriers can be altered to some extent or entirely lost. The *in vitro* cytotoxicity of curcumin with two Pluronic micelle formulations was investigated and compared to that of the free drug through MTT assay on HeLa cells and results showed that encapsulated curcumin did not lose their anticancer effect. The curcumin incorporated Pluronic micelles showed lower cytotoxic behavior when compared with free curcumin itself. Such an increase in the IC_{50} of the micellar formulation of drug is likely because of the delayed and sustained release behavior of curcumin from the micelle core (Lee et al., 2007; Jeong et al., 2009). In case of *in vitro* cell dosing of free curcumin organic solvent DMSO was used for effective solubilization, which is not suitable for *in vivo* applications. The Pluronic encapsulated curcumin was used without any organic solvent, which provides greater opportunity for safe *in vivo* administration of the drug. However, polymeric micelles themselves did not significantly affect the survivability of tumor cells and showed good cytocompatibility. Almost 90% of tumor cells were survived at highest concentration of polymeric micelles. Strong fluorescence of curcumin was observed mainly in cytoplasm of the cells rather than the cell nuclei (Figure 3.9). It suggests that both the Pluronic micelles

are efficient nanovehicle to transport the drug molecules inside the cancer cells. After the transport to the cytoplasm the drug released from the carrier slowly and killed the cells (Figure 3.10).

3.5 Conclusions

In this chapter, we have described the development of micellar formulations based on Pluronic tri-block copolymers for increasing the solubility of lipophilic curcumin. The potential of Pluronic micelles as a nanocarrier for curcumin was evaluated by estimating the encapsulation efficiency, *in vitro* drug release and *in vitro* cytotoxicity of drug loaded micelles against HeLa cells. Curcumin encapsulated Pluronic formulations were successfully freeze-dried and reconstituted without addition of cryoprotectants. These preliminary in vitro results suggest that Pluronic micelle based nanoformulation may be a promising delivery system for curcumin for clinical application in cancer chemotherapy. But further *in vivo* studies are required to proof this hypothesis.

4.1 Introduction

Drug delivery systems based on food proteins hold much promise because of their biocompatibility and biodegradability (Chen et al., 2006). Caseins are the major milk proteins (~80% of total protein in milk) and naturally exist as colloidal particles called casein micelles (CM). Casein proteins have excellent emulsification, gelation and water binding properties and are widely used in food industry for various food products. Microspheres of casein prepared by glutaraldehyde cross-linking have been used for oral delivery of anticancer drugs such as doxorubicin, mitoxantrone etc (Willmott et al., 1992; Knepp et al., 1993). But the natural structure of casein micelle (CM) as such has not been used for drug delivery. Only recently researchers have used this natural protein micelle for drug or nutraceutical encapsulation. Huppertz et al (2007) prepared microgel and nanogel particles from casein micelles, whereas Semo et al (2007) used it as a natural nano-capsular vehicle for lipophilic nutraceutical vitamin D.

Milk casein micelles are part of the milk transport system whereby nutrients are passed from mother to suckling offspring. They are primary source of amino acids and calcium phosphates to neonates (Fox and Brodkorb, 2008). These micelles are almost spherical aggregates stabilized as colloidal suspension in milk and composed of four phosphoproteins namely α_{s1}-casein, α_{s2}-casein, β-casein and κ-casein. They are held together in micellar nanostructure by hydrophobic interactions and by bridging of calcium-phosphate nanoclusters (colloidal calcium phosphate, CCP) bound to phosphorylated serine residues of the casein side chains (De Kruif and Holt, 2003). CCP plays a crucial role in maintaining micellar integrity. Three of the caseins (α_{s1}, α_{s2}, and β-casein) contain centers of phosphorylation (at least 3 phosphoserine residues in close proximity) that can bind to the

amorphous CCP cluster, thereby forming a stabilizing protein shell. Both α_{s1} and α_{s2}-casein contain more than one phosphate center and can thus act as a linking agent between nanoclusters (Horne, 1986). The surface of the micelles is covered primarily with κ-casein, which provides a hydrophilic, charged and diffuse surface layer and stabilizes the micelles through intermicellar electrostatic and steric repulsion, similar to a polyelectrolyte brush (De Kruif and Zhulina, 1996) (Scheme 4.1). In this chapter we have studied the complexation of chemopreventive agent curcumin with the natural nanostructure of casein micelles and its application in drug delivery to cancer cells. The interaction between curcumin and casein micelle was investigated using steady-state fluorescence spectroscopy. The binding constant of the curcumin to the low polarity regions of CM was calculated from fluorescence data and the probable binding region of curcumin in CM were characterized. We also investigated the potential of CM as carrier of curcumin.

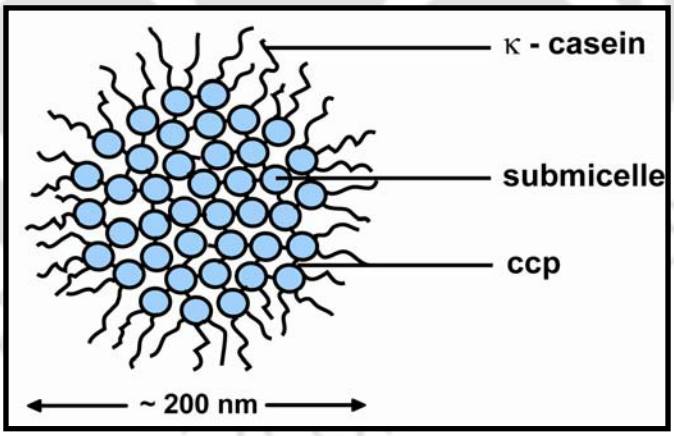

Scheme 4.1: Schematics of a single casein micelle (CM). The nanostructure of CM is made of several submicelles (small circles) which consist of hydrophobic αs_1-casein, αs_2-casein and β-casein. The submicelles are held together by colloidal calcium phosphate (CCP) which binds with phosphorylated serine residues of the casein proteins. κ-casein remains outside the micelle and act as polyelctrolyte brush to stabilize the CM.

4.2. Materials and Methods

4.2.1 Materials

Curcumin, MTT and casein hydrolysate was purchased from Himedia Laboratory (Mumbai, India). Calcium chloride and Tris-base were purchased from Merck (Mumbai, India). SDS-PAGE molecular weight markers were from Sigma (Bangalore, India). All other reagents used were of analytical grade.

4.2.2 Purification of casein micelles

Casein micelle was purified from fresh cow milk collected from local dairy according to Diaz et al (1996) with slight modifications. The milk was skimmed by centrifugation at 1500 g for 30 minute at 4ºC. The skimmed milk was stored at 4ºC with 0.05% (w/v) sodium azide to prevent microbial growth if not used immediately. Casein micelles were purified from skimmed milk by centrifuging at 25000 g for 30 minute at 20ºC. The pellet containing casein micelle was then redispersed in Tris buffer (10 mM, pH 7.4) containing 10 mM $CaCl_2$. This centrifugation redispersion process was repeated five times to wash out any whey proteins that are loosely adsorbed over the casein micelle surface. The casein content in the solution was measured by Bradford assay (Bradford, 1976) using bovine serum albumin (BSA) as standard.

4.2.3 Gel electrophoresis analysis

SDS-PAGE was carried out as described by Laemmli (1970) using a Bio-Rad mini gel electrophoresis unit. Total milk protein and isolated CM samples were loaded onto a 12%

gel and electrophoresed under constant current (20 mA). Proteins in the gel were stained using coomassie brilliant blue R-250. The gel was photographed using a gel documentation system (BioRad, USA).

4.2.4 Stability of casein micelle suspension

To determine the stability of the CM suspension upon dilution we measured "the wavelength (λ) dependence of turbidity (τ) of the suspensions", represented as (Gatti et al., 1999):

$$\alpha = -\left(\frac{d\log\tau}{d\log\lambda}\right)$$

Where, α was obtained from the slope of log τ vs log λ plots in the 400-800 nm wavelength range. Turbidity measurements were done using UV-visible spectrophotometer (Cary-100 Bio, Varian). Turbidity (τ) was calculated using the following equation (Pitkowski et al., 2008):

$$\tau = \ln\left(\frac{I_0}{I}\right)\frac{1}{L}$$

Where, I and I_0 were transmitted intensity and incident intensity of light respectively. L was the sample path length. In our case L was 1 cm. The measurements were done with freshly prepared samples.

4.2.5 Physical characterization of CM suspension

The size of CM solution was measured in a dynamic light scattering particle size analyzer (LB-550, Horiba, Japan) equipped with a 650 nm laser light source. Measurements were carried out at 90° scattering angle at room temperature.

Morphology evaluation of the CM was performed by scanning electron microscopy (SEM) and atomic force microscopy (AFM). For SEM analysis a drop of CM solution was placed on foil paper, air dried, coated with gold in a sputter coater (Quorum Technologies, UK) and observed under electron microscope (LEO 1430 VP, UK). For AFM analysis a drop of CM solution was placed over freshly cleaved mica surface and dried under nitrogen stream. Images were taken in non-contact mode (Picoscan, Molecular Imaging, USA).

4.2.6 Fluorescence Spectroscopy

The binding of curcumin with casein micelles was quantified by fluorescence spectrophotometry. Steady state fluorescence measurements were carried out in a Spex FluoroMax-3 spectrofluorimeter (HORIBA Jobin Yvon Inc, USA). The fluorescence of curcumin was measured by keeping its concentration constant at 5 μM and varying the CM concentration from 0 to 20 μM. The emission spectra were recorded from 450 to 700 nm with an excitation wavelength of 420 nm. The slit widths were 2 and 5 for excitation and emission respectively. CM solutions without curcumin were used as controls for fluorescence measurements.

Protein intrinsic fluorescence was measured at constant CM concentration (10 μM) in the presence of 0, 1, 1.5, 2, 2.5, 3, 3.5, 4, 4.5 and 5 μM curcumin. Emission spectra were recorded from 300 to 450 nm (at an excitation wavelength of 280 nm) and from 315 to 450 nm (at an excitation wavelength of 295 nm) individually. In this case free curcumin solutions without CM were used as control and fluorescence was recorded similarly.

In both cases the fluorescence spectra of controls were subtracted from respective spectra of samples to cancel out any contribution due to Raman peak and other scattering artifacts. For

calculation of binding constant, corrections for inner filter effect was made using the following equation (Gatti et al., 1998):

$$FI_{corr} = FI_{obs} \times 10^{-0.5(\mathrm{Aex}+\mathrm{Aem})}$$

Where FI_{corr} is the corrected fluorescence intensity and FI_{obs} is the background subtracted fluorescence intensity of the sample. A_{ex} and A_{em} are the measured absorbance of the samples at the excitation and emission wavelengths, respectively.

To study the binding of curcumin to the submicelles, casein submicelle solution was prepared by dissociating CM with 0.1M sodium citrate. The dissociation of CM was confirmed by reduction in turbidity of the suspension (Panouillé et al., 2004). Curcumin was added to this solution at a final concentration of 5 μM. The same concentration of curcumin was also added to a solution of casein hydrolysate. The curcumin fluorescence was recorded in both the solutions as above and compared with that of intact CM solution.

4.2.7 Cell Culture and cytotoxicity assay

Human cervical cancer cell line HeLa was a gift from National Centre for Cell Sciences (Pune, India). Cells were maintained in DMEM containing 2 mM L-glutamine, 1.5 g/L sodium bicarbonate, 0.1 mM non essential amino acids and 1.0 mM sodium pyruvate supplemented with 10% FBS (heat inactivated) and 1% antibiotic-antimycotic solution (1000 U/ml penicillin G, 10 mg/ml streptomycin sulfate, 5mg/ml gentamycin and 25 μg/ml amphotericin B). Cells were cultured at 37°C in a humidified atmosphere supplied with 5% CO_2.

The cell viability was assessed by MTT assay, which is based on the reduction of MTT by the mitochondrial dehydrogenase of live cells to a purple formazan product (Mosmann, 1983). HeLa cells ($1x10^4$) were seeded in a 96-well plate (CellBind, Corning, USA). After 24 h of growth the medium was exchanged by the medium containing each of the following substances: empty CM, free curcumin and CM-curcumin complex. The curcumin stock solution (5 mM) was prepared in ethanol. From the stock solution, aliquots of curcumin were rapidly added to the culture medium to give the final concentrations of free curcumin. In case of CM-curcumin complex, the stock curcumin was diluted with CM solution in culture media. After 48 h treatment, media were removed and cells were washed with phosphate buffer saline (PBS). Then 100 µl of MTT (0.5 mg/ml) in culture medium was added to each well and incubated for 4 h at 37 ºC. After incubation the media was removed and 100 µl of DMSO was added in each well to solubilize the formazan crystals. Amount of formazan formed in each well was determined by measuring the absorbance at 570 nm using a multiwell plate reader (Biorad Microplate Reader, Model 680, CA, USA). The cell viability was calculated by following equation:

$$\text{Cell Viability (\%)} = \left(\frac{A_{treated}}{A_{control}}\right) x\ 100$$

Where, $A_{treated}$ was the absorbance of the treated cells and $A_{control}$ was the absorbance of untreated cells. The IC_{50} was measured as the concentration of drug at which 50% cells were viable in comparison with that of the control.

4.2.8 Cellular uptake of curcumin

HeLa cells were seeded in a 24 well plate at a seeding density of $1x10^4$ cells per well in 1 ml of growth medium and allowed to attach for 24 h. For the studies of concentration dependent uptake, cells were treated with equivalent dose of free curcumin and CM-curcumin complex and incubated for 4 h. After the incubation, media was removed and cells were washed twice with PBS. To extract curcumin, cells were lysed by adding methanol. The cell lysate was centrifuged at 10000 rpm for 10 minute at 4ºC. Curcumin content in the supernatant was measured using fluorescence spectrophotometer (λ_{ex} = 420 nm and λ_{em} = 540 nm).

4.2.9 Microscopic study

The effect of CM-curcumin complex on the morphology of HeLa cells was assessed by microscopy. Cells were seeded onto 35 mm culture plates (CellBind, Corning, USA) and incubated for 24h for attachment and then treated with CM-curcumin complex containing 30 μM curcumin. Control experiments were carried out by treating similarly plated cells with CM alone. The plates were taken out from the incubator at different time intervals and observed under inverted phase contrast microscope (Eclipse TS100, Nikon, USA) with 40X objective. Photographs were taken by a digital camera (Coolpix 5400, Nikon, USA) attached with the microscope. Simultaneously, fluorescence was observed by excitation with blue filter.

4.3. Results

In SDS-PAGE analysis the gel showed four distinct bands in the lane of casein micelle with molecular weight ranging from 26 to 37 kDa whereas, in the lane of skimmed milk many other bands were clearly visible (Fig 4.1). Although the molecular weights of different caseins are in the range of 19.0-25.0 kDa, they have been reported to behave abnormally in Laemmli gels (Basch et al., 1985). We observed that, our result was similar to that of Vincenzetti et al (2008) and for the stoichiometric calculations we have taken the average molecular weight of the caseins to be 23.5 kDa according to Gatti et al (1995).

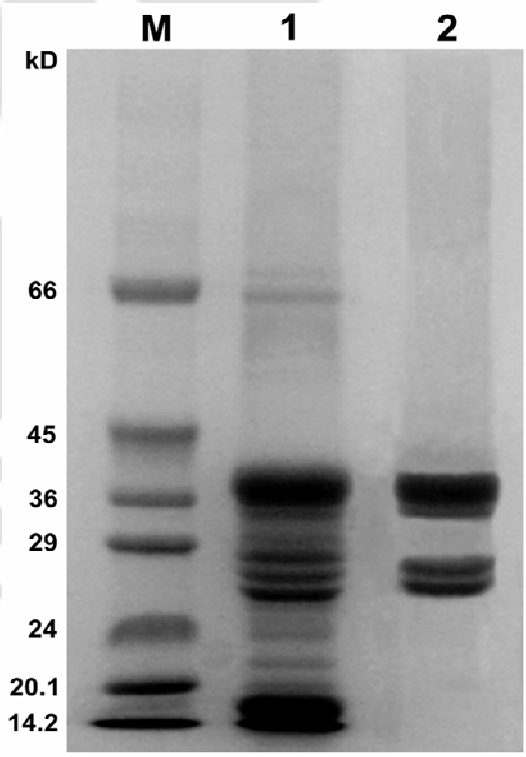

Figure 4.1: SDS-PAGE of molecular weight marker (Lane M); skimmed milk (Lane 1) and purified casein micelle (Lane 2): the 4 distinct bands with molecular weight ranging from 37 to 26 kDa belongs to αs1-casein, αs2-casein, β-casein and κ-casein respectively.

Isolated micelles were redispersed as suspension in tris buffer (pH 7.4) containing 10 mM $CaCl_2$. Ca^{+2} are necessary for stable CM suspension preparation (Gatti et al., 1995). The turbidity (τ) of purified CM suspension was determined at 400 and 600 nm with different CM concentrations. We observed a linear increase of τ with CM concentration at both the wavelength (Fig 4.2A). The wavelength dependence of turbidity (α) measurements is shown in Fig 4.2B, where the value of α remained nearly constant with the change in CM concentrations.

The size of the casein micelles measured by DLS revealed that the mean diameter of the protein particles was 166.3 (± 33.1) nm (Fig.4.3). SEM and AFM analysis showed that the nanoparticles were roughly spherical in shape (Fig. 4.4 and 4.5). SEM and AFM data were in good agreement with the DLS measurement. The morphology and size of CM-Curcumin complex was similar to that of free CM.

The baseline spectrum of CM suspension showed high absorbance values because of the high degree of Rayleigh scattering present in the samples (Fig 4.6A). To get the spectra of curcumin a difference spectrum was generated by subtracting the CM suspension spectrum from CM-curcumin spectrum. The difference spectrum revealed that the curcumin bounded to CM shows absorbance maxima at 424 nm (Fig 4.6B).

The binding constant was estimated from the increase of the fluorescence intensity of a fixed concentration of curcumin in the presence of increasingly added concentration of CM. There was a blue shift of the curcumin emission maximum and significant increase in fluorescence intensity with increasing concentration of CM (Fig.4.7). Fig. 4.8 represents the variations of curcumin fluorescence intensity with increasing CM concentrations. The plot shows that the fluorescence intensity of curcumin increased initially and gradually leveled off in the higher

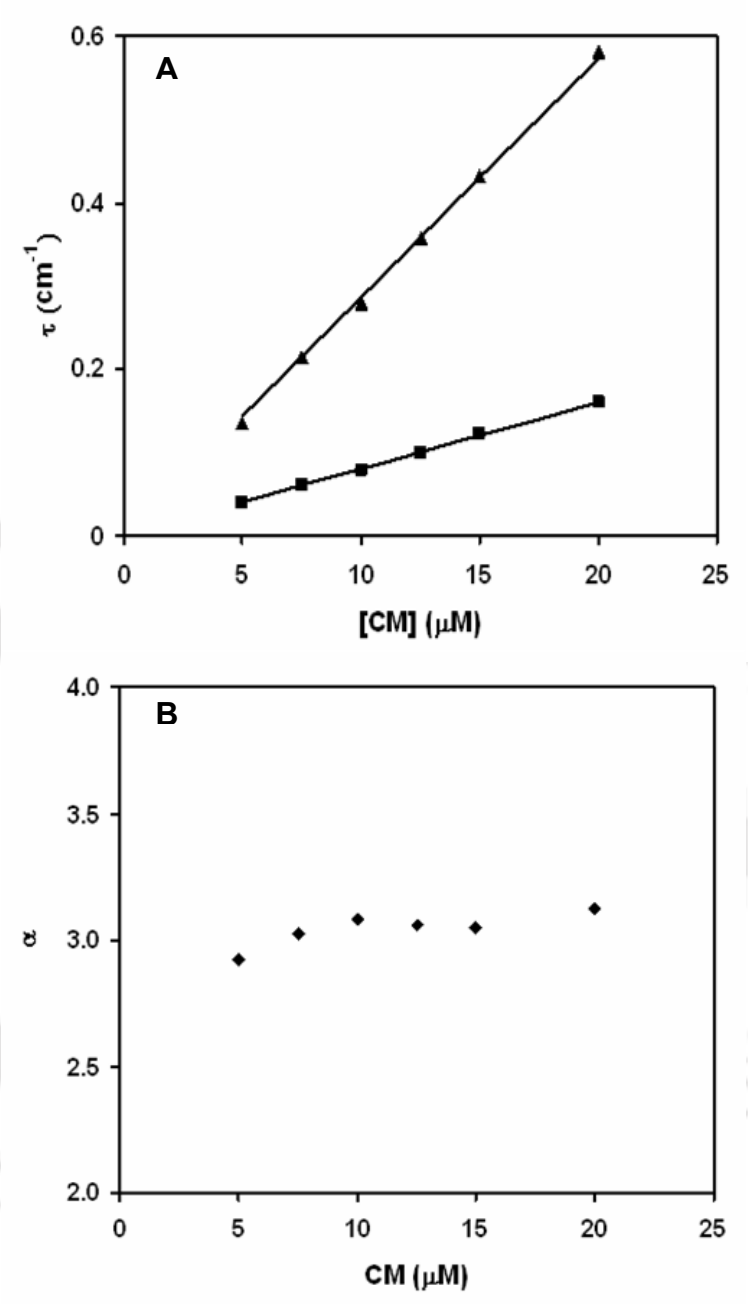

Figure 4.2: Stability of casein micelle (CM) suspensions in Tris buffer (pH 7.4) containing 10 mM $CaCl_2$. (A) Turbidity (τ) of purified CM suspension at wavelength of 400 nm (▲) and 600 nm (■) showing a linear change with different CM concentrations. (B) Change of α (wavelength dependence of turbidity) with different CM concentrations. The α value remained nearly constant.

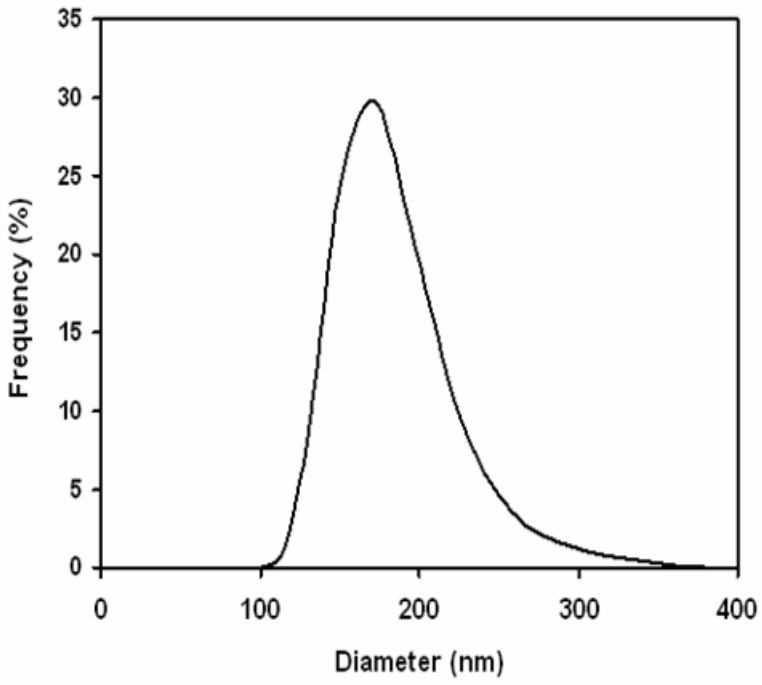

Figure 4.3: Size distribution of CM suspension measured by DLS. The average diameter of the CM particles was found to be 166.3 nm.

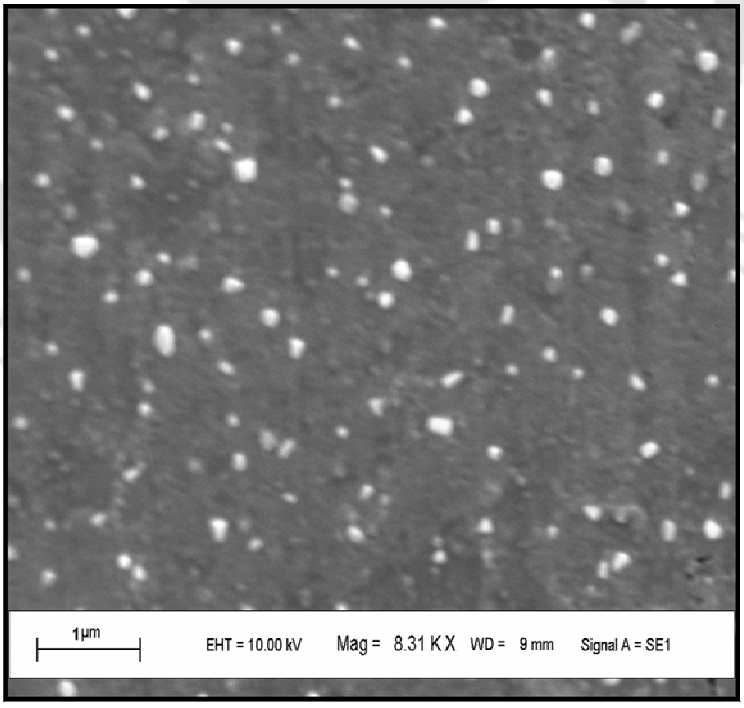

Figure 4.4: Observation of CM particles under scanning electron microscope (SEM).

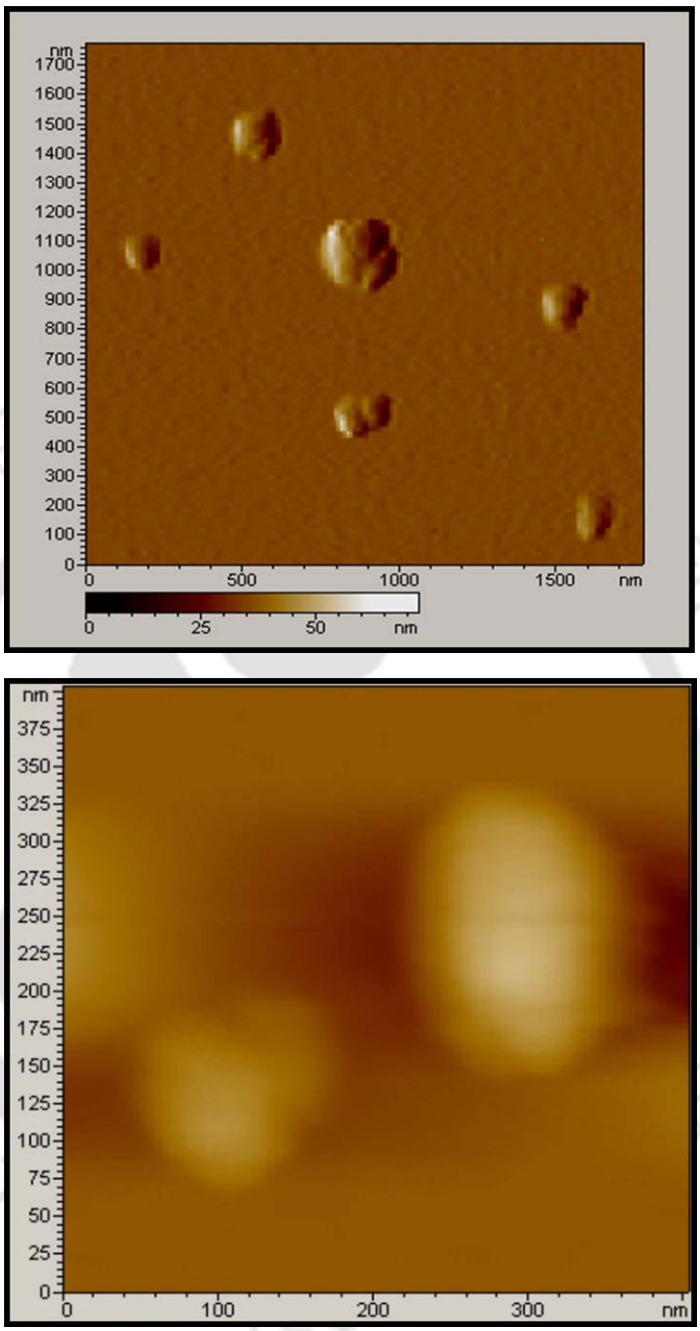

Figure 4.5: Morphology analysis of CM particles by AFM. Particles were almost spherical in shape with average size distribution of 200 nm.

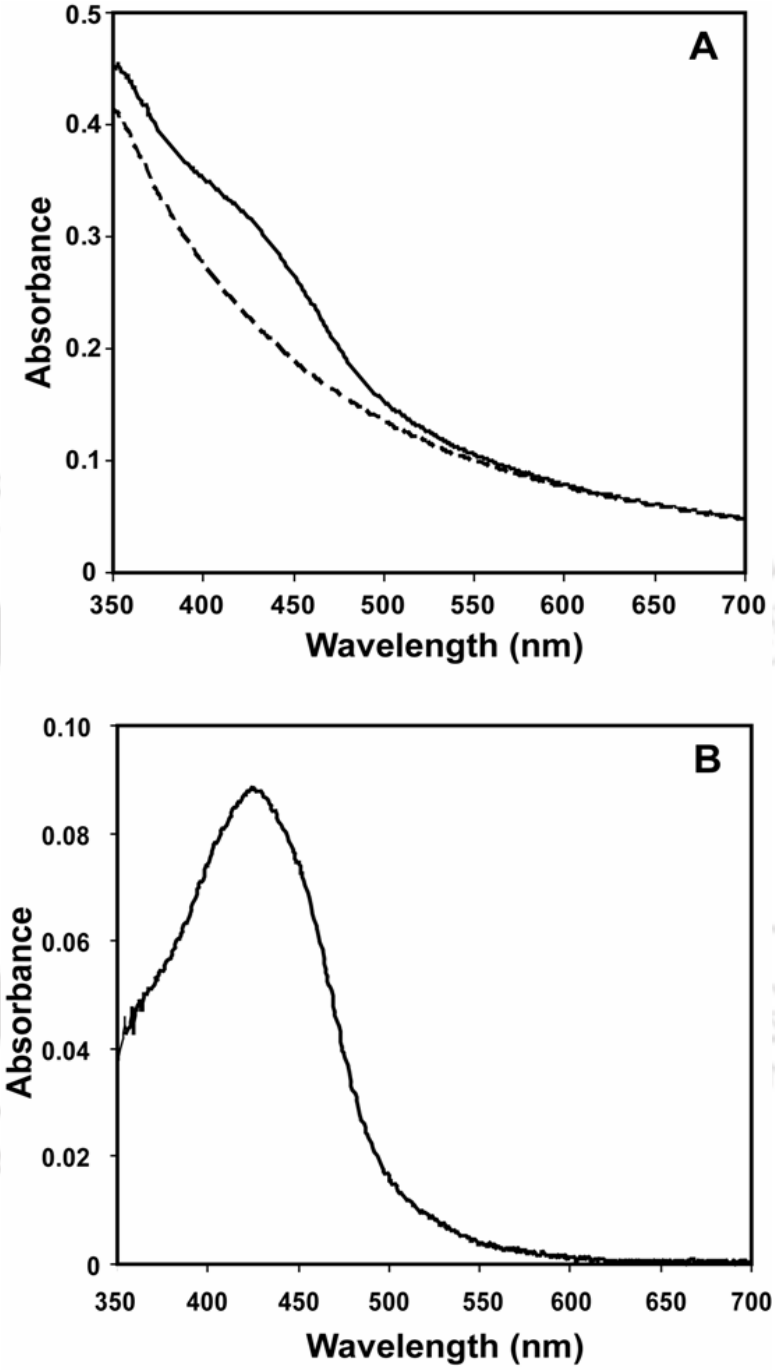

Figure 4.6: (A) Absorption spectra of CM suspension (broken line) and CM-curcumin complex (solid line). Difference spectra (B) revealed that the curcumin bound to CM shows absorption maxima at 424 nm.

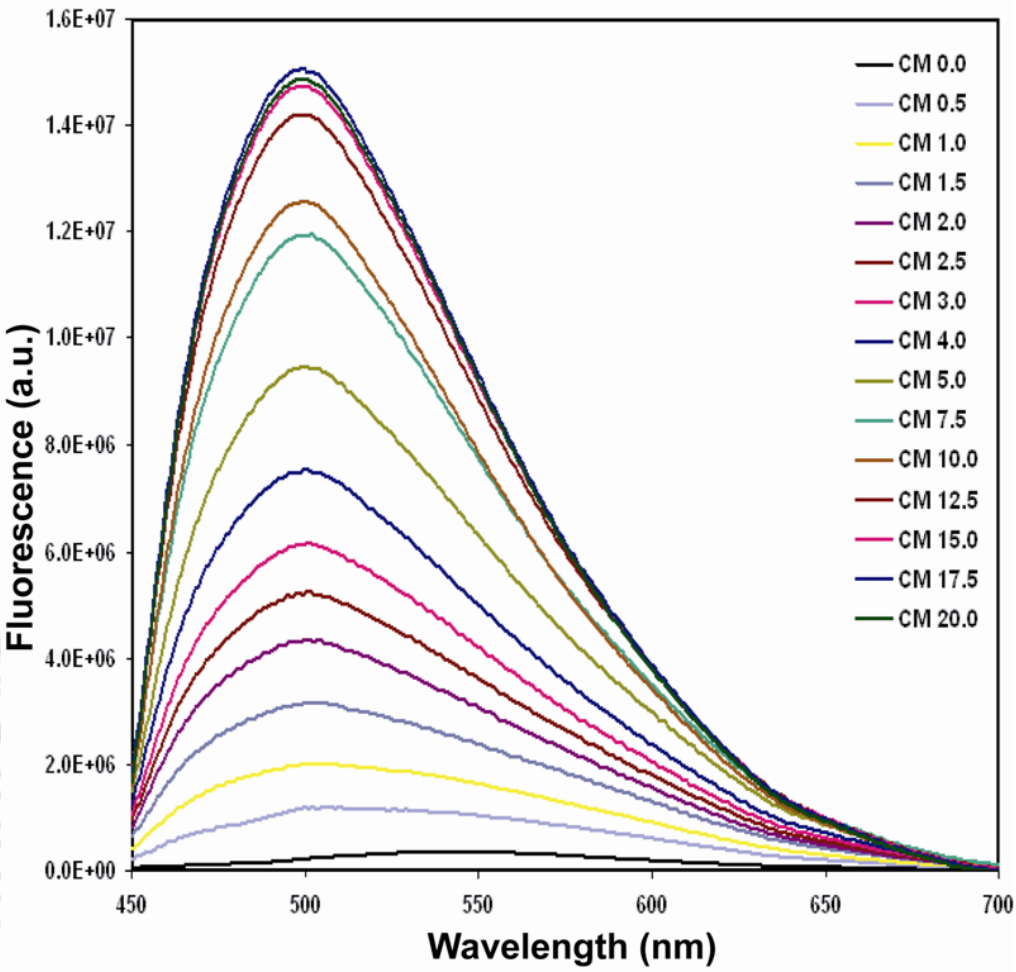

Figure 4.7: Fluorescence emission spectra of 5 μM curcumin in buffer solution (pH 7.4) in presence of CM at different concentrations (a) 0 (b) 0.5 (c) 1.0 (d) 1.5 (e) 2.0 (f) 2.5 (g) 3.0 (h) 4.0 (i) 5.0 (j) 10.0 (k) 12.5 (l) 15.0 (m) 17.5 and (n) 20.0 μM respectively. Excitation wavelength was 420 nm.

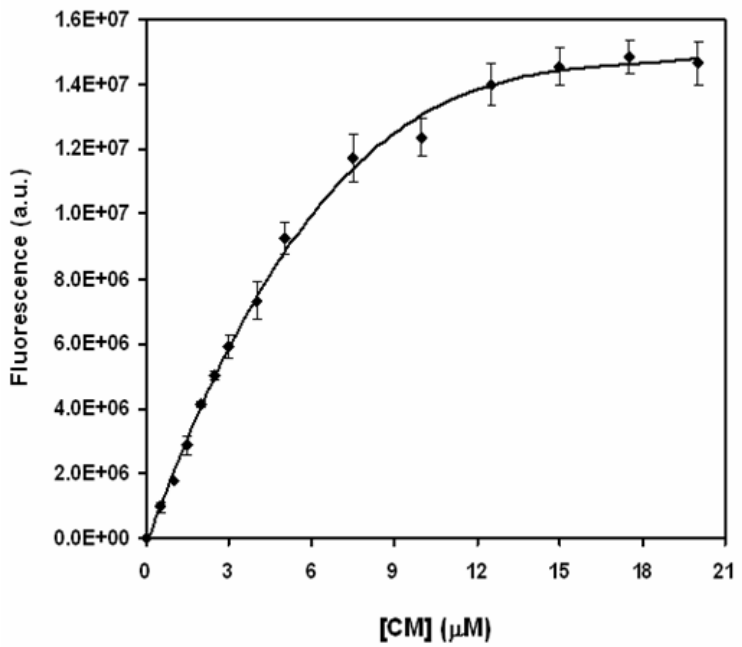

Figure 4.8: Change of curcumin fluorescence intensity at 500 nm in the presence of increasing concentrations of CM. It showed that 17 μM CM is required for saturation of 5 μM curcumin binding.

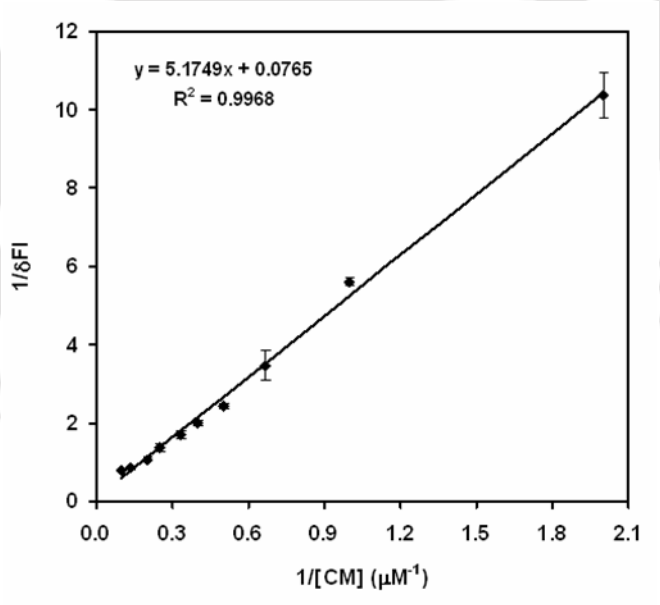

Figure 4.9: Double reciprocal plot of [CM] vs change in curcumin fluorescence intensity (△FI). Binding constant (K_b) was estimated to be 1.48 X 10^4 M^{-1} between curcumin and CM from the plot.

concentration of CM. The saturation concentration of CM required for complete binding of 5 μM curcumin was 17 μM. The binding constant was determined by the following equation (Gatti et al., 1995; Liang et al., 2008):

$$\frac{1}{\Delta FI} = \frac{1}{\Delta FI_{max}} + \frac{1}{K_b \Delta FI_{max}[CM]}$$

Where, ΔFI is the change of curcumin fluorescence intensity in the presence and absence of CM; ΔFI_{max} is the maximal change of curcumin fluorescence intensity; K_b is the binding constant and [CM] is the concentration of casein micelles.

The intensity data was used to plot the double reciprocal plot, 1/ [CM] vs $1/\Delta FI$ (Fig.4.9). The intercept of the double reciprocal plot on the $1/\Delta FI$ axis measures $1/\Delta FI_{max}$, which was used to calculate the binding constant from the value of slope in the plot. The binding constant was estimated to be 1.48 X 10^4 M^{-1}.

Intrinsic fluorescence of protein has been widely used to investigate the interaction and binding of drug molecules to proteins in solution. At the excitation wavelength of 280 nm, both tryptophan (Trp) and tyrosine (Tyr) residues have fluorescence emission but when the excitation wavelength is 295 nm, only the Trp residue shows a fluorescence emission. CM shows strong fluorescence emission with a peak at 342 nm upon excitation at 280 nm. Fig.4.10 shows the fluorescence emission spectra of CM suspension in the presence of different concentrations of curcumin with an excitation wavelength of 280 nm. The intensities of fluorescence emission of CM at 342 nm decreased gradually with the increase of drug concentration. When excited at 295 nm the CM solution showed fluorescence maxima at 344 nm. Fig. 4.12 shows the fluorescence quenching spectra of CM before and

after incubation with different concentrations of curcumin at an excitation of 295 nm. The quenching data were also analyzed according to the Stern-Volmer equation:

$$\frac{F_0}{F} = 1 + K_{SV}[Q]$$

Where, F_0 and F are the fluorescence intensities in the absence and presence of curcumin respectively, $[Q]$ is the drug concentration and K_{SV} is the Stern-Volmer quenching constant. The Stern-Volmer plot for CM fluorescence quenching by curcumin was shown in Fig. 4.11 & 4.13. The plot of F_0/F versus Q was found to be linear in both the cases i.e. for 280 and 295 nm excitation. The Stern-Volmer quenching constant (K_{sv}) was found to be $11.3X10^4$ M^{-1} (for 280 nm excitation and 342 nm emission) and $8.3X10^4$ M^{-1} (for 295 nm excitation and 344 nm emission). The Stern-Volmer quenching constant (K_{sv}) can be further expressed as:

$$K_{SV} = k_q X\ \tau_0$$

Where, k_q is the fluorescence quenching rate constant and τ_0 is the lifetime of the fluorophore in the absence of quencher. For, caseins the value of τ_0 is known to be approximately $4 X 10^{-9}$ s (Chakraborty and Basak, 2007). The k_q values for CM fluorescence quenching by curcumin was calculated from above equation and shown in Table 4.1.

Table 4.1: Quenching of CM fluorescence by curcumin.

Excitation wavelength (nm)	**K_{SV} (M^{-1})**	**k_q ($M^{-1}s^{-1}$)**
280	$11.3 X 10^4$	$4.52 X 10^{14}$
295	$8.3 X 10^4$	$3.32 X 10^{14}$

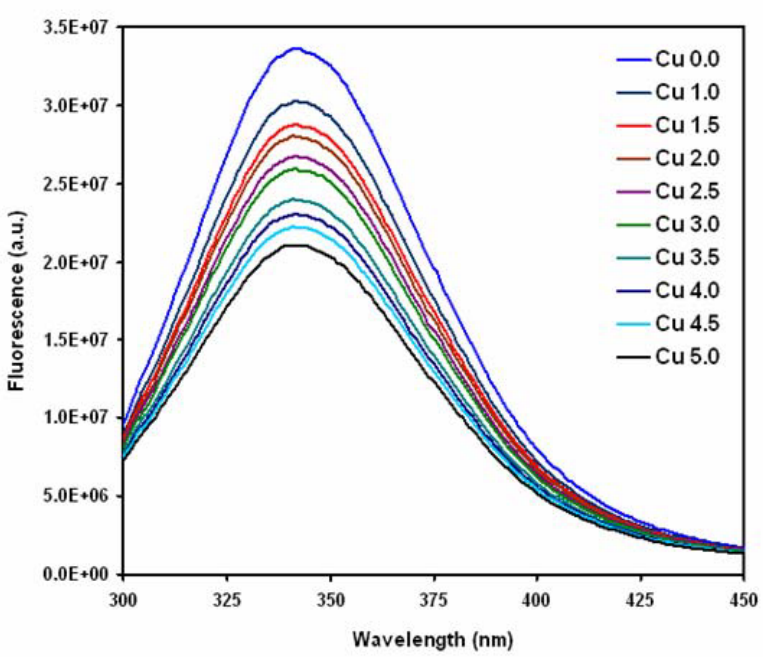

Figure 4.10: Quenching of CM intrinsic fluorescence by curcumin. Fluorescence emission spectra of CM suspension at excitation wavelengths of 280 nm in presence of (i) 0 (ii) 1 (iii) 1.5 (iv) 2.0 (v) 2.5 (vi) 3.0 (vii) 3.5 (viii) 4.0 (ix) 4.5 and (x) 5.0 μM curcumin respectively.

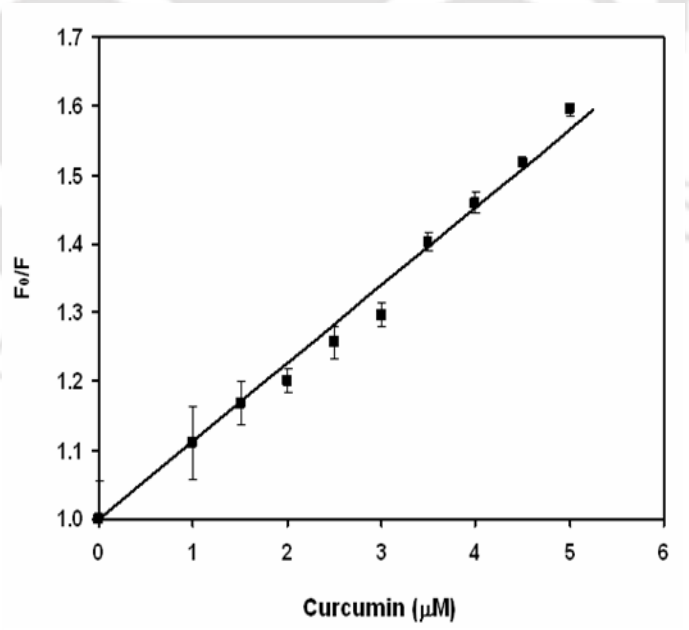

Figure 4.11: Stern-Volmer plot of protein fluorescence quenching when excitation wavelength was 280 nm.

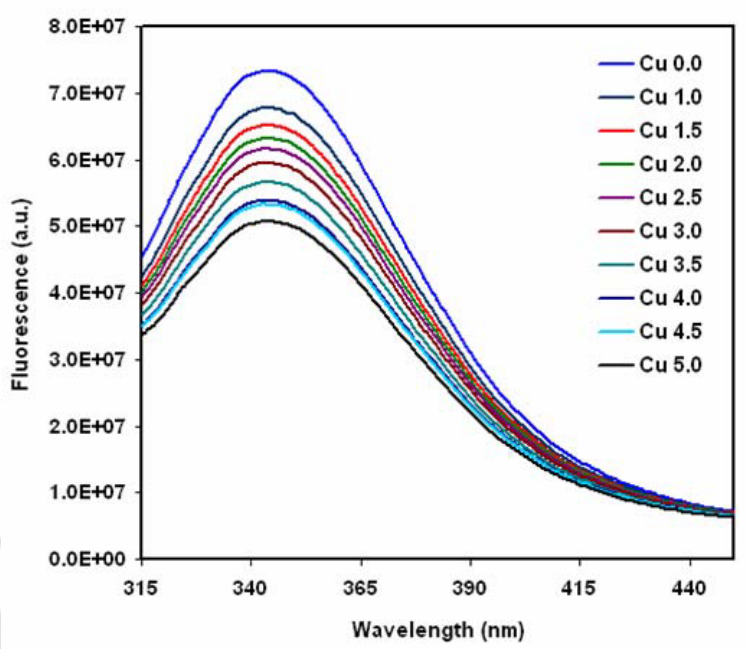

Figure 4.12: Fluorescence emission spectra of CM suspension at excitation wavelengths of and 295 nm in presence of (i) 0 (ii) 1 (iii) 1.5 (iv) 2.0 (v) 2.5 (vi) 3.0 (vii) 3.5 (viii) 4.0 (ix) 4.5 (x) 5.0 μM curcumin respectively.

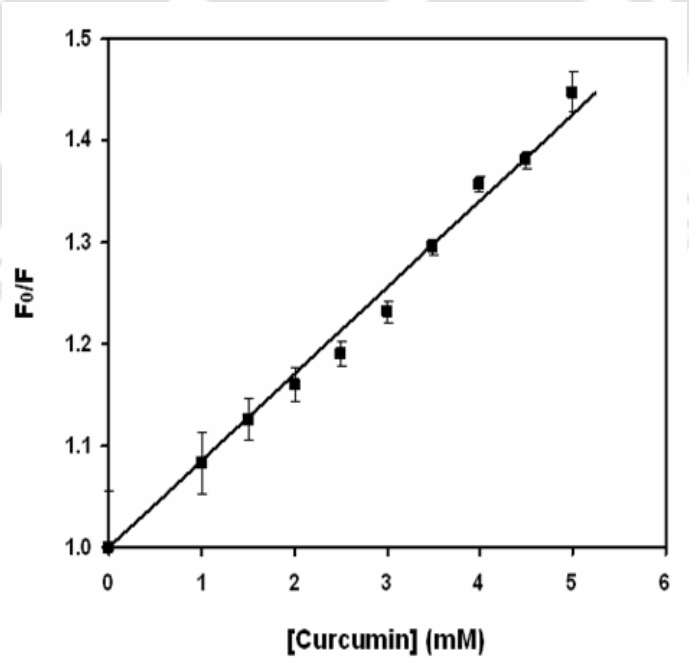

Figure 4.13: Stern-Volmer plot of protein fluorescence quenching when excitation wavelength was 295 nm.

To further investigate the binding of curcumin to CM, we studied the curcumin fluorescence with dissociated casein micelles and casein hydrolysate. Casein micelles dissociate into smaller subunits (average size of 10 to 20 nm) called submicelles after removal of CCP by chelating agent (Panouillé et al., 2004) (Scheme 4.2). The fluorescence of curcumin complexed with both dissociated and intact CM solution showed well defined peak at 500 nm (Fig 4.14). However curcumin added to a solution of casein hydrolysate, did not showed significant fluorescence intensity (Fig. 4.14).

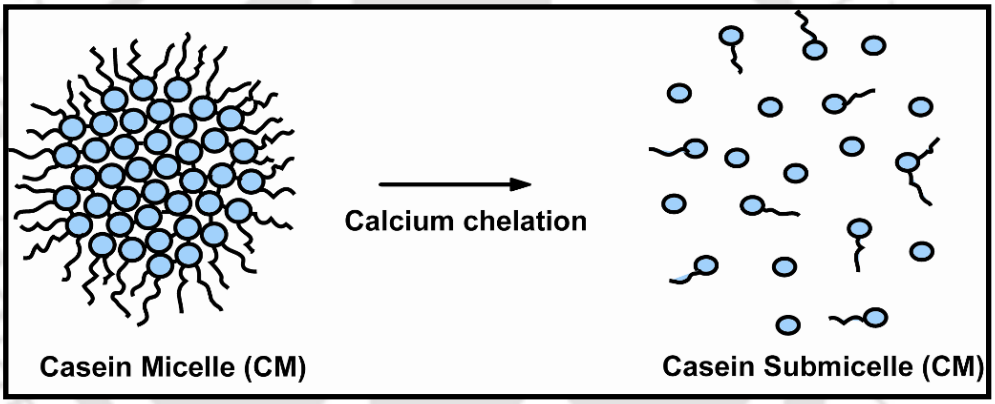

Scheme 4.2: Dissociation of casein micelle into submicelles by removal of CCP through calcium chelation.

To compare the cytotoxicity of free and CM bound drug, HeLa cells were exposed to a series of equivalent concentrations of free or CM-curcumin complex for 48 hours, and the percentage of viable cells was quantified using MTT assay. A dose dependent decrease in cell viability was noticed in both cases (Fig 4.15). CM-curcumin complex exerts a comparable cytotoxic effect with respect to free curcumin on HeLa cells at the same dose. The values of IC_{50} for CM-curcumin complex and free curcumin were found to be 12.69 and

14.85 μM respectively. This indicates that the curcumin remain active after complexation with CM. The cellular uptake study of free curcumin and CM-curcumin complex shows a concentration dependent increase in uptake (Fig 4.16).

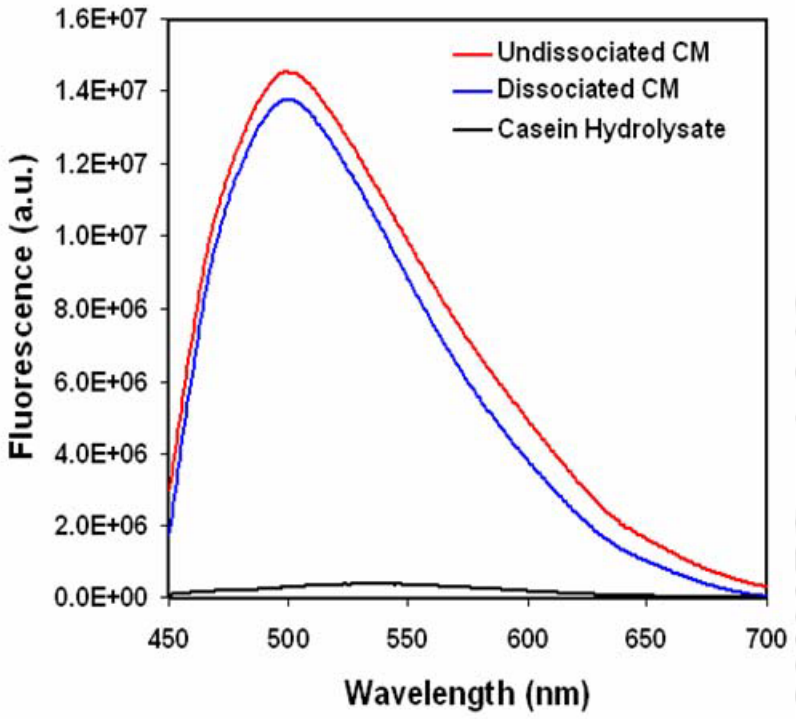

Figure 4.14: Fluorescence emission spectra of curcumin in presence of undissociated CM and dissociated CM showed high fluorescence intensity due to complexation by hydrophobic interactions and the same with casein hydrolysate showed poor fluorescence intensity due to lack of hydrophobic domains.

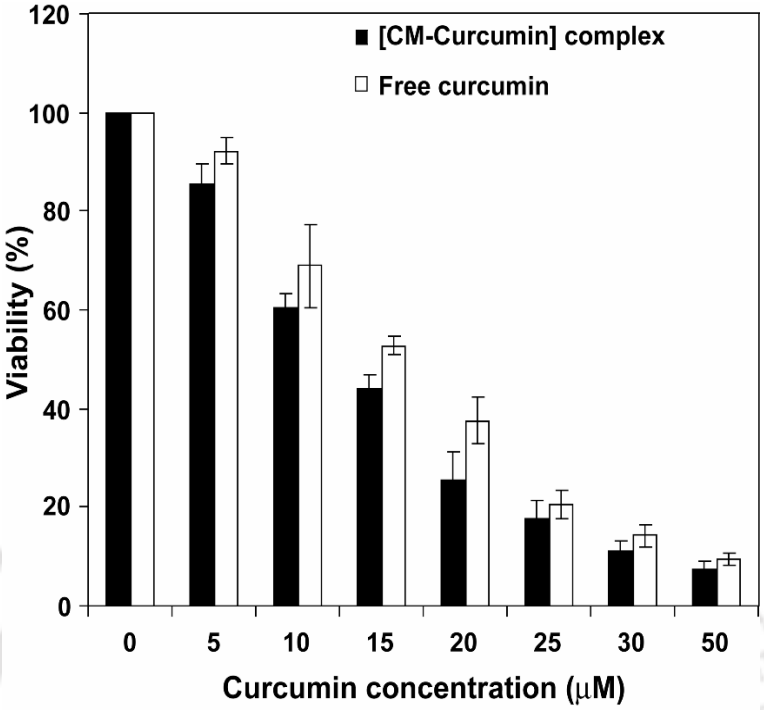

Figure 4.15: Cytotoxicity assay of free curcumin (□) and CM-curcumin complex (■) on *in vitro* cultured HeLa cells. CM-curcumin complex showed comparable cytotoxic effect to free curcumin.

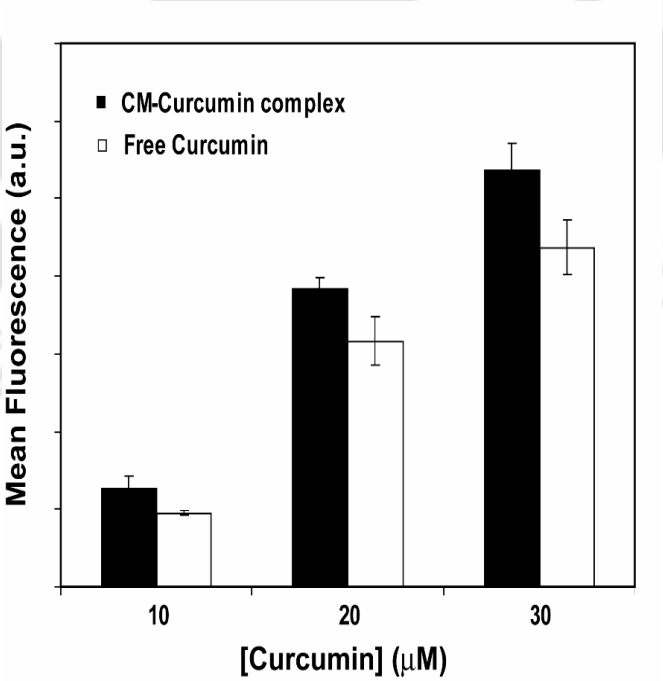

Figure 4.16: Cellular uptake study of CM-curcumin complex (■) and free curcumin (□) on *in vitro* cultured HeLa cells.

We examined morphological changes in the HeLa cells after treatment with CM-curcumin complex by microscopic observation. Intracellular green fluorescence of curcumin proves that the HeLa cells efficiently took up the CM-curcumin complex. The cells treated with the CM-curcumin complex underwent marked morphologic changes compared with the vehicle control (Fig 4.17). CM-curcumin treated HeLa cells underwent retraction of cellular processes and showed apoptotic characteristics such as cell shrinkage, membrane blebbing, rounding etc. with increase in incubation time (Fig 4.17B). When cells were treated with CM-curcumin complex for 24 h, cells displayed a rounded morphology and detached from the substratum (Fig 4.17B3). Following 48 h exposure, cellular fragmentation was extensive and few cells remained adherent (Fig 4.17B4). In contrast, control cells treated with CM without drug were well spread with flattened morphology shows nontoxicity of CM. We also observed the intracellular green fluorescence of curcumin in case of treated cells. No fluorescence was observed in case of control cells.

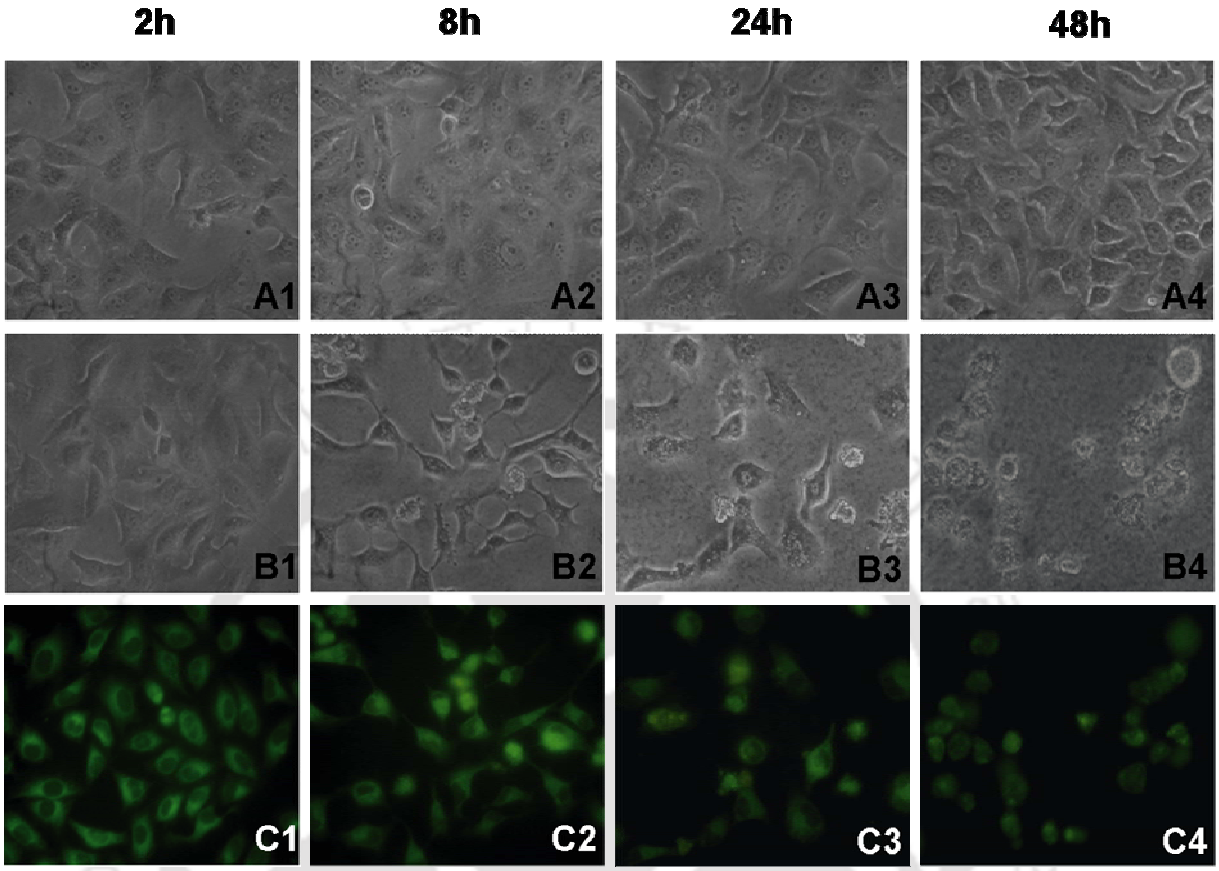

Figure 4.17: Microscopic observation of CM-curcumin complex induced morphological changes with time in HeLa cells. (A1-A4) Control cells treated with CM without drug showed no change of morphology with time. (B1-B4) Cells treated with CM-curcumin complex containing 30 μM curcumin exhibited marked morphological changes due to apoptosis. (C1-C4) Intracellular green fluorescence of curcumin revealed that the complex was efficiently internalized into the cells.

4.4 Discussions

The protein composition of isolated casein micelles was analyzed by SDS-PAGE. Four bands in the lane of CM corresponds to 4 casein proteins which forms the micelle structure together i.e. αs_1, αs_2, β and κ- casein. The whole skimmed milk showed more bands as whey proteins were present there. The SDS-PAGE confirms that no whey proteins were present in the purified CM suspension.

We have used α as the parameter to study the stability of CM suspension. The suspension is unstable if the size of the particles present in the solution changes with dilution. It has been reported previously that the values of α is related to CM size (Gatti et al., 1995 and 1999). Increasing values of CM size shows a decrease in α value. In our case, we observed that the value of α was nearly constant for different CM concentrations, suggesting that the purified casein micelles were stable against dilution in the buffer solution. The CM particles were found to be nearly spherical in shape and their average size was below 200 nm which is good for passive targeting of tumor tissues.

In our study we found that in the absence of CM when free curcumin was excited at 420 nm it showed a low intensity broad fluorescence peak at 540 nm in aqueous solution. Upon binding to CM the fluorescence spectrum of curcumin was blue shifted to a well-defined peak at 500 nm and intensity increased sharply as a function of CM concentration (Fig 6A). This observation was in good agreement with previous reports of interaction of curcumin with other proteins. The binding of curcumin to BSA and HSA showed fluorescence maxima at 510 and 500 nm respectively (Barik et al., 2003; Kunwar et al., 2006). The authors attributed this blue shifting of peak to the binding of curcumin into the hydrophobic domain of the protein molecules.

It is well documented in literature that casein micelles possess a great deal of hydrophobicity. Hydrophobic fluorescent probes such as ANS, nile red, pyrene and TNS binds strongly to the casein micelles through hydrophobic and electrostatic interactions (Gatti et al., 1995 and 199; Liu et al., 2007). Our observations suggest that curcumin molecules bind within the nonpolar regions of casein micelles through hydrophobic interaction. Curcumin has two phenolic OH groups with pK_a values at 8.38 and 9.88 in aqueous solution (Bernabé-Pineda et al., 2004). So, at pH 7.4 curcumin will be in the neutral from. Thus, binding due to charge interactions can be ruled out. The interaction of curcumin with CM can be represented as:

Curcumin + Casein Micelle (CM) = [CM-Curcumin] Complex

We used the change of curcumin fluorescence intensity upon binding to casein micelles to determine the binding parameters. This change in fluorescence intensity suggests that in the presence of CM the curcumin molecules are transferred from polar aqueous solution to the nonpolar hydrophobic domains of CM. The linearity of the plot suggests that curcumin interacts with CM suspension to form 1:1 complexes (Liang et al., 2008).

Addition of increasing concentration of curcumin caused a progressive reduction of the fluorescence intensity, but the maximum emission wavelength remains unchanged. This indicates that there is no change in the local dielectric environment of the Trp residues. The hydrophobic interior of casein micelles mainly consists of α_{s1} and β-casein. α_{s1}-casein contains two Trp residues at positions 164 and 199 where β-casein has one Trp residue at position 143 (Alaimo et al., 1999; Farrell et al., 2001). So, it is likely that curcumin molecules can bind any or all of these Trp residues. As casein micelles consist of mixtures of proteins and they are natively unfolded proteins, so it is difficult to predict the exact

position of binding of curcumin molecules. Since, the quenching of CM fluorescence by curcumin at 280 nm is more distinct than at 295 nm we suggest that apart from tryptophan residues, the tyrosine residues also involved in CM-curcumin interactions. The quenching process can be both static and dynamic. Static quenching occurs in the ground state by formation of non-fluorophoric dark complex in the presence of quencher and dynamic quenching occurs by the interaction of quencher with fluorophore in the excited state (Lakowicz, 2007). Our analysis showed that for excitation at 280 and 295 nm, the values for k_q obtained was in the scale of 10^{14} (Table 4.1). Since, the maximum values of k_q for a diffusion-controlled quenching process is about 2 X 10^{10} $M^{-1}s^{-1}$, the higher value obtained here suggests that the dominating quenching mechanism is static.

The low fluorescence intensity of curcumin in casein hydrolysate solution suggests that curcumin molecules are not present in sufficient nonpolar environment. As casein hydrolysate is composed of short peptides, they do not form aggregated structure with hydrophobic domains in aqueous solution. In contrast, the unique assembly of casein submicelles provides sufficient nonpolar environment to the bound curcumin molecules. This data further supports the possibility that in CM-curcumin complex, curcumin molecules were bound to the hydrophobic regions of CM, which are located in the submicelles. The uptake of CM-curcumin complex was comparable with the uptake of free curcumin at equivalent concentrations. Similar result was also obtained by Kunwar et al (2006) with human serum albumin (HSA) bound curcumin. This uptake profile explains the results of cytotoxicity assay and indicates that CM has the potential as delivery vehicle for hydrophobic drugs. Our results also suggest that the CM-curcumin complex was efficiently internalized by HeLa cells (Scheme 4.3) and produced cytotoxic effects (Figure 4.17). Thus

curcumin, which is poorly soluble in water, can be formulated in a nanosized colloidal system using CM.

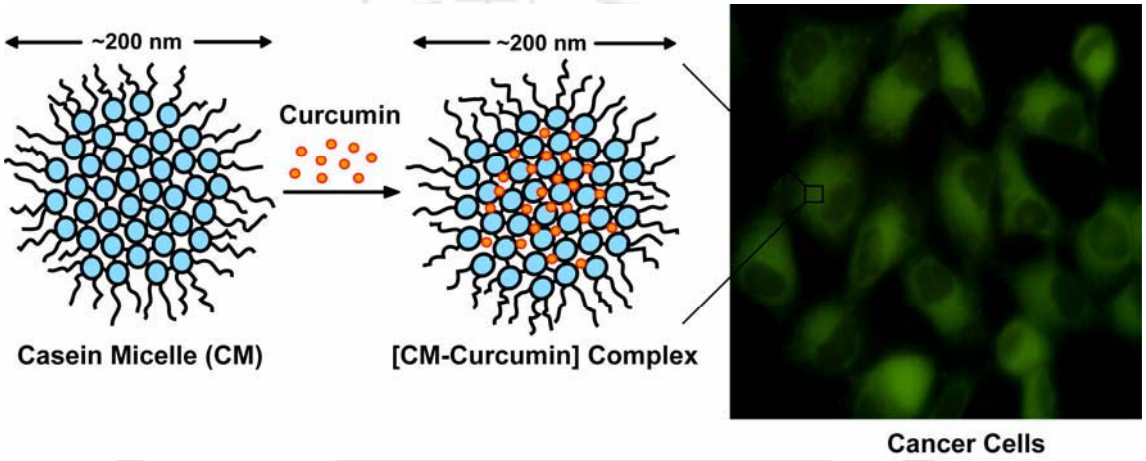

Scheme 4.3: Complex formation between curcumin and casein micelle (CM) and subsequent internalization of CM–curcumin complex to cancer cells.

4.5 Conclusions

In this study, we have prepared CM-curcumin complex, which can be an alternative drug formulation of curcumin for cancer therapy. We report for the first time the fluorescence spectroscopy study of the interaction between curcumin and casein micelles. It was observed that curcumin molecules interact with casein micelles by binding to the low polarity regions of CM. Under physiological buffer conditions the CM-curcumin yielded a nanoformulation, which exhibited similar cytotoxic effects on HeLa cells, compared with an equal dose of free curcumin. As casein is an edible protein, so the complex has potential as oral dose of curcumin; however, further studies are required to confirm this hypothesis.

Summary
&
Future Directions

SUMMARY

The present investigation was focused on the development of nanocarriers from polymeric materials for delivery of curcumin to cancer cells. We have used different polymers i.e. synthetic and natural for the preparation of nanocarriers. The curcumin encapsulation and the efficiency of as prepared nanocarriers were tested on *in vitro* cultured cancer cell line.

Synthetic mPEG-PA polymeric nanocarrier for curcumin delivery to cancer cells

We have prepared an amphiphilic polymer (mPEG-PA) by conjugating hydrophobic palmitic acid (PA) to the end of hydrophilic polymer mPEG in a single step reaction. The conjugation was carried out though ester linkage which is degradable inside the cells by the action of enzymes such as esterase. The synthesis of the mPEG-PA conjugate and presence of ester linkage was confirmed through ^{1}HNMR and FT-IR spectroscopy. mPEG-PA can self-assemble in aqueous solution to form micelle nanostructures. The micelleization of the conjugate was studied by fluorescence spectroscopy using pyrene as a fluorescent probe and the CMC of the conjugate was calculated to be 0.12 g/L. The structures of the self-aggregated micelles were spherical with average size below 50 nm as obtained by AFM and DLS studies. The micelle nanocarrier successfully encapsulated curcumin in its hydrophobic core and produced clear orange color solution. The encapsulation was also confirmed by enhanced blue shifted fluorescence spectrum of curcumin in the aqueous micelle solution. Drug encapsulated mPEG-PA nanoparticles showed good pH stability in physiological condition (pH 7.4), in simulated gastric fluid (pH 1.2) and in simulated intestinal fluid (pH 6.8). In physiological pH (7.4), the nanocarriers were able to retain ~90% of loaded drug which is promising for the long circulation and passive targeting of tumors by EPR effect. This conjugate is a potential model system for enzyme triggered drug release systems as

demonstrated by *in vitro* studies for enzyme-mediated degradation and release of encapsulated drug with lipase and HeLa cell lysate. The encapsulation of curcumin in mPEG-PA micelles did not affected its anticancer activity as the IC_{50} of free curcumin and encapsulated curcumin against HeLa cells was comparable.

Formulation of curcumin in Pluronic nanocarriers for cancer chemotherapy

We have also used commercially available tri-block copolymer Pluronic for encapsulation and delivery of curcumin. Pluronics, which are FDA approved synthetic polymer is an attractive material for drug delivery due to its easy availability, low cost, nontoxicity, biocompatibility, well-studied physical properties and ease of preparation. The utility of Pluronic block copolymers were already proven by its extensive use for the formulation and delivery of many hydrophobic drugs. But, to the best of our knowledge, Pluronic micelles has not been used for curcumin encapsulation. So, we have used two commonly used Pluronic i.e. F127 and F68 for the preparation of curcumin formulations. The formulations were analyzed for curcumin encapsulation efficiency, loading content, *in vitro* drug release and stability. The Pluronic micelles were effective in solubilization of curcumin in aqueous solution and Pluronic F127 showed higher encapsulation efficiency than Pluronic F68. The physical interaction of curcumin encapsulated in Pluronic nanocarriers was evident by UV-visible and fluorescence spectroscopy. AFM study showed that the drug encapsulated micelles were spherical in shape with diameters below 100 nm. Controlled release of curcumin from micelle nanocarriers were observed *in vitro* in physiological conditions. In comparison with the release from Pluronic F68 micelles, drug release from Pluronic F127 micelles was slower. The T_{50} value (time required for release of 50% of the encapsulated drug) for curcumin release form Pluronic F68 and F127 formulations were 36 and 144h

respectively. To analyze the drug release kinetics and mechanism, data were analyzed using the four kinetic models, (i) Zero order, (ii) First order, (iii) Higuchi model and (iv) Power law model. The analysis showed that models of Higuchi and Power law were best fitted with drug release kinetics data and the predominant mechanism behind the curcumin release from the Pluronic micelle formulations was diffusion. Stability studies revealed the the formulation can be stored in dry powder form by lyophilization and reconstitute in aqueous solution just before use. Observations under fluorescence microscope revealed that Pluronic encapsulated micelles were efficiently internalized within the HeLa cells and exert cytotoxic effects. The IC_{50} of curcumin with Pluronic F127 and F68 micelle formulations was found to be 17.45 μM and 16.01 μM respectively.

Natural food protein based nanoparticles for curcumin delivery to cancer cells

Finally, taking inspiration from traditional use of administering herbal medicines with milk we used natural nanostructures of casein micelles for curcumin delivery to cancer cells. Casein micelles were purified from bovine milk by simple centrifugation procedure and redispersed in buffer solution. SEM and AFM studies showed that the particles were roughly spherical in shape with an average size distribution of ~200 nm. Steady state fluorescence spectroscopy of the CM-curcumin complex formation revealed that curcumin molecules formed complexes with casein micelles (CM-curcumin complex) by binding to the low polarity regions of CM through hydrophobic interaction. The binding constant for the CM-curcumin interaction was calculated to be 1.48 X 10^4 M^{-1}. Fluorescence quenching showed that, upon binding curcumin molecules quenches the intrinsic fluorescence of caseins and further analysis revealed that the probable binding of curcumin was in the submicelles and near to the tryptophan residues in the proteins. The utility of casein micelles as carrier of

curcumin was evaluated on *in vitro* cultured HeLa cells. Cytotoxicity studies on HeLa cells revealed that the IC_{50} of free curcumin and CM-curcumin complex was 14.85 and 12.69 μM respectively. As caseins are edible proteins, so the CM-Curcumin complex has the potential to be an oral dose of curcumin but further studies and modifications are required.

Thus, in this thesis we have used biocompatible and safe materials for the preparation of nanocarriers for curcumin delivery to cancer cells. The nanocarriers provided readily aqueous solution/suspension of curcumin without use of any organic solvents, so they can be used for easy dosing of the drug. Basically we have done the preliminary assessment of the developed nanocarriers for curcumin delivery, which showed potential for clinical application in cancer chemotherapy but further developments and research is required.

FUTURE DIRECTIONS

Our attempt to develop nanocarriers for curcumin delivery to cancer cells yielded a novel mPEG-PA nanocarrier, a Pluronic based nanoformulation and the novel use of naturally existing nanostructure of casein micelles for drug delivery. However at the end of the investigation we could foresee many areas in which further investigations could yield potentially new and beneficial information as summarized below.

- Determination of the exact pathways involved in cellular uptake of nanocarrier mediated transport of curcumin in cancer cells. Normally the free drug enters the cells by diffusion whereas nanocarriers enter the cells via endocytosis (Bareford and Swaan, 2007). The endocytosis pathways of nanocarriers may vary depending on the properties of carrier.

So, the exact analysis of the endocytosis pathways of three different carriers of curcumin will be helpful for the design of future nanocarriers for similar drugs.

- Molecular insight into the cytotoxic effect of nanocarrier encapsulated curcumin on cancer cells. It has been proved that free curcumin acts on different signaling molecules inside the cells to exert its cytotoxic effect (Reuter et al., 2008). So, it will be of fundamental importance to know how nanocarrier encapsulated curcumin affects the signaling molecules inside the cells in comparison to free curcumin.
- Most importantly, the *in vivo* study of nanocarriers is required to know their true potential as drug carrier. The biodistribution of the nanocarriers in animal model is required to know about their *in vivo* stability, and ability of passive targeting of tumor tissues. It will also help to know whether any kind of side effects exists or not.
- Attachment of cancer cell specific ligands to these nanocarrier surfaces for active targeting to tumors is likely to increase the efficiency of nanocarriers by enhanced uptake through receptor mediated endocytosis (Gu et al., 2007).
- A smart nanocarrier can be prepared by replacing the ester linkage of the mPEG-PA conjugate with other linkages which can be cleaved by the enzymes over expressed in cancer cells (e.g. cathepsin B) (Oh et al., 2007).
- The casein micelles showed potential as carrier for hydrophobic drugs. As caseins are food grade proteins, this nanocarrier can be used for oral delivery of hydrophobic drugs. But it can not be used at its native form, because it is susceptible to degradation by proteases in gut. The potential of casein micelles as an oral drug delivery by improving the nano-structural/architectural stability through internal crosslinking of protein chains present in each particle.

Bibliography

1. Aggarwal BB and Harikumar KB. Potential therapeutic effects of curcumin, the abti-inflammatory agent, against neurodegenarative, cardiovascular, pulmonary, metabolic, autoimmune and neoplastic diseases. *The International Journal of Biochemistry & Cell Biology* 40-59, 2009.
2. Aggarwal BB, Kumar A and Bharti AC. Anticancer potential of curcumin: preclinical and clinical studies. *Anticancer Research* 23, 363-398, 2003.
3. Agnihotri SA, Mallikarjuna NN and Aminabhavi TM. Recent advances on chitosan based micro and nanoparticles in drug delivery. *Journal of Controlled Release* 100, 5-28, 2004.
4. Ahmad Z, Pandey R, Sharma S and Khuller GK. Pharmacokinetic and pharmacodynamic behaviour of antitubercular drugs encapsulated in alginate nanoparticles at two doses. *International Journal of Antimicrobial Agents* 27, 409-416, 2006.
5. Ahmed F, Pakunlu RI, Brannan A, Bates F, Minko T and Discher DE. Biodegradable polymersomes loaded with both paclitaxel and doxorubicin permeate and shrink tumors, inducing apoptosis in proportion to accumulated drug. *Journal of Controlled Release* 116, 150-158, 2006.
6. Ahuja N, Katare OP and Singh B. Studies on dissolution enhancement and mathematecical modeling of a poorly water-soluble drug using water-soluble carriers. *European Journal of Pharmaceutics Biopharmaceutics* 65, 26-38, 2007.
7. Akiyoshi K, Deguchi S, Moroguchi N, Sumaguchi S and Sunamoto J. Self-aggregates of hydrophobitized polysaccharides in water-formation and characteristics of nanoparticles. *Macromolecules* 26, 3062–3068, 1993.
8. Alaimo MH, Farrell HM and Germann MW. Conformational analysis of the hydrophobic peptide α_{s1}-casein(136–196). *Biochimica et Biophysica Acta* 1431, 410-420, 1999.
9. Aldaye FA, Palmer AL, Sleiman HF. Assembling materials with DNA as the guide. *Science* 321, 1795–1799, 2008.
10. Alexiou C, Arnold W, Klein RJ, Parak FG, Hulin P, Bergemann C, Erhardt W, Wagenpfeil S and Lübbe AS. Locoregional cancer treatment with magnetic drug targeting. *Cancer Research* 60, 6641-6648, 2000.

11. Allen C, Han J, Yu Y, Maysinger D and Eisenberg A. Polycaprolactone-*b*-poly(ethylene oxide) copolymer micelles as a delivery vehicle for dihydrotestosteron. *Journal of Controlled Release* 63, 275-286, 2000.
12. Allen C, Maysinger D and Eisenberg A. Nano-engineering block copolymer aggregates for drug delivery. *Colloids and Surfaces B* 16, 3-27, 1999.
13. Allen TM and Cullis PR. Drug delivery systems: Entering the mainstream. *Science* 303, 1818-1822, 2004.
14. Angelova N and Hunkeler D. Rationalizing the design of polymeric biomaterials. *Trends in Biotechnology* 17, 409–421, 1999.
15. Aoki H, Takada Y, Kondo S, Sawaya R, Aggarwal BB and Kondo Y. Evidence that curcumin suppresses the growth of malignant gliomas in vitro and in vivo through induction of autophagy: role of Akt and ERK signaling pathways. *Molecular Pharmacol*ogy 72, 29-39, 2007.
16. Astete CE and Sabliov CM. Synthesis and characterization of PLGA nanoparticles. *Journal of Biomaterial Science, Polymer Edition* 17, 247-289, 2006.
17. Aumelas A, Serrero A, Durand A, Dellacherie E and Leonard M. Nanoparticles of hydrophobically modified dextrans as potential drug carrier systems. *Colloids and Surfaces B* 59, 74-80, 2007.
18. Azarmi S, Huang Y, Chen H, McQuarrie S, Abrams D, Roa W, Finlay WH, Miller GG and Lobenberg R. Optimization of a two-step desolvation method for preparing gelatin nanoparticles and cell uptake studies in 143B osteosarcoma cancer cells. *Journal of Pharmacy and Pharmaceutical Science* 9, 124-132, 2006.
19. Azuine M and Bhide SV. Chemopreventive effect of turmeric against stomach and skin tumors induced by chemical carcinogens in Swiss mice. *Nutrition and Cancer* 17, 77-83, 1992.
20. Babu PS and Srinivasan K. Influence of dietary curcumin and cholesterol on the progression of experimentally induced diabetes in albino rat. Molecular and Cellular Biochemistry 152, 13-21, 1995.
21. Badar H, Ringsdorf H and Schmidt B. Water soluble polymers in medicine. *Angewandte Makromolecular Chemistry* 123, 457-485, 1984.

22. Bajgai M, Aryal S, Lee D, Park SJ and Kim H. Physicochemical characterization of self-assembled poly(ε-caprolactone) grafted dextran nanoparticles. *Colloid and Polymer Science* 286, 517-524, 2008.
23. Bala I, Hariharan S and Kumar MN. PLGA nanoparticles in drug delivery: the state of the art. *Critical Reviews in Therapeutic Drug Carrier Systems* 21, 387-422, 2004.
24. Balthasar S, Michaelis K, Dinauer N, von Briesen H, Kreuter J and Langer K. Preparation and characterisation of antibody modified gelatin nanoparticles as drug carrier system for uptake in lymphocytes. *Biomaterials* 26, 2723-2732, 2005.
25. Bareford LM and Swaan PW. Endocytic mechanisms for targeted drug delivery. Advanced Drug Delivery Reviews 59, 748-758, 2007.
26. Barik A, Priyadarsni KI and Mohan H. Photophysical studies on binding of curcumin to bovine serum albumin. *Photochemistry and Photobiology* 77, 597-603, 2003.
27. Basch JJ, Douglas FW, Procino LS, Holsinger VH and Farrell HM. Quantitation of casein and whey proteins of processed milks and whey protein concentrates, application of gel electrophoresis and comparison with Harland-Ashworth procedure. *Journal of Dairy Science* 68, 23-31, 1985.
28. Batrakova E and Kabanov A. Pluronic block copolymers: Evolution of drug delivery concept from inert nanocarriers to biological response modifiers. *Journal of Controlled Release* 130, 98-106, 2008.
29. Bernabé-Pineda M, Ramírez-Silva MT, Romero-Romo M, González-Vergara E and Rojas-Hernández A. Determination of acidity constants of curcumin in aqueous solution and apparent rate constant of its decomposition. *Spectrochimica Acta Part A* 60, 1091-1097, 2004.
30. Bianco A, Kostarelos K and Prato M. Applications of carbon nanotubes in drug delivery. *Current Opinion in Chemical Biology* 9, 674–679, 2005.
31. Bisht S, Feldmann G, Soni S, Ravi R, Karikar C, Maitra A and Maitra A. Polymeric nanoparticle encapsulated curcumin (”nanocurcumin”): a novel strategy for human cancer therapy. *Journal of Nanobiotechnology* 5, 3-20, 2007.
32. Bodnar M, Hartmann JF and Borbely J. Preparation and characterization of chitosan based nanoparticles. *Biomacromolecules* 6, 2521–2527, 2005.

33. Bohorquez, M., Koch, C., Trygstad, T., Pandit, N., 1999. A study of the temperature dependent micellization of Pluronic F127. *Journal of Colloid and Interface Science* 216, 34-40, 2008.

34. Borges O, Cordeiro-da-Silva A, Romeijn SG, Amidi M, de Sousa A, Borchard G and Junginger HE. Uptake studies in rat Payer's patches, cytotoxicity and release studies of alginate coated chitosan nanoparticles for mucosal vaccination. *Journal of Controlled Release* 114, 348-358, 2006.

35. Bosquets S, Carbo N, Almendro V, Quiles MT, Lopez-Soriano FJ and Argiles JM. Curcumin, a natural product present in turmeric, decreases tumor growth but does not behave as an anticachectic compound in a rat model. *Cancer Letter* 167, 33-38, 2001.

36. Bradford MM. A rapid and sensitive method for the quantitation of microgram quantities of protein utilizing the principle of protein-dye binding. *Analytical Biochemistry* 72, 248-254, 1976.

37. Brannon-Peppas L and Blanchette JO. Nanoparticles and targeted systems for cancer therapy. *Advanced Drug Delivery Reviews* 56, 1649-1659, 2004.

38. Bromberg L. Polymeric micelles in oral chemotherapy. Journal of Controlled Release 128, 99-112, 2008.

39. Bush JA, Cheung Jr. KJ and Li G. Curcumin induces apoptosis in human melanoma cells through a Fas receptor/caspase-8 pathway independent of p53. *Experimental Cell Research* 271, 305-314, 2001.

40. Byrne JD, Betancourt T and Peppas LB**.** Active targeting schemes for nanoparticle systems in cancer therapeutics. Advanced Drug Delivery Reviews 60, 1615-1626, 2008.

41. Cafaggi S, Russo E, Stefani R, Leardi R, Caviglioli G, Parodi B, Bignardi G, Totero D, Aiello C and Viale M. Preparation and evaluation of nanoparticles made of chitosan or *N*-trimethyl chitosan and a cisplatinalginate complex. *Journal of Controlled Release* 121, 110-123, 2007.

42. Chakraborty A and Basak S. pH-indced structural transitions of caseins. *Journal of Photochemistry and Photobiology* B 87, 191-199, 2007.

43. Chavanpatil MD, Khdair A and Panyam J. Surfactant-polymer nanoparticles: A novel platform for sustained and enhanced cellular delivery of water-soluble molecules. *Pharmaceutical Research* 24, 803-810, 2007a.

44. Chavanpatil MD, Khdair A, Gerard B, Bachmeier C, Miller DW, Shekhar MPV and Panyam J. Surfactant–Polymer Nanoparticles Overcome P-Glycoprotein-Mediated Drug Efflux. *Molecular Pharmaceutics* 4, 730-738, 2007b.
45. Chen JF, Ding HM, Wang JX and Shao L. Preparation and characterization of hollow silica nanoparticles for drug delivery applications. *Biomaterials* 25, 723-727, 2004.
46. Chen L, Remondetto GE and Subirade M. Food protein-based materials as nutraceutical delivery systems. *Trends in Food Science and Technology* 17, 272-283, 2006.
47. Cheng G, Aponte AM and Ramirez CA. Cross-linked amino acid-containing polyanhydrides for controlled drug release applications. *Polymer* 45, 3157-3162, 2004.
48. Cheung RY, Ying Y, Rauth AM, Marcon N and Wu XY. Biodegradable dextran-based microspheres for delivery of anticancer drug mitomycin C. Biomaterials 26, 5375-5385, 2005.
49. Chiappetta DA and Sosnik A. Poly(ethylene oxide)-poly(propylene oxide) block copolymer micelles as drug delivery agents: Improved hydrosolubility, stability and bioavailability of drugs. *European Journal of Pharmaceutics Biopharmaceutics* 66, 303-317, 2007.
50. Chignell CF, Bilski P, Reszka KJ, Motten AG, Sik RH and Dahl TH. Spectral and photochemical properties of curcumin. *Photochemistry and Photobiol*ogy 59, 295-302, 1994.
51. Cho K, Wang X, Nie S, Chen Z and Shin DM. Therapeutic nanoparticles for drug delivery in cancer. *Clinical Cancer Research* 14, 1310-1316, 2008.
52. Chowdhary RK, Chansarkar N, Sharif I, Hioka N and Dolphin D. Formulation of benzoporphyrin derivatives in Pluronics. *Photochemistry and Photobiology* 77, 299-303, 2003.
53. Couvreur P and Vauthier C. Intelligent design to treat complex disease. Pharmaceutical Research 23, 1417-1450, 2006.
54. Croy SC and Kwon GS. The effects of Pluronic block copolymers on the aggregation state of nystatin. *Journal of Controlled Release* 95, 161-171, 2004.
55. Dang W, Daviau T, Ying P, Zhao Y, Nowotnik D, Clow CS, Tyler B and Brem H. Effects of GLIADEL® wafer initial molecular weight on the erosion of wafer and release of BCNU. *Journal of Controlled Release* 42, 83-92, 1996.

56. Danson S, Ferry D, Alakhov V, Margison J, Kerr D, Jowle D, Brampton M, Halbert G and Ranson M. Phase I dose escalation and pharmacokinetic study of pluronic polymer-bound doxorubicin (SP1049C) in patients with advanced cancer. *British Journal of Cancer* 90, 2085-2091, 2004.
57. Davda J and Labhasetwar V. Characterization of nanoparticle uptake by endothelial cells. *International Journal of Pharmaceutics* 233, 51-59, 2002.
58. Davis ME and Brewster ME. Cyclodextrin-based pharmaceutics: past, present and future. *Nature Reviews Drug Discovery* 3, 1023-1035, 2004.
59. De Kruif CG and Holt C. Casein micelle structure, function and interactions**.** In *Advanced dairy chemistry-1 proteins part A*; Fox, P. F., Mcsweeney, P. L. H., Eds.; Kluwer academic/Plenum publisher: New York, 233-276, 2003.
60. De Kruif CG and Zhulina EB. κ-casein as a polyelectrolyte brush on the surface of casein micelles. *Colloids and Surfaces A* 117, 151-159, 1996.
61. Deodhar SD, Sethi R and Srimal RC. Preliminary study on antirheumatic activity of curcumin (diferuloyl methane). *Indian Journal of Medical Research* 71, 632-634, 1980.
62. Desai N, Trieu V, Yao Z, Louie L, Ci S, Yang A, Tao C, De T, Beals B, Dykes D, Noker P, Yao R, Labao E, Hawkins M and Soon-Shiong P, Increased antitumor activity, intratumor paclitaxel concentrations, and endothelial cell transport of cremophor-free, albumin-bound paclitaxel, ABI-007, compared with cremophor-based paclitaxel. *Clinical Cancer Research* 12, 1317–1324, 2006.
63. Diaz O, Gouldsworthy AM and Leaver J. Identification of peptides released from casein micelles by limited trypsinolysis. *Journal of Agriculture and Food Chemistry* 44, 2517-2522, 1996.
64. Discher DE and Eisenberg A. Polymer vesicles. *Science* 297, 967-973, 2002.
65. Dobson J. Magnetic nanoparticles for drug delivery. *Drug Development Research* 67, 55-60, 2006.
66. Dorai T, Cao YC, Dorai B, Buttyan R and Katz AE. Therapeutic potential of curcumin in human prostate cancer. III. Curcumin inhibits proliferation, induces apoptosis, and inhibits angiogenesis of LNCaP prostate cancer cells in vivo. *Prostate* 47, 293–303, 2001.

67. Dreis S, Rothweiler F, Michaelis M, Cinatl Jr. J, Kreuter J and Langer K. Preparation, characterisation and maintenance of drug efficacy of doxorubicin-loaded human serum albumin (HSA) nanoparticles. *Internationational Journal of Pharmaceutics* 341, 207-214, 2007.

68. Dubey PK, Mishra V, Jain S, Mahor S and Vyas SP. Liposomes modified with cyclic RGD peptide for tumor targeting. *Journal of Drug Targeting* 12, 257-264, 2004.

69. Duclairoir C, Irache JM, Nakache E, Orecchioni AM, Chabenat C and Popineau Y. Gliadin nanoparticles: formation, all-trans-retinoic acid entrapment and release, size optimization. *Polymer International* 79, 327-333, 1999.

70. Duclairoir C, Orecchioni AM, Depraetere P, Osterstock F and Nakache E. Evaluation of gliadins nanoparticles as drug delivery systems: a study of three different drugs. International Journal of Pharmaceutics 353, 133-144, 2003.

71. Egan ME, Pearson M, Weiner SA, Rajendran V, Rubin D, Pagel JG, Canny S, Du K, Lukacs GL and Caplan MJ. Curcumin, a major constituent of turmeric, corrects cystic fibrosis defects. Science 304, 600-603, 2004.

72. Elbert DL and Hubbell JA. Surface treatments of polymers for biocompatibility. *Annual Review of Material Science* 26, 365-394, 1996.

73. Erben CM, Goodman RP, Turberfield AJ. Single-molecule protein encapsulation in a rigid DNA cage. *Angewandte Chemie Int.* 45, 7414-7417, 2006.

74. Exner AA, Krupka TM, Scherrer K and Teets JM. Enhancement of carboplatin toxicity by Pluronic block copolymers. *Journal of Controlled Release* 106, 188-197, 2005.

75. Ezpeleta I, Irache JM, Stainmesse S, Chabenat C, Gueguen J, Popineau Y and Orecchion AM. Gliadin nanoparticles for the controlled release of all-*trans*-retinoic acid. *International Journal of Pharmaceutics* 131, 191-200, 1996a.

76. Ezpeleta I, Irache JM, Stainmesse S, Gueguen J and Orecchion AM. Preparation of small sized particles from vicilin (vegetal protein from *Pisum sativum L.*) by coacervation. *European Journal of Pharmaceutics Biopharmaceutics* 42, 36-41, 1996b.

77. Farrell HM, Wickham ED, Unruh JJ, Qi PX and Hoagland PD. Secondary structural studies of bovine caseins: temperature dependence of β-casein structure as analyzed by circular dichroism and FTIR spectroscopy and correlation with micellization. *Food Hydrocolloids* 15, 341-354, 2001.

78. Feazell RP, Ratchford NN, Dai H and Lippard SJ. Soluble single-walled carbon nanotubes as longboat delivery systems for platinum(IV) anticancer drug design. *Journal of American Chemical Society* 129, 8438-8439, 2007.

79. Ferrari M. Cancer Nanotechnology: opportunities and challenges. *Nature Reviews Cancer* 5, 161-171, 2005.

80. Fox PF and Brodkorb A. The casein micelle: historical aspects, current concepts and significance. *International Dairy Journal* 18, 735-740, 2008.

81. Freitas C and Müller RH. Correlation between long-term stability of solid lipid nanoparticles (SLN) and crystallinity of the lipid phase. *European Journal of Pharmaceutics Biopharmaceutics* 47, 125-132, 1999.

82. Friess W. Collagen– biomaterial for drug delivery. *European Journal of Pharmaceutics and Biopharmaceutics* 45, 113-136, 1998.

83. Fung LK and Saltzman WM. Polymeric implants for cancer chemotherapy. *Advanced Drug Delivery Reviews* 26, 209-230, 1997.

84. Gabizon A, Shmeeda H, Horowitz AT and Zalipsky S. Tumor cell targeting of liposome-entrapped drugs with phospholipid-anchored folic acid-PEG conjugates. *Advanced Drug Delivery Reviews* 56, 1177-1192, 2004.

85. Gao J, Ming J, He B, Fan Y, Gu Z and Zhang X. Preparation and characterization of novel polymeric micelles for 9-nitro-20(S)-camptothecin delievry. *European Journal of Pharmaceutical Sciences* 34, 85-93, 2008.

86. Gao Z, Lukyanov AN, Singhal A and Torchilin VP. Diacyllipid-polymer micelles as nanocarriers for poorly soluble anticancer drugs. *Nano Letters* 2, 979 -982, 2002.

87. Gatti CA, Alvarez EM and Sala VS. Effect of anion citrate on the mineral composition of artificial casein micelles. *Journal of Agriculture and Food Chemistry* 47, 141-144, 1999.

88. Gatti CA, Risso PH and Pires MS. Spectrofluorometric study on surface hydrophobicity of bovine casein micelles in suspension and during enzymic coagulation. *Journal of Agriculture and Food Chemistry* 43, 2339-2344, 1995.

89. Gatti CA, Risso PH and Zerpa SM. Study of the inhibitory effect of hydrophobic fluorescent markers on the enzymic coagulation of bovine casein micelles: action of TNS. *Food Hydrocolloids* 12, 393-400, 1998.

90. Gaucher G, Dufresne MH, Sant VP, Kang N, Maysinger D and Leroux JC. Block copolymer micelles: Preparation, characterization and application in drug delivery. *Journal of Controlled Release*109, 169-188, 2005.

91. Gebhardt BM and Kaufman HE. Collagen as a delivery system for hydrophobic drugs: studies with cyclosporine. *Journal of Ocular Pharmacolgy and Therapeutics* 11, 319-327, 1995.

92. General S and Thunemann AF. pH-sensitive nanoparticles of poly(amino acid) dodecanoate complexes. *International Journal of Pharmaceutical Sciences* 230, 11-24, 2001.

93. George M and Abraham TE. Polyionic hydrocolloids for the intestinal delivery of protein drugs: alginate and chitosan – a review. *Journal of Controlled Release* 114, 1-14, 2006.

94. Ghosh P, Han G, De M, Kim CK and Rotello VM. Gold nanoparticles in delivery applications. *Advanced Drug Delivery Reviews* 60, 1307-1315, 2008.

95. Goel A, Kunnumakkara AB and Aggarwal BB. Curcumin as "Curecumin": from kitchen to clinic. *Biochemical Pharmacology* 75, 787-809, 2008.

96. Grabar KC, Freeman RG, Hommer MB and Natan MJ. Preparation and characterization of Au colloid monolayers. *Analytical Chemistry* 67, 735-743, 1995.

97. Gregoriadis G, Leathwood PD and Ryman BE. Enzyme entrapment in liposomes. *FEBS Letter* 14, 95-–99, 1971.

98. Gregoriadis G, Wills EJ, Swain CP and Tavill AS. Drug-carrier potential of liposomes in cancer chemotherapy. *Lancet* 1, 1313-1316, 1974.

99. Gronenberg DA, Giersig M, Welte T and Pison U. Nanoparticle based diagnosis and therapy. *Current Drug Targets* 7, 643-648, 2006.

100. Gu FX, Karnik R, Wang AZ, Alexis F, Levy-Nissenbaum E, Hong S, Langer RS and Farokhzad OC. Targeted nanoparticles for cancer therapy. Nano Today 2, 14-21, 2007.

101. Gu XG, Schmitt M, Hiasa A, Nagata Y, Ikeda H, Sasaki Y, Akiyoshi, K, Sunamoto J, Nakamura H, Kuribayashi K and Shiku H. A novel hydrophobized polysaccharide/ oncoprotein complex vaccine induces in vitro and in vivo cellular and humoral immune responses against HER2-expressing murine sarcomas. *Cancer Research* 58, 3385-3390, 1998.

102. Gunasekaran S, Ko S and Xiao L. Use of whey proteins for encapsulation and controlled delivery applications. *Journal of Food Engineering* 83, 31-40, 2007.

103. Gupta AK and Gupta M. Synthesis and surface engineering of iron oxide nanoparticles for biological applications. *Biomaterials* 26, 3995-4021, 2005.

104. Gupta M and Gupta AK. Hydrogel pullulan nanoparticles encapsulating pBUDLacZ plasmid as an efficient gene delivery carrier. *Journal of Controlled Release* 99, 157-166, 2004.

105. Hamada H, Ishihara K, Masuoka N, Mikuni K and Nakajima N. Enhancement of water-solubility and bioactivity of paclitaxel using modified cyclodextrins. *Journal of Bioscience and Bioengineering* 102, 369-371, 2006.

106. Hamaguchi T, Matsumura Y, Suzuki M, Shimizu K, Goda R, Nakamura I, Nakatomi I, Yokoyama M, Kataoka K and Kakizoe T. NK105, a paclitaxel-incorporating micellar nanoparticle formulation, can extend in vivo antitumour activity and reduce the neurotoxicity of paclitaxel. *British Journal of Cancer* 92, 1240-1246, 2005.

107. Hans ML and Lowman AM. Biodegradable nanoparticles for drug delivery and targeting. *Current Opinion in Solid State and Materials Science* 6, 319-327, 2002.

108. Hatcher H, Planalp R, Cho J, Torti FM and Torti SV. Curcumin: from ancient medicine to current clinical trials. *Cellular and Molecular Life Sciences* 65, 1631-1652, 2008.

109. Hawker CJ and Fréchet JM. Preparation of polymers with controlled molecular architecture. A new convergent approach to dendritic macromolecules. *Journal of American Chemical Soceity* 112, 7638–7647, 1990.

110. Hawkins MJ, Soon-Shiong P and Desai N. Protein nanoparticles as drug carriers in clinical medicine. *Advanced Drug Delivery Reviews* 60, 876-885, 2008.

111. Hernandez JR, Checot F, Gnanou Y and Lecommandoux S. Toward 'smart' nano-objects by self-assembly of block copolymers in solution. *Progress in Polymer Science* 1-34, 2005.

112. Higuchi T. Mechanisms of sustained action mediation. Theoretical analysis of rate of release of solid drugs dispersed in solid matrices. *Journal of Pharmaceutical Science* 52, 1145–1149, 1963.

113. Hirayama F and Uekama K. Cyclodextrin-based controlled drug release system. Advanced Drug Delivery Reviews 36, 125-141, 1999.

114. Hong K, Kirpotin DB, Park JB, Shao Y, Shalaby R, Colbern G, Benz CC, Papahadjopoulos D. Anti-HER2 immunoliposomes for targeted drug delivery. *Annals of New York Academy of Sciences* 886, 293-296, 2006.

115. Horkay F and Basser PJ. Osmotic observations on chemically cross-linked DNA gels in physiological salt solutions. *Biomacromolecules*, 5, 232–237, 2004.

116. Horne DS. Steric stabilization and casein micelle stability. *Journal of Colloid and Interface Science* 111, 250-260, 1986.

117. Horvath G, Premkumar T, Boztas A, Lee E, Jon S and Geckeler KE. Supramolecular nanoencapsulation as a tool: solubilization of the anticancer drug trans-dichloro(dipyridine)platinum(II) by complexation with β-cyclodextrin. Molecular Pharmaceutics 5, 358-363, 2008.

118. Hosta L, Pla-Roca M, Arbiol J, Lpez-Iglesias C, Samitier J, Cruz LJ, Kogan MJ and Albericio F. Conjugation of kahalalide F with gold nanoparticles to enhance in vitro antitumoral activity. *Bioconjugate Chemistry* 20, 138–146, 2009.

119. Huang M, Smart RC, Wong CQ and Conney AH. Inhibitory effect of curcumin, chlorogenic acid, caffeic acid, and ferulic acid on tumor promotion inmouse skin by 12-O-tetradecanoylphorbol-13-acetate. *Cancer Research* 48, 5941-5946, 1988.

120. Huang X, Jain PK, El-Sayed IH and El-Sayed MA. Gold nanoparticles and nanorods in medicine: From cancer diagnostics to photothermal therapy. *Nanomedicine* 2, 681-693, 2007.

121. Huppertz T, Smiddy MA and De Kruif CG. Biocompatible Micro-Gel Particles from Cross-Linked Casein Micelles. *Biomacromolecules* 8, 1300-1305, 2007.

122. Ijima S. Helical microtubles of graphitic carbon. *Nature* 354, 56–58, 1991.

123. Ireson CR, Jones DJL, Orr S, Coughtrie MWH, Boocock DJ, Williams ML, Farmer PB, Steward WP and Gescher AJ. Metabolism of the cancer chemopreventive agent curcumin in human and rat intestine. *Cancer Epidemiology Biomarkers & Prevention* 11, 105-111, 2002.

124. Ireson CR, Orr S, Jones DJL, Verschoyle R, Lim C, Luo J, Howells L, Plummer S, Jukes R, Williams M, Steward WP and Gescher A. Characterization of metabolites of the chemopreventive agent curcumin in human and rat hepatocytes and in the rat *in vivo*, and evaluation of their ability to inhibit phorbol ester-induced prostaglandin E_2 production. *Cancer Research* 61, 1058-1064, 2001.

125. Itokazu M, Sugiyama T, Ohno T, Wada E and Katagiri Y. Development of porous apatite ceramic for local delivery of chemotherapeutic agents. *Journal of Biomedical Material Research A* 39, 536-538, 1998.
126. Jain RA. The manufacturing techniques of various drug loaded biodegradable poly(lactide-*co*-glycolide) (PLGA) devices. *Biomaterials* 21, 2475- 2490, 2000.
127. Jain RK. Vascular and interstitial barriers to delivery of therapeutic agents in tumors. *Cancer Metastasis Review* 9, 253-266, 1990.
128. Jain SK and DeFilipps RA. Medicinal plants of India. Reference Publications, Algonac MI, 120, 1991.
129. Janes KA, Fresneau MP, Marazuela A, Fabra A and Alonso MJ. Chitosan nanoparticles as delivery systems for doxorubicin. *Journal of Controlled Release* 73, 255-267, 2001.
130. Jeong Y, Na HS, Cho KO, Lee HC, Nah JW and Cho CS. Antitumor activity of adriamycin incorporated polymeric micelles of poly (γ-bezyl L-glutamate)/ poly (ethylene oxide). *International Journal of Pharmaceutics* 365, 150, 156, 2009.
131. Jones MC and Leroux JC. Polymeric micelles – a new generation of colloidal drug carriers. *European Journal of Pharmaceutics Biopharmaceutics* 48, 101-111, 1998.
132. Kabanov AV, Batrakova EV and Alakhov VY. Pluronic® block copolymrs as novel polymer therapeutics for drug and gene delivery. *Journal of Controlled Release* 82, 189-212, 2002.
133. Karmali PP, Kotamraju VR, Kastantin M, Black M, Missirlis D, Tirrell M and Ruoslahti E. Targeting of albumin-embedded paclitaxel nanoparticles to tumors. *Nanomedicine* 5, 73-82, 2005.
134. Kataoka K, Harada A, and Nagasaki Y. Block copolymer micelles for drug delivery: design, characterization and biological significance. *Advanced Drug Delivery Reviews* 47, 113-131, 2001.
135. Kato Y, Onishi H and Machida Y. Contribution of chitosan and its derivatives to cancer chemotherapy. *In Vivo* 19, 301-310, 2005.
136. Kaul G and Amiji M. Long-circulating poly(ethylene glycol) modified gelatin nanoparticles for intracellular delivery. *Pharmaceutical Research* 19, 1061-1067, 2002.

137. Kaul G and Amiji M. Biodistribution and targeting potential of poly(ethylene glycol)-modified gelatin nanoparticles in subcutaneous murine tumor model. *Journal of Drug Targeting* 12, 585-591, 2004.
138. Kaur IP, Bhandari R, Bhandari S and Kakkar V. Potential of solid lipid nanoparticles in brain targeting. *Journal of Controlled Release* 127, 97-109, 2008.
139. Kawasaki ES and Player A. Nanotechnology, nanomedicine and the development of new, effective therapies for cancer. Nanomedicine 1, 101-109, 2005.
140. Kester M, Heakal Y, Fox T, Sharma A, Robertson GP, Morgan TT, Altinoglu E, Tabakovic A, Parette MR, Rouse SM, Velasco VR and Adair JH. Calcium phosphate nanocomposite particles for in vitro imaging and encapsulated chemotherapeutic drug delivery to cancer cells. *Nano Letters* 8, 4116-4121, 2008.
141. Khopde SM, Priyadarsini, Palit DK and Mukherjee T. Effect of solvent on the excited state photophysical properties of curcumin. *Photochemistry and Photobiology* 72, 625-631, 2000.
142. Kim C, Lee SC, Kang SW, Kwon IC, Kim Y, Jeong SY. Synthesis and the micellar characteristics of poly(ethylene oxide)-deoxycholic acid conjugates. *Langmuir* 16, 4792-4797, 2000.
143. Kim IS, Kim SH. Evaluation of polymeric nanoparticles composed of cholic acid and methoxy poly(ethylene glycol). International Journal of Pharmaceutics 226, 23-29, 2001.
144. Kim JH, Kim YS, Kim S, Park JH, Kim K, Choi K, Chung H, Jeong SY, Park RW, Kim IS and Kwon IC. Hydrophobically modified glycol chitosan nanoparticles as carriers for paclitaxel. *Journal of Controlled Release* 111, 228-234, 2006.
145. Kim JH, Kim YS, Park K, Kang E, Lee S, Nam HY, Kim K, Park JH, Chi DY, Park RW, Kim IS, Choi K and IC Kwon. Self-assembled glycol chitosan nanoparticles for the sustained and prolonged delivery of antiangiogenic small peptide drugs in cancer therapy. *Biomaterials* 29, 1920-1930, 2008.
146. Kim TY, Kim DW, Chung JY, Shin SG, Kim SC, Heo DS, Kim NK and Bang YJ. Phase I and pharmacokinetic study of genexol-PM, a cremophor-free, polymeric micelle formulated paclitaxel, in patients with advanced malignancies. *Clinical Cancer Research* 10, 3708-3716, 2004.

147. Knepp WA, Jayakrishna A, Quigg JM, Sitren HS, Bagnall JJ and Goldberg EP. Synthesis, properties and intratumoral evaluation of mitoxantrone loaded casein microspheres in Lewis lung carcinoma. *Journal of Pharmacy and Pharmacology* 45, 887-891, 1993.

148. Koda J, Venook A, Walser E, et al. Phase I/II trial of hepatic intraarterial delivery of doxorubicin hydrochloride adsorbed to magnetic targeted carriers in patients with hepatocarcinoma. *European Journal of Cancer* 38, S18, 2002.

149. Kono K, Liu M and Fréchet JM. Design of dendritic macromolecules containing folate or methotrexate residues. *Bioconjugate Chemistry* 10, 1115-1121, 1999.

150. Kontermann RE. Immunoliposomes for cancer therapy. *Current Opinion in Molecular Therapy* 8, 39-45, 2006.

151. Korsmeyer RW, Gurny R, Doelker E, Buri P and Peppas NA. Mechanisms of solute release from porous hydrophilic polymers. *International Journal of Pharmaceutics* 15, 25-35, 1983.

152. Kost J and Langer R. Responsive polymeric delivery systems. *Advanced Drug Delivery Reviews* 6, 19-50, 1991.

153. Kostarelos K. Rational design and engineering of delivery systems for therapeutics: biomedical exercise in colloid and surface science. *Advances in Colloid and Interface Science* 106, 147-168, 2003.

154. Kreuter J. Nanoparticulate systems for brain delivery of drugs. *Advanced Drug Delivery Reviews* 47, 65-81, 2001.

155. Kumar N, Langer RS and Domb AJ. Polyanhydrides: an overview. *Advanced Drug Delivery Reviews* 54, 889-910, 2002.

156. Kumar V, Lewis SA, Mutalik S, Shenoy DB, Venkatesh, Udupa N. Biodegradable microspheres of curcumin for treatment of inflammation. *Indian Journal of Physiology and Pharmacology* 46, 209-217, 2002.

157. Kunwar A, Barik A, Pandey R and Priyadarsini KI. Transport of liposomal and albumin loaded curcumin to living cells: An absorption and fluorescence spectroscopic study. *Biochimica et Biophysica Acta* 1760, 1513-1520, 2006.

158. Kuttan R, Bhanumathy P, Nirmala K and George MC. Potential anticancer activity of turmeric (*Curcuma longa*). *Cancer Letter* 29, 197-202, 1985.

159. Kwon G, Suwa S, Yokoyama M, Okano T, Sakurai Y and Kataoka K. Enhanced tumor accumulation and prolonged circulation times of micelle-forming poly(ethylene oxide-aspartate) block copolymer–adriamycin conjugates. *Journal of Controlled Release* 29, 17-23, 1994.

160. Kwon GS. Diblock copolymer nanoparticles for drug delivery. Critical *Reviews in Therapeutic Drug Carrier Systems* 15, 481-512, 1998.

161. Kwon GS. Polymeric micelles for delivery of poorly water-soluble compounds. *Critical Reviews in Therapeutic Drug Carrier Systems* 20, 357-403, 2003.

162. Kwon GS and Kataoka K. Block copolymer micelles as long-circulating drug vehicles. *Advanced Drug Delivery Reviews* 16, 295-309, 1995.

163. Laemmli UK. Cleavage of structural proteins during the assembly of the head of bacteriophage. *Nature* 277, 680-685, 1970.

164. Lakowich JR. Principles of Fluorescence Spectroscopy. 3rd Edition, Springer, 2007.

165. Lambert G, Fattal E and Couvreur P. Nanoparticulate systems for the delivery of antisense oligonucleotides. *Advanced Drug Delivery Reviews* 47, 99-112, 2001.

166. Lampe V and Milobedaska J. *Berichte der Deutschen Chemischen Gesellschaft* 46, 2235, 1913.

167. Langer K, Balthasar S, Vogel V, Dinauer N, von Briesen H and Schubert D. Optimization of the preparation process for human serum albumin (HSA) nanoparticles. *Internationational Journal of Pharmaceutics* 257, 169-180, 2003.

168. Langer R. New methods of drug delivery. *Science* 249, 1527–1533, 1990.

169. Langer R. Biomaterials in drug delivery and tissue engineering: one laboratory's experience. *Accounts of Chemical Research* 33, 94-101, 2000.

170. Lao C, Ruffin M, Normolle D, Heath D, Murry S and Bailey J. Dose escalation of a curcuminoid formulation. *BMC Complemetary Alternative Medicine* 6, 10-15, 2006.

171. Lasic DD. Doxorubicin in sterically stabilized liposomes. *Nature* 380, 561-562, 1996.

172. Lasic DD and Papahadjopoulos D. Medical applications of liposomes. Elsevier, Amesterdam, 1998.

173. Leclerc PL, Remondetto GE, Ramassamy C and Subirade M. Whey protein nanospheres as drug carriers for oral administration. In Conference on Bioencapsulation, Kingston, 24-26, 2005.

174. Lee CC, Gillies ER, Fox ME, Guillaudeu SJ, Fréchet JM, Dy EE and Szoka FC. A single dose of doxorubicin-functionalized bow-tie dendrimer cures mice bearing C-26 colon carcinomas. *PNAS* 103, 16649–16654, 2006.

175. Lee CC, MacKay JA, Fréchet JM and Szoka FC. Designing dendrimers for biological applications. *Nature Biotechnology* 23, 1517-1526, 2005.

176. Lee CH, Singla A and Lee Y. Biomedical applications of collagen. *International Journal of Pharmaceutics* 221, 1-22, 2001.

177. Lee H, Soo PL, Liu J, Butler M and Allen C. Polymeric micelles for formulation of anti-cancer drugs. In: Amiji, M.M.(Ed), Nanotechnology for cancer therapy. CRC Press, New York, 317-355, 2007.

178. Lee HJ, Yang SR, An EJ and Kim JD. Biodegradable Polymersomes from Poly(2-hydroxyethyl aspartamide) grafted with lactic acid oligomers in aqueous solution. *Macromolecules* 39, 4938-4940, 2006.

179. Lee JH, Jung SW, Kim IS, Jeong Y, Kim YH, Kim SH. Polymeric nanoparticle composed of fatty acids and poly(ethylene glycol) as a drug carrier. International Journal of Pharmaceutics 251, 23-32, 2003.

180. Lee KY, Jo WH, Kwon IC, Kim YH and Jeong SY. Physico-chemical characteristics of self-aggregates of hydrophobically modified chitosans. *Langmuir* 14, 2329-2332, 1998.

181. Lee M, Lo AC, Cheung PT, Wong D and Chan BP. Drug carrier systems based on collagen–alginate composite structures for improving the performance of GDNF-secreting HEK293 cells. *Biomaterials* 30, 1214-1221, 2009.

182. Lee WC and Chu IM. Preparation and degradation behavior of polyanhydrides nanoparticles. *Journal of Biomedical Material Research B* 84, 138-146, 2007.

183. Lemarchand C, Gref R and Couvreur P. Polysaccharide-decorated nanoparticles. *European Journal of Pharmaceutics and Biopharmaceutics* 58, 327-341, 2004.

184. Lemoine D, Francois C, Kedzierewicz F, Preat V, Hoffman M and Maincent P. Stability study of nanoparticles of poly(ε-caprolactone), poly(d,l-lactide) and poly(d,l-lactide-co-glycolide). *Biomaterials* 17, 2191-2197, 1996.

185. Leo E, Vandelli MR, Cameroni R and Forni F. Doxorubicin-loaded gelatin nanoparticles stabilized by glutaraldehyde: Involvement of the drug in the cross-linking process. *Internationational Journal of Pharmaceutics* 155, 75-82, 1997.

186. Leroux JC, Allémann E, Jaeghere FD, Eric Doelker and Robert Gurny. Biodegradable nanoparticles – from sustained release formulations to improved site specific drug delivery. *Journal of Controlled Release* 39, 339-350, 1996.

187. Lertsutthiwong P, Noomun K, Jongaroonngamsang N, Rojsitthisak P and Nimmanni U. Preparation of alginate nanocapsules containing turmeric oil. *Carbohydrate Polymers* 74, 209-214, 2008.

188. Levine DH, Ghoroghchian PP, Freudenberg J, Zhang G, Therien MJ, Greene MI, Hammer DA and Murali R. Polymersomes: A new multi-functional tool for cancer diagnosis and therapy. *Methods* 46, 25-32, 2008.

189. Li L, Braiteh FS and Kurzrock R. Liposome encapsulated curcumin: In vitro and in vivo effects on proliferation, apoptosis, signaling and angiogenesis. *Cancer* 104, 1322-1331, 2005.

190. Li MX, Zhuo RX annd Qu FQ. Synthesis and characterization of novel biodegradable poly (ester amide) with ether linkage in the backbone chain. *Journal of Polymer Science A* 40, 4550-4555, 2002.

191. Liang L, Tajmir-Riahi HA and Subirade M. Interaction of β-lactoglobulin with resveratrol and its biological implications. *Biomacromolecules* 9, 50-56, 2008.

192. Liggins RT and Burt HM. Polyether-polyester diblock copolymers for the preparation of paclitaxel loaded polymeric micelle formulations. Advanced Drug Delivery Reviews 54, 191–202, 2002.

193. Lim GP, Chu T, Yang F, Beech W, Frautschy SA and Cole GM. The curry spice curcumin reduces oxidative damage and amyloid pathology in an Alzeimer transgenic mouse. Journal of Neuroscience 21, 8370-8377, 2001.

194. Lin C, Liu Y and Yan H. Designer DNA nanoarchitectures. *Biochemistry* 48, 1663–1674, 2009.

195. Liu Y and Guo R. Interaction between casein and sodium dodecyl sulfate. *Journal of Colloid and Interface Science* 315, 685-692, 2007.

196. Liu Z, Chen K, Davis C, Sherlock S, Cao Q, Chen X and Dai H. Drug delivery with carbon nanotubes for in vivo cancer treatment. Cancer Research, 68, 6652-6660, 2008.

197. Liu Z, Sun X, Ratchford NN and Dai H. Supramolecular chemistry on water soluble carbon nanotubes for drug loading and delivery. *ACS Nano* 1, 50-56, 2007.

198. Lopez-Leon T, Carvalho EL, Seijo B, Ortega-Vinuesa JL and Bastos-Gonzalez D. Physicochemical characterization of chitosan nanoparticles: Electrokinetic and stability behavior. *Journal of Colloid and Interface Science* 283, 344-351, 2005.

199. LoTempio MM, Veena MS, Steele HL, Ramamurthy B, Ramalingam TS and Cohen AN. Curcumin suppresses growth of head and neck squamous cell carcinoma, *Clinical Cancer Research* 11, 6994-7002, 2005.

200. Lu AH, Salabas EL and Schuth F. Magnetic nanoparticles: Synthesis, protection, functionalization and application. *Angewandte Chemie International* 46, 1222-1244, 2007a.

201. Lu J, Liong M, Zink JI and Fuyuhiko Tamanoi. Mesoporous silica nanoparticles as a delivery system for hydrophobic anticancer drugs. *Small* 3, 1341-1346, 2007b.

202. Lu J, Liong M, Sherman S, Xia T, Kovochich M, Nel A, Zink J; Tamanoi, Fuyuhiko. Mesoporous silica nanoparticles for cancer therapy: energy-dependent cellular uptake and delivery of paclitaxel to cancer cells. *Nanobiotechnology* 3, 89-95, 2007c.

203. Lu Z, Yeh TK, Tsai M, Au JL and Wientjes MG. Paclitaxel loaded gelatin nanoparticles for intravesical bladder cancer therapy. *Clinical Cancer Research* 10, 7677-7684, 2004.

204. Lubbe A.S., Bergemann C., Huhnt W., Fricke T., Riess H., Brock J. W. and Huhn D. Preclinical experiences with magnetic drug targeting: tolerance and efficacy. *Cancer Research* 56, 4694-4701, 1996a.

205. Lubbe A.S., Bergemann C., Riess H., et al. Clinical experiences with magnetic drug targeting phase I syudy with 4'- epidoxorubicin in 14 patients with adnaced solid tumors. *Cancer Research* 56, 4686-4693, 1996b.

206. Lukyanov AN, Torchilin VP. Micelles from lipid derivatives of water-soluble polymers as delivery systems for poorly soluble drugs. *Advanced Drug Delivery Reviews* 56, 1273-1289, 2004.

207. Ma Z, Haddadi A, Molavi O, Lavasanifar A, Lai R and Samuel J. Micelles of poly(ethylene oxide)-b-poly(ε-caprolactone) as vehicles for the solubilization, stabilization and controlled delivery of curcumin. *Journal of Biomedical Materials Research A* 86, 300-310, 2008.

208. Maeda H. The enhanced permeability and retention (EPR) effect in tumor vasculature: the key role of tumor-selective macromolecular drug targeting. *Advances in Enzyme Regulation* 41, 189-207, 2001.

209. Maeda H, Wu J, Sawa T, Matsumura Y and Hori K. Tumor vascular permeability and the EPR effect in macromolecular therapeutics: a review. *Journal of Controlled Release* 65, 271-284, 2000.

210. Mahady GB, Pendland SL, Yun G and Lu ZZ. Turmeric (*Curcuma longa*) and curcumin inhibit the growth of *Helicobacter pylori*, a group 1 carcinogen. *Anticancer Research* 22, 4179-4181, 2002.

211. Maheshwari R, Singh AK, Gaddipati J and Srimal RC. Multiple biological activities of curcumin: A short review. *Life Science* 78, 2081-2087, 2006.

212. Mahmoud NN, Carothers AM, Grunberger D, Bilinski RT, Churchill MR, Martucci C, Newmark HL and Bertagnolli MM. Plant phenolics decrease intestinal tumors in an animal model of familial adenomatous polyposis. *Carcinogenesis* 21, 921-927, 2000.

213. Majoros IJ, Myc A, Thomas T, Mehta CB and. Baker Jr. JR. PAMAM dendrimer-based multifunctional conjugate for cancer therapy: synthesis, characterization, and functionality. *Biomacromolecules* 7, 572–579, 2006.

214. Mandal M, Kundu S, Ghosh SK, Panigrahi S, Sau TK, Yusuf SM and Pal T. Magnetite nanoparticles with tunable gold or silver shell. *Journal of Colloid and Interface Science* 286, 187-194, 2005.

215. Markman M, Gordon AN, McGuireWP and Muggia FM. Liposomal anthracycline treatment for ovarian cancer. *Seminars in Oncology* 31, 91-105, 2004.

216. Martin del Valle EM. Cyclodextrin and their uses: a review. *Process Biochemistry* 39, 1033-1046, 2004.

217. Matsumara Y and Maeda H. A new concept for macromolecular therapeutics in cancer chemotherapy – mechanism of tumoritropic accumulation of proteins and the antitumor agent SMANCS. *Cancer Research* 46, 6387-6392, 1986.

218. Matsumura Y, Hamaguchi T, Ura T, Muro K, Yamada Y, Shimada Y, Shirao K, Okusaka T, Ueno H, Ikeda M and Watanabe N. Phase I clinical trial and pharmacokinetic evaluation of NK911, a micelle-encapsulated doxorubicin. *British Journal of Cancer* 91, 1775-1781, 2004.

219. McNally SJ, Harrison EM, Ross JA, Garden OJ and Wigmore SJ, Curcumin induces heme oxygenase 1 through generation of reactive oxygen species, p38 activation and phosphatase inhibition. *International Journal of Molecular Medicine* 19, 165-172, 2007.

220. Mehvar R. Dextrans for targeted and sustained delivery of therapeutic and imaging agents. *Journal of Controlled Release* 69, 1-25, 2000.

221. Memisoglu EB, Vural I, Bochot A, Renoir JM, Duchene D and Atilla AH. Tamoxifen citrate loaded amphiphilic β-cyclodextrin nanoparticles: In vivo characterization and cytotoxicity. *Journal of Controlled Release* 104, 489-496, 2005.

222. Meng F, Hiemstra C, Engbers GHM and Feijen J. Biodegradable polymersomes. *Macromolecules* 36, 3004-3006, 2003.

223. Meng F, Zhong Z and Feijen J. Stimuli-Responsive Polymersomes for Programmed Drug Delivery. *Biomacromolecules* 10, 197-209, 2009.

224. Min KH, Park K, Kim YS, Bae SM, Lee S, Jo HG, Park RW, Kim IS, Jeong SY, Kim K and Kwon IC. Hydrophobically modified glycol chitosan nanoparticles-encapsulated camptothecin enhance the drug stability and tumor targeting in cancer therapy. *Journal of Controlled Release* 127, 208-218, 2008.

225. Mirshahi T, Irache JM, Gueguen AM and Orecchioni AM. Development of drug delivery systems from vegetal proteins: legumin nanoparticles. *Drug Dev Ind Pharm* 22, 841-846, 1996.

226. Missirlis D, Kawamura R, Tirelli N and Hubbell JA. Doxorubicin encapsulation and diffusional release from stable, polymeric, hydrogel nanoparticle. *European Jounal of Pharmaceutical Sciences* 29, 120-129, 2006.

227. Mitra A, Chakrabarti J, Banerji A, Chatterjee A and Das BR. Curcumin, a potential inhibitor of MMP-2 in human laryngeal squamous carcinoma cells HEp2. *Journal of Environmental Pathology Toxicology and Oncology* 25, 679-690, 2006.

228. Mitra S, Gaur U, Ghosh PC and Maitra AN. Tumour targeted delivery of encapsulated dextran–doxorubicin conjugate using chitosan nanoparticles as carrier. *Journal of Controlled Release* 74, 317-323, 2001.

229. Moghimi S, Garcia ML, Al-Hanbali OAR and Rutt KJ. Polymeric nanoparticles as drug carriers and controlled release implant devices. In Nanoparticulates as Drug Carriers, Imperial College Press, 29-42, 2006.

230. Moran MC, Miguel MG and Lindman B. DNA gel particles: Particle preparation and release characteristics. *Langmuir*, 23, 6478–6481, 2007.

231. Morgan MT, Nakanishi Y, Kroll DJ, Griset AP, Carnahan MA, Wathier M, Oberlies NH, Manikumar G, Wani MC and Grinstaff MW. Dendrimer encapsulated camptothecins: increased solubility, cellular uptake, and cellular retention affords enhanced anticancer activity *in vitro*. *Cancer Research* 66, 11913-11921, 2006.

232. Mosmann T. Rapid colorimetric assay for cellular growth and survival: application to proliferation and cytotoxicity assays. *Journal of Immunological Methods* 65, 55-63, 1983.

233. Muller RH, Mader K and Gohla S. Solid lipid nanoparticles (SLN) for controlled drug delivery – a review of the state of the art. *European Journal of Pharmaceutics Biopharmaceutics* 50, 61-77, 2000.

234. Na K and Bae YH. Self-Assembled hydrogel nanoparticles responsive to tumor extracellular pH from pullulan derivative/sulfonamide conjugate: characterization, aggregation and adriamycin release in vitro. *Pharmaceutical Research* 19, 681-687, 2002.

235. Na K, Lee TB, Park KH, Shin EK, Lee YB and Choi HK. Self-assembled nanoparticles of hydrophobically-modified polysaccharide bearing vitamin H as a targeted anti-cancer drug delivery system. *European Journal of Pharmaceutical Sciences* 18, 165-173, 2003.

236. Nakanishi T, Fukushima S, Okamoto K, Suzuki M, Matsumura Y, Yokoyama M, Okano T, Sakurai Y and Kataoka K. Development of the polymer micelle carrier system for doxorubicin. *Journal of Controlled Release* 74, 295-302, 2001.

237. Neerman MF, Chen HT, Parrish AR and Simanek EE. Reduction of drug toxicity using dendrimers based on melamine, *Molecular Pharmaceutics* 1, 390–393, 2004.

238. Nishiyama N and Kataoka K. Current state, achievements and future prospects of polymeric micelles as nanocarriers for drug and gene delivery. *Pharmacology & Therapeutics* 2006.

239. Niwa T, Takeuchi H, Hino T, Kunou N and Kawashima Y. Preparations of biodegradable nanospheres of water-soluble and insoluble drugs with D,L-lactide/glycolide copolymer by a novel spontaneous emulsification solvent diffusion method, and the drug release behavior. *Journal of Controlled Release* 25, 89-98, 1993.

240. Oh KT, Yin H, Lee ES and Bae YH. Polymeric nanovehicles for anticancer drugs with triggering release mechanisms. *Journal of Materials Chemistry* 3987-4001, 2007.

241. Ohulchanskyy TY, Roy I, Goswami LN, Chen Y, Bergey EJ, Pandey RK, Oseroff AR and Prasad PN. Organically modified silica nanoparticles with covalently incorporated photosensitizer for photodynamic therapy of cancer. *Nano Letters* 7, 2835-2842, 2007.

242. Olbrich C, Geßner A, Kayser O and Müller RH, Lipid–drug-conjugate (LDC) nanoparticles as an alternative carrier system with high drug content. *Proc. Int. Symp. Control. Rel. Bioact. Mater.* 27, 295–296, 2000.

243. Ooya T, Lee J and Park K. Hydrotropic dendrimers of generations 4 and 5: synthesis, characterization, and hydrotropic solubilization of paclitaxel, *Bioconjugate Chemistry* 15, 1221–1229, 2004.

244. Owens DE and Peppas NA. Opsonization, biodistribution and pharmacokinetics of polymeric nanoparticles. *International Journal of Pharmaceutics* 307, 93-102, 2006.

245. Paciotti GF, Kingston DGI and Tamarkin L. Colloidal gold nanoparticles: a novel nanoparticle platform for developing multifunctional tumor-targeted drug delivery vectors. *Drug Developmental Research* 67, 47-54, 2006.

246. Paciotti GF, Myer L, Weinreich D, Goia D, Pavel N, McLaughlin RE and Tamarkin L. Colloidal gold: a novel nanoparticle vector for tumor directed drug delivery. *Drug Delivery* 11, 169–183, 2004.

247. Pan MH, Chang WL, Lin-Shiau SY, Ho CT and Lin JK. Induction of apoptosis by garcinol and curcumin through cytochrome *c* release and activation of caspases in human leukemia HL-60 cells. *Journal of Agriculture and Food Chemistry* 49, 1464-1474, 2001.

248. Pan MH, Huang TM and Lin JK. Biotransformation of curcumin through reduction and glucoronidation in mice. *Drug Metabolism and Disposition* 27, 486-494, 1999.

249. Pan X, Yao P and Jiang M. Simultaneous nanoparticle formation and encapsulation driven by hydrophobic interaction of casein-*graft*-dextran and *β*-carotene. *Journal of Colloid and Interface Science* 315, 456-463, 2007.

250. Panouillé M, Nicolai T and Durand D. Heat induced aggregation and gelation of casein submicelles. *International Dairy Journal* 14, 297-303, 2004.

251. Panyam J and Labhasetwar V. Biodegradable nanoparticles for drug and gene delivery to cells and tissue. *Advanced Drug Delivery Reviews* 55, 329-347, 2003.

252. Papahadjopoulos D, Allen TM, Gabizon A, Mayhew E, Matthay K, Huang SK, Lee KD, Woodle MC, Lasic DD and Redemann C. Sterically stabilized liposomes: improvements in pharmacokinetics and antitumor therapeutic efficacy. *Proc Natl Acad Sci USA* 88, 11460-11464, 1991.

253. Park JW, Benz CC and Martin FJ. Future directions of liposome-and immunoliposome-based cancer therapeutics. *Seminars in Oncology* 31, 196-205, 2004.

254. Park JW, Hong K, Kirpotin DB, Papahadjopoulos D, Benz CC. Immunoliposomes for cancer treatment. *Advances in Pharmacology* 40, 399-435, 1997.

255. Pato C, Borgne ML, Baut GL, Pape PL, Marion D and Douliez JP. Potential application of plant lipid transfer proteins for drug delivery. *Biochemical Pharmacology* 62, 555-560, 2001.

256. Patri AK, Myc A, Beals J, Thomas TP, Bander NH and Baker Jr. JR, Synthesis and *in vitro* testing of J591 antibody–dendrimer conjugates for targeted prostate cancer therapy. *Bioconjugate Chemistry* 15, 1174–1181, 2004.

257. Paul and Sharma CP. Porous hydroxyapatite nanoparticles for intestinal delivery of insulin. *Trends in Biomaterials and Artificial Organs* 14, 37-38, 2001.

258. Paul W and Sharma CP. Ceramic Drug Delivery: A Perspective. *Journal of Biomaterials Applications* 17, 253-263, 2003.

259. Peer D, Karp JM, Hong S, Farokhzad OC, Margalit R and Langer R. Nanocarriers as an emerging platform for cancer therapy. *Nature Nanotechnology* 2, 751-760, 2007.

260. Pillai O and Panchagnula R. Polymers in drug delivery. *Current Opinion in Chemical Biology* 5, 447-451, 2001.

261. Pitkowski A, Nicolai T and Durand D. Scattering and turbidity study of the dissociation of casein by calcium chelation. *Biomacromolecules* 9, 369-375, 2008.

262. Piwocka K, Bielak-Mijewska A and Sikora E. Curcumin induces caspase-3-independent apoptosis in human multidrug-resistant cells. *Annals of New York Academy of Sciences* 973, 250-254, 2002.

263. Pridgen EM, Langer R and Farokhzad OC. Biodegradable, polymeric nanoparticle delivery systems for cancer therapy. Nanomedicine 2, 669-680, 2007.

264. Qi L, Xu Z and Chen M. *In vitro* and *in vivo* suppression of hepatocellular carcinoma growth by chitosan nanoparticles. *European Journal of Cancer* 43, 184-193, 2007.

265. Qiu F, Feng J, Wu DQ, Zhang XZ and Zhuo RX. Nanosized micelles self-assembled from amphiphilic dextran-graft-methoxypolyethylene glycol/poly(ε-caprolactone) copolymers. *European Polymer Journal* 45, 1024-1031, 2009.

266. Quintana A, Raczka E, Piehler L, Lee I, Myc A, Majoros I, Patri AK, Thomas T, Mule J and Baker Jr. JR. Design and function of a dendrimer-based therapeutic nanodevice targeted to tumor cells through the folate receptor. *Pharmaceutical Research* 19, 1310-1316, 2002.

267. Radtke M and Müller RH. NLC - nanostructured lipid carriers: the new generation of lipid drug carriers. *New Drugs* 2, 48–52, 2001.

268. Rajaonarivony M, Vauthier C, Couarraze G, Puisieux F and Couvreur P. Development of a new drug carrier made from alginate. *Journal of Pharmaceutical Sciences* 82, 912–917, 1993.

269. Rao CNR and Cheetham AK. Science and technology of nanomaterials: current status and future prospects. *Journal of Material Chemisry* 11, 2887-2894, 2001.

270. Rapoport N, Pitt WG, Sun H and Nelson JL. Drug delivery in polymeric micelles: From in vitro to in vivo. *Journal of Controlled Release* 91, 85-95, 2003.

271. Ravindranath V and Chandrasekhara N. Absorption and tissue distribution of curcumin in rats. *Toxicology* 16, 259-265, 1980.

272. Reddy LH, Sharma RK, Chuttani K, Mishra AK and Murthy RSR. Influence of administration route on tumor uptake and biodistribution of etoposide loaded solid nanoparticles in Dalton's lymphoma tumor bearing mice. *Journal of Controlled Release* 105, 285-290, 2005.

273. Reuter S, Eifes S, Dicato M, Aggarwal BB and Diederich M. Modulation of anti-apoptotic and survival pathways by curcumin as a strategy to induce apoptosis in cancer cells. *Biochemical Pharmacology* 1340-1351, 2008.

274. Rieux A, Fievez V, Garinot M, Schneider YJ and Préat V. Nanoparticles as potential oral delivery systems of proteins and vaccines: a mechanistic approach. *Journal of Controlled Release*116, 1-27, 2006.

275. Rosen H and Abribat T. The rise and rise of drug delivery. *Nature Reviews Drug Discovery* 4, 381-385, 2005.

276. Rosenholm JM, Meinander A, Peuhu E, Niemi R, Eriksson JE, Sahlgren C and Linden M. Targeting of porous hybrid silica nanoparticles to cancer cells. *ACS Nano*, 3, 197-206, 2009.

277. Rossler B, Kreuter J and Scherer D. Collagen microparticles: preparation and properties. *Journal of Microencapsulation* 12, 49-57, 1995.

278. Roy I, Ohulchanskyy TY, Pudavar HE, Bergey EJ, Oseroff AR, Morgan J, Dougherty TJ and Prasad PN. Ceramic-based nanoparticles entrapping water-insoluble photosensitizing anticancer drugs: a novel drug-carrier system for photodynamic therapy. *Journal of American Chemical Society* 125, 7860-7865, 2003.

279. Ruszczak Z and Friess W. Collagen as a carrier for on-site delivery of antibacterial drugs. *Advanced Drug Delivery Reviews* 55, 1679-1698, 2003.

280. Salamaso S, Bersani S, Semenzato A and Caliceti P. New cyclodextrin bioconjugates for active tumour targeting. *Journal of Drug Ttargeting* 15, 379-390.

281. Sarmento B, Ferreira D, Veiga F and Ribeiro A. Characterization of insulin-loaded alginate nanoparticles produced by ionotropic pre-gelation through DSC and FTIR studies. *Carbohydrate Polymers* 66, 1-7, 2006.

282. Schiffelers RM and Storm G. Liposomal nanomedicines as anticancer therapeutics: Beyond targeting tumor cells. *International Journal of Pharmaceutics* 364, 258-264, 2008.

283. Schmidt HT, Gray BL, Wingert PA and Ostafin AE. Assembly of aqueous-cored calcium phosphate nanoparticles for drug delivery. *Chemistry of Materials* 16, 4942-4947, 2004.

284. Semo E, Kesselman E, Danino D and Livney YD. Casein micelle as a natural nano-capsular vehicle for nutraceuticals. *Food Hydrocolloids* 21, 936-942, 2007.

285. Senyei AE, Widder KJ and Czerlinski C. Magnetic guidance of drug carrying microspheres. *Journal of Applied Physics* 49, 3578-3583, 1978.

286. Seppala JV, Helminen AO and Korhonen H. Degradable polyesters through chain linking for packaging and biomedical applications. *Macromolecular Bioscince* 4, 208-217, 2004.

287. Serpe L, Catalano MG, Cavalli R, Ugazio E, Bosco O, Canaparo R, Muntoni E, Frairia R, Gasco MR, Eandi M, Zara GP. Cytotoxicity of anticancer drug incorporated in solid

lipid nanoparticles on HT-29 colorectal cancer cell line. *European Journal of Pharmaceutics Biopharmaceutics* 58, 673-680, 2004.

288. Sezgin Z, Yuksel N and Baykara T. Preparation and characterization of polymeric micelles for solubilization of poorly soluble anticancer drugs. *European Journal of Pharmaceutics Biopharmaceutics* 64, 261-268, 2006.
289. Shaikh J, Ankola DD, Beniwal V, Singh D and Ravi Kumar MNV. Nanoparticle encapsulation improves oral bioavailability of curcumin by at least 9-fold when compared to curcumin administered with piperine as absorption enhancer. *European Journal of Pharmaceutical Sciences* (in press).
290. Shankar T, Shantha N, Ramesh H, Murthy I and Murthy V. Toxicity studies on turmeric (Curcuma longa): acute toxicity studies in rats, guineapigs & monkeys. *Indian Journal of Experimental Biology* 18, 73-75, 1980.
291. Shen L and Ji HF. Theoretical study on physicochemical properties of curcumin. *Spectrochimica Acta A* 67, 619-623, 2007.
292. Shi KNW and Dai H. Carbon Nanotubes as Intracellular Protein Transporters: Generality and Biological Functionality. *Journal of American Chemical Society* 127, 6021-6026, 2005.
293. Shishodia S, Sethi G and Aggarwal BB. Curcumin: getting back to the roots. *Annals of* New York *Academy of Sciences* 1056, 206-217, 2005.
294. Shishodia S, Singh T and Chaturvedi MM, Modulation of transcription factors by curcumin. *Advances in Experimental Medicine and Biology* 595, 127-148, 2007.
295. Shoba G, Joy D, Joseph T, Majeed M, Rajendran R and Srinivas PS. Influence of piperine on the pharmacokinetics of curcumin in animals and human volunteers. *Planta Medica* 64, 353-356, 1998.
296. Shuai X, Ai H, Nasongkla N, Kim S and Gao J. Micellar carriers based on block copolymers of poly(epsilon-caprolactone) and poly(ethylene glycol) for doxorubicin delivery. Journal of Controlled Release 98, 415-426, 2004.
297. Shukla R, Thomas T, Peters J, Kotlyar A, Myc A and Baker Jr JR. Tumor angiogenic vasculature targeting with PAMAM dendrimer-RGD conjugates. *Chemical Communications* 5739-5741, 2005.

298. Shukla R, Thomas TP, Peters JL, Desai AM, Kukowska-Latallo J, Patri AK, Kotlyar A and Baker Jr. JR. HER2 specific tumor targeting with dendrimer conjugated anti-HER2 mAb. *Bioconjugate Chemistry* 17, 1109-1115, 2006.

299. Sidhu GS, Singh AK, Thaloor D, Banaudha KK, Patnaik GK, Srimal RC and Maheshwari RK. Enhancement of wound healing by curcumin in animals. *Wound Repair Regeneration* 6, 167-177, 1998.

300. Siebenlist U, Franzoso G and Brown K. Structure, regulation and function of NF-κB. *Annual Review of Cell Biology* 10, 405-455, 1994.

301. Sindhwani P, Hampton JA, Baig MM, Keck R, Selman SH. Curcumin prevents intravesical tumor implantation of the MBT-2 tumor cell line in C3H mice. *The Journal of Urology* 166, 1498-2501, 2001.

302. Singh S, Hu X, Srivastava SK, Singh M, Xia H, Orchard JL and Zaren HA. Mechanism of inhibition of benzo[a]pyrene-induced forestomach cancer in mice by dietary curcumin. *Carcinogenesis* 19, 1357-1360, 1998.

303. Sinha VR, Bansal K, Kaushik R, Kumria R and Trehan A. Poly-epsilon-caprolactone microspheres and nanospheres: an overview. *International Journal of Pharmaceutics* 278, 1-23, 2004.

304. Slowing II, Vivero-Escoto JL, Wu CW and Lin VSY. Mesoporous silica nanoparticles as controlled release drug delivery and gene transfection carriers. *Advanced Drug Delivery Reviews* 60, 1278-1288, 2008.

305. Soppimath K, Aminabhavi T, Kulkarni A and Rudzinski W. Biodegradable polymeric nanoparticles as drug delivery devices. *Journal of Controlled Release* 70, 1-20, 2001.

306. Sou K, Inenaga S, Takeoka S and Tsuchida E. Loading of curcumin into macrophages using lipid based nanoparticles. *International Journal of Pharmaceutics* 352, 287-293, 2008.

307. Sreepriya M and Bali G. Effects of administration of embelin and curcumin on lipid peroxidation, hepatic glutathione antioxidant defense and hematopoietic system during *N*-nitrosodiethylamine/phenobarbital-induced hepatocarcinogenesis in Wistar rats. *Molecular and Cellular Biochemistry* 284, 49–55, 2006.

308. Steinhauser I, Spänkuch B, Strebhardt K and Langer K. Trastuzumab-modified nanoparticles: Optimisation of preparation and uptake in cancer cells. *Biomaterials* 27, 4975-4983, 2006.

309. Sudarshan NR, Hoover DG and Knorr D. Antibacterial action of chitosan. *Food Biotechnology* 6, 257–272, 1992.

310. Sui Z, Salto R, Li J, Craik C and Ortiz de Montellano PR. Inhibition of the HIV-1 and HIV-2 proteases by curcumin and curcumin boron complexes. Bioinorganic Medicinal Chemistry 1, 415-422, 1993.

311. Sukhorukov GB, Volodkin DV, Gunther AM, Petrov AI, Shenoy DB and Mohwald H. Porous calcium carbonate microparticles as templates for encapsulation of bioactive compounds, *Journal of Materials Chemistry* 14, 2073–2081, 2004.

312. Sunamoto J and Ushio K. Folate-modified cholesterol-bearing pullulan, a new cancer targeted nanoparticle drug carrier: synthesis and applications. *Journal of Bioactive and Compatible Polymers* 21, 603-617, 2006.

313. Szejtli J. Introduction and general overview of cyclodextrin chemistry. *Chemical Review* 98, 1743-1754, 1998.

314. Tang H, Duan X, Feng X, Liu L, Wang S, Li Y and Zhu D. Fluorescent DNA–poly(phenylenevinylene) hybrid hydrogels for monitoring drug release. *Chemical Communications* 641-643, 2009.

315. Thomas TP, Patri AK, Myc A, Myaing MT, Ye JY, Norris TB and Baker Jr. JR, *In vitro* targeting of synthesized antibody-conjugated dendrimer nanoparticles. *Biomacromolecules* 5, 2269-2274, 2004.

316. Thoren L. The dextrans – clinical data. *Developments in Biological Standardization* 48, 157-167, 1981.

317. Tiyaboonchai W and Limpeanchob N. Formulation and characterization of amphotericin B – chitosan – dextran sulfate nanoparticles. *International Journal of Pharmaceutics* 329, 142-149, 2007.

318. Tiyaboonchai W, Woiszwillo J, Sims RC and Middaugh RC. Insulin containing polyethyleneumine – dextran sulfate nanoparticles. *International Journal of Pharmaceutics* 255, 139-151, 2003.

319. Tkachenko AG, Xie H, Coleman DM, Ryan J, Glomm W, Franzen S and Feldheim DL. Cellular trajectories of peptide-modified gold nanoparticle complexes: Comparison of nuclear localization signals and peptide transduction domains. Bioconjugate Chemistry 15, 482, 2004.

320. Tomalia DA, Baker H, Dewald J, Hall M, Kallos G, Martin S, Roeck J, Ryder J and Smith P. A new class of polymers: starburst-dendritic macromolecules. *Polymer Journal* 17, 117-132, 1985.

321. Torchilin VP. Recent advances with liposomes as pharmaceutical carriers. *Nature Reviews Drug Discovery* 4, 145-160, 2005.

322. Torchilin VP. Structure and design of polymeric surfactant-based drug delivery systems. *Journal of Controlled Release* 73,137-172, 2001.

323. Torchilin VP. Micellar nanocarriers: pharmaceutical perspectives. *Pharmaceutical Research* 24, 1-16, 2007.

324. Trewyn BG, Giri S, Slowing II and Lin VSY. Mesoporous silica nanoparticle based controlled release, drug delivery, and biosensor systems. *Chemical communications* 3236–3245, 2007a.

325. Trewyn BG, Nieweg JA, Zhao Y and Lin VSY. Biocompatible mesoporous silica nanoparticles with different morphologies for animal cell membrane penetration. *Chemical Engineering Journal* 137, 23–29, 2007b.

326. Trewyn BG, Slowing II, Giri S, Chen HT and Lin VSY. Synthesis and Functionalization of a mesoporous silica nanoparticle based on the sol–gel process and applications in controlled release. *Accounts of Chemical Research* 40, 846–853, 2007c.

327. Tseng CL, Wang TW, Dong GC, Wu SY, Young TH, Shieh MJ, Lou PJ and Lin FH. Development of gelatin nanoparticles with biotinylated EGF conjugation for lung cancer targeting. *Biomaterials* 28, 3996-4005, 2007.

328. Uchida A, Shinto Y, Araki N and Ono K. Slow release of anticancer drugs from porous calcium hydroxyapatite ceramic. *Journal of Orthopaedic Research* 10, 440-445, 2005.

329. Uchino H, Matsumura Y, Negishi T, Koizumi F, Hayashi T, Honda T, Nishiyama N, Kataoka K, Naito S and Kakizoe T. Cisplatin-incorporating polymeric micelles (NC-6004) can reduce nephrotoxicity and neurotoxicity of cisplatin in rats. *British Journal of Cancer* 93, 678-687, 2005.

330. Ueno Y, Futagawa H, Takagi Y, Ueno A and Mizushima Y. Drug-incorporating calcium carbonate nanoparticles for a new delivery system. *Journal of Controlled Release* 103, 93-98, 2005.

331. Uhrich KE, Cannizzaro SM, Langer RS and Shakesheff KM. Polymeric systems for controlled drug release. *Chemical Reviews* 99, 3181-3198, 1999.

332. Um SH, Lee JB, Park N, Kwon SY, Umbach CC and Luo D. Enzyme-catalyzed assembly of DNA hydrogel. *Nature Materials* 5, 797–801, 2006.

333. Vila A, Sánchez A, Tobío M, Calvo P and Alonso MJ**.** Design of biodegradable particles for protein delivery. *Journal of Controlled Release* 78, 15-24, 2002.

334. Vincenzatti S, Polidori P, Mariani P, Cammertoni N, Fantuz F and Vita A. Donkey's milk protein fractions characterization. *Food Chemistry* 106, 640-649, 2008.

335. Vonarbourg A, Passirani C, Saulnier P, Benoit JP. Parameters influencing the stealthiness of colloidal drug delivery systems. *Biomaterials* 27, 4356-4373, 2006.

336. Wang D, Veena MS, Stevenson K, Tang C, Ho B, Suh JD, Duarte VM, Faull KF, Mehta K, Srivatsan ES and Wang MB. Liposome encapsulated curcumin suppresses growth of head and neck squamous cell carcinoma *in vitro* and in xenografts through the inhibition of nuclear factor κB by an AKT-independent pathway. *Clinical Cancer Research* 14, 6228, 2008.

337. Wang YJ, Pan MH, Cheng AL, Lin LI, Ho YS, Hsieh CY. Stability of curcumin in buffer solutions and characterization of its degradation products. Journal of Pharmaceutical Biomedical Analysis 15, 1867-1876, 1997.

338. Wang YS, Liu LR, Jiang Q and Zhang QQ. Self-aggregated nanoparticles of cholesterol modified chitosan conjugate as a novel carrier of epirubicin. *European Polymer Journal* 43, 43-51, 2007.

339. Watanabe M, Kawano K, Yokoyama M, Opanasopit P, Okano T and Maitani Y. Preparation of camptothecin-loaded polymeric micelles and evaluation of their incorporation and circulation stability. *International Journal of Pharmaceutics* 308, 183-189, 2006.

340. Westesen K, Bunjes H and Koch MHJ. Physicochemical characterization of lipid nanoparticles and evaluation of their drug loading capacity and sustained release potential. *Journal of Controlled Release* 48, 223-236, 1997.

341. WHO Website: http://www.who.int/mediacentre/factsheets/fs297/en/index.html.

342. Widder KJ, Senyei AE and Ranney DF. Magnetically responsive microspheres and other carriers for the biophysical targeting of antitumor agents. *Advances in Pharmacology and Chemotherapy* 16, 213-271, 1979.

343. Wilhelm M, Zhao CL, Wang YC, Xu RL, Winnik MA, Mura JL, Riess G and Croucher MD. Poly(styrene-ethylene oxide) block copolymer micelle formation in water: a fluorescence probe study. *Macromolecules* 24, 1033-1040, 1991.

344. Willmott N, Magee GA, Cummings J, Halbert GW and Smyth JM. Doxorubicin loaded casein microspheres: protein nature of drug incorporation. *Journal of Pharmacy and Pharmacology* 44, 472-475, 1992.

345. Win KY and Feng SS. Effects of particle size and surface coating on cellular uptake of polymeric nanoparticles for oral delivery of anticancer drugs. *Biomaterials* 26, 2713-2722, 2005.

346. Wolinsky JB and Grinstaff MW. Therapeutic and diagnostic applications of dendrimers for cancer treatment. Advanced Drug Delivery Reviews 60, 1037-1055, 2008.

347. Wong HL, Bendayan R, Rauth AM, Li Y and Wu XY. Chemotherapy with anticancer drugs encapsulated in solid lipid nanoparticles. *Advanced Drug Delivery Reviews* 59, 491-504, 2007.

348. Woo JH, Kim YH, Choi YJ, Kim DG, Lee KS, Bae JH, Min DS, Chang JS, Jeong YJ, Lee YH, Park JW and Kwon TK. Molecular mechanisms of curcumin-induced cytotoxicity: induction of apoptosis through generation of reactive oxygen species, down-regulation of Bcl-XL and IAP, the release of cytochrome *c* and inhibition of Akt. *Carcinogenesis* 24, 1199–1208, 2003.

349. Woodle MC. Sterically stabilized liposome therapeutics. *Advanced Drug Delivery Reviews* 16, 249–265, 1995.

350. Wu G, Barth RF, Yang W, Kawabata S, Zhang L, and Green-Church K. Targeted delivery of methotrexate to epidermal growth factor receptor-positive brain tumors by means of cetuximab (IMC-C225) dendrimer bioconjugates, *Molecular Cancer Therapy* 5, 52-59, 2006.

351. Yang W, Cheng Y, Xu T, Wang X and Wen L. Targeting cancer cells with biotin–dendrimer conjugates. *European Journal of Medicinal Chemistry* 44, 862-868, 2009.

352. Yoo HS and Park TG. Biodegradable polymeric micelles composed of doxorubicin conjugated PLGA–PEG block copolymer. *Journal of Controlled Release* 70, 63-70, 2001.

353. Young S, Wong M, Tabata Y and Mikos AG. Gelatin for as a delivery vehicle the controlled release of bioactive molecules. *Journal of Controlled Release* 109, 256-274, 2005.

354. Yoysungnoen P, Wirachwong P, Bhattarakosol P, Niimi H and Patumraj S. Effects of curcumin on tumor angiogenesis and biomarkers, COX-2 and VEGF, in hepatocellular carcinoma cell-implanted nude mice. *Clin Hemorheol Microcirc* 34, 109–115, 2006.

355. Yuan F, Dellian M, Fukumura D, Leuniq M, Berk DA, Torchilin VP and Jain RK. Vascular permeability in a human tumor xenograft – molecular-size dependence and cutoff size. Cancer Research 55, 3752-3756, 1995.

356. Zamboni WC. Liposomal, nanoparticle, and conjugated formulations of anticancer agents. *Clinical Cancer Research* 11, 8230-8234, 2005.

357. Zhang DY, Shen XZ, Wang JY, Dong L, Zheng YL and Wu LL. Preparation of chitosan-polyaspartic acid-5-fluorouracil nanoparticles and its anti-carcinoma effect on tumor growth in nude mice. *World Journal of Gastroenterology* 14, 3554-3562, 2008.

358. Zhang L, Gu FX, Chan JM, Wang AZ, Langer RS and Farokhzad OC. Nanoparticles in medicine: therapeutic applications and developments. *Clinical Pharmacology and Therapeutics* 83, 761-769, 2008.

359. Zheng C, Qiu L and Zhu K. Novel polymersomes based on amphiphilic graft polyphosphazenes and their encapsulation of water-soluble anti-cancer drug. Polymer 50, 1173-1177, 2009.

360. Zhu J and Li P. Synthesis and characterization of poly(methyl methacrylate)/casein nanoparticles with a well-defined core-shell structure. *Journal of Polymer Science Part A* 41, 3346-3353, 2003.

Publications

Available online at www.sciencedirect.com
ScienceDirect
Acta Biomaterialia 4 (2008) 1752–1761
Acta BIOMATERIALIA
www.elsevier.com/locate/actabiomat

Synthesis of novel biodegradable and self-assembling methoxy poly(ethylene glycol)–palmitate nanocarrier for curcumin delivery to cancer cells

Abhishek Sahu, Utpal Bora *, Naresh Kasoju, Pranab Goswami

Biomaterials and Tissue Engineering Laboratory, Department of Biotechnology, Indian Institute of Technology Guwahati, Guwahati 781 039, Assam, India

Received 17 January 2008; received in revised form 17 April 2008; accepted 25 April 2008
Available online 11 May 2008

Abstract

A novel polymeric amphiphile, mPEG–PA, was synthesized with methoxy poly(ethylene glycol) (mPEG) as the hydrophilic and palmitic acid (PA) as the hydrophobic segment. The conjugate prepared in a single-step reaction showed minimal toxicity on HeLa cells. ^{1}H nuclear magnetic resonance imaging and Fourier transform infrared spectroscopy revealed that the conjugation was through an ester linkage, which is biodegradable. Enzymes having esterase activity, such as lipase, can degrade the conjugate easily, as observed by in vitro studies. mPEG–PA conjugate undergoes self-assembly in an aqueous environment, as evidenced by fluorescence spectroscopic studies with pyrene as a probe. The mPEG–PA conjugate formed micelles in the aqueous solution with critical micelle concentration of 0.12 g l^{-1}. Atomic force microscopy and dynamic light scattering studies showed that the micelles were spherical in shape, with a mean diameter of 41.43 nm. The utility of mPEG–PA to entrap the potent chemopreventive agent curcumin in the core of nanocarrier was investigated. The encapsulation of a highly hydrophobic compound like curcumin in the nanocarrier makes the drug readily soluble in an aqueous system, which can increase the ease of dosing and makes intravenous dosing possible. Drug-loaded micelle nanoparticles showed good stability in physiological condition (pH 7.4), in simulated gastric fluid (pH 1.2) and in simulated intestinal fluid (pH 6.8). This micellar formulation can be used as an enzyme-triggered drug release carrier, as suggested by in vitro enzyme-catalyzed drug release using pure lipase and HeLa cell lysate. The IC_{50} of free curcumin and encapsulated curcumin was found to be 14.32 and 15.58 μM, respectively.

Keywords: Nanocarrier; Curcumin; Anticancer; Micelle; Bioavailability

1. Introduction

Curcumin is a low-molecular-weight natural polyphenol isolated from turmeric (*Curcuma longa*) that has low intrinsic toxicity but a wide range of pharmacological activity, including antitumor, antioxidant, anti-amyloid and anti-inflammatory properties [1]. It is a potent inhibitor of NF-κB, a transcription factor implicated in the pathogenesis of several malignancies [2], and also inhibits the production of various cytokines, including tumor necrosis factor-α and interleukin-1β [3]. Pre-clinical studies of curcumin have shown its ability to inhibit carcinogenesis in a variety of cell lines, including breast, cervical, colon, gastric, hepatic, leukemia, oral epithelial, ovarian, pancreatic and prostate cancer [4]. As a result, interest is increasing in the clinical development of this compound as a cancer chemopreventive agent [5]. Despite all these promising characteristics, a major problem with curcumin is its extreme low solubility in aqueous solutions, which limits its bioavailability and clinical efficacy [6]. In a clinical study, Shoba et al. showed that after oral administration of 2 g kg^{-1} of curcumin to rats a maximum serum concentration of 1.35 ± 0.23 μg ml^{-1} was observed at time 0.83 h, whereas in humans the same dose of curcumin resulted in

* Corresponding author. Tel.: +91 0361 2582215; fax: +91 0361 2582249.
E-mail addresses: ubora@iitg.ernet.in, ubora@rediffmail.com (U. Bora).

1742-7061/$ - see front matter © 2008 Acta Materialia Inc. Published by Elsevier Ltd. All rights reserved.
doi:10.1016/j.actbio.2008.04.021

extremely low (0.006 ± 0.005 μg ml^{-1} at 1 h) serum levels [7]. To increase its aqueous solubility and bioavailability, attempts have been made through encapsulation in liposome, polymeric nanoparticle, lipid-based nanoparticle, biodegradable microsphere, cyclodextrin and hydrogel [8–14]. One possible way of increasing its aqueous solubility is encapsulation within the core of a micellar nanocarrier [15–18].

Interest in nanocarriers for cancer chemotherapy is growing [19]. Polymeric micelles has gained attention as nanocarriers [20–22] due to several advantages, such as (i) their low toxicity; (ii) their high stability; (iii) their small size (<200 nm), which has made them ideal candidate for passive targeting of solid tumor tissue sites by enhanced permeation and retention (EPR) effect [23]; and (iv) they can be prepared in large quantities easily and reproducibly. Several drugs formulated in polymeric micelles are in clinical trial development for the treatment of various cancers [24,25]. Studies on polymeric micelles prepared from block copolymers have been carried out by many groups [26,27], but synthesis of block copolymers by polymerization reaction is a tedious multistep process that requires expertise. Recently many studies have been conducted on self-aggregation behavior of hydrophobically modified water-soluble polymers that can self-assemble to form micelles in the aqueous phase [28,29]. Studies have proved that polymeric amphiphiles consisting of hydrophilic poly(ethylene glycol) (PEG) and hydrophobic low-molecular-weight natural components such as diacyllipid, fatty acid and bile salts can form self-aggregated micelles [30–33].

In this study, we describe a simple method of synthesis and characterization of a novel polymeric amphiphile based on methyl poly(ethylene glycol) (mPEG) as the hydrophilic and palmitate (PA) as the hydrophobic segment. PEG is a well-known biocompatible polymer with an antifouling property and palmitate is a naturally occurring fatty acid in animals. The nonionic hydrophilic PEG shell can suppress opsonin adsorption and subsequent clearance by the mononuclear phagocyte system, thereby prolonging the circulation time, and influences the pharmacokinetics and biodistribution of the drug delivery system [34,35], whereas the hydrophobic core of PA can solubilize curcumin.

The conjugate was synthesized in a single-step reaction. The PEG chain was conjugated with PA through an ester linkage that can be degraded inside the cells. The mPEG–PA conjugate forms self-assembled micelle nanoparticles with hydrophobic anticancer drug curcumin in the core. We also demonstrate enzyme-triggered release of the drug through hydrolysis of the ester linkage of the amphiphilic conjugate by lipase.

2. Materials and methods

2.1. Materials

mPEG (mol. wt. 5000) and palmitoyl chloride was purchased from Fluka (Bangalore, India) and Aldrich (Bangalore, India), respectively. Curcumin was from Himedia Laboratories (Mumbai, India). Porcine pancreatic lipase was from Sigma (Bangalore, India). All the solvents used in the study were of analytical grade and obtained from Merck (Mumbai, India).

Human cervical cancer cell line (HeLa) was obtained from National Centre for Cell Science (Pune, India). Cells were maintained in Eagle's minimum essential medium, containing 2 mM L-glutamine, 1.5 g l^{-1} sodium bicarbonate, 0.1 mM non-essential amino acids and 1.0 mM sodium pyruvate, supplemented with 10% fetal bovine serum and 1% antibiotic antimycotic solution (1000 U ml^{-1} penicillin G, 10 mg ml^{-1} streptomycin sulfate, 5 mg ml^{-1} gentamycin and 25 μg ml^{-1} amphotericin B). Cells were cultured at 37 °C in a humidified atmosphere supplied with 5% CO_2.

2.2. Synthesis of mPEG–PA conjugate

The conjugation of mPEG–PA was carried out by reacting mPEG with palmitoyl chloride. mPEG (1 mM) was dissolved in toluene and mixed with triethylamine (final concentration 1 mM). A solution of palmitoyl chloride (1.1 mM) in toluene was added dropwise and stirred continuously for 3 h at 60 °C. The solution was then filtered through filter paper (Whatman, grade 1) to remove the precipitated triethylamine hydrochloride salt. Then mPEG–PA conjugate was precipitated from filtrate by adding cold diethyl ether. The conjugate was characterized by ^{1}H nuclear magnetic resonance imaging (NMR; Mercury Plus 400 MHz, Varian, CA, USA) and Fourier transform infrared (FTIR; Spectrum One, Perkin Elmer, MA, USA) spectroscopy.

2.3. Preparation of self-assembled micellar nanoparticles of mPEG–PA conjugate

The dry powder of mPEG–PA conjugate was dissolved in phosphate-buffered saline (PBS; 0.01 M, pH 7.4) and sonicated for 30 min to get an optically clear solution. The critical micelle concentration (CMC) of mPEG–PA was determined by using pyrene as a hydrophobic fluorescence probe. The CMC was determined based on the intensity of pyrene excitation spectra and shift of the spectra with increasing mPEG–PA concentrations. The pyrene solutions (6×10^{-6} M) in acetone were added to the test tubes and evaporated to remove the solvent. Solutions of mPEG–PA micelles in PBS (0.01 M, pH 7.4) were then added to the test tubes in concentrations ranging from 0.001 to 1 mg ml^{-1}, bringing the final concentration of pyrene to 6.0×10^{-7} M. The solutions were vortexed and kept overnight at 37 °C to equilibrate pyrene with the micelles. Steady-state fluorescence excitation spectra of pyrene were measured at an emission wavelength of 390 nm (Fluoro Max-3, Jobin Yvon, Horiba, USA) with slit widths of 2.5 and 5.0 nm for excitation and emission, respectively.

2.4. Dynamic light scattering (DLS) and atomic force microscopy (AFM) studies

Size distribution of mPEG–PA micelles before and after drug loading (2.5 mg ml^{-1} in 0.01 M PBS, pH 7.4) were analyzed by DLS (Zetasizer NanoZS, Malvern Instruments, Worcestershire, UK) using an argon laser beam at 633 nm and 90° scattering angle. The shape of the micelle nanoparticles before and after drug loading was characterized by AFM (Picoscan, Molecular Imaging, CA, USA). A drop of micellar solution (2.5 mg ml^{-1}) was placed on freshly cleaved mica. After 1 min of incubation the surface was gently rinsed with deionized water to remove unbound micelles. The samples were air dried at room temperature and mounted on the microscope scanner. The micelle shape was observed and imaged in non-contact mode.

2.5. Encapsulation of curcumin in micellar nanoparticle

The encapsulation efficiency of curcumin was studied in different concentrations of mPEG–PA. Curcumin solution in methanol was added to the solution of mPEG–PA in chloroform to obtain different drug:polymer ratios ranging from 1:20 to 1:100. Methanol was evaporated under vacuum to produce a film consisting of mPEG–PA/curcumin mixture. Micelles were formed by extensive vortexing of the film in PBS. Nonencapsulated curcumin was separated by centrifugation of the micelle suspension at 5000 rpm (Sigma 4K-15 refrigerated centrifuge, Germany) for 10 min and quantified spectrophotometrically (Cary 100 BIO UV–Vis spectrophotometer, Varian, CA, USA) at 425 nm. The entrapment efficiency was calculated by following equation:

$$\text{Encapsulation efficiency (\%)} = \frac{(\text{Total amount of curcumin} - \text{Free curcumin})}{\text{Total amount of curcumin}} \times 100$$

The micelle-loaded curcumin was characterized by absorption and fluorescence spectra.

2.6. In vitro stability of drug-loaded micelle

Curcumin-loaded mPEG–PA (100 mg) was dispersed in 10 ml of physiological buffer (0.01 M PBS, pH 7.4), simulated gastric fluid (0.2 g sodium chloride and 0.7 ml concentrated HCl in 100 ml water, pH 1.2) and simulated intestinal fluid (0.68 mg KH_2PO_4 and 7.7 ml of 0.2 M NaOH in 100 ml water, pH 6.8) separately and incubated at 37 °C under gentle agitation. Drug retention was studied at different time intervals, ranging from 6 to 48 h. The percentage of drug retained was determined with the following equation:

$$\text{Drug retention (\%)} = \frac{(\text{Total curcumin encapsulated} - \text{Released curcumin})}{\text{Total curcumin encapsulated}} \times 100$$

2.7. Enzyme-catalyzed degradation of micelle and in vitro drug release

To examine the degradation of micelle and site of action of enzyme, 50 mg of mPEG–PA was dissolved in 10 ml of 0.1 M PBS (pH 7.4) containing bovine pancreatic lipase (0.5 mg ml^{-1}) and kept at 37 °C. After 48 h the precipitate was collected and washed several times with water, then dried. The dried precipitate was recrystallized from chloroform and analyzed by ^{1}H NMR to confirm the cleavage site.

To estimate the drug release by enzyme-catalyzed degradation of micelle, the lipase solution in PBS (0.01 M, pH 7.4) was added to the drug-loaded micelle solution at a final concentration of 0.5 mg ml^{-1} and incubated at 37 °C. Samples were collected at different time intervals ranging from 2 to 48 h and the released curcumin was estimated as described in Section 2.5. The release was quantified as follows:

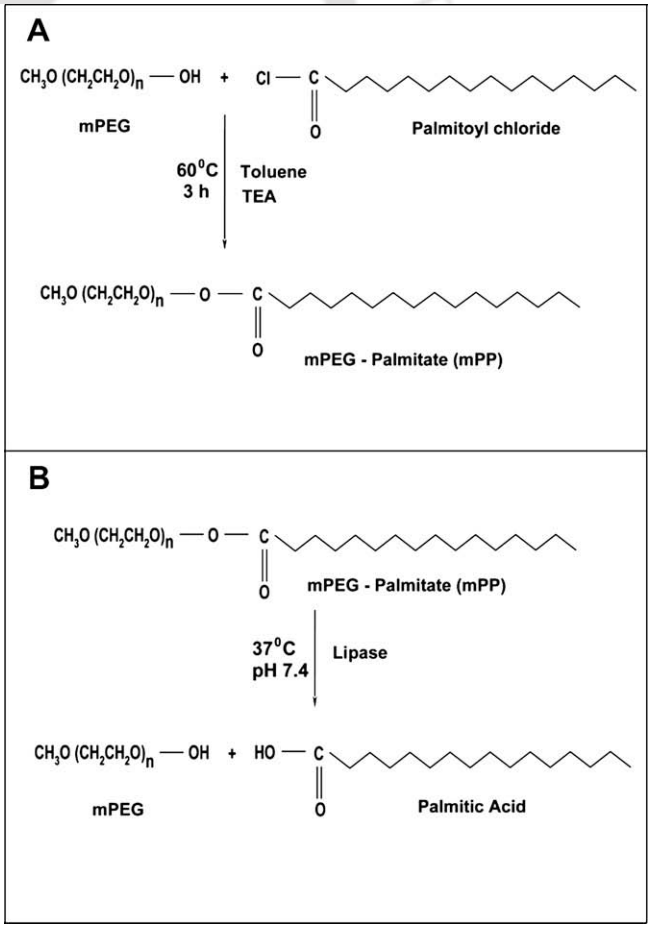

Scheme 1. (A) Synthesis of methoxy poly(ethylene glycol)–palmitate (mPEG–PA) conjugate. The hydrophilic mPEG was conjugated to hydrophobic palmitate through an ester linkage by reacting with palmitoyl chloride. (B) Lipase-catalyzed degradation of mPEG–PA. Lipase hydrolyzes the ester bond of mPEG–PA to yield mPEG and palmitic acid in physiological conditions (0.01 M PBS, pH 7.4).

$$\text{Release } (\%) = \frac{\text{Released curcumin}}{\text{Total curcumin}} \times 100$$

To study the drug release by cellular enzymes, cell lysate was obtained from HeLa cells by mechanical lysis. Cells were mechanically disrupted by vigorous passage (10 times) through a needle using a 2 ml syringe. Then the solution was centrifuged at 10,000*g* (10 min, 4 °C) and supernatant was collected carefully. The supernatant containing intracellular enzymes was added to the drug-loaded micelle solution and drug release was quantified as above.

2.8. Confocal laser scanning microscopy and cytotoxicity studies

To visualize the cellular uptake of drug-loaded micelle HeLa cells were grown in 35 mm culture plate up to 80% confluency. Cells were treated with 15 μM free and micelle-encapsulated curcumin. As curcumin is insoluble in aqueous solution, the free curcumin was dissolved with the aid of dimethylsulfoxide (DMSO). The final concentration of DMSO in the culture medium was always <0.1%. After 2 h, cells were examined under a confocal laser scanning microscope (LSM 510 Meta, Zeiss, Germany) for intracellular curcumin fluorescence. The cytotoxicity of the free and encapsulated curcumin was determined by methylthiazoletetrazolium (MTT) dye assay, as described by Mosmann [36]. HeLa cells were seeded into a 96-well cell culture plate at a density of 1×10^4 cells well^{-1} and grown for 24 h before the assay. The cells were then exposed to a series of different concentrations of free and encapsulated curcumin (1–30 μM) for 48 h followed by addition of 100 μl MTT (0.5 mg/ml) in culture medium to each well and incubated for 4 h. Empty micelle was used to test the cytotoxicity of the nanocarrier. After incubation 100 μl of DMSO was added to each well and absorbance

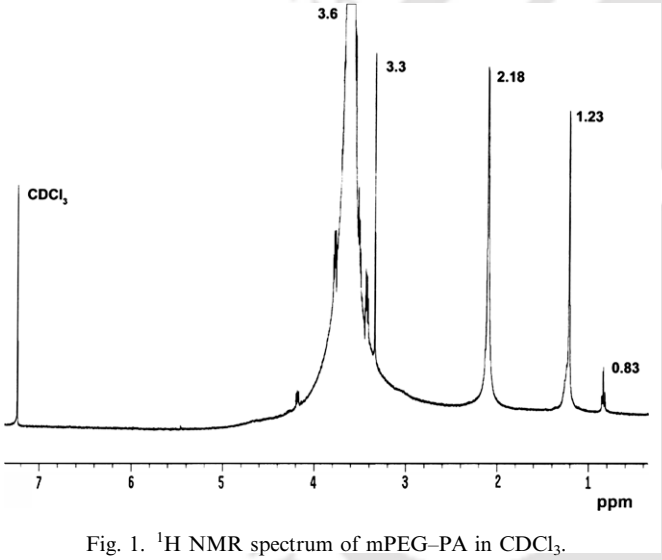

Fig. 1. ^{1}H NMR spectrum of mPEG–PA in $CDCl_3$.

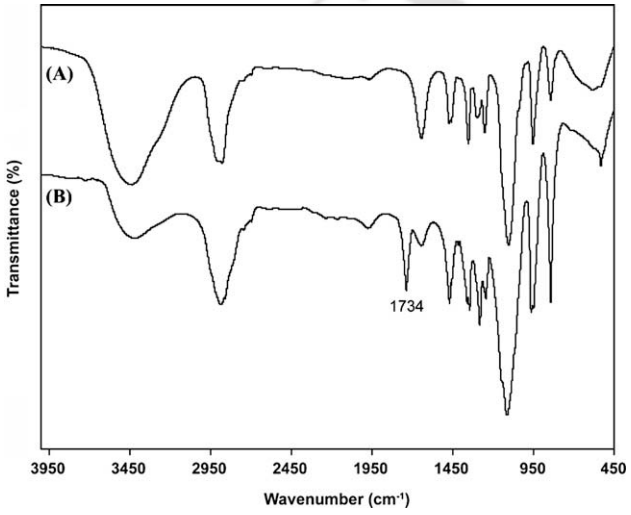

Fig. 2. FTIR spectrum of mPEG (A) and mPEG–PA (B) conjugate. The peak at 1734 cm^{-1} in the spectrum of mPEG–PA confirms the presence of an ester linkage in the conjugate.

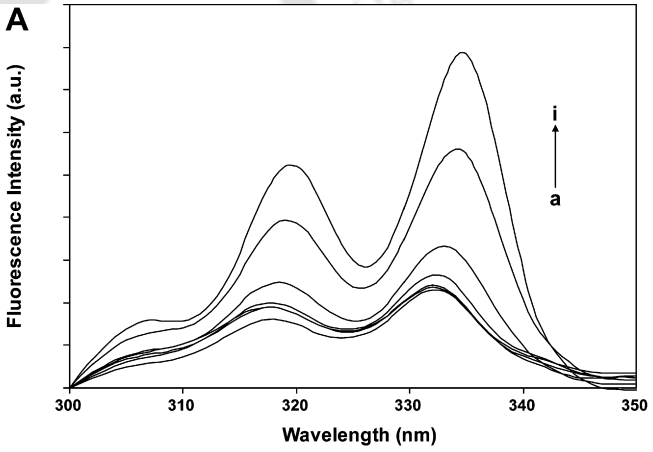

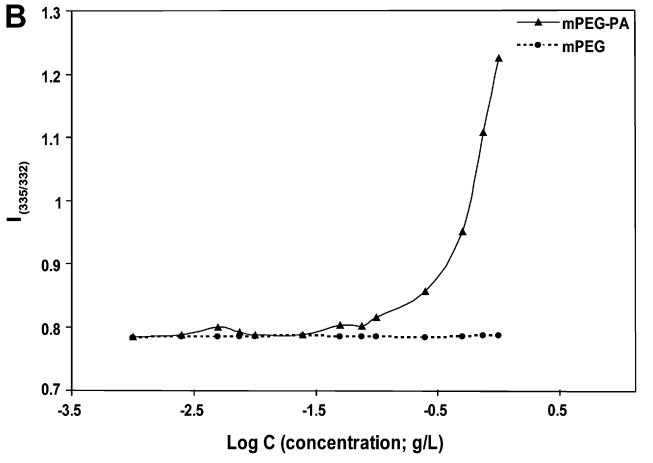

Fig. 3. (A) Fluorescence excitation spectra of pyrene (6×10^{-7} M) in mPEG–PA solution (0.01 M PBS, pH 7.4) with concentrations of: (a) 0.001, (b) 0.005, (c) 0.01, (d) 0.05, (e) 0.1, (f) 0.25, (g) 0.5, (h) 0.75 and (i) 1.0 mg ml^{-1}. (B) Plot of intensity ratio ($I_{335/332}$) from pyrene excitation spectra as a function of log (concentration) for mPEG–PA and mPEG. The CMC value of mPEG–PA conjugate was calculated from the crossover point of $I_{335/332}$.

was measured at 570 nm using a microplate reader (Biorad Microplate Reader, Model 680, CA, USA). The cell viability was expressed as a percentage of the control by following equation:

$$\text{Viability } (\%) = N_t/N_c \times 100$$

where N_t is the absorbance of the cells treated with free curcumin or curcumin loaded micelles and N_c was the absorbance of the untreated cells.

3. Results and discussion

mPEG–PA conjugate was prepared in a single-step reaction. The palmitoyl chloride reacts with the hydroxyl group of mPEG to provide an ester linkage, as shown in Scheme 1A and confirmed by ^{1}H NMR (Fig. 1) and FTIR (Fig. 2) spectra. NMR signals at δ 3.6 and δ 3.3 are due to the methylene protons of PEG oxyethylene unit and protons of the methoxy end group, respectively. Coupling of the

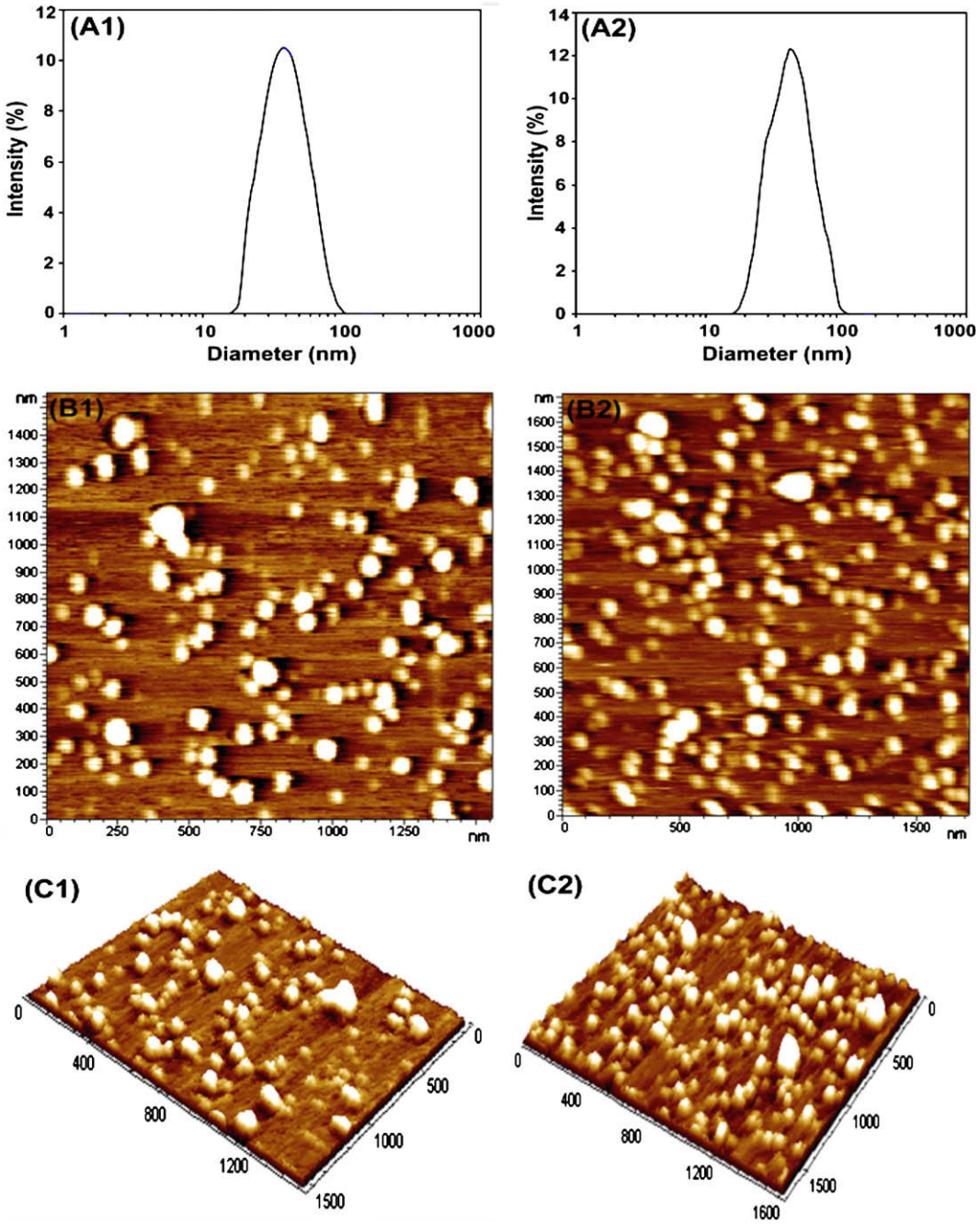

Fig. 4. Size distribution of (A1) blank and (A2) curcumin-loaded mPEG–PA micelle as measured by DLS. The average hydrodynamic diameter of the blank and curcumin-encapsulated micelles was found to be 41.43 and 47.36 nm, respectively. AFM images of (B1, C1) blank and (B2, C2) curcumin-loaded mPEG–PA micelle. The micelles were spherical in shape, as seen in the topographic images (B1, B2). C1 and C2 represent the three-dimensional views of B1 and B2, respectively.

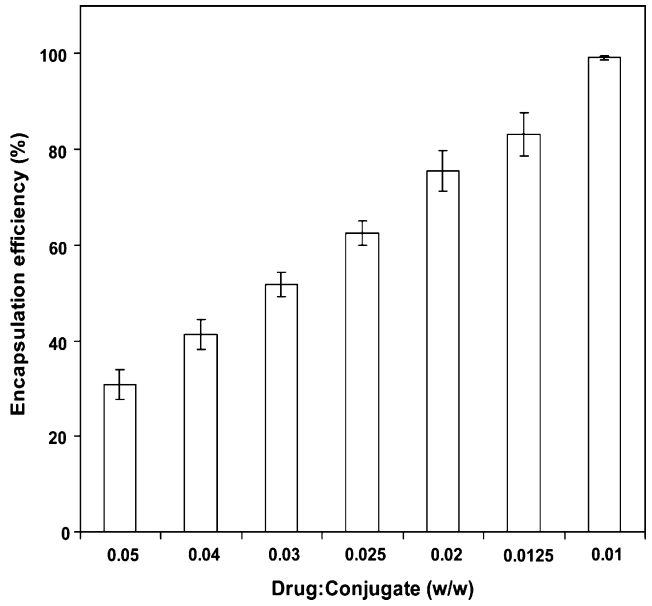

Fig. 5. Drug loading: curcumin encapsulation with different concentrations of mPEG–PA. Drug encapsulation was dependent on the drug to polymer ratio.

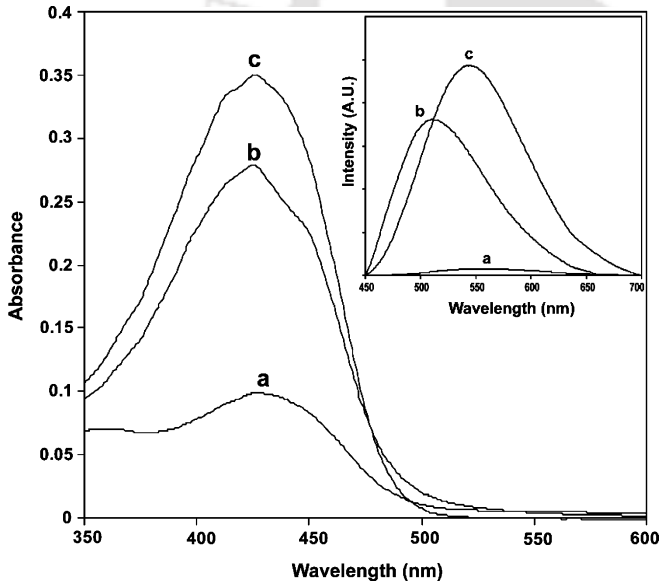

Fig. 6. Ultraviolet–visible absorbance spectra of curcumin in different solutions. (a) Curcumin in aqueous solution containing 10% methanol; (b) curcumin loaded in mPEG–PA micelle; (c) methanolic solution of curcumin. The inset corresponds to the fluorescence emission spectra of the respective curcumin solutions when excited at 420 nm.

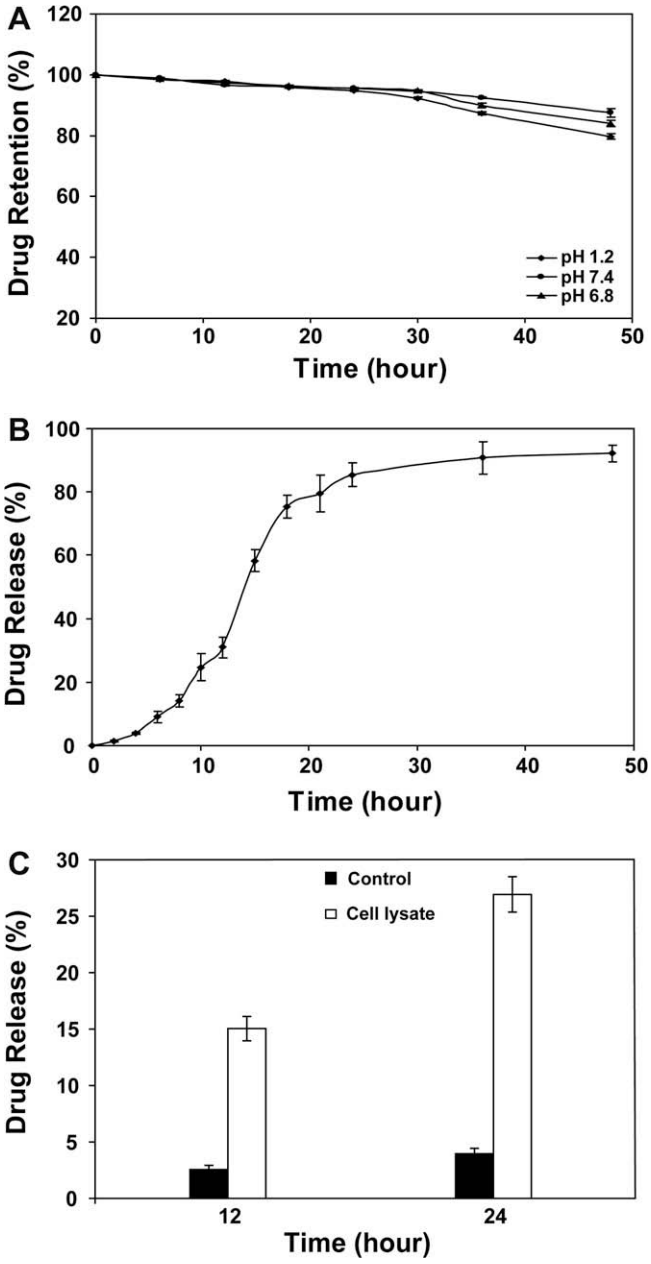

Fig. 7. (A) In vitro stability of curcumin loaded mPEG–PA micelle in PBS (pH 7.4), simulated gastric fluid (pH 1.2) and simulated intestinal fluid (pH 6.8) at 37 °C. (B) Lipase-catalyzed release of drug (curcumin) from micelle nanoparticle in PBS (pH 7.4) at 37 °C. (C) Drug release from micelle nanoparticle by HeLa cell lysate. Drug release was greater in the presence of cell lysate with respect to the control.

palmitate residue to mPEG was confirmed by the appearance of signals in the region δ 0.8–2.4 ppm. The IR spectrum of mPEG–PA conjugate shows a sharp peak at 1734 cm^{-1} due to the stretching vibration of the ester bond. This peak was not present in the spectrum of mPEG, which confirms the formation of mPEG–PA conjugate via ester linkage.

The amphiphilic nature of the polymeric amphiphile consisting of a hydrophobic palmitate and a hydrophilic PEG segment provides the opportunity to form micelles in water with a palmitate core and a PEG shell. The formation of self-aggregates in aqueous solution was studied by fluorescence spectroscopy where pyrene was used as the fluorescent probe. We observed strong fluorescence when mPEG–PA micelles were formed in the presence of pyrene in an aqueous solution against control experiments carried out with pyrene alone in water. This is because pyrene behaves as a self-quenching agent in a polar environment

and exhibits fluorescence when located inside or close to the hydrophobic domain of micelle (Fig. 3A). With the increase in the concentration of mPEG–PA the fluorescence intensity increased, indicating that the pyrene was transferred from aqueous solution to the less polar hydrophobic interior of the self-aggregated micelle. The partitioning of pyrene brought about the shift in its excitation peak from 332 to 335 nm. The CMC of micelle was determined from the curve showing relationship between changes in intensity ($I_{335/332}$) of pyrene with the log (concentration) of mPEG–PA (Fig. 3B). At low concentrations, the intensity ($I_{335/332}$) value remains nearly unchanged, but with further increasing mPEG–PA concentration the intensity begins to increase significantly, implying the onset of self-assembly. The CMC was calculated from the crossover point and its value was 0.12 g l^{-1}. This value of CMC was much lower than low-molecular-weight surfactants (e.g. 2.3 g l^{-1} for sodium dodecyl sulfate in water). It indicates that micelles formed from mPEG–PA conjugate were thermodynamically stable and could preserve stability without dissociation after dilution caused by intravenous injection. However, in the control, where only mPEG was used, no appreciable change in pyrene fluorescent intensity was observed over all the concentrations, clearly indicating that in this concentration range mPEG cannot aggregate to form a micelle-like structure. This implies that the presence

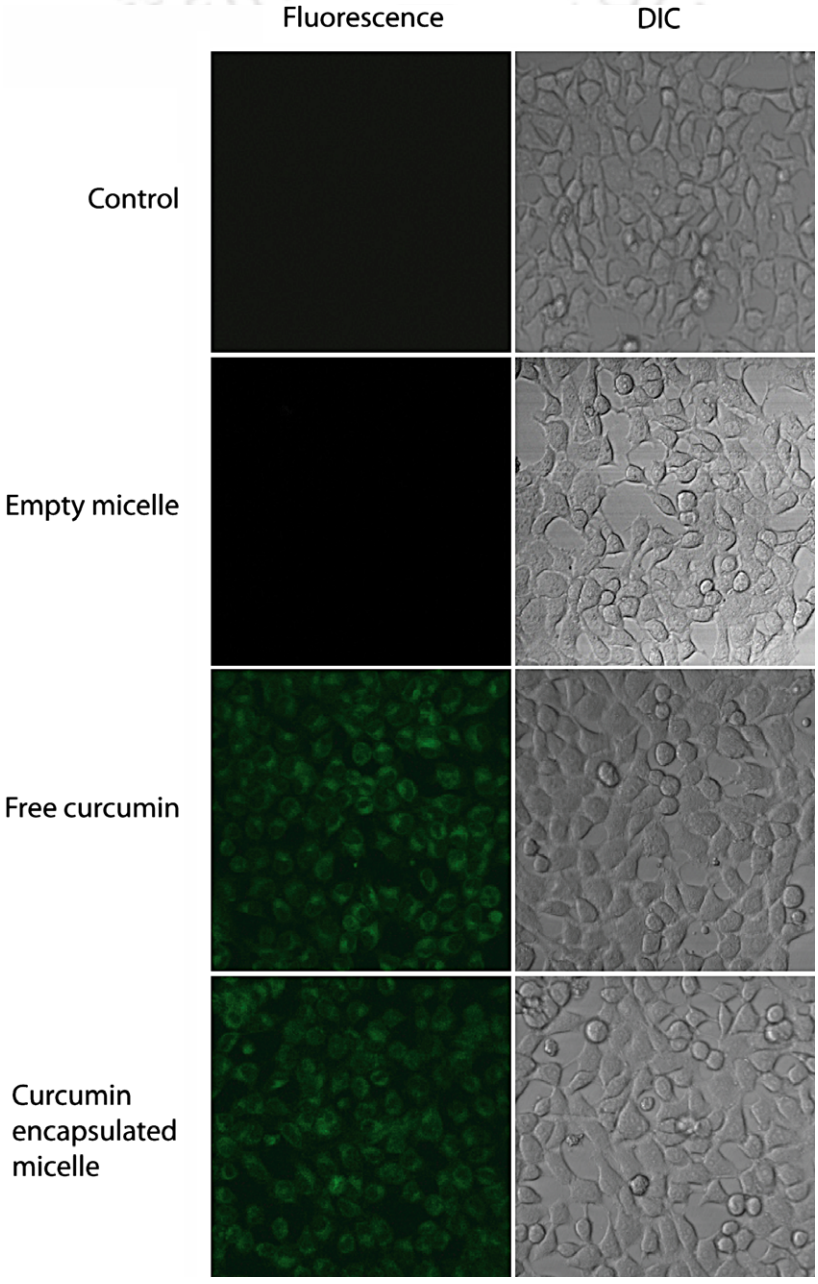

Fig. 8. Differential interference contrast (DIC) and fluorescence confocal images of internalization of free and micelle-loaded curcumin by HeLa cells. The green fluorescence of curcumin inside the cells can be observed clearly. Cells were visualized at 2 h after treatment.

of hydrophobic palmitate chain is necessary for micelle formation.

The size and morphology of the self-assembled micelle nanoparticles of mPEG–PA were determined by light-scattering measurements and AFM. The mean diameters of the blank and drug-loaded micelles were found to be 41.43 and 47.36 nm, respectively, with a narrow size distribution in the DLS experiment (Fig. 4A). The increase of micelle size can be attributed to the expansion of core after drug loading. This average size of the drug-loaded mPEG–PA micelles was lower than the size of curcumin-loaded lipid-based nanoparticles [11] and comparable to the other nano-formulations of curcumin [10,16,17]. The small size of this formulation can be advantageous for passive targeting of tumor tissues by the EPR effect. The AFM image taken in non-contact mode showed that the micelles were spherical in shape before and after drug loading (Fig. 4B). The size observed in the AFM was in good agreement with that measured by DLS.

To investigate whether these nanocarriers could be used advantageously for encapsulating the highly hydrophobic drug curcumin for delivery to cancer cells, we studied the encapsulation of curcumin by the novel mPEG–PA conjugate and subsequent internalization to HeLa cells. The encapsulation efficiency of curcumin in mPEG–PA micelles was dependent on the drug to conjugate ratio. The encapsulation efficiency was found to be 31% when drug to conjugate ratio (w/w) was 0.05. The encapsulation efficiency increases with increasing amount of mPEG–PA. At a drug:conjugate ratio of 0.01 the encapsulation efficiency was close to 100%. So, when the drug to polymer ratio was high, the encapsulation was lower, and it increased as the ratio decreased (Fig. 5).

The micelle-encapsulated curcumin shows distinct photophysical properties (Fig. 6). Curcumin in aqueous solution (10% methanol solution was used to solubilize curcumin, which was insoluble in pure water) has weak absorption, with a peak at around 425 nm. The absorption intensity of encapsulated curcumin increased sharply towards that of curcumin dissolved in methanol alone. The fluorescence spectra also exhibited similar behavior. In aqueous solution it shows a weak broad peak at 550 nm, whereas the micelle-loaded curcumin shows a well-defined blue-shifted fluorescent peak at 500 nm with high intensity. This increase of absorption and fluorescence intensity suggests that curcumin in mPEG–PA is encapsulated in the hydrophobic core of the micelle.

For effective passive targeting of cancerous tissues, drug-loaded micelles should be able to retain the drug for a prolonged time in circulation. We observed that mPEG–PA micelles exhibited high in vitro stability in physiological conditions (pH 7.4). Micelles can retain more than 95% of incorporated curcumin for the first 24 h. Drug retention inside the micelles after 36 and 48 h of incubation was over 92% and 87%, respectively (Fig. 7A). After 48 h of incubation in simulated gastric fluid (pH 1.2) 80% of the drug was retained, and in case of simulated intestinal fluid it was 84%. Thus the micellar formulation has very high stability under broad physiological pH conditions.

The mPEG–PA conjugate is biodegradable, as evidenced by enzyme degradation studies. When lipase acted on mPEG–PA micelle we anticipated the release of free mPEG into the solution and palmitic acid as an insoluble precipitate (Scheme 1B). ^{1}H NMR of the precipitate showed four peaks, at δ 0.88, 1.3, 1.6 and 2.18, which confirmed that the precipitate was palmitic acid (data not shown), as per the proposed scheme, and that micelle degradation occurred due to the cleavage of the ester bond of the conjugate. In vitro lipase-catalyzed release of curcumin from the core of the micelle was observed for 48 h. Fig. 7B indicates that the enzyme-catalyzed release of curcumin occurred in a controlled manner. In the first 12 h only 30% of curcumin was released from the micelle, which increased up to 85% by 24 h. Thereafter there was a drop in the rate of release, until finally 92% of curcumin was released in total by 48 h.

To verify that the ester linkage of mPEG–PA can be cleaved inside the cells to release the entrapped drug, we performed an in vitro experiment with HeLa cell lysate. The cell lysate successfully degraded the micelles to release curcumin (Fig. 7C). About 15% and 26% drug release was observed after 12 and 24 h, respectively, upon exposure to HeLa cell lysate that contains enzymes such as esterase and lipases.

Taking advantage of the intrinsic green fluorescence of curcumin, we studied its cellular uptake by confocal microscopy. The microscopic images of control cells without any drug exposure and cells incubated with empty mPEG–PA micelles did not show any fluorescence, whereas the images of cells treated with encapsulated and free curcumin exhibited green fluorescence due to the internalized curcumin (Fig. 8). So, cells can internalize micelle

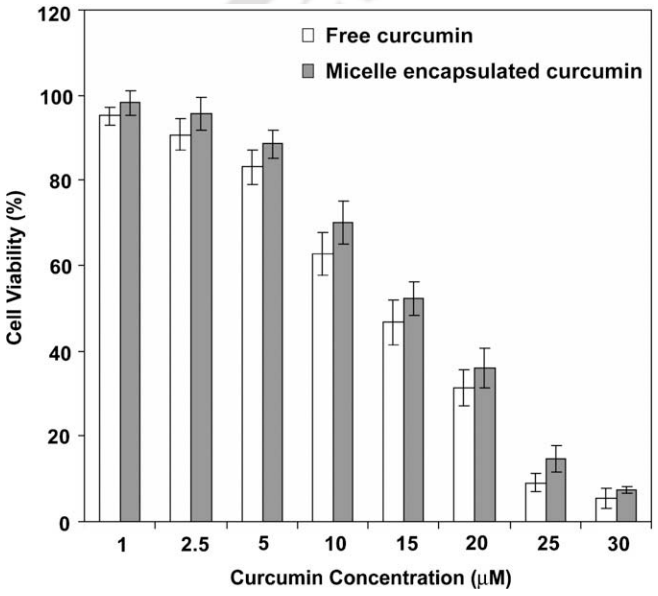

Fig. 9. Cytotoxicity assay: cell viability of HeLa cells exposed to free curcumin and mPEG–PA micelle-encapsulated curcumin.

encapsulated curcumin as effectively as free curcumin. However, the mPEG–PA-encapsulated curcumin has the added advantage of enhanced solubility and can therefore be used directly without any organic solvent.

The empty micelle was found to be nontoxic at 2.5 mg ml^{-1} (data not shown) and was used for curcumin encapsulation. Results of the cytotoxicity assay showed that encapsulated curcumin ($IC_{50} = 15.58$ μM) inhibited cell proliferation comparably to free curcumin ($IC_{50} = 14.32$ μM) (Fig. 9).

4. Conclusions

We have prepared a novel biodegradable polymeric mPEG palmitate amphiphilic conjugate that forms spherical micelles in aqueous solution through a process of self-assembly. The advantages of this conjugate is that it can be synthesized in a single-step reaction, shows minimal toxicity on HeLa cells and can successfully encapsulate hydrophobic drug, as exhibited with studies involving the chemopreventive agent curcumin. Encapsulation of curcumin in the core of the micelles increased the aqueous solubility of the drug. Drug-loaded nanocarriers showed good stability over a wide pH range. The small size of the drug-loaded micelles is promising for passive targeting of tumors through the EPR effect. Thus, this novel micellar nanoencapsulation may improve the bioavailability of curcumin and will make this drug amenable to intravenous dosing without affecting its anticancer properties. This conjugate is a potential model system for encapsulating hydrophobic drugs and preparation of enzyme-triggered release systems, as demonstrated by in vitro studies for enzyme-mediated degradation and release of encapsulated drug with lipase and HeLa cell lysate.

Acknowledgements

This work was funded by the Department of Biotechnology, Government of India. A.S and N.K. thank IIT Guwahati for financial support in the form of fellowship.

References

[1] Maheshwari RK, Singh AK, Gaddipati J, Srimal RC. Multiple biological activities of curcumin: a short review. Life Sci 2006;78:2081–7.
[2] Singh S, Aggarwal BB. Activation of transcription factor NF-κB is suppressed by curcumin (diferulolylmethane). J Biol Chem 1995;270:24995–5000.
[3] Abe Y, Hashimoto S, Horie T. Curcumin inhibition of inflammatory cytokine production by human peripheral blood monocytes and alveolar macrophages. Pharmacol Res 1999;39:41–7.
[4] Aggarwal BB, Kumar A, Bharti AC. Anticancer potential of curcumin: preclinical and clinical studies. Anticancer Res 2003;23:363–98.
[5] Sharma RA, Gescher AJ, Steward WP. Curcumin: the story so far. Eur J Cancer 2005;41:1955–68.
[6] Anand P, Kunnumakkara AB, Newman RA, Aggarwal BB. Bioavailability of curcumin: problems and promises. Mol Pharm 2007;4:807–18.
[7] Shoba G, Joy D, Joseph T, Majeed M, Rajendran R, Srinivas PS. Influence of piperine on the pharmacokinetics of curcumin in animals and human volunteers. Planta Med 1998;64:353–6.
[8] Li L, Ahmed B, Mehta K, Kurzrock R. Liposomal curcumin with and without oxaliplatin: effects on cell growth, apoptosis and angiogenesis in colorectal cancer. Mol Cancer Ther 2007;6:1276–82.
[9] Kunwar A, Barik A, Pandey R, Priyadarsini KI. Transport of liposomal and albumin loaded curcumin to living cells: an absorption and fluorescence spectroscopic study. Biochim Biophys Acta 2006;1760:1513–20.
[10] Bisht S, Feldmann G, Soni S, Ravi R, Karikar C, Maitra A, et al. Polymeric nanoparticle-encapsulated curcumin (''nanocurcumin''): a novel strategy for human cancer therapy. J Nanobiotechnol 2007;5:3.
[11] Sou K, Inenaga S, Takeoka S, Tsuchida E. Loading of curcumin into macrophages using lipid-based nanoparticles. Int J Pharm 2008;352:287–93.
[12] Kumar V, Lewis SA, Mutalik S, Shenoy DB, Venkatesh, Udupa N. Biodegradable microspheres of curcumin for treatment of inflammation. Ind J Physiol Pharmacol 2002;46:209–17.
[13] Salmaso S, Bersani S, Semenzato A, Caliceti P. New cyclodextrin bioconjugates for active tumor targeting. J Drug Target 2007;15:379–90.
[14] Vemula PK, Li J, John G. Enzyme catalysis: tool to make and break amygdalin hydrogelators from renewable resources: a delivery model for hydrophobic drugs. J Am Chem Soc 2006;128:8932–8.
[15] Ma Z, Shayeganpour A, Brocks DR, Lavasanifar A, Samuel J. High-performance liquid chromatography analysis of curcumin in rat plasma: application to pharmacokinetics of polymeric micellar formulation of curcumin. Biomed Chromatogr 2007;21:546–52.
[16] Letchford K, Liggins R, Burt H. Solubilization of hydrophobic drugs by methoxy poly(ethylene glycol)-block–polycaprolactone diblock copolymer micelles: theoretical and experimental data and correlations. J Pharm Sci 2008;97:1179–90.
[17] Ma Z, Haddadi A, Molavi O, Lavasanifar A, Lai R, Samuel J. Micelles of poly(ethylene oxide)-b-poly(ε-caprolactone) as vehicles for the solubilization, stabilization, and controlled delivery of curcumin. J Biomed Mater Res A, doi:10.1002/jbm.a.31584.
[18] Chen HC, Lin HY, Lin CC, Lee MH. The encapsulation of curcumin in micelles. In: Proceedings of the IEEE 31st annual northeast bioengineering conference; 2005. p. 275–6.
[19] Peer D, Karp JM, Hong S, Farokhzad OC, Margalit R, Langer R. Nanocarriers as an emerging platform for cancer therapy. Nat Nanotechnol 2007;2:751–60.
[20] Torchilin VP. Micellar nanocarriers: pharmaceutical perspectives. Pharm Res 2007;24:1–16.
[21] Jones MC, Leroux JC. Polymeric micelles – a new generation of colloidal drugs. Eur J Pharm Biopharm 1999;48:101–11.
[22] Kwon GS. Polymeric micelles for delivery of poorly water-soluble compounds. Crit Rev Ther Drug Carr Syst 2003;20:357–403.
[23] Maeda H, Wu J, Sawa T, Matsumura Y, Hori K. Tumor vascular permeability and the EPR effect in macromolecular therapeutics: a review. J Control Release 2000;65:271–84.
[24] Kim TY et al. Phase I and pharmacokinetic study of genexol-PM, a cremophor-free, polymeric micelle-formulated paclitaxel, in patients with advanced malignancies. Clin Cancer Res 2004;10:3708–16.
[25] Matsumura Y et al. Phase I clinical trial and pharmacokinetic evaluation of NK911, a micelle-encapsulated doxorubicin. Br J Cancer 2004;91:1775–81.
[26] Kataoka K, Harada A, Nagasaki Y. Block copolymer micelles for drug delivery: design, characterization and biological significance. Adv Drug Deliv Rev 2001;47:113–31.
[27] Gaucher G, Dufresne MH, Sant VP, Kang N, Maysinger D, Leroux JC. Block copolymer micelles: preparation, characterization and application in drug delivery. J Control Release 2005;109:169–88.
[28] Lukyanov AN, Torchilin VP. Micelles from lipid derivatives of water-soluble polymers as delivery systems for poorly soluble drugs. Adv Drug Deliv Rev 2004;56:1273–89.

[29] Torchilin VP. Structure and design of polymeric surfactant-based drug delivery systems. J Control Release 2001;73:137–72.
[30] Gao Z, Lukyanov AN, Singhal A, Torchilin VP. Diacyllipid-polymer micelles as nanocarriers for poorly soluble anticancer drugs. Nano Lett 2002;2:979–82.
[31] Lee JH, Jung SW, Kim IS, Jeong Y, Kim YH, Kim SH. Polymeric nanoparticle composed of fatty acids and poly(ethylene glycol) as a drug carrier. Int J Pharm 2003;251:23–32.
[32] Kim IS, Kim SH. Evaluation of polymeric nanoparticles composed of cholic acid and methoxy poly(ethylene glycol). Int J Pharm 2001;226:23–9.
[33] Kim C, Lee SC, Kang SW, Kwon IC, Kim Y, Jeong SY. Synthesis and the micellar characteristics of poly(ethylene oxide)–deoxycholic acid conjugates. Langmuir 2000;16:4792–7.
[34] Owens DE, Peppas NA. Opsonization, biodistribution and pharmacokinetics of polymeric nanoparticles. Int J Pharm 2006;307:93–102.
[35] Vonarbourg A, Passirani C, Saulnier P, Benoit JP. Parameters influencing the stealthiness of colloidal drug delivery systems. Biomaterials 2006;27:4356–73.
[36] Mosmann T. Rapid colorimetric assay for cellular growth and survival: application to proliferation and cytotoxicity assays. J Immunol Methods 1983;65:55–63.

Fluorescence Study of the Curcumin−Casein Micelle Complexation and Its Application as a Drug Nanocarrier to Cancer Cells

Abhishek Sahu, Naresh Kasoju, and Utpal Bora*

Biomaterials and Tissue Engineering Laboratory, Department of Biotechnology, Indian Institute of Technology Guwahati, Guwahati-781039 Assam, India

Received June 24, 2008; Revised Manuscript Received August 14, 2008

In milk caseins exists a natural nanostructure, which can be exploited as a carrier of hydrophobic drugs. Here we investigated the complex formation of curcumin with bovine casein micelles (CMs) and its use as a vehicle for drug delivery to cancer cells. DLS studies of the CM suspension that was stable in buffer solution (pH 7.4) showed an average size distribution of <200 nm. SEM and AFM studies showed that the particles were roughly spherical in shape. Steady-state fluorescence spectroscopy of the CM−curcumin complex formation revealed that curcumin molecules formed complexes with CMs (CM−curcumin complex) through hydrophobic interactions. The binding constant for the CM−curcumin interaction was calculated to be 1.48×10^4 M^{-1}, as determined by the curcumin fluorescence. Fluorescence quenching showed that curcumin molecules quench the intrinsic fluorescence of caseins upon binding. We evaluated the utility of CMs as carriers of curcumin by using in vitro cultured HeLa cells. Cytotoxicity studies of HeLa cells revealed that the IC_{50} of free curcumin and the CM−curcumin complex was 14.85 and 12.69 μM, respectively.

Introduction

In recent years, nanocarriers (NCs) have been receiving much attention as potential drug carriers in cancer therapy.[1] NCs have the potential to improve the therapeutic index of currently available drugs by increasing drug efficacy, lowering drug toxicity, and achieving steady-state therapeutic levels of drugs over an extended period of time. NCs also improve drug solubility and stability and allow the development of potentially effective new chemical entities that have been stalled during the preclinical or clinical development as a result of suboptimal pharmacokinetics or biochemical properties.[2] Various NCs such as inorganic and polymeric nanoparticles, dendrimers, liposomes, polymeric micelles, and biomolecules such as gelatin and albumin have been used to prepare nanoparticles for drug delivery applications.[3,4]

Drug delivery systems that are based on food proteins hold much promise because of their biocompatibility and biodegradability.[5] Caseins, the major milk proteins, have excellent emulsification and gelation and water binding properties and are widely used in the food industry for various food products. Microspheres of casein that are prepared by glutaraldehyde cross-linking have been used for the oral delivery of anticancer drugs such as doxorubicin, mitoxantrone, and so forth.[6,7] However, the natural structure of casein micelle (CM) as such has not been used for drug delivery. Only recently have researchers used this natural protein micelle for drug or nutraceutical encapsulation. Huppertz et al. prepared microgel and nanogel particles from CMs, whereas Semo et al. used them as natural nanocapsular vehicles for lipophilic nutraceutical vitamin D.[8,9]

Milk CMs are part of the milk transport system in which nutrients are passed from the mother to suckling offspring. They are a primary source of amino acids and calcium phosphates for neonates. These micelles are almost spherical aggregates that are stabilized as a colloidal suspension in milk. They are composed of four phosphoproteins, namely, α_{s1}-casein, α_{s2}-casein, β-casein, and κ-casein, at a molar ratio of about 4:1:4:1.3. They are held together in the micellar nanostructure by hydrophobic interactions and by the bridging of calcium phosphate nanoclusters (colloidal calcium phosphate, CCP) that are bound to phosphorylated serine residues of the casein side chains.[10] CCP plays a crucial role in the maintenance of the micellar integrity. Three of the caseins (α_{s1}-, α_{s2}-, and β-casein) contain centers of phosphorylation (at least three phosphoserine residues in close proximity) that can bind to the amorphous MCP cluster and thereby form a stabilizing protein shell. Both α_{s1}- and α_{s2}-casein contain more than one phosphate center and can thus act as linking agents between nanoclusters.[11] The surface of the micelles is primarily covered with κ-casein, which provides a hydrophilic, charged, and diffuse surface layer and stabilizes the micelles through intermicellar electrostatic and steric repulsion, which is similar to a polyelectrolyte brush.[12]

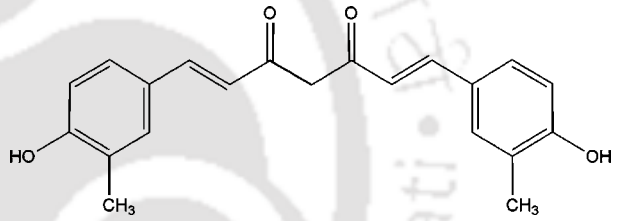

Figure 1. Chemical structure of curcumin.

Curcumin (diferuloylmethane) is a low-molecular-weight, natural polyphenolic compound that is isolated from the rhizome of turmeric (*Curcuma longa*). It is a lipophilic fluorescent molecule with phenolic groups and conjugated double bonds (Figure 1). It has a low intrinsic toxicity but a wide range of pharamacological activities including antioxidant, anti-inflammatory, antimicrobial, antiamyloid, and antitumor properties.[13,14]

* To whom correspondence should be addressed. Tel: +91-361-2582215. Fax: +91-361-2582249. E-mail: ubora@iitg.ernet.in, ubora@rediffmail.com.

10.1021/bm800683f CCC: $40.75
Published on Web 09/12/2008

Preclinical studies of curcumin have shown its ability to inhibit carcinogenesis in a variety of cell lines that include breast, cervical, colon, gastric, hepatic, leukemia, oral epithelial, ovarian, pancreatic, and prostate cancer.[15] The ability of curcumin to induce apoptosis in cancer cells without cytotoxic effects on healthy cells makes it a potential compound for drug development against cancer.[15,16] The molecular mechanism that underlie curcumin's selective toxicity against tumor cells are not clearly understood. An in vitro study of limited cells lines revealed that curcumin increases the levels of superoxide, downregulates the expression of bcl-2, depletes cellular glutathione, and lowers glutathione *S*-transferase activity, which leads to cell death by apoptosis, whereas normal cells that were treated with curcumin did not show any such altered activities and did not follow the pathway to death.[17] However, various studies have revealed a much more complex picture that shows that curcumin interacts with multiple molecular targets that affect the many processes that are involved in cancer, including the inhibition of NF-$\kappa\beta$ and TNF-α, the release of cytochrome c, the generation of reactive oxygen species (ROS), and so forth.[15,18,19]

The major problem with curcumin is its extremely low solubility in aqueous solution (2.99×10^{-8} M) and its poor bioavailability, which limits its clinical efficacy.[20,21] Attempts have been made through encapsulation in polymeric micelles, liposomes, polymeric nanoparticles, lipid-based nanoparticles, and hydrogels to increase its aqueous solubility and bioavailability.[22−27]

In this article, we have reported the complexation of chemopreventive agent curcumin with the natural nanostructure of CMs and its application in drug delivery to cancer cells. We investigated the interaction between curcumin and CM by using steady-state fluorescence spectroscopy. The binding constant of the curcumin to the low-polarity regions of CM was calculated from fluorescence data, and the probable binding region of curcumin in CM was characterized. We also investigated CM's potential as a carrier of curcumin. Our results suggest that CM can make a complex with curcumin, and the CM−curcumin complex was efficiently internalized by HeLa cells.

Materials and Methods

Chemicals. Curcumin, 3,4,5-dimethylthiazol-2-yl-2−5-diphenyltetrazolium bromide (MTT), and casein hydrolysate were purchased from Himedia Laboratory (Mumbai, India). Calcium chloride and Tris base were purchased from Merck (Mumbai, India). SDS-PAGE molecular weight markers were purchased from Sigma (Bangalore, India). All other reagents used were of analytical grade.

Purification of Casein Micelles. Casein micelle was purified from fresh cow milk that was collected from a local dairy according to Diaz et al.[28] with slight modifications. The milk was skimmed by centrifugation at 1500*g* for 30 min at 4 °C. The skimmed milk was stored at 4 °C with 0.05% (w/v) sodium azide to prevent microbial growth if it was not used immediately. Casein micelles were purified from skimmed milk by centrifugation at 25 000*g* for 30 min at 20 °C. The pellet that contained CM was then redispersed in Tris buffer (10 mM, pH 7.4) containing 10 mM $CaCl_2$. This centrifugation redispersion process was repeated five times to wash out any whey proteins that were loosely adsorbed over the CM surface. We measured the casein content in the solution by the Bradford assay[29] by using bovine serum albumin (BSA) as the standard.

Gel Electrophoresis Analysis. We carried out SDS-PAGE as described by Laemmli[30] by using a Bio-Rad mini gel electrophoresis unit. Total milk protein and isolated casein were loaded onto a 12% gel and were electrophoresed under a constant current (20 mA). We stained proteins in the gel by using Coomassie Brilliant Blue R-250. The gel was photographed by the use of a gel documentation system (BioRad).

Stability of the Casein Micelle Solution. To determine the stability of the CM suspension upon dilution, we measured the wavelength (λ) dependence of the turbidity (τ) of the suspensions, which is represented as[31]

$$\alpha = -\left(\frac{d\log \tau}{d\log \lambda}\right)$$

where α was obtained from the slope of log τ versus log λ plots in the 400−800 nm wavelength range.

We measured turbidity by using a UV−visible spectrophotometer (Cary-100 Bio, Varian). Turbidity (τ) was calculated by the use of the following equation[32]

$$\tau = \ln\left(\frac{I_0}{I}\right)\frac{1}{L}$$

where I and I_0 are the transmitted and incident intensities of light, respectively. L was the sample path length. In our case, L was 1 cm.

The measurements were conducted with freshly prepared samples.

Physical Characterization of the CM Suspension. The size of the CM solution was measured in a dynamic light scattering particle size analyzer (LB-550, Horiba, Japan) that was equipped with a 650 nm laser light source. Measurements were carried out at 90° scattering angle at room temperature.

The morphology evaluation of the CM was performed by scanning electron microscopy (SEM) and atomic force microscopy (AFM). For SEM analysis, a drop of CM solution was placed on foil paper, was air dried, was coated with gold, and was observed under microscope (LEO 1430 VP, UK). For AFM analysis, a drop of CM solution was placed on a freshly cleaved mica surface and was dried under nitrogen stream. Images were taken in noncontact mode (Picoscan, Molecular Imaging).

Fluorescence Spectroscopy. The binding of curcumin with CMs was quantified by fluorescence spectrophotometry. Steady-state fluorescence measurements were carried out in a Spex FluoroMax-3 spectrofluorimeter (Horiba Jobin Yvon). We measured the fluorescence of curcumin by keeping its concentration constant at 5 μM and by varying the CM concentration from 0 to 20 μM. The emission spectra were recorded from 450 to 700 nm with an excitation wavelength of 420 nm. The slit widths were 2 and 5 for excitation and emission, respectively. CM solutions without curcumin were used as controls for fluorescence measurements.

Protein intrinsic fluorescence was measured at a constant CM concentration (10 μM) in the presence of 0, 1, 1.5, 2, 2.5, 3, 3.5, 4, 4.5, and 5 μM curcumin. Emission spectra were individually recorded from 300 to 450 nm (at an excitation wavelength of 280 nm) and from 315 to 450 nm (at an excitation wavelength of 295 nm). In this case, free curcumin solutions without CM were used as controls, and fluorescence was similarly recorded.

In both cases, the fluorescence spectra of controls were subtracted from the respective spectra of samples to cancel out any contribution that was due to the Raman peak and other scattering artifacts. For the calculation of the binding constant, we made corrections for the inner filter effect by using the following equation[33]

$$FI_{corr} = FI_{obs} \times 10^{-0.5(A_{ex}+A_{em})}$$

where FI_{corr} and FI_{obs} are the corrected and background-subtracted fluorescence intensities of the sample and A_{ex} and A_{em} are the measured absorbances of the samples at the excitation and emission wavelengths, respectively.

To study the binding of curcumin to the submicelles, we prepared a casein submicelle solution by dissociating CM with 0.1 M sodium citrate. The dissociation of CM was confirmed by the reduction in turbidity of the suspension.[34] Curcumin was added to this solution at a final concentration of 5 μM. The same concentration of curcumin

was also added to a solution of casein hydrolysate. The curcumin fluorescence was recorded in both of the solutions as above and was compared with that of the intact CM solution.

Cell Culture and Cytotoxicity Assay. Human cervical cancer cell line HeLa was a gift from the National Centre for Cell Sciences (Pune, India). Cells were maintained in DMEM containing 2 mM L-glutamine, 1.5 g/L sodium bicarbonate, 0.1 mM nonessential amino acids, and 1.0 mM sodium pyruvate that was supplemented with 10% FBS (heat inactivated) and 1% antibiotic−antimycotic solution (1000 U/mL penicillin G, 10 mg/mL streptomycin sulfate, 5 mg/mL gentamycin, and 25 μg/mL amphotericin B). Cells were cultured at 37 °C in a humidified atmosphere that was supplied with 5% CO_2.

The cell viability was assessed by MTT assay, which is based on the reduction of MTT by the mitochondrial dehydrogenase of live cells to a purple formazan product.[35] HeLa cells (1×10^4) were seeded in a 96-well plate (CellBind, Corning). After 24 h of growth, the medium was exchanged for the medium that contained each of the following substances: empty CM, free curcumin, and the CM−curcumin complex. The curcumin stock solution (5 mM) was prepared in ethanol. From the stock solution, aliquots of curcumin were rapidly added to the culture medium to give the final concentrations of free curcumin. In the case of the CM−curcumin complex, the stock curcumin was diluted with CM solution in culture media. After 48 h of treatment, media were removed and cells were washed with phosphate-buffered saline (PBS). Then, 100 μL of MTT (0.5 mg/mL) in the culture medium was added to each well and incubated for 4 h at 37 °C. After incubation, the medium was removed, and 100 μL of DMSO was added to each well to solubilize the formazan crystals. We determined the amount of formazan that formed in each well by measuring the absorbance at 570 nm by using a multiwell plate reader (Biorad microplate reader, model 680, CA). The cell viability was calculated by following equation

$$\text{cell viability } (\%) = \left(\frac{A_{\text{treated}}}{A_{\text{control}}}\right) \times 100$$

where A_{treated} and A_{control} are the absorbances of the treated and untreated cells, respectively. The IC_{50} was measured as the concentration of drug at which 50% cells were viable compared with that of the control.

Cellular Uptake of Curcumin. HeLa cells were seeded in a 24-well plate at a seeding density of 1×10^4 cells per well in 1 mL of growth medium and were allowed to attach for 24 h. For the studies of concentration-dependent uptake, cells were treated with equivalent doses of free curcumin and the CM−curcumin complex and were incubated for 4 h. After the incubation, the medium was removed and the cells were washed twice with PBS. To extract curcumin, we lysed the cells by adding methanol. The cell lysate was centrifuged at 10 000 rpm for 10 min at 4 °C. The curcumin content in the supernatant was measured by the use of a fluorescence spectrophotometer ($\lambda_{ex} = 420$ and $\lambda_{em} = 540$ nm).

Microscopic Study. The effect of the CM−curcumin complex on the morphology of HeLa cells was assessed by microscopy. Cells were seeded onto 35 mm culture plates (CellBind, Corning) and were incubated for 24 h for attachment and were then treated with the CM−curcumin complex that contained 30 μM curcumin. We carried out control experiments by treating similarly plated cells with CM alone. The plates were removed from the incubator at different time intervals and were observed under inverted phase contrast microscope (Eclipse TS100, Nikon) with a 40× objective. Photographs were taken by a digital camera (Coolpix 5400, Nikon) that was attached to the microscope. Simultaneously, we observed fluorescence by excitation with a blue filter.

Results and Discussion

The protein composition of isolated CMs was analyzed by SDS-PAGE. The gel showed four distinct bands in the lane of CM with molecular weights ranging from 26 to 37 kDa (Figure 2). Although the molecular weights of different caseins are in the 19.0−25.0 kDa range, they have been reported to behave abnormally in Laemmli gels.[36] We observed that our result was similar to that of Vincenzetti et al.,[37] and for the stoichiometric calculations, we have taken the average molecular weight of the caseins to be 23.5 kDa according to Gatti et al.[38]

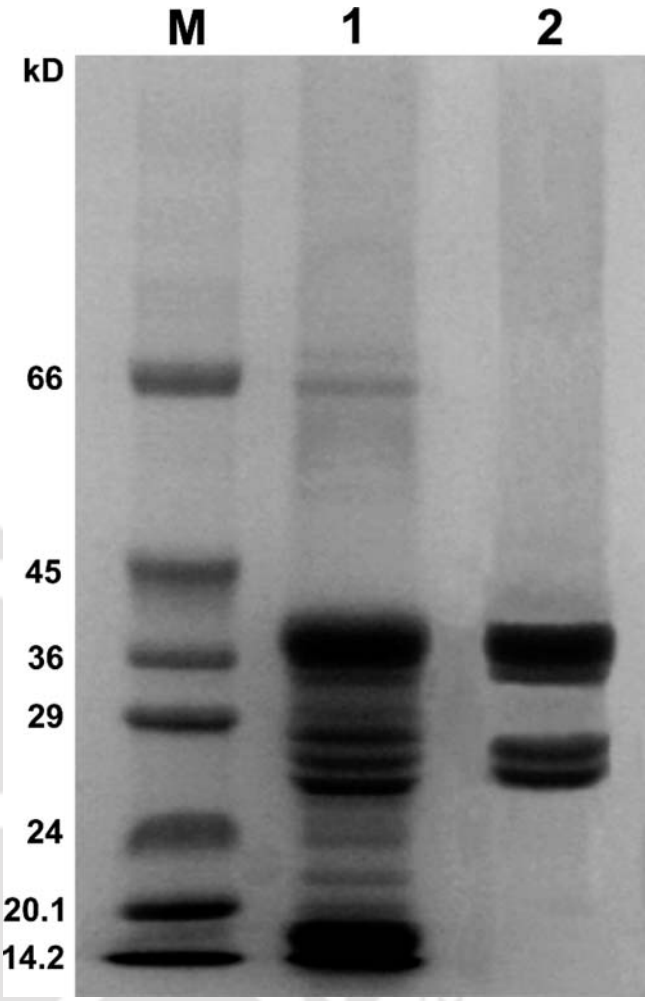

Figure 2. SDS-PAGE of molecular weight marker (lane M), skimmed milk (lane 1), and purified casein micelle (lane 2). In lane 2, the four distinct bands with molecular weights ranging from 37 to 26 kDa belong to α_{s1}-casein, α_{s2}-casein, β-casein, and κ-casein, respectively.

Isolated micelles were redispersed as a suspension in Tris buffer (pH 7.4) that contained 10 mM $CaCl_2$. Ca^{2+} ions are necessary for a stable CM suspension preparation.[38] The turbidity (τ) of the purified CM suspension was determined at 400 and 600 nm at different CM concentrations. We observed a linear increase in τ with CM concentration at both wavelengths (Figure 3A). We have also calculated values of α at different CM concentrations. It was previously reported that the value of α is related to CM size.[31,38] Increasing the value of CM size shows a decrease in the α value. In our case, we observed that the value of α was nearly constant for different CM concentrations, which suggests that the purified CMs were stable against dilution in the buffer solution.

The size of the CMs that were measured by DLS revealed that the mean diameter of the protein particles was 166.3 (±33.1) nm (Figure 4A, inset). SEM and AFM analyses showed that the nanoparticles were roughly spherical in shape (Figure 4A,B). SEM and AFM data were in good agreement with the DLS

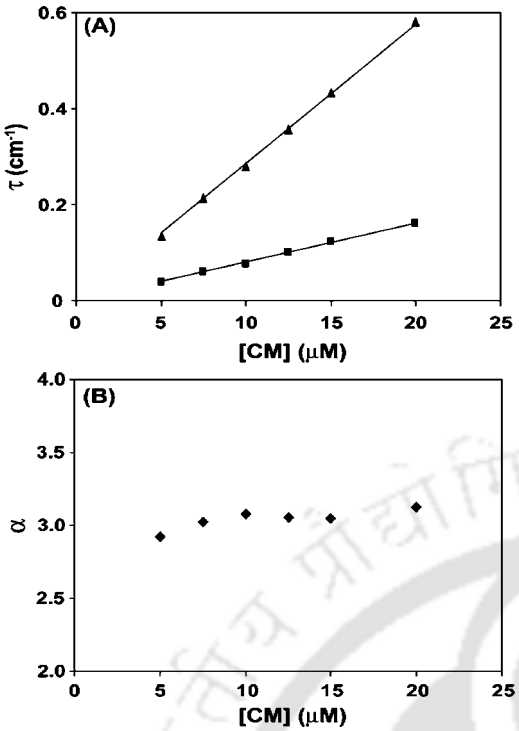

Figure 3. Stability of the casein micelle (CM) suspensions in Tris buffer (pH 7.4) containing 10 mM $CaCl_2$. (A) Turbidity (τ) of the purified CM suspension at wavelengths of 400 (▲) and 600 nm (■). A linear change with different CM concentrations is shown. (B) Change in α (wavelength dependence of turbidity) with different CM concentrations. The α value remained nearly constant.

measurement. The morphology and the size of the CM−curcumin complex were similar to those of free CM (data not shown).

The baseline spectrum of the CM suspension showed high absorbance values because of the high degree of Rayleigh scattering that was present in the samples (Figure 5). To get the spectra of curcumin, we generated a difference spectrum by subtracting the CM suspension spectrum from the CM−curcumin spectrum. The difference spectrum revealed that the curcumin bound to CM shows absorbance maxima at 424 nm (Figure 5, inset).

Curcumin has intrinsic fluorescence properties. The photophysical properties and fluorescence spectra of curcumin are very sensitive to the polarity of the environment and show significant solvent-dependent shifts in emission maxima.[39] In our study, we found that when free curcumin was excited at 420 nm in the absence of CM it showed a low-intensity broad fluorescence peak at 540 nm in aqueous solution. When curcumin bound CM, its fluorescence spectrum was blue shifted to a well-defined peak at 500 nm, and the intensity sharply increased as a function of CM concentration (Figure 6A). This observation was in good agreement with previous reports of the interaction of curcumin with other proteins. The binding of curcumin to BSA and human serum albumin (HSA) showed fluorescence maxima at 510 and 500 nm, respectively.[40,41] The authors attributed this blue shifting of the peak to the binding of curcumin to the hydrophobic domain of the protein molecules. It is well documented in literature that CMs possess a great deal of hydrophobicity. Hydrophobic fluorescent probes such as ANS, Nile Red, pyrene, and TNS strongly bind to the CMs through hydrophobic and electrostatic interactions.[33,38,42] Our observations suggest that curcumin molecules bind within the nonpolar regions of CMs through hydrophobic interactions. Curcumin has two phenolic OH groups with pK_a values of 8.38

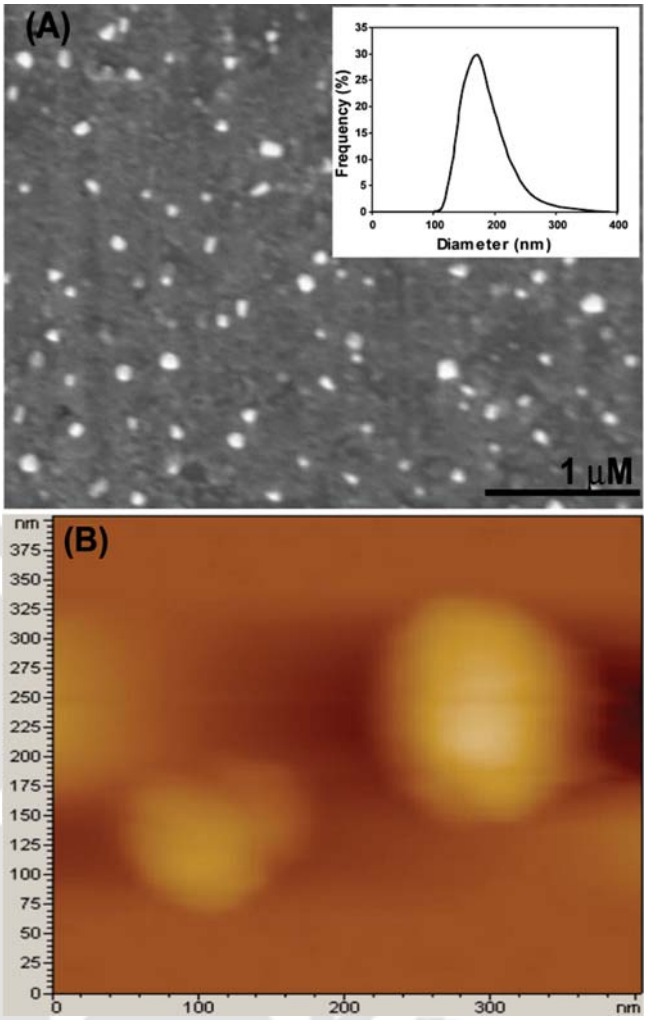

Figure 4. Size and morphology of casein micelle. (A) SEM and (B) AFM analyses displayed a roughly spherical morphology of purified casein micelles and an average particle size of 166.3 nm, which was further confirmed by the DLS measurement (inset of A).

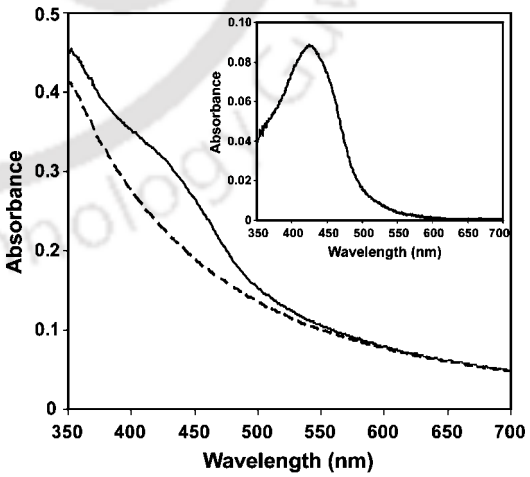

Figure 5. Absorption spectra of the CM suspension (---) and the CM−curcumin complex (−). Difference spectra (inset) revealed that the curcumin bound to CM shows absorption maxima at 424 nm.

and 9.88 in aqueous solution.[43] At pH 7.4, curcumin will be in the neutral from. Therefore, binding that is due to charge interactions can be ruled out. The interaction of curcumin with CM can be represented as curcumin + CM = [CM−curcumin] complex.

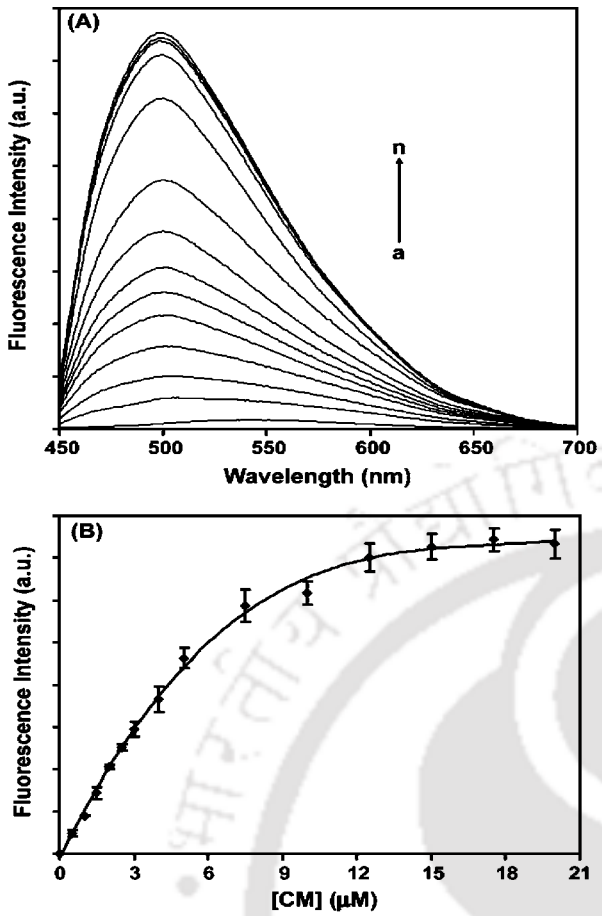

Figure 6. (A) Fluorescence emission spectra of 5 μM curcumin in buffer solution (pH 7.4) in the presence of CM at different concentrations (a) 0, (b) 0.5, (c) 1.0, (d) 1.5, (e) 2.0, (f) 2.5, (g) 3.0, (h) 4.0, (i) 5.0, (j) 10.0, (k) 12.5, (l) 15.0, (m) 17.5, and (n) 20.0 μM. The excitation wavelength was 420 nm. (B) Change in curcumin fluorescence intensity at 500 nm in the presence of increasing concentrations of CM. This shows that 17 μM CM is required for the saturation of 5 μM curcumin binding.

We used the change in the curcumin fluorescence intensity upon curcumin's binding to CMs to determine the binding parameters. The binding constant was estimated from the increase in the fluorescence intensity of a fixed concentration of curcumin in the presence of an increasing concentration of added CM. There was a blue shift of the curcumin emission maximum and a significant increase in the fluorescence intensity with an increasing concentration of CM (Figure 6A). This change in the fluorescence intensity suggests that in the presence of CM the curcumin molecules are transferred from the polar aqueous solution to the nonpolar hydrophobic domains of CM. Figure 6B represents the variations of curcumin fluorescence intensity with increasing CM concentrations. The plot shows that the fluorescence intensity of curcumin initially increased and gradually leveled off in the higher concentration of CM. The saturation concentration of CM that is required for the complete binding of 5 μM curcumin was 17 μM. The binding constant was determined by the following equation[38,44]

$$\frac{1}{\Delta FI} = \frac{1}{\Delta FI_{max}} + \frac{1}{K_b \Delta FI_{max}[CM]}$$

where ΔFI is the change in the curcumin fluorescence intensity in the presence and absence of CM, ΔFI_{max} is the maximal change in the curcumin fluorescence intensity, K_b is the binding constant, and [CM] is the concentration of CM.

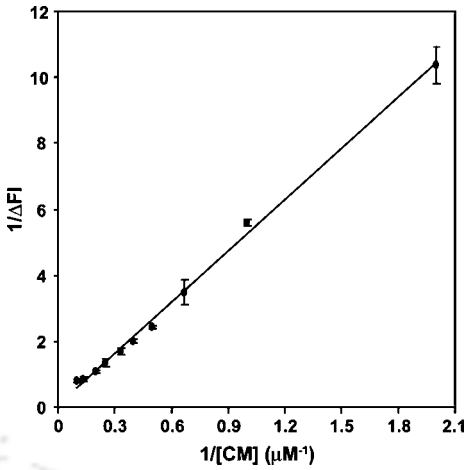

Figure 7. Double-reciprocal plot of [CM] versus the change in the curcumin fluorescence intensity (ΔFI). Binding constant (K_b) was estimated to be 1.48×10^4 M^{-1} between curcumin and CM from the plot.

The intensity data were used to plot the double-reciprocal plot 1/[CM] versus $1/\Delta FI$ (Figure 7). The intercept of the double-reciprocal plot on the $1/\Delta FI$ axis is $1/\Delta FI_{max}$, which was used to calculate the binding constant from the value of the slope in the plot. The binding constant was estimated to be 1.48×10^4 M^{-1}. The linearity of the plot suggests that curcumin interacts with the CM suspension to form 1:1 complexes.[44]

The intrinsic fluorescence of proteins has been widely used to investigate the interaction and binding of drug molecules to proteins in solution. At the excitation wavelength of 280 nm, both tryptophan (Trp) and tyrosine (Tyr) residues have fluorescence emission, but when the excitation wavelength is 295 nm, only the Trp residue shows fluorescence emission. CM shows strong fluorescence emission with a peak at 342 nm upon excitation at 280 nm. Figure 8A shows the fluorescence emission spectra of CM suspension in the presence of different concentrations of curcumin with an excitation wavelength of 280 nm. The intensity of the fluorescence emission of CM at 342 nm gradually decreased with the increase in drug concentration. When it was excited at 295 nm, the CM solution showed fluorescence maxima at 344 nm. Figure 8C shows the fluorescence quenching spectra of CM before and after incubation with different concentrations of curcumin at an excitation at 295 nm. The addition of increasing concentrations of curcumin caused a progressive reduction in the fluorescence intensity, but the maximum emission wavelength remained unchanged. This indicates that there is no change in the local dielectric environment of the Trp residues. The hydrophobic interior of CMs mainly consists of α_{s1}- and β-casein, and α_{s1}-casein contains two Trp residues at positions 164 and 199, whereas β-casein has one Trp residue at position 143.[45,46] Therefore, it is likely that curcumin molecules can bind any or all of these Trp residues. CMs consist of a mixtures of proteins, and they are natively unfolded proteins, so it is difficult to predict the exact position of binding of curcumin molecules. The quenching data were analyzed according to the Stern−Volmer equation

$$\frac{F_0}{F} = 1 + K_{SV}[Q]$$

where F_0 and F are the fluorescence intensities in the absence and presence of curcumin, respectively, [Q] is the drug concentration, and K_{SV} is the Stern−Volmer quenching constant. The Stern−Volmer plot for CM fluorescence quenching by

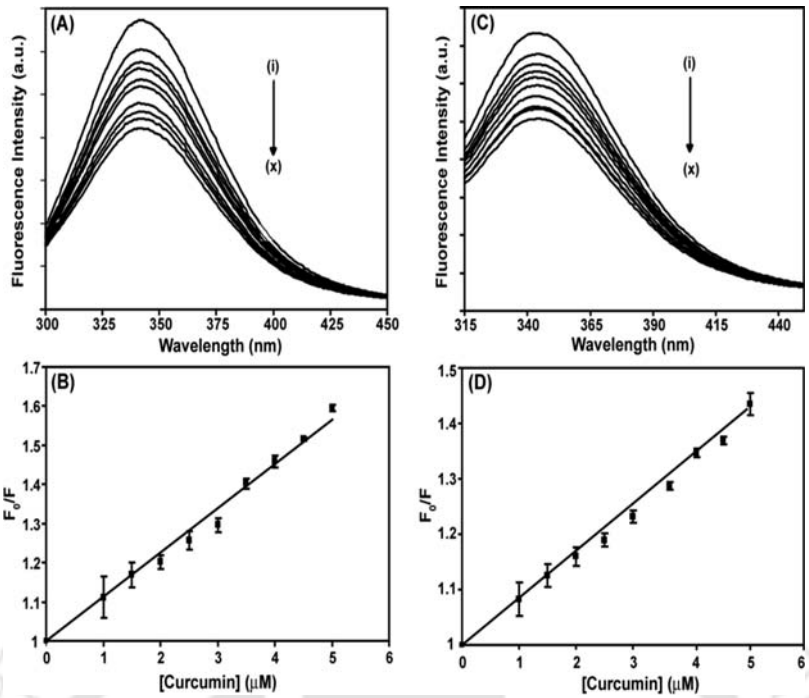

Figure 8. Quenching of CM intrinsic fluorescence by curcumin. Fluorescence emission spectra of the CM suspension at excitation wavelengths of (A) 280 (C) and 295 nm in presence of (i) 0, (ii) 1, (iii) 1.5, (iv) 2.0, (v) 2.5, (vi) 3.0, (vii) 3.5, (viii) 4.0, (ix) 4.5, and (x) 5.0 μM curcumin. Corresponding Stern−Volmer plots are shown in (B) and (D), respectively.

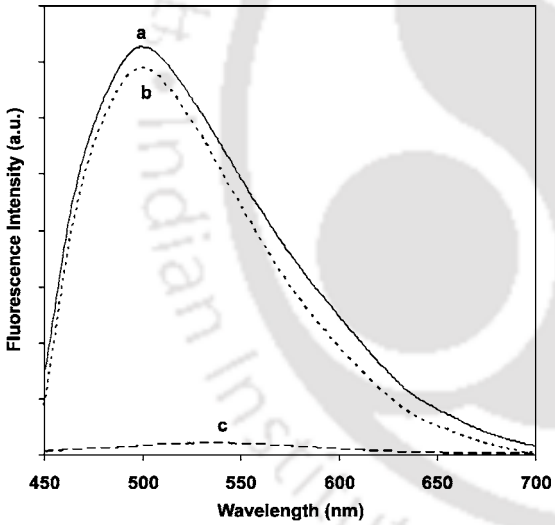

Figure 9. Fluorescence emission spectra of curcumin in the presence of (a) nondissociated CM; (b) dissociated casein submicelles, which showed a high fluorescence intensity because of complexation by hydrophobic interactions; and (c) casein hydrolysate, which showed a poor fluorescence intensity because of the lack of hydrophobic domains.

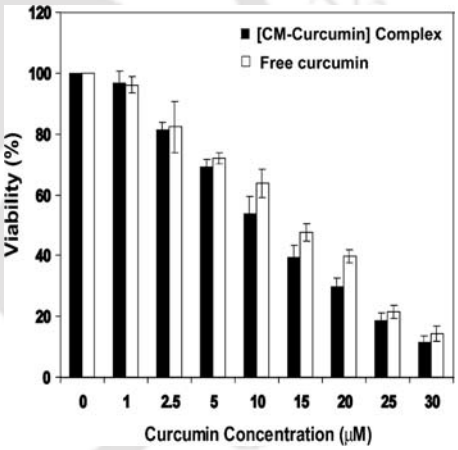

Figure 10. Cytotoxicity assay of free curcumin (□) and CM−curcumin complex (■) on in vitro cultured HeLa cells. The CM−curcumin complex showed a cytotoxic effect that was comparable to that of free curcumin.

curcumin is shown in Figure 8B,D. The plot of F_0/F versus [Q] was found to be linear in both of the cases, that is, for 280 and 295 nm excitation. The Stern−Volmer quenching constant (K_{sv}) was found to be 11.3 × 10^4 M^{-1} for 280 and 342 nm emission and 8.3 × 10^4 M^{-1} for 295 and 344 nm emission. Because the quenching of CM fluorescence by curcumin at 280 nm is more distinct than it is at 295 nm, we suggest that apart from Trp residues the Tyr residues are also involved in CM−curcumin interactions.

To investigate the binding of curcumin to CM further, we studied the curcumin fluorescence with dissociated CMs and casein hydrolysate. Casein micelles dissociate into smaller subunits (average size of 10−20 nm) called submicelles after the removal of CCP by a chelating agent.[34] The fluorescence of curcumin that was complexed with both dissociated and intact CM solution showed a well-defined peak at 500 nm (Figure 9). However, curcumin that was added to a solution of casein hydrolysate did not show significant fluorescence intensity (Figure 9). The low fluorescence intensity of curcumin in casein hydrolysate solution suggests that curcumin molecules are not present in a sufficiently nonpolar environment. Because casein hydrolysate is composed of short peptides, it does not form an aggregated structure with hydrophobic domains in aqueous solution. In contrast, the unique assembly of casein submicelles provides a sufficient nonpolar environment for the bound curcumin molecules. These data further support the possibility that in the CM−curcumin complex curcumin molecules were bound to the hydrophobic regions of CM, which are located in the submicelles.

Therefore, curcumin, which is poorly soluble in water, can be formulated in a colloidal system by the use of CM.

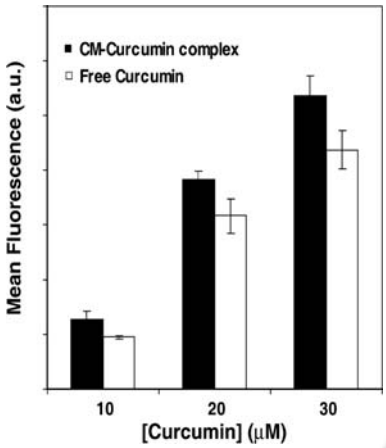

Figure 11. Cellular uptake study of CM−curcumin complex (■) and free curcumin (□) on in vitro cultured HeLa cells.

Furthermore, to compare the cytotoxicities of free and CM-bound drug, we exposed HeLa cells to a series of equivalent concentrations of free circumin or the CM−curcumin complex for 48 h, and the percentage of viable cells was quantified by the use of the MTT assay. A dose-dependent decrease in the cell viability was noticed in both cases (Figure 10). The CM−curcumin complex exerts a comparable cytotoxic effect with respect to free curcumin on HeLa cells at the same dose. The IC_{50} values for the CM−curcumin complex and the free curcumin were found to be 12.69 and 14.85 μM, respectively. CM itself was found to be nontoxic (data not shown). This indicates that the curcumin remains active after complexation with CM.

The therapeutic application of hydrophobic, poorly water-soluble molecules is associated with serious problems such as poor absorption and bioavailability upon oral administration. The formation of drug aggregates results in highly localized concentrations at the sites of deposition that are associated with local toxicity, which is compelling many pharmaceutical companies to exclude poorly soluble compounds very early in their screening process regardless of how active these compounds are toward their molecular targets.[47,48] A potential therapeutic agent such as curcumin, which suffers from similar problems, requires a suitable carrier/delivery system to overcome them without compromising its activity. The above result shows that this delivery system could be a promising choice for administering curcumin without the loss of its therapeutic efficacy.

The cellular uptake study of free curcumin and the CM−curcumin complex shows a concentration-dependent increase in uptake (Figure 11). The uptake of the CM−curcumin complex was comparable to the uptake of free curcumin at equivalent concentrations. Similar results were obtained with HSA-bound curcumin by Kunwar et al.[41] This uptake profile explains the results of the cytotoxicity assay and indicates that CM has the potential to be a delivery vehicle for hydrophobic drugs.

We examined morphological changes in the HeLa cells after treatment with the CM−curcumin complex by microscopic observation. Intracellular green fluorescence of curcumin proves that the HeLa cells efficiently took up the CM−curcumin complex. The cells that were treated with the CM−curcumin complex underwent marked morphological changes compared with the vehicle control (Figure 12). CM−curcumin-treated HeLa cells underwent a retraction of cellular processes and

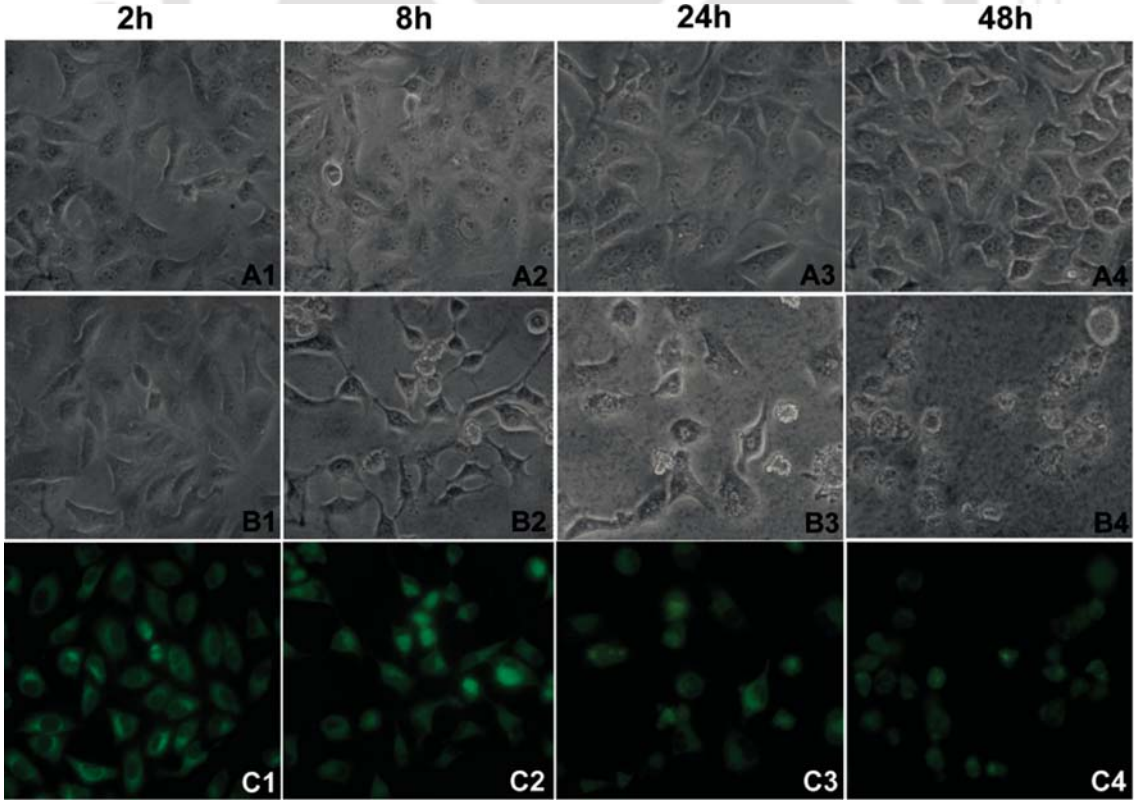

Figure 12. Microscopic observation of the CM−curcumin-complex-induced morphological changes with time in HeLa cells. (A1−4) Control cells that were treated with CM without drug showed no change in morphology with time. (B1−4) Cells that were treated with the CM−curcumin complex containing 30 μM curcumin exhibited marked morphological changes as a result of apoptosis. (C1−4) Intracellular green fluorescence of curcumin revealed that the complex was efficiently internalized in the cells.

showed apoptotic characteristics such as cell shrinkage, membrane blebbing, rounding, and so forth, with an increase in incubation time (Figure 12B). When cells were treated with the CM−curcumin complex for 24 h, cells displayed a rounded morphology and detached from the substratum (Figure 12B3). Following 48 h of exposure, cellular fragmentation was extensive, and few cells remained adherent (Figure 12B4). In contrast, control cells that were treated with CM without drug were well spread with a flattened morphology, which shows the nontoxicity of CM. We also observed the intracellular green fluorescence of curcumin in the case of treated cells. No fluorescence was observed in the case of control cells (data not shown).

Conclusions

We successfully prepared the CM−curcumin complex, which can be an alternative drug formulation of curcumin for cancer therapy. We report for the first time the fluorescence spectroscopy study of the interaction between curcumin and CMs. It was observed that curcumin molecules interact with CMs by binding the low-polarity regions of CM. Under physiological buffer conditions, the CM−curcumin complex yielded a nanoformulation, which exhibited similar cytotoxic effects on HeLa cells compared to an equal dose of free curcumin. Because casein is an edible protein, the complex has the potential to be an oral dose of curcumin; however, further studies are required to confirm this hypothesis.

Acknowledgment. The DBT and DST of the Government of India funded this work. A.S and N.K. thank IITG and MHRD of the Government of India for financial support in the form of a fellowship.

References and Notes

(1) Peer, D.; Karp, J. M.; Hong, S.; Farokhzad, O. C.; Margalit, R.; Langer, R. *Nat. Nanotechnol.* **2007**, *2*, 751–760.
(2) Alexis, F.; Rhee, J.; Richie, J. P.; Radovic-Moreno, A. F.; Langer, R.; Farokhzad, O. C. *Urol. Oncol.* **2008**, *26*, 74–85.
(3) Lu, Z.; Yeh, T.; Tsai, M.; Au, J. L.; Wientjes, M. G. *Clin. Cancer Res.* **2004**, *10*, 7677–7684.
(4) Dreis, S.; Rothweiler, F.; Michaelis, M.; Cinatl, J.; Kreuter, J.; Langer, K. *Int. J. Pharm.* **2007**, *341*, 207–214.
(5) Chen, L.; Remondetto, G. E.; Subirade, M. *Trends Food Sci. Technol.* **2006**, *17*, 272–283.
(6) Willmott, N.; Magee, G. A.; Cummings, J.; Halbert, G. W.; Smyth, J. M. *J. Pharm. Pharmacol.* **1992**, *44*, 472–475.
(7) Knepp, W. A.; Jayakrishna, A.; Quigg, J. M.; Sitren, H. S.; Bagnall, J. J.; Goldberg, E. P. *J. Pharm. Pharmacol.* **1993**, *45*, 887–891.
(8) Huppertz, T.; Smiddy, M. A.; De Kruif, C. G. *Biomacromolecules* **2007**, *8*, 1300–1305.
(9) Semo, E.; Kesselman, E.; Danino, D.; Livney, Y. D. *Food Hydrocolloids* **2007**, *21*, 936–942.
(10) De Kruif, C. G.; Holt, C. Casein Micelle Structure, Functions, and Interactions. In *Advanced Dairy Chemistry: Proteins, Part A*, 3rd ed.; Fox, P. F., McSweeney, P. L. H. Eds.; Kluwer Academic/Plenum: New York, 2003; Vol. 1, pp 233−276.
(11) Horne, D. S. *J. Colloid Interface Sci.* **1986**, *111*, 250–260.
(12) De Kruif, C. G.; Zhulina, E. B. *Colloids Surf., A* **1996**, *117*, 151–159.
(13) Maheshwari, R. K.; Singh, A. K.; Gaddipati, J.; Srimal, R. C. *Life Sci.* **2006**, *78*, 2081–2087.
(14) Ono, K.; Hasegawa, K.; Naike, H.; Yamada, M. *J. Neurosci. Res.* **2004**, *75*, 742–750.
(15) Aggarwal, B. B.; Kumar, A.; Bharti, A. C. *Anticancer Res.* **2003**, *23*, 363–398.
(16) Hatcher, H.; Planalp, H.; Cho, J.; Torti, F. M.; Torti, S. V. *Cell. Mol. Life Sci.* **2008**, *65*, 1631–1652.
(17) Syang-ai, C.; Leela Kumari, A.; Khar, A. *Mol. Cancer Ther.* **2004**, *3*, 1101–1108.
(18) Kamath, R.; Jiang, Z.; Sun, G.; Yalowich, J. C.; Baskaran, R. *Mol. Pharmacol.* **2007**, *71*, 61–72.
(19) Singh, S.; Aggarwal, B. B. *J. Biol. Chem.* **1995**, *270*, 24995–25000.
(20) Letchford, K.; Liggins, R.; Burt, H. *J. Pharm. Sci.* **2008**, *97*, 1179–1190.
(21) Anand, P.; Kunnumakkara, A. B.; Newman, R. A.; Aggarwal, B. B. *Mol. Pharmacol.* **2007**, *4*, 807–818.
(22) Sahu, A.; Bora, U.; Kasoju, N.; Goswami, P. *Acta Biomater.*, in press.
(23) Ma, Z.; Haddadi, A.; Molavi, O.; Lavasanifar, A.; Lai, R.; Samuel, J. *J. Biomed. Mater. Res., Part A* **2008**, *86*, 300–310.
(24) Li, L.; Ahmed, B.; Mehta, K.; Kurzrock, R. *Mol. Cancer Ther.* **2007**, *6*, 1276–1282.
(25) Bisht, S.; Feldmann, G.; Soni, S.; Ravi, R.; Karikar, C.; Maitra, A. *J. Nanobiotechnol.* **2007**, *5*, 3.
(26) Sou, K.; Inenaga, S.; Takeoka, S.; Tsuchida, E. *Int. J. Pharm.* **2008**, *352*, 287–293.
(27) Vemula, P. K.; Li, J.; John, G. *J. Am. Chem. Soc.* **2006**, *128*, 8932–8938.
(28) Diaz, O.; Gouldsworthy, A. M.; Leaver, J. *J. Agric. Food Chem.* **1996**, *44*, 2517–2522.
(29) Bradford, M. M. *Anal. Biochem.* **1976**, *72*, 248–254.
(30) Laemmli, U. K. *Nature* **1970**, *277*, 680–685.
(31) Gatti, C. A.; Alvarez, E. M.; Sala, V. S. *J. Agric. Food Chem.* **1999**, *47*, 141–144.
(32) Pitkowski, A.; Nicolai, T.; Durand, D. *Biomacromolecules* **2008**, *9*, 369–375.
(33) Gatti, C. A.; Risso, P. H.; Zerpa, S. M. *Food Hydrocolloids* **1998**, *12*, 393–400.
(34) Panouillé, M.; Nicolai, T.; Durand, D. *Int. Dairy J.* **2004**, *14*, 297–303.
(35) Mosmann, T. *J. Immunol. Methods* **1983**, *65*, 55–63.
(36) Basch, J. J.; Douglas, F. W.; Procino, L. S.; Holsinger, V. H.; Farrell, H. M. *J. Dairy Sci.* **1985**, *68*, 23–31.
(37) Vincenzatti, S.; Polidori, P.; Mariani, P.; Cammertoni, N.; Fantuz, F.; Vita, A. *Food Chem.* **2008**, *106*, 640–649.
(38) Gatti, C. A.; Risso, P. H.; Pires, M. S. *J. Agric. Food Chem.* **1995**, *43*, 2339–2344.
(39) Chignell, C. F.; Bilski, P.; Reszka, K. J.; Motten, A. G.; Sik, R. H.; Dahl, T. H. *Photochem. Photobiol.* **1994**, *59*, 295–302.
(40) Barik, A.; Priyadarsni, K. I.; Mohan, H. *Photochem. Photobiol.* **2003**, *77*, 597–603.
(41) Kunwar, A.; Barik, A.; Pandey, R.; Priyadarsini, K. I. *Biochim. Biophys. Acta* **2006**, *1760*, 1513–1520.
(42) Liu, Y.; Guo, R. *J. Colloid Interface Sci.* **2007**, *315*, 685–692.
(43) Bernabé-Pineda, M.; Ramírez-Silva, M. T.; Romero-Romo, M.; González-Vergara, E.; Rojas-Hernández, A. *Spectrochim. Acta, Part A* **2004**, *60*, 1091–1097.
(44) Liang, L.; Tajmir-Riahi, H. A.; Subirade, M. *Biomacromolecules* **2008**, *9*, 50–56.
(45) Alaimo, M. H.; Farrell, H. M.; Germann, M. W. *Biochim. Biophys. Acta* **1999**, *1431*, 410–420.
(46) Farrell, H. M.; Wickham, E. D.; Unruh, J. J.; Qi, P. X.; Hoagland, P. D. *Food Hydrocolloids* **2001**, *15*, 341–354.
(47) Lipinski, C. A. *J. Pharmacol. Toxicol. Methods* **2000**, *44*, 235–249.
(48) Lipinski, C. A.; Lombardo, F.; Dominy, B. W.; Feeney, P. J. *Adv. Drug Delivery Rev.* **2001**, *46*, 3–26.

BM800683F

Other Publications

J Mater Sci: Mater Med (2009) 20:171–175
DOI 10.1007/s10856-008-3549-4

Microwave mediated rapid synthesis of chitosan

Abhishek Sahu · Pranab Goswami · Utpal Bora

Received: 22 March 2007 / Accepted: 18 July 2008 / Published online: 14 August 2008

Abstract Chitosan is synthesized by deacetylating chitin with NaOH solution under microwave irradiation. The process describes a rapid synthesis procedure in comparison to conventional methods. The microwave-synthesized chitosan was characterized by Ninhydrin test, Fourier transform-infrared spectroscopy and X-ray diffraction measurements. The experimental results show that the degree of deacetylation increased with increasing irradiation time. A degree of deacetylation of 85.3% was achieved after irradiating chitin with 45% NaOH solution in a microwave for 5.5 min at 900-watt power. This method can be very useful for synthesizing low molecular weight chitosan with rapid and clean chemistry.

1 Introduction

Chitosan is as an environment friendly polymer due to its biodegradability, easy availability and renewability. It is widely used in water treatment [1], chromatography [2], cosmetics, textiles [3] etc. It is a nontoxic biocompatible natural polymer having bacteriostatic and fungistatic activity [4–7] making it an interesting material for biomedical applications like drug delivery [8], gene delivery [9] and tissue engineering [10].

Chitosan is obtained by *N*-deacetylation of chitin, the second most widely available polysaccharide after cellulose. Chemically chitin is composed of β (1 → 4)-linked *N*-acetyl-D-glucosamine and chitosan is composed of β (1 → 4)-linked *N*-acetyl-D-glucosamine and D-glucosamine residues.

Several methods have been reported for preparation of chitosan from chitin such as alkali treatment at high temperature [11], alkali treatment at high temperature with intermittent washing with water [12], use of water miscible organic solvents [13] and enzymatic *N*-deacetylation [14]. Commercially chitosan is produced by *N*-deacetylation of chitin with highly concentrated sodium hydroxide solution (40–50% w/v) in high temperature and pressure. The process takes several hours to produce chitosan with significant degree of deacetylation (DD).

In recent years microwave chemistry has received much attention as it can speed up the reaction rate by orders of magnitude over conventional heating. In spite of it, the use of microwave irradiation for carrying out chemical reactions for biotechnological processes is few. Recently Nahar and Bora [15] used microwave irradiation for the covalent immobilization of proteins. Microwave irradiation has been used for the chemical modification of chitosan [16–18]. Peniston and Johnson [19] have patented a process to obtain chitosan from chitin, that also uses microwave treatment. In this communication, we report the simple and rapid method for the *N*-deacetylation of chitin for producing chitosan using microwave irradiation and subsequent characterization in detail.

2 Experimental

2.1 Material

Chitin with average molecular weight ~400 kD was obtained from Himedia, India. Sodium hydroxide, acetic acid

A. Sahu · P. Goswami · U. Bora (✉)
Biomaterials and Tissue Engineering Laboratory, Department of Biotechnology, Indian Institute of Technology Guwahati, Guwahati 781039, Assam, India
e-mail: ubora@iitg.ernet.in; ubora@rediffmail.com

and ninhydrin were purchased from Merck, India. Glucosamine hydrochloride was obtained from SRL, India. All other reagents were of analytical grade from Merck, India.

2.2 Deacetylation of chitin by microwave irradiation at constant power

Two grams of chitin were transferred to a 250 ml conical flask and 25 ml 45% w/v NaOH solution was added and mixed. The conical flask was placed on the centre of the turntable of the microwave oven (LG MC8083MLR microwave oven, LG electronics, India) and irradiated for 0.5, 1.0, 2.0, 3.0, 3.5, 4.0, 4.5, 5.0 and 5.5 min at 900 watts. The products were filtered and washed with double distilled water until the pH of the filtrate became 7.0. The residue obtained after filtration was dried in a hot air oven at 50°C until constant dry weight was attained and were used for further analysis. In control experiment, deacetylation was carried out at 121°C temperature and 15 psi pressure for 4 h.

2.3 Ninhydrin test

Ninhydrin test was carried out according to the method of Prochazkova et al. [20] with slight modifications. Ninhydrin solution was prepared by dissolving 1 mg of reagent in 1 ml of methanol. Five hundred microlitre of ninhydrin solution were added to 2 mg of chitosan in 500 µl deionized water. The tubes were immediately capped, briefly shaken and incubated in a water bath at 70°C for 30 min then cooled below 30°C in a cold-water bath. The tubes were then vigorously stirred in a vortex mixture followed by a brief centrifugation. The solution was pipetted into a cuvette and absorbance recorded at 570 nm in Cary-100 UV–Vis spectrophotometer (Varian, USA). The DD values were calculated using glucosamine hydrochloride as a standard.

2.4 FTIR analysis

A 2% w/w mixture of chitosan and potassium bromide (KBr) was ground into a fine powder using an agate mortar and subsequently compressed into a disc. Each disc was scanned at a resolution of 1 cm^{-1} over a frequency region of 450 to 4,000 cm^{-1} using a FTIR spectrophotometer (Perkin Elmer Spectrum One, USA) and the characteristic peaks of IR transmission spectra were recorded.

2.5 XRD

X-ray diffraction of powder samples was done using a Bruker D8 advance X-ray diffractometer (Bruker Axs Inc. Germany) under the following operating conditions: 40 kV and 40 mA with Cu-Kα_1 radiation at λ 1.54184 Å and acceptance slot at 0.1 mm. Approximately 20 mg of chitosan powder was spread on a sample stage, and the relative intensity was recorded in the scattering range (2θ) of 5–40° in steps of 0.04°.

2.6 Viscometric analysis

Chitosan solutions were prepared in solvent containing 0.5 M CH_3COOH and 0.25 M NaCl. The viscosities of the solutions were measured in an Ostwald viscometer at 25°C. The solution and solvent viscosity are used to calculate the relative viscosity (η_r), specific viscosity (η_{sp}) and intrinsic viscosity ([η]).

$$\text{Relative viscosity } (\eta_r) = {}^{t}/_{t_0} \quad (1)$$

$$\text{Specific viscosity } (\eta_{sp}) = \eta_r - 1 \quad (2)$$

$$\text{Reduced viscosity } (\eta_{red}) = {}^{\eta_{sp}}/_{c} \quad (3)$$

$$\text{Intrinsic viscosity } ([\eta]) = (\eta_{red}) \text{ when } c \rightarrow 0 \quad (4)$$

where t is the running time of the sample solution, t_0 is the running time of the solvent and c is the sample concentration in g/dl. The intrinsic viscosities are obtained by extrapolating η_{red} to zero concentration.

Average molecular weights of all the samples are calculated by using classical Mark–Houwink relationship

$$[\eta] = K_m M_w^a \quad (5)$$

where 'K_m' and 'a' are Mark-Houwink parameters. Values of K_m (2.14×10^{-3} dl/g) and a (0.657) were as defined by Rege and Block [21] with 0.5 M CH_3COOH-0.25 M NaCl solvent system.

3 Results and discussion

In recent years microwave irradiation has attracted a considerable amount of attention and is becoming an increasingly popular method for chemical reactions as it offers a clean, cheap, and convenient method of heating resulting in higher yields and shorter reaction times. The main advantage of microwave mediated chemistry is that it results in instantaneous 'in core' heating of materials in a homogeneous and selective manner which cannot be otherwise attained in conventional heating within a short time. Despite an increasing amount of literature on microwave chemistry, its use in biotechnology has remained limited. Here we report that microwave heating can be used to prepare a biopolymer like chitosan more efficiently than conventional heating.

In a typical experiment, chitin and highly concentrated NaOH were reacted under microwave for different time

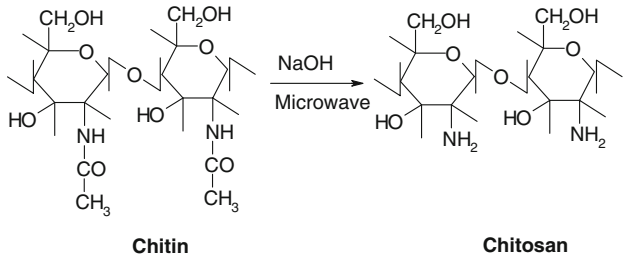

Scheme 1 Deacetylation of chitin by microwave irradiation

periods (0.5–5.5 min). Under alkaline conditions deacetylation of chitin ($-NHCOCH_3$) to chitosan ($-NH_2$) occurs as shown in Scheme 1. The DD values of chitosan increased almost linearly with irradiation time and reached a maximum of 85.3% at 5.5 min as determined by the ninhydrin test (Fig. 1).

The formation of chitosan from chitin by microwave irradiation was confirmed by FTIR spectroscopy (Fig. 2). Chitosan has a characteristic band at $\sim$3,450 cm^{-1} which can be attributed to $-NH_2$ and –OH stretching vibration [22]. Chitin has a sharp band at 1,377 cm^{-1} which is due to the symmetrical deformation or rocking of the CH_3 group and the band at 1,626 cm^{-1} is attributable to the stretching of CN vibration of the superimposed C=O group linked to –OH group by hydrogen bonding [23, 24]. Due to high deacetylation these peaks are weakly visible in the chitosan spectra. Further in the chitosan spectra the peak at $\sim$1,645 cm^{-1} indicated that the hydrogen interactions are less accentuated and the hydroxyl groups exist freely due to removal of acetyl group [25].

The conversion process was further confirmed by XRD analysis (Fig. 3). The characteristic sharp peak of chitin at

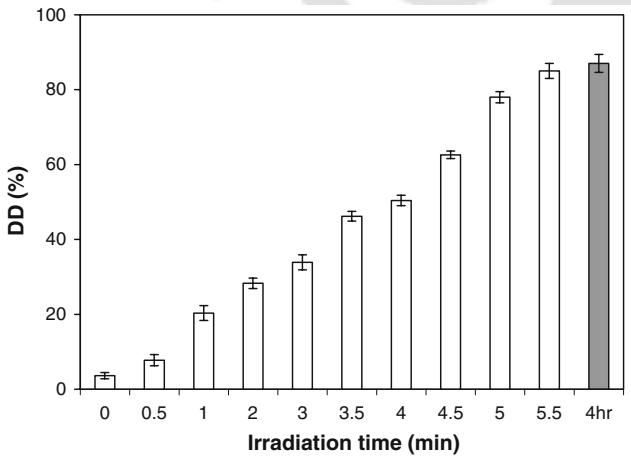

Fig. 1 DD values of chitosan after microwave irradiation for 0.5, 1.0, 2.0, 3.0, 3.5, 4.0, 4.5, 5.0 and 5.5 min at 900 W (hollow columns) and conventional heating (solid dark column), as determined by the ninhydrin test. The DD value of Chitosan obtained at 5.5 min is comparable to that obtained at 4 h at 121°C and 15 psi (conventional heating)

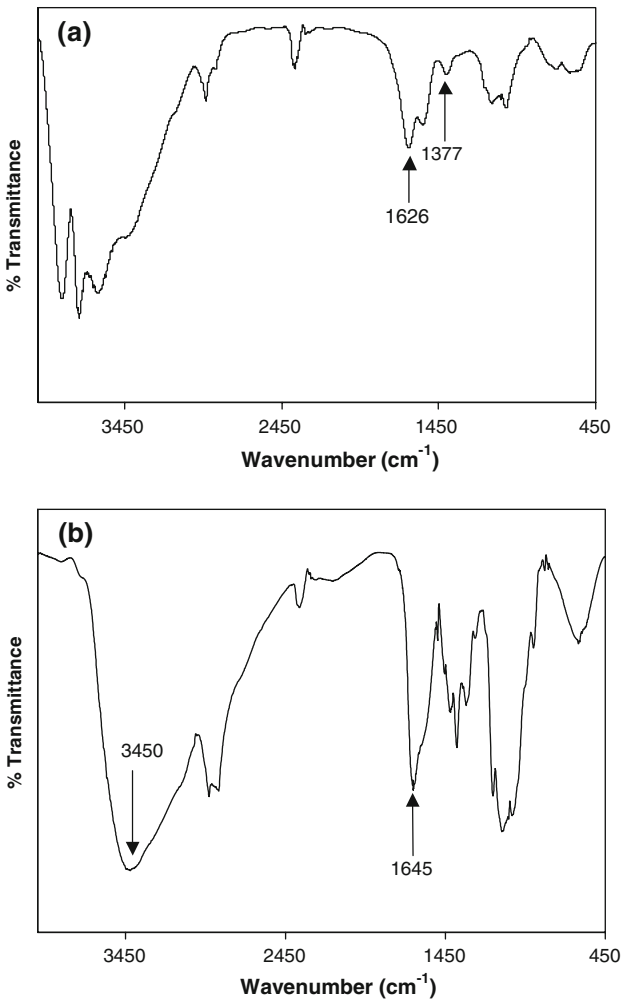

Fig. 2 FT-IR spectrum of (**a**) chitin and (**b**) chitosan formed after 5.5 min of microwave irradiation of chitin at 900 watt

2θ of 9.24° and 19.2° decreased considerably and became broad after 5.5 min of microwave irradiation. It gave clear indication of the formation of chitosan as described by Zhang et al. [26].

Finally, to determine the molecular weights of chitosan formed we carried out viscometric analysis. Viscometric analysis requires a polymer to be soluble in a suitable medium. The solubility of chitosan in acidic buffer is dependent on DD values. The chitosan formed after 4.0, 4.5, 5.0 and 5.5 min of microwave irradiation revealed good solubility and were therefore taken for viscometric analysis. We found that intrinsic viscosity of the samples decreased with increasing microwave irradiation time (Fig. 4). Table 1 shows that the molecular weight decreased as DD of chitosan increased with microwave irradiation time. Further we observed that molecular weight of chitosan prepared by microwave irradiation showed more decrease than that prepared by conventional heating technique. Liu et al. [17] observed a similar phenomenon while preparing *N*-phthaloyl chitosan using microwave

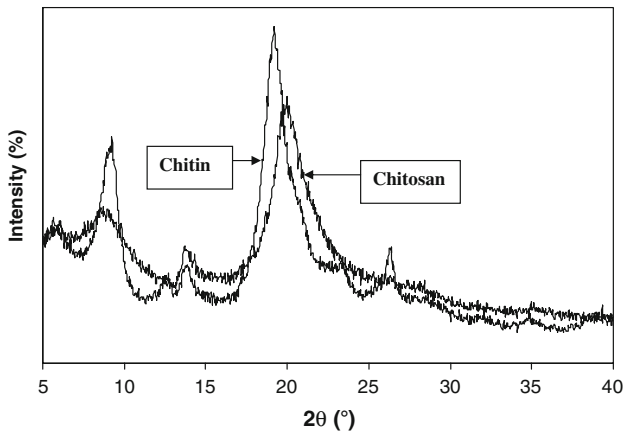

Fig. 3 Comparison of X-ray diffractograms of chitin and chitosan formed after 5.5 min microwave irradiation. Decrease of peaks at 2θ of 9.24° and 19.2° indicates the formation of chitosan from chitin due to microwave irradiation

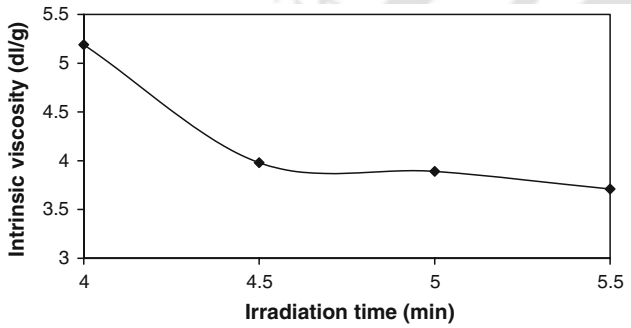

Fig. 4 Intrinsic viscosity of chitosan solutions formed after microwave irradiation of 4.0, 4.5, 5.0 and 5.5 min, respectively

Table 1 Molecular weight and DD of chitosan as a function of different microwave irradiation time

Iradiation time (min)	Mw (kD)	DD (%)
4.0	142.06	49.2
4.5	94.84	62.5
5.0	91.59	76.2
5.5	85.22	85.3
Conventional heating (121°C, 4 h)	244.34	87.0

irradiation and attributed this to the fact that microwave accelerated splits of chitosan chains. Therefore this method can be very useful for synthesizing low molecular weight chitosan with rapid and clean chemistry.

4 Conclusion

Conventionally chitosan is prepared by deacetylation of chitin using high temperatures. In this study we used microwave for deacetylation of chitin. The successful conversion of chitin to chitosan was confirmed by detailed characterization with FTIR, XRD and viscometric analysis. The in core heating through microwave can raise the temperature and speeds up the reaction by many folds over conventional heating. When chitin is reacted with a 45% w/v NaOH solution under microwave, the deacetylation reaction occurs very fast leading to a DD of 85.3% in as low as 5.5 min whereas conventional heating takes about 4 h to achieve this DD. We foresee the design of a microwave reactor using this simple, fast and reproducible method for continuous synthesis of chitosan with high DD.

Acknowledgement This work was financially supported by the Department of Biotechnology, Govt. of India project (BT/PR6759/BRB/10/446/2005). A. Sahu thanks MHRD, Govt of India and IITG for the financial support in the form of fellowship. We thank the reviewers for their constructive criticism and critical inputs.

References

1. C.M. Elson, D.H. Davies, E.R. Hayes, Removal of arsenic from contaminated drinking water by a chitosan/chitin mixture. Water Res. **14**, 1307–1311 (1980). doi:10.1016/0043-1354(80)90190-6
2. M. Yilmaz, G. Bayramoglu, M.Y. Arica, Separation and purification of lysozyme by reactive green 19 immobilized membrane affinity chromatography. Food Chem. **89**, 11–18 (2005). doi:10.1016/j.foodchem.2004.01.072
3. E. Pascual, M.R. Julià, The role of chitosan in wool finishing. J. Biotechnol. **89**, 289–296 (2001). doi:10.1016/S0168-1656(01)00311-X
4. X.G. Chen, C.H. Liu, C.G. Liu, X.H. Meng, C.M. Lee, H.J. Park, Preparation and biocompatibility of chitosan microcarriers as biomaterial. Biochem. Eng. J. **27**, 269–274 (2006). doi:10.1016/j.bej.2005.08.021
5. P. Gualtieri, L. Barsanti, V. Passarelli, Harvesting *Euglena fracilis* cells with a nontoxic flocculant. J. Microbiol. Methods **8**, 327–332 (1988). doi:10.1016/0167-7012(88)90031-0
6. H.K. No, N.Y. Park, S.H. Lee, S.P. Meyers, Antibacterial activity of chitosans and chitosan oligomers with different molecular weights. Int. J. Food Microbiol. **74**, 65–72 (2002). doi:10.1016/S0168-1605(01)00717-6
7. S. Roller, N. Covill, The antifungal properties of chitosan in laboratory media and apple juice. Int. J. Food Microbiol. **47**, 67–77 (1999). doi:10.1016/S0168-1605(99)00006-9
8. A.D. Sezer, J. Akbuga, Release characteristics of chitosan treated alginate beads: II. Sustained release of a low molecular drug from chitosan treated alginate beads. J. Microencapsul. **16**, 687–696 (1999). doi:10.1080/026520499289176
9. U. Guliyeva, F. Öner, S. Özsoy, R. Haziroğlu, Chitosan microparticles containing plasmid DNA as potential oral gene delivery system. Eur. J. Pharm. Biopharm. **62**, 17–25 (2006). doi:10.1016/j.ejpb.2005.08.006
10. Z. Li, H.R. Ramay, K.D. Hauch, D. Xiao, M. Zhang, Chitosan–alginate hybrid scaffolds for bone tissue engineering. Biomaterials **26**, 3919–3928 (2005). doi:10.1016/j.biomaterials.2004.09.062
11. A. Castelli, L. Bergamasco, P.L. Beltrame, B. Focher, Adv. Chitin Sci. **1**, 198–203 (1996)
12. S. Mima, M. Miya, M. Iwamoto, S. Yoshikawa, Highly deacetylated chitosan and its properties. J. Appl. Polym. Sci. **28**, 1909–1917 (1983). doi:10.1002/app.1983.070280607

13. I. Batista, G.A.F. Roberts, A novel, facile technique for deacetylating chitin. Makromol Chem. **191**, 429–434 (1990). doi:10.1002/macp.1990.021910217
14. A. Martinou, D. Kafetzopoulos, V. Bouriotis, Chitin deacetylation by enzymatic means: monitoring of deacetylation processes. Carbohydr. Res. **273**, 235–242 (1995). doi:10.1016/0008-6215(95)00111-6
15. P. Nahar, U. Bora, Microwave-mediated rapid immobilization of enzymes onto an activated surface through covalent bonding. Anal. Biochem. **328**, 81–83 (2004). doi:10.1016/j.ab.2003.12.031
16. H.C. Ge, D.K. Luo, Preparation of carboxymethyl chitosan in aqueous solution under microwave irradiation. Carbohydr. Res. **340**, 1351–1356 (2005). doi:10.1016/j.carres.2005.02.025
17. L. Liu, Y. Li, Y. Li, Y.E. Fang, Rapid N-phthaloylation of chitosan by microwave irradiation. Carbohydr. Polymers **57**, 97–100 (2004). doi:10.1016/j.carbpol.2004.04.009
18. V. Singh, A. Tiwari, D.N. Tripathi, R. Sanghi, Microwave enhanced synthesis of chitosan-*graft*-polyacrylamide. Polymer **47**, 254–260 (2006). doi:10.1016/j.polymer.2005.10.101
19. Q.T. Peniston, E.L. Johnson, Process for activating chitin by microwave treatment and improved activated chitin product. Patent USPTO 4159932, 1979
20. S. Prochazkova, K.M. Vårum, K. Ostgaard, Quantitative determination of chitosans by ninhydrin. Carbohydr. Polymers **38**, 115–122 (1999). doi:10.1016/S0144-8617(98)00108-8
21. P.R. Rege, L.H. Block, Chitosan processing: influence of process parameters during acidic and alkaline hydrolysis and effect of the processing sequence on the resultant chitosan's properties. Carbohydr. Res. **321**, 235–245 (1999). doi:10.1016/S0008-6215(99)00172-X
22. D.R. Bhumkar, V.B. Pokharkar, Studies on effect of pH on cross-linking of chitosan with sodium tripolyphosphate: a technical note. AAPS Pharm. Sci. Tech. **7**(2), (2006)
23. J. Majtán, K. Bíliková, O. Markovič, J. Gróf, G. Kogan, J. Šimúth, Isolation and characterization of chitin from bumblebee (*Bombus terrestris*). Int. J. Biol. Macromol. **40**, 237–241 (2007). doi:10.1016/j.ijbiomac.2006.07.010
24. A.T. Paulino, J.I. Simionato, J.C. Garcia, J. Nozaki, Characterization of chitosan and chitin produced from silkworm chrysalides. Carbohydr. Polymers **64**, 98–103 (2006). doi:10.1016/j.carbpol.2005.10.032
25. M.L. Duarte, M.C. Ferreira, M.R. Marvão, J. Rocha, An optimised method to determine the degree of acetylation of chitin and chitosan by FTIR spectroscopy. Int. J. Biol. Macromol. **31**, 1–8 (2002). doi:10.1016/S0141-8130(02)00039-9
26. Y. Zhang, C. Xue, Y. Xue, R. Gao, X. Zhang, Determination of the degree of deacetylation of chitin and chitosan by X-ray powder diffraction. Carbohydr. Res. **340**, 1914–1917 (2005). doi:10.1016/j.carres.2005.05.005

Available online at www.sciencedirect.com
ScienceDirect
Food Research International 41 (2008) 1–15
FOOD RESEARCH INTERNATIONAL
www.elsevier.com/locate/foodres

Review

Indian medicinal herbs as sources of antioxidants

Shahin Sharif Ali, Naresh Kasoju, Abhinav Luthra, Angad Singh, Hallihosur Sharanabasava, Abhishek Sahu, Utpal Bora *

Department of Biotechnology, Indian Institute of Technology Guwahati, Guwahati 781039, Assam, India

Received 13 July 2007; accepted 3 October 2007

Abstract

Currently there has been an increased interest globally to identify antioxidant compounds that are pharmacologically potent and have low or no side effects for use in preventive medicine and the food industry. As plants produce significant amount of antioxidants to prevent the oxidative stress caused by photons and oxygen, they represent a potential source of new compounds with antioxidant activity. Traditional herbal medicines form an important part of the healthcare system of India. Ayurveda, supposed to be the oldest medical system in the world, provides potential leads to find active and therapeutically useful compounds from plants. Considering the growing interest in assessing the antioxidant capacity of herbal medicine in this review we discuss about rarely reviewed 24 plants reported to have antioxidant properties. Some of the plants reviewed are part of multi-herbal preparations while others are used singly. Certain herbs like *Amaranthus paniculatus*, *Aerva lanata*, *Coccinia indica* and *Coriandrum sativum* are used as vegetables indicating that these plants could be source of dietary antioxidant supplies, which is another emerging area of research.

Keywords: Antidiabetic; Antioxidants; Ayurveda; Flavonoids; Indian herbs

Contents

* Corresponding author. Tel.: +91 361 258 2215; fax: +91 361 258 2249.
E-mail addresses: ubora@iitg.ernet.in, ubora@rediffmail.com (U. Bora).

0963-9969/$ - see front matter © 2007 Elsevier Ltd. All rights reserved.
doi:10.1016/j.foodres.2007.10.001

1. Introduction

Antioxidants help organisms deal with oxidative stress, caused by free radical damage. Free radicals are chemical species, which contains one or more unpaired electrons due to which they are highly unstable and cause damage to other molecules by extracting electrons from them in order to attain stability.

Reactive oxygen species (ROS) formed in vivo, such as superoxide anion, hydroxyl radical and hydrogen peroxide, are highly reactive and potentially damaging transient chemical species. These are continuously produced in the human body, as they are essential for energy supply, detoxification, chemical signaling and immune function. ROS are regulated by endogenous superoxide dismutase, glutathione peroxidase and catalase but due to over-production of reactive species, induced by exposure to external oxidant substances or a failure in the defense mechanisms, damage to cell structures, DNA, lipids and proteins (Valko, Rhodes, Moncol, Izakovic, & Mazur, 2006) occur which increases risk of more than 30 different disease processes (Aruoma, 1998). The most notorious among them being neurodegenerative conditions like Alzheimer's disease (AD) (Smith et al., 1996, Smith, Rottkamp, Nunomura, Raina, & Perry, 2000), mild cognitive impairment (MCI) (Guidi, Galimberti, Lonati, & Novembrino, 2006) and Parkinson's disease (PD) (Bolton, Trush, Penning, Dryhurst, & Monks, 2000). Other neurodegenerative diseases significantly associated with oxidative stress include multiple sclerosis, Creutzfeldt–Jacob disease and meningoencephalitis. All these diseases are associated with significant increases in the specific and persistent lipid peroxidation marker F_2-isoprostane (Greco, Minghetti, & Levi, 2000). Other diseases include highly disabling vascular pathologies like cardiovascular disease (CVD) and cardiac failure (Jha, Flather, Lonn, Farkouh, & Yusuf, 1995), alcohol-induced liver disease (ALD) (Arteel, 2003) and Ulcerative colitis (Ramakrishna, Varghese, Jayakumar, Mathan, & Balasubramanian, 1997) and cancer caused by a complex of different causes, of which RNS/ROS is a component. Valko et al. (2007) have done an extensive review on the effect of free radicals and antioxidants in normal physiological functions and human disease. The hydroxyl radical is known to react with all components of the DNA molecule, damaging both the purine and pyrimidine bases and also the deoxyribose backbone (Halliwell & Gutteridge, 1999). Besides DNA ROS also attack other cellular components involving polyunsaturated fatty acid residues of phospholipids (Siems, Grune, & Esterbauer, 1995), side chains of all amino acid residues of proteins, in particular cysteine and methionine residues (Stadtman, 2004).

Interestingly the body posses defence mechanisms against free radical-induced oxidative stress, which involve preventative mechanisms, repair mechanisms, physical defenses and antioxidant defenses. Enzymatic antioxidant defenses include superoxide dismutase (SOD), glutathione peroxidase (GPx), catalase (CAT) etc. Non-enzymatic antioxidants are ascorbic acid (vitamin C), α-tocopherol (vitamin E), glutathione (GSH), carotenoids, flavonoids, etc. All these act by one or more of the mechanisms like reducing activity, free radical-scavenging, potential complexing of pro-oxidant metals and quenching of singlet

oxygen. A brief description of mechanism of actions of some antioxidants in different disease is described in Table 1. It is possible to reduce the risks of chronic diseases and prevent disease progression by either enhancing the body's natural antioxidant defenses or by supplementing with proven dietary antioxidants (Stanner, Hughes, Kelly, & Buttriss, 2004). This is one of the reasons why discovery and synthesis of novel antioxidants is a major active area.

Synthetic antioxidants like butylated hydroxytoluene (BHT) and butylated hydroxyanisole (BHA) commonly used in processed foods have side effects and are carcinogenic (Branen, 1975; Ito, Fukushima, Hassegawa, Shibata, & Ogiso, 1983). In recent years, the use of natural antioxidants present in food and other biological materials has attracted considerable interest due to their presumed safety, nutritional and therapeutic value (Ajila, Naidu, Bhat, & Rao, 2007). Nutraceuticals are supposed to hold the key to a healthy society in the coming future. Antioxidants derived from fruits, vegetables, spices and cereals are very effective and have reduced interference with the body's ability to use free radicals constructively (Kahkonen et al., 1999; Wolfe, Xianzhong, & Liu, 2003). Natural antioxidants mainly come from plants in the form of phenolic compounds (flavonoids, phenolic acids and alcohols, stilbenes, tocopherols, tocotrienols) ascorbic acid and carotenoids. The quest for natural antioxidants for dietary, cosmetic and pharmaceutical uses has become a major industrial and scientific research challenge over the last two decades. Efforts to gain extensive knowledge regarding the power of antioxidants from plants and to tap their potential are therefore on the increase.

Table 1
Mechanism of action of various antioxidants against different disease

Compound	Pathology	Mechanism of action	References
Catalase (CAT)	Cancer, diabetic retinopathy	Destroys hydrogen peroxide in high concentration by catalysing its two-electron dismutation into oxygen and water	Schonbaum and Chance (1976)
Glutathione peroxidase (GPx)	Neurodegenerative diseases	Catalyse the reduction of hydroperoxides at the expense of GSH. In this process, hydrogen peroxide is reduced to water whereas organic hydroperoxides are reduced to alcohols	Ursini et al. (1995)
Superoxide dismutase (SOD)	Neurodegenerative diseases	Catalyse the one-electron dismutation of superoxide into hydrogen peroxide and oxygen	Fridovich (1997)
Alkaloids	Cancer, Neurodegenerative diseases, chronic inflammation	Shown a variety of biological activities such as inhibition of topoisomerase I and II; cytotoxicity against different tumor cell lines	Radisky et al. (1993) and Gunasekera et al. (2003)
Catechins	Neurodegenerative diseases	Enhance activity of SOD and catalase	Levites et al. (2001)
Carotenoids	Cancer, diabetic retinopathy, chronic inflammation	Mainly act as physical quenchers of reactive oxygen	Sundquist et al. (1994)
α-tocopherol	Cancer, neurodegenerative diseases, chronic inflammation	Scavenges lipid peroxyl radicals (LOO) through hydrogen atom transfer	Burton and Ingold (1981)
(−)-EGCG	Neurodegenerative conditions	Decreases the expression of proapototic genes (bax, bad, caspase-1 and -6, cyclin dependent kinase inhibitor) thus maintaining the integrity of the mitochondrial membrane	Levites et al. (2003)
(−)-EGCG	Cancer, diabetic retinopathy, chronic inflammation	Suppression of angiogenesis by inhibiting growth factor triggered activation of receptors and PKC. Downregulation of VEGF production in tumour cells. Repression of AP-1, NF-_B and STAT-1 transcription factor pathways	Wollin and Jones (2001)
Ferulic acid	Diabetes	Decrease lipid peroxidation and enhances the level of glutathione and antioxidant enzymes	Balasubashini et al. (2004)
Glutathione	Cancer	Glutathione in the nucleus maintains the redox state of critical protein sulphydryls that are necessary for DNArepair and expression	Gérard Monnier and Chaudiere (1996)
Proanthocyanidin (GSPE)	Cardiovascular disorders	Inhibitory effects on proapoptotic and cardioregulatory genes. Modulating apoptotic regulatory bcl-XL, p53 and c-myc genes	Bagchi et al. (2003)
Phenolics	Cancer, diabetic retinopathy, chronic inflammation	Inhibit the oxidation of lipids, fats, and proteins (RH) by donation of a phenolic hydrogen atom to the free radical	Aruoma et al. (1993)
Quercetin, Kaempferol, genistein, resveratrol	Colon cancer	Suppresses COX-2 expression by inhibiting tyrosine kinases important for induction of COX-2 gene expression	Lee et al. (1998)
Tannins	Cardiovascular disorders	Tannins are known to enhance synthesis of nitric oxide and relax vascular segments precontracted with norepinephrine	Dwivedi (2007)

In developing countries like India where poverty and malnutrition is rampant, knowledge of plant derived antioxidants could reduce the cost of health care. India has a rich history of using various herbs and herbal components for treating various diseases. Many Indian plants have been investigated for their beneficial use as antioxidants or source of antioxidants using presently available experimental techniques. Scartezzini and Speroni (2000) have reviewed extensively about *Curcuma longa*, *Magnifera indica*, *Momordica charantia*, *Phyllanthus emblica*, *Santalum album*, *Swertia chirata*, *Withania somnifera* that have antioxidant activity and used in Indian traditional medicine. Recently Govindarajan et al. (2003) has reviewed *Acorus calamus*, *Aloe vera*, *Andrographis paniculata*, *Asparagus racemosus*, *Azadirachta indica*, *Bacopa monnieri*, *Desmodium gangeticum*, *Glycyrrhiza glabra*, *Picrorhiza kurroa*, *Psoralea corylifolia*, *Semecarpus anacardium*, *Terminalia chebula*, *Tinospora cordifolia*. Apart from these 20 plants numerous other plants used in Indian traditional medicine are reported to show antioxidant activity. The present review deals with an exclusive list of such plants based on information collected from various literatures dealing with herbs found in India having antioxidant property.

2. Assay methods for antioxidants

Several methods are used to measure the antioxidant activity of a biological material. The most commonly used ones are those involving chromogen compounds of radical nature that stimulate the reductive oxygen species. These methods are popular due to their ease, speed and sensitivity. The presence of antioxidants leads to the disappearance of these radical chromogens; the most widely used ones being the ABTS and DPPH methods. Some other commonly used assays like FRAP assay, ORAC assay, PCL assay, etc are mentioned below.

2.1. ABTS or TEAC assay

The Trolox equivalent antioxidant capacity (TEAC) assay was reported first by Miller, Rice-Evans, Davies, Gopinathan, and Milner (1993) and Rice-Evans and Miller (1994) and then modified by Re et al. (1999). The TEAC assay is based on the inhibition by antioxidants of the absorbance of the radical cation of 2,2′-azinobis (3-ethylbenzothiazoline 6-sulfonate) (ABTS), which has a characteristic long-wavelength absorption spectrum showing maxima at 660, 734 and 820 nm. Generation of the ABTS radical cation forms the basis of one of the spectrophotometric methods that have been applied to the measurement of the total antioxidant activity of various substances. The experiments are carried out using a decolorization assay, which involves the generation of the ABTS chromophore by the oxidation of ABTS with potassium persulphate. It is applicable to both hydrophilic and lipophilic compounds. The ABTS solution is diluted and absorbance measured in about 10 min after the initial mixing of different concentrations of the extracts with 1ml of the solution. Trolox, a water-soluble analogue of vitamin E is used as the reference standard. The assay has been widely used in many recent studies related to detection of antioxidant property of plant (Dastmalchi, DamienDorman, Laakso, & Hiltunen, 2007; Srinivasan, Chandrasekar, Nanjan, & Suresh, 2007).

2.2. DPPH method

This method was given by Brand-Williams, Cuvelier, and Berset (1995) and later modified by Sánchez-Moreno, Larrauri, and Saura-Calixto (1998). It is one of the most extensively used antioxidant assay for plant samples. Recently the assay has been used to determine antioxidant activity in *Tanacetum* (Tepe & Sokmen, 2007), *Moldavian balm* (Dastmalchi et al., 2007) and *Phyllanthus amarus* (Lim & Murtijaya, 2007). This method is based on scavenging of the 1,1-diphenyl-2-picrylhydrazyl radical (DPPH) from the antioxidants, which produces a decrease in absorbance at 515 nm. When a solution of DPPH is mixed with a substance that can donate a hydrogen atom, the reduced form of the radical is generated accompanied by loss of colour. This delocalization is also responsible for the deep violet colour, characterized by an absorption band in ethanol solution at about 520 nm.

Representing the DPPH radical by Z^* and the donor molecule by AH, the primary reaction is:

$$Z^* + AH \rightarrow ZH + A^*$$

2.3. FRAP assay

Ferric reducing ability of plasma (FRAP) assay is a technique to determine the total antioxidant power interpreted as the reducing capability. The FRAP assay was first given by Benzie and Strain (1999). This assay was very recently used by Lim and Murtijaya (2007), Netzel, Netzel, Tian, Schwartz, and Konczak (2007) and Soobrattee, Bahorun, Neergheen, Googoolye, and Aruoma (in press) for establishing the antioxidant activity of different plant species. In this assay reductants (“antioxidants”) in the sample reduce Fe (III)/tripyridyltriazine complex, present in stoichiometric excess, to the blue ferrous form, with an increase in absorbance at 593 nm. $\not\Delta A$ is proportional to the combined (total) ferric reducing/antioxidant power (FRAP value) of the antioxidants in the sample. The final results were expressed as micromole Trolox equivalents (TE) per gram on dried basis (*i*mol TE/g, db).

$$Fe(TPTZ)_2(III) + ArOH \rightarrow Fe(TPTZ)_2(II) + ArOH^+$$

2.4. ORAC assay

The oxygen radical absorbance capacity (ORAC) assay is based largely on the work reported by Glazer’s (1990). It uses beta-phycoerythrin (PE) as an oxidizable protein substrate and 2,2′-azobis (2-amidinopropane) dihydrochloride

(AAPH) as a peroxyl radical generator or Cu^{2+}–H_2O_2 as a hydroxyl radical generator. To date, it is the only method that takes free radical action to completion and uses an area-under-curve (AUC) technique for quantitation and thus, combines both inhibition percentage and the length of inhibition time of the free radical action by antioxidants into a single quantity. The assay has been widely used in many recent studies related to plant (Almeida, Fernandes, Lima, Costa, & Bahia, 2008; Soobrattee et al., in press; Zhao et al., in press).

2.5. TRAP assay

The total radical trapping parameter (TRAP) assay of Wayner, Burton, Ingold, and Locke (1985) was the most widely used method for measuring total antioxidant capacity of plasma or serum during the last decade. Schlesier, Harwat, Böhm, and Bitsch (2002) employed TRAP assay to evaluate the antioxidant property of tea and various fruit juice while Actis-goretta, Mackenzie, Oteiza, and Fraga (2002) did antioxidant assay in red wine. The TRAP assay uses peroxyl radicals generated from 2,2′-azobis (2-amidinopropane) dihydrochloride (AAPH) and peroxidizable materials contained in plasma or other biological fluids. After adding AAPH to the plasma, the oxidation of the oxidizable materials is monitored by measuring the oxygen consumed during the reaction. During an induction period, this oxidation is inhibited by the antioxidants in the plasma. The length of the induction period (lag phase) is compared to that of an internal standard, Trolox (Aldrich, Milwaukee, WI, USA) (6-hydroxyl-2,5,7,8,-tetramethylchroman-2-carboxylic acid), and then quantitatively related to the antioxidant capacity of the plasma.

2.6. Dichlorofluorescin-diacetate (DCFH-DA) based assay

Another method that also measures TRAP is the spectrophotometric assay reported recently by Valkonen and Kuusi (1997). Amado et al. (2007) have reported a rapid and easy assay method involving dichlorofluorescin-diacetate. This assay uses AAPH to generate peroxyl radicals and DCFH-DA as the oxidizable substrate for the peroxyl radicals. The oxidation of DCFH-DA by peroxyl radicals converts DCFH-DA to dichlorofluorescein (DCF). DCF is highly fluorescent (Ex 480 nm, Em 526 nm) and also has absorbance at 504 nm. Therefore, the produced DCF can be monitored either fluorometrically or spectrophotometrically. DCFH-DA assay has been used to determine the antioxidant property of *Gongronema latifolium* leaves (Ugochukwu & Cobourne, 2003), Labrador tea (*Ledum groenlandicum* Retzius) leaves (Dufour et al., 2007), and grape juice (Rozenberg, Howell, & Aviram, 2006).

2.7. Cyclic voltammetry method

The cyclic voltammetry procedure reported recently by Kohen, Beit-Yannai, Berry, and Tirosh (1999) evaluates the overall reducing power of low molecular weight antioxidants in a biological fluid or tissue homogenate. Following preparation, the sample is introduced into a well in which three electrodes are placed: the working electrode (e.g., glassy carbon), the reference electrode (Ag/AgCl), and the auxiliary electrode (platinum wire). The potential is applied to the working electrode at a constant rate (100 mV/s) either toward the positive potential (evaluation of reducing equivalent) or toward the negative potential (evaluation of oxidizing species). During operation of the cyclic voltammetry, a potential current curve is recorded (cyclic voltammogram). Recently quantitative determination of the phenolic antioxidants using voltammetric techniques was described by Raymundo, Paula, Franco, and Fett (2007). In case of plant samples Chatterjee et al. (2007) determine the antioxidant property of green pepper (*Piper nigrum* L.) and lignans from fresh mace (*Myristica fragrans*). While Kilmartin and Hsu (2003) determine antioxidant property of green, oolong and black teas, and in coffee using cyclic voltammetry method.

2.8. TOSC assay

Winston, Regoli, Dugas, Fong, and Blanchard (1998) recently reported an assay called total oxyradical scavenging capacity (TOSC) assay. MacLean, Murr, and DeEll (2003) used this assay to determine the antioxidant activity of plant tissues. It is based on the oxidation of alpha-keto-γ-methiolbutyric acid (KMBA) to ethylene by peroxyl radicals produced from AAPH. The ethylene formation, which is partially inhibited in the presence of antioxidants, is monitored by gas chromatographic analysis of head space from the reaction vessel. The TOSC is calculated according to the equation: $\text{TOSC} = 100 - (\int \text{SA} / \int \text{CA} \times 100)$, where $\int$SA and $\int$CA are the integrated area from the curve defining the sample and control reactions, respectively.

2.9. Photochemiluminescence (PCL) assay

PCL assay was initially used by Popov, Lewin, and Baehr (1987). Popov and Lewin (1994, 1996) have extensively studied this technique to determine water-soluble and lipid-soluble antioxidants. The photochemiluminescence measures the antioxidant capacity, towards the superoxide radical, in lipidic (ACL) and water (ACW) phase. This method allows the quantification of both the antioxidant capacity of hydrophilic and/or lipophilic substances, either as pure compounds of complex matrix from different origin: synthetic, vegetable, animal, human, etc. The PCL method is based on an acceleration of the oxidative reactions in vitro about 1000 faster than the normal conditions, because the presence of an appropriate photosensitizer. The PCL is a very quick and sensitive measurement method. Using the PCL assay Chua, Tung, and Chang (in press) determined antioxidant property in *Cinnamomum osmophloeum* Kaneh and Wang et al. (2006) determine antioxidant property in marigold flowers.

3. Indian plants with antioxidant activity

The number of plant species in India is estimated to be over 45,000 representing about 7% of the world's flora (http://www.inheritanceindia.co.in). Medicinal plants, as a group, comprise approximately 8000 species and account for about 50% of all the higher flowering plant species of India. India is one of the richest countries in the world as regards genetic resource of medicinal and aromatic plants. It constitutes 11% of total known world flora having medicinal property. Ayurveda has been in practice in India for more than 3500 years and the first recorded book on Ayurvedic medicine was *Charaka Samhita* dates back to 600 BC. The traditional healers have used this resource since time immemorial for the benefit of mankind. As already stated some plants with antioxidant activity have been reviewed earlier. Here we discuss a list of plants in addition to these as below.

3.1. *Aerva lanata (L.) Schult (Pindi kura)*

A. lanata is an erect or prostrate herbaceous weed, common throughout the hotter parts of India like Tamil Nadu, Andhra Pradesh and Karnataka. It is also found in Sri Lanka, Arabia, Egypt, tropical Africa, Indonesia, Malaysia, Papua New Guinea, Philippines and Australia. *A. lanata* is endowed with flavonoids, alkaloids, steroids, polysaccharides, tannins, saponins, etc. (Afaq, Tajuddin, & Afridi, 1991; Chandra & Sastry, 1990; Zapesochnaya, Kurkin, Okhavov, & Hiroshnikov, 1992) The in vitro antioxidant studies of the ethanol extract of *A. lanata* exhibited 1,1-diphenyl-2-picrylhydrazyl (DPPH) scavenging properties (Shirwaikar, Issac, & Malini, 2004). Flavonoids, which are well-known antioxidants and free radical scavengers, such as kaempferol 3-rhamnoside and kaempferol 3-rhamnogalactoside have been reported to be present in *A. lanata* (Afaq et al., 1991). The significant hepatoprotective, nephroprotective and antioxidant effect of *A. lanata* may be due to presence of alkaloids and its inhibitory effect on microsomal Cyt P450 enzyme or on lipid peroxidation (Nevin & Vijayammal, 2005).

3.2. *Amaranthus paniculatus L. (Rajgriha, Bush greens, Caterpillar amaranth)*

It belongs to the family Amaranthaceae and commonly called as Amaranth. It grows on broken waste ground, in short grassland and in shady places in forests. Presumably of Central American origin, it is now cultivated and naturalized worldwide. *A. paniculatus* has a high content of beta-carotene, ascorbic acid (vitamin C) and folate which can be a rich source of antioxidants. Members of Amaranthaceae are good natural sources of carotenoids, vitamin C, nutritionally critical lysine, methionine and proteins (Bhatia & Jain, 2003). The ability of *A. paniculatus* extract to act as a free radical scavenger or hydrogen donor was revealed by DPPH radical-scavenging activity assay. (Amin, Norazaidah, & Hainida, 2006).

3.3. *Aristolochia bracteolata Lam. (Worm killer, Indian Birthwort)*

A. bracteolata is a perennial herb, the leaves of which are used by the native tribals and villagers of the Chittoor District of Andhra Pradesh in India for the rapid healing of cuts and wounds. It is also distributed along Tropical Africa, Oman, Saudi Arabia, United Arab Emirates, Yemen, Pakistan and Sri Lanka. The ethanol extract of the shade-dried leaves of *A. bracteolata* was studied for its effect on wound healing in rats, using incision, excision and dead-space wound models. The plant showed a definite, positive effect on wound healing, with a significant increase in the level of two powerful antioxidant enzymes, super oxide dismutase and catalase, in the granuloma tissue. Preliminary phytochemical screening revealed the presence of alkaloids, saponins, glycosides, steroids, tannins, phenolic compounds and flavonoid glycosides (Shirwaikar, Somashekar, Udupa, Udupa, & Somashekar, 2003).

3.4. *Cissampelos pareira (Ambastha, Laghupatha)*

C. pareira is a sub-erect or climbing herb used in Indian traditional medicine (Vaidya, 1998). The plant is common in orchards, hedges, parks and gardens on moist soils distributed throughout tropical and subtropical India and on the hilly tracts along watercourses. It is also found in Mexico and Southern America. The leaves, eaten as potherb and are reported to be cooling. Crushed leaves are boiled with rice and given as a tonic and in heart complaints; fresh juice is applied in eye-diseases. Plant juice with jaggery and egg is given internally for minor injuries (Anonymous, 1992). The roots possess astringent, mildly tonic, diuretic, stomachic, antilithic, analgesic, antipyretic activities and are prescribed for treating cough, dyspepsia, dropsy, urino-genital troubles such as prolapsus uteri, cystitis, haemorrhage, menorrhagia and calcular nephritis (Kirtikar & Basu, 1933). The root and leaves contain several alkaloids and essential oil. The methiodide and methchloride derivatives of alkaloid hayatine were reported to be potent neuromuscular blocking agents that lower blood pressure (Amresh Reddy, Rao, & Shirwaikar, 2004; Anonymous, 1992). In ethnomedicine, this plant finds mention for its antidiarrhoeal properties (Jain, 1991).

3.5. *Coccinia indica Wight & Arn. (Little Gourd, Kovai)*

C. indica grows abundantly all over India, Tropical Africa, Australia, Fiji and through out the oriental countries. Indigenous people use various parts of the plant to get relief from diabetes mellitus. The plant has also been used extensively in Ayurvedic and Unani practice in the Indian subcontinent (Chopra, Chopra, Handa, & Kapur, 1958). Mukerjee, Ghosh, and Datta (1972) showed that

the aqueous and ethanolic extract of *C. indica* leaves possess hypoglycemic activity. Several years ago, Hossain, Shibib, and Rahman (1992) examined the effect of *C. indica* leaf preparation and showed that it depressed the activity of the enzyme glucose-6-phosphatase. *C. indica* leaf extract possesses an antioxidant activity, which may be attributed to its protective action on lipid peroxidation and to the enhancing effect on cellular antioxidant defence contributing to the protection against oxidative damage in streptozotocin diabetes (Venkateswaran & Pari, 2002).

3.6. Coriandrum sativum L. (Coriander)

It is an annual herb probable originated in mediterranean region, now extensively cultivated in India, Russia, Central Europe, Turkey, Morocco, Argentina and the United States of America. The fruits are aromatic, bitter, have antiinflammatory and diuretics property. It aids digestion and useful in vitiated conditions of *pitta*, burning sensation, cough, bronchitis, vomiting, dyspepsia, diarrhoea, dysentery, gout, rheumatism, intermittent fevers and giddiness (Varier, 1994). Coriander seeds have been shown to have antiperoxidative properties (Chitra & Leelamma, 1999). The activity of polyphenolic compounds from coriander seeds on oxidative damage induced by H_2O_2 in human lymphocytes has been shown (Hashim, Lincy, Remya, Teena, & Anila, 2005). Quercetin 3-glucuronide, isoquercitrin and rutin have been separated and identified in coriander fruits (Kunzemann & Herrmann, 1977). Guerra, Melo, and Filho (2005) determine antioxidant activity of the fractions, containing approximately 1.50 mg of carotenoids by the coupled oxidation of the β-carotene and the linoleic acid. While Wangensteen, Samuelsen, and Malterud (2004) and Wong and Kitts (2006) confirmed antioxidant property of *C. sativum* using DPPH assay.

3.7. Coscinium fenestratum Colebr. (Tree turmeric)

C. fenestratum, indigenous to India and Sri Lanka, also found in Cambodia, Vietnam, Indonesia and Malaysia is used in ayurveda and siddha medicine. The alcoholic extract of the stems are used for treatment of diabetes and dyspepsia (Punitha et al., 2005; Varier, 1994; Shirwaikar et al., 2005). It is reported to have hypotensive and hepatoprotective actions (Singh, Singh, Bani, & Malhotra, 1990; Venukumar & Latha, 2004). The stem contains berberine, ceryl alcohol, hentriacontane, sitosterol, palmitic acid, oleic acid and saponin, together with some resinous material (Anonymous, 1992). Roots contain tertiary alkaloids, berlambine, dihydroberlambine and noroxyhydrastinine (Datta, Mathur, & Baruah, 1988). The antioxidant activity of *C. fenestratum* may be due to the presence of berberine and phenolic compounds (Punitha, Rajendran, Shirwaikar, & Shirwaikar, 2005).

3.8. Cynodon dactylon (L.) Pers. (Dhub grass, Bermuda, Bahama grass, Hariali, Durva, Haritali)

This grass grows throughout India and in almost all parts of the world. It forms an important part of Ayurvedic medicine. The juice is used in hysteria, epilepsy and insanity (Rajvaidya, 1935). Auddy et al. (2003) have studied and demonstrated the antioxidant properties of *C. dactylon* using ABTS assay.

3.9. Cyperus rotundus L. (Nut grass, Coco grass)

C. rotundus is a pantropic weed that grows throughout India. It is a traditional medicinal plant appearing not only among Indian drugs but Chinese and Japanese natural drugs as well. It forms an ingredient of Amrita Bindu, a salt-spice-herbal mixture formulated by Shanmugasundaram, Sujatha, and Shanmugasundaram (1994) based on Indian system of medicine that can control inflammation and degenerative disorders, slowing the aging process (Natarajan, Narasimhan, Shanmugasundaram, & Shanmugasundaram, 2006). It is used for the treatment of spasms, stomach disorder and antiinflammatory diseases (Gupta, Palit, Singh, & Bhargava, 1971; Seo et al., 2001). It has remarkable hypotensive (Li, 1992) and antipyretic effects (Vedavathy & Rao, 1991). *C. rotundus* has been found to exhibit significant antioxidant and antimutagenic activities. The preliminary chemical study of the tested extracts of *C. rotundus* revealed the presence of important quantities of flavonoids, tannins and coumarins in total oligomers flavonoids (TOF) and methanol extracts. Ethyl acetate extract has shown the presence of sterols and flavonoids, while antioxidant nature was proved by DPPH assay (Kilani et al., 2005).

3.10. Enicostemma littorale Blume (Nahi, Maja-makka booti)

It is a small herb, found throughout India and commonly used as an antidiabetic agent by rural folks of Gujarat. Also found in tropical Africa, Southeast Asia and Malaysia. It is cited in ancient literature as an antimalarial, antipyretic and as a laxative (Vyas, Sharma, Sharma, & Khanna, 1979). It contains phenols, tannins, flavonoids, glycosides, anthroquinones, sterols (Vasu, Modi, Thaikoottathil, & Gupta, 2005), gentianine and swertiamarin (Govindachari, Sathe, & Vishwanathan, 1966; Vishwakarma, Rajani, Bagul, & Goyal, 2004). Studies have also confirmed its antidiabetic effect (Vijayvargia, Kumar, & Gupta, 2000; Maroo, Vasu, Aalinkeel, & Gupta, 2002, 2003a, Maroo, Vasu, & Gupta, 2003b; Murali, Upadhyaya, & Goyal, 2002; Upadhyay & Goyal, 2004; Srinivasan, Padmanabhan, & Prince, 2005) and hypoglycemic, antioxidant and hypolipidaemic potential (Vasu et al., 2005). This herb is also known for its antiinflammatory (Sadique, Chandra, Thenmozhi, & Elango, 1987) and anticancer property (Kavimani & Manisenthlkumar, 2000).

Recently aerial part of *Enicostemma littorale* was reported to show hypolipidaemic effect in *p*-dimethylaminobenzene (*p*-DAB) induced hepatotoxic animals (Gopal, Gnanamani, Udayakumar, & Sadulla, 2004; Vasu et al., 2005).

3.11. Evolvulus alsinoides L. (Slender dwarf, Morning glory)

Found throughout India it is used in insanity, epilepsy and nervous debility (Chatterjee, 1990). Also present in Alabama, Florida and Texas (USA) and through out Southern America. In Ayurveda it is used for the treatment of degenerative diseases. Both ethanolic extract and water infusion of *E. alsinoides* have been found to have antioxidant effects, shown by the inhibition of lipid peroxidation and ABTS assay (Auddy et al., 2003).

3.12. Fagonia cretica L. (Dhanyavas)

Fagonia cretica L. is a small spiny undershrub, mostly found in dry calcareous rocks throughout western India and Pakistan. Also found in Algeria, Egypt, Morocco, Tunisia, Cape Verde, Saudi Arabia and Cyprus. It has been reported to contain a wide variety of antioxidants and have been in use in the eastern system of medicine for various disorders. It is effective in elevating the glutathione (GSH) levels and expression of the γ-glutamylcysteine ligase (GCLC). It also exhibits strong free radical scavenging properties against reactive oxygen and nitrogen species as revealed by electron paramagnetic resonance spectroscopy, diminishing the expression of iNOS gene. Therefore, it attenuate oxidative stress mediated cell injury during oxygen glucose deprivation (OGD) and exert the above effects at both the cytosolic as well as at gene expression levels and may be effective therapeutic tool against ischemic brain damage. Further protective ability may be attributed to the GSH and vitamin C content of *F. cretica* (Rawal, Muddeshwar, & Biswas, 2004).

3.13. Gymnema montanum Hook.f. (Madhunasni)

G. montanum, a rare, endangered and endemic plant species is distributed in India mainly in Western Ghats (Hooker, 1883). Also present in West Tropical Africa, Southern Africa, China, Japan, Sri Lanka, Thailand, Vietnam, Indonesia and Malaysia. *G. montanum* ethanolic leaf extract possess antihyperglycemic and antiperoxidative effect. It has been reported to be rich in gymnemagenin and gymnemic acids that are responsible for antihyperglycemic effect (Murakami et al., 1996). The decrease in lipid peroxides, increase in reduced glutathione, ascorbic acid (vitamin C) and α-tocopherol (vitamin E). In the study by Ananthan et al. (2003) has shown treatment of diabetic rats with leaf extract increased the antioxidant levels.

3.14. Hygrophila auriculata (Schumach.) Heine (syn. Asteracantha longifolia Nees)

This indigenous plant is widely distributed throughout the Indian subcontinent and possess antitumor, hypoglycaemic antibacterial, free radical scavenging and lipid peroxidation activities (Mazumdar, Gupta, Maiti, & Mukhejee, 1997; Boily & Vanpuyvelde, 1986; Vlietinck et al., 1995). Now the plant is widely distributed through out Tropical Africa, Nepal, Pakistan, Sri Lanka, Cambodia, Laos, Myanmar, Thailand, Vietnam and Malaysia. The roots, seeds and ashes of the plant are extensively used in the traditional system of medicine for ailments like jaundice, hepatic obstruction, rheumatism, inflammation, urinary infections and gout. In ayurveda it is used for the treatment of diabetes and dysentery (Chopra, Nayar, & Chopra, 1986).

The seeds are diuretic, aphrodisiac and used prophylactically for curing asthma, jaundice and liver ailments and as an ingredient of at least ten polyherbal formulations with established hepatoprotective action (Jayatilak, Pardanani, Murty, & Seth, 1976; Handa, Sharma, & Chakraborti, 1986; Asolkar, Kakkar, & Chakre, 1992; Singh & Handa, 1995).

Methanolic extracts of seeds showed hepatoprotective activity in rats with thioacetamide and paracetamol-induced liver damage and hepatocarcinogenesis (Singh & Handa, 1995; Ahmed, Rahman, Mathur, Athur, & Sultana, 2001). Ahmed et al. (2001) showed that plant extract inhibits CCl_4 induced oxidative stress and proliferative response. The root extract was also studied for its in vitro antioxidant activity using ferric thiocyanate (FTC) and thiobarbituric acid (TBA) methods (Shanmugasundaram & Venkataraman, 2006).

3.15. Phyllanthus amarus Schumach. & Thonn. (Bhumyamalaki)

P. amarus is a herb with rigid, short and prostrate stems. It is found in parts of South India, Florida, Mexico and throughout the Southern America. It is used in Ayurvedic system of medicine to combat many liver disorders (Sane, Kuber, & Menon, 1995) and is a well-known antiviral agent (Thyagarajan, Jayaram, & Valliammai, 1990). *P. amarus* showed antitumor, anticarcinogenic and radio protective activities (Rajeshkumar et al., 2002; Harikumar & Kuttan, 2004). *P. amarus* contains several active ingredients like tannins, phyllanthin, hypophyllanthin, polyphenols, quercetin, astragalin and some ellgitannins like catechin and epigallocatechin (Foo, 1995). *P. amarus* has antiseptic properties, and is used to treat gonorrhea, jaundice and mammary abscesses (Basharat, 1998). *P. amarus* has been reported to possess antidiabetic, anticancer, anti-inflammatory activities (Kiemer, Hartung, Huber, & Vollmar, 2003; Rajeshkumar et al., 2002; Srividya & Periwal, 1995).

3.16. Phyllanthus debilis Klein ex Willd

It is a monoecious, erect, annual herbs distributed in Bhutan, India and Sri Lanka. *P. debilis* shows the highest antioxidant property as compared to all the other plants belonging to the genus *Phyllanthus* as proved experimentally by Kumaran and Karunakaran (2007) using different antioxidant assays such as total antioxidant activity, free radical scavenging, superoxide anion radical scavenging, hydrogen peroxide scavenging, nitric oxide scavenging, reducing power and metal ion chelating activities. The antioxidant property of *P. debilis* can be attributed to the presence of phenolic compounds, flavonoids and flavonols (Kumaran & Karunakaran, 2007).

3.17. Phyllanthus maderaspatensis L

It is widely distributed in India, Pakistan, Yemen and Sri Lanka including some parts of Tropical Africa, Indonesia and Australia. *P. maderaspatensis* is a traditional herbaceous medicinal plant. The leaves are expectorant, diaphoretic, and useful in strangury and sweats. The seeds have a bad taste and are carminative, laxative and tonic to the liver, diuretic and useful in bronchitis, earache, griping, ophthalmia and ascites. The hepatoprotective activities of different extracts (*n*-hexane, alcohol and water) of *P. maderaspatensis* (whole plant) and choleretic activity of the most active extract have been studied along with the hydroxyl radical scavenging and antilipid peroxidation activities of these extracts. *P. maderaspatensis* has been evaluated for its antihepatotoxic and choleretic activities. The plant extracts (*n*-hexane, ethyl alcohol or water) has been shown to possess a remarkable hepatoprotective activity against acetaminophen-induced hepatotoxicity as judged from the serum marker enzymes (Asha, Akhila, Wills, & Subramoniam, 2004). The water and ethyl alcohol extracts showed moderate activity compared to the *n*-hexane extract, which showed activity at low doses as well. The *n*-hexane extract is known to exhibit choleretic activity, in vitro hydroxyl radical scavenging activity and inhibition of lipid peroxidation. (Asha et al., 2004) *P. maderaspatensis* is used for headaches, as a laxative and diuretic (Kumaran & Karunakaran, 2007).

3.18. Phyllanthus niruri L. (Bhumyamalki)

P. niruri is a perennial herb distributed throughout India including some parts of USA and Mexico and through out Southern America. Whole plant, fresh leaves and fruits are used to treat hepatitis (Chopra et al., 1986), hypolipidaemia (Khanna, Rizvi, & Chander, 2002) and viral disease (Venkateswaran, Millman, & Blumberg, 1987; Wang, Cheng, Li, Meng, & Malik, 1994). Several bioactive molecules, such as lignans, phyllanthin, hypophyllanthin, flavonoids, glycosides and tannins, have been shown to be present in the extracts of *P. niruri* (Rajeshkumar et al., 2002). Shamasundar et al. (1985) have shown that phyllanthin and hypophyllanthin protect cells against carbon tetrachloride cytotoxicity whereas triacontanal protects against galactosamine toxicity. *P. niruri* is used as one of the components of a multiherbal preparation for treating liver ailments (Kapur, Pillai, Hussain, & Balani, 1994).

Methanolic and aqueous extract of leaves and fruits of *P. niruri* showed inhibition of membrane lipid peroxidation (LPO), scavenging of 1,1-diphenyl-2picrylhydrazyl (DPPH) radical and inhibition of reactive oxygen species (ROS) in vitro (Chatterjee, Sarkar, & Parames, 2006). Antioxidant activities of the extracts were also demonstrable in vivo by the inhibition of the carbon tetrachloride induced formation of lipid peroxides in the liver of rats by pretreatment with the extracts (Harish & Shivanandappa, 2006).

Apart from this protein fraction isolated from of *P. niruri* partially prevented nimesulide induced hepatic disorder and possesses both preventive and curative activities against chemically induced oxidative stress in mice (Chatterjee et al., 2006).

3.19. Phyllanthus urinaria L. (Pitirishi, Budhatri)

P. urinaria is herb found through out the Indian Subcontinent, oriental countries and Northwestern Pacific, particularly used as a diuretic and for the treatment of dysentery (Basharat, 1998). The antioxidant activity of *P. urinaria* in comparison with other plants of the genus *Phyllanthus* has been examined using different antioxidant assays such as total antioxidant activity, free radical scavenging (DPPH assay), superoxide anion radical scavenging, hydrogen peroxide scavenging, nitric oxide scavenging, reducing power and metal ion chelating activities in the study by Kumaran and Karunakaran (2007).

3.20. Phyllanthus virgatus G.Forst. (Chitrak)

It is distributed mainly in India, Bhutan and Nepal including some other parts of Orantal Asia, Australia and Pacific ilands. The antioxidant properties of *P. virgatus* were intermediate to those of the other plants of the genus *Phyllanthus* as reported by Kumaran and Karunakaran (2007).

3.21. Plumbago zeylanica Linn (Plumbaginaceae)

P. zeylanica is an important medicinal plant, distributed in the tropical regions of India. It is also found throughout the Tropical Africa and some parts of Oriental Asia, Australia, Yemen and Pacific islands. The herb *P. zeylanica* in Amrita Bindu is known for inhibitory effects against superoxide and nitric oxide production (Natarajan et al., 2006; Seo et al., 2001). Natarajan et al. (2006) found antioxidant property of the plant using ABTS assay. It is used as chemopreventive agent against intestinal neoplasia (Natarajan et al., 2006; Sugie et al., 1998).

Table 2
Worldwide distribution of plants with antioxidant activities used in traditional Indian remedies

Land Mass	Plant Species																							
	Aerva lanata	*Amaranthus paniculatus*	*Aristolochia bracteolate*	*Cissampelos pareira*	*Coccinia indica*	*Coriandrum sativum*	*Cosciniun fenestratum*	*Cynodon dactylon*	*Cyperus rotundus*	*Enicostemma littorale*	*Enicostemma littorale*	*Fagonia cretica*	*Gymnema montanum*	*Hygrophila auriculata*	*Phyllanthus amarus*	*Phyllanthus debilis*	*Phyllanthus maderaspatensis*	*Phyllanthus niruri*	*Phyllanthus urinaria*	*Phyllanthus virgatus*	*Plumbago zeylanica*	*Rubia cordifolia*	*Striga orobanchioides*	*Trichopus zeylanicus*
Afghanistan																						+		
Arabian peninsula	+		+									+					+				+			
Australia	+				+												+			+	+		+	
Bhutan & Nepal														+		+								
Cape Verde												+												
Central America				+											+			+						
Central Europe						+																		
China									+				+									+		
Cyprus												+												
Eastern Siberia																						+		
Egypt	+											+												
Indonesia	+						+						+				+					+		
Japan									+				+									+		
Malaysia	+						+			+			+	+										+
Mongolia																						+		
Morocco						+						+												
Pacific islands	+				+														+	+	+			
Pakistan			+											+			+							
Philippines																						+		
Russia						+																		
South Africa													+											
South America				+		+					+				+			+						
Southeast Asia	+						+			+			+	+					+			+		+
Sri Lanka	+		+										+	+		+	+							+
Thailand													+	+										+
Through out Asia																				+	+		+	
Tropical Africa	+		+		+					+		+	+	+			+				+	+	+	
Turkey						+																		
USA						+					+				+			+						
Vietnam							+						+	+								+		
World wide		+						+																

3.22. *Rubia cordifolia L. (Indian madder, madderwort)*

It is a perennial, herbaceous climber, roots long, cylindrical, flexuose, with a thin red bark and common throughout the hilly tracts of India from the Northern western Himalayas, eastward ascending to 2500 m (Sivarajan & Balachandran, 1994). It is also distributed through out Tropical Africa, Afghanistan, Eastern Siberia, Mongolia, China, Japan, Vietnam, Indonesia and Philippines. *R. cordifolia* has been shown to exert cell/neuroprotective properties via preventing the depletion and increasing GSH (glutathione) levels by inducing GCLC (γ-glutamylcysteine ligase) expression, reducing oxidant levels by direct scavenging, and decreasing iNOS expression. The protective ability may be attributed to the GSH and vitamin C content of the herb (Rawal et al., 2004).

3.23. *Striga orobanchioides Benth*

S. orobanchioides is a parasitic plant that lives on the roots of various plants. It is distributed in the hills, usually on red and gravelly soils of India and in the warmer regions of Asia, Africa and Australia. In Ayurvedic medicine, the plant is described as antidiabetic (Chopra et al., 1986). Studies have shown significant antiimplantation and estrogenic activity of ethanolic and aqueous extracts of the

whole plant (Hiremath, Badami, Swamy, Patil, & Londonkar, 1994). The ethanolic extract has also shown significant antiandrogenic and antibacterial (Hiremath, Swamy, Badami, & Meena, 1996a, 1997), antihistaminic and mast cell stabilising activities (Harish, Nagur, & Badami, 2001). The ethanolic extract of *S. orobanchioides* possesses strong antioxidant properties as evidenced by the significant increase in the level of catalase, SOD and ascorbic acid and decrease in the levels of thio-barbituric acid reactive substances (TBARS). Badami, Gupta, and Suresh (2003) confirmed antioxidant property of this plant by DPPH and nitric oxide radical inhibition assays. A large number of flavonoids including apigenin and luteolin are known to possess strong antioxidant properties (Raj & Shalini, 1999; Badami et al., 2003).

3.24. *Trichopus zeylanicus Gaertn. (Arogyappacha)*

T. zeylanicus is a wild plant of a rare genus, found growing in the Agasthyar hilly forests of Kerala, India. It is also found in Malay Peninsula, Sri Lanka and Thailand. The tribal inhabitants (Kani tribe) of this area use this plant as a health tonic and rejuvenator (Evans, Subramoniam, Rajasekharan, & Pushpangadan, 2002; Sharma, Pushpangandan, Chopra, Rajasekharan, & Amma, 1989). Exploration and identification of the active constituent(s) of *T. zeylanicus* that increases the non-specific resistance of the body to combat harmful influence of stress has been carried out (Singh et al., 2005). The antioxidant properties of *T. zeylanicus* were established on free radicals (DPPH and ABTS), its ability to reduce iron, lipoxygenase activity and hydrogen peroxide-induced lipid peroxidation. *T. zeylanicus* contains, polyphenols and sulfhydryl compounds, which have the ability to scavenge reactive oxygen species (Tharakan, Dhanasekaran, & Manyam, 2005).

4. Conclusions

In this review we have focussed on 24 plants used in India for their antioxidant properties, which have been rarely reviewed. The most common use of these herbs was found to be in liver disease as hapatoprotective agents and in diabetics. Other major applications of these herbs were in the form of a neuroprotective, anticancer, antitumor, antistress, dermal wound healing, cardiovascular protection, antidiarrhoea and anticholesterol activity. Among different families of antioxidants, flavanoids and tannins are most recurring followed by phenolics, ascorbic acid and alkaloids.

Though invitro antioxidant assays has been carried out in the reported plants, invivo tests remains to be done in majority of them. The clinical efficacies of many plant preparations used are not yet validated. The mechanism of action of some of the identified antioxidants is known (Table 1) but as the active ingredients in many plants extract possessing antioxidant properties remains to be identified a complete picture is yet to emerge. A further elucidation of both known and yet to be identified natural antioxidants clubbed with newly emerging technology metabolomics could help disease prevention and cure using simple herbs. Herbs like *Amaranthus paniculatus*, *Aerva lanata*, *Coccinia indica* and *Coriandrum sativum* are used as vegetables indicating that these plants could be source of dietary antioxidant supplies. The worldwide distribution of these plants was verified using the Germplasm Resources Information Network (GRIN) maintained by USDA and presented in Table 2. Interestingly a vast majority of these plats are also available in other parts of the world. Therefore if a systematic investigation is initiated the traditional medicinal systems practised in India can offer promising leads for the discovery of potent antioxidants that can have therapeutic and dietary use globally.

References

Actis-goretta, L., Mackenzie, G. G., Oteiza, P. I., & Fraga, C. G. (2002). Comparative study on the antioxidant capacity of wines and other plant-derived beverages. *Alcohol and Wine in Health and Disease, 957*, 279–283.

Afaq, S. H., Tajuddin, S., & Afridi, R. (1991). Bisheri Booti (*Aerva lanata*) some lesser known uses and pharmacognosy. *Ethnobotany, V*, 37–40.

Ahmed, S., Rahman, A., Mathur, M., Athur, M., & Sultana, S. (2001). Antitumor promoting activity of *Asteracantha longifolia* against experimental hepatocarinogenesis in rats. *Food and Chemical Toxicology, 39*, 19–28.

Ajila, C. M., Naidu, K. A., Bhat, U. J. S., & Rao, P. (2007). Bioactive compounds and antioxidant potential of mango peel extract. *Food Chemistry, 105*, 982–988.

Almeida, I. F., Fernandes, E., Lima, J. L. F. C., Costa, P. C., & Bahia, F. M. (2008). Walnut (*Juglans regia*) leaf extracts are strong scavengers of pro-oxidant reactive species. *Food Chemistry, 106*, 1014–1020.

Amado, L. L., Jaramillo, M. D., Rocha, A. M., Ferreira, J. L. R., Garcia, L. M., Ramos, P. B., et al. (2007). A new method to evaluate total antioxidant capacity against reactive oxygen and nitrogen species (RONS) in aquatic organisms. *Comparative Biochemistry and Physiology – Part A: Molecular & Integrative Physiology, 148*, S75–S76.

Amin, I. Y., Norazaidah, K. I., & Hainida, E. (2006). Antioxidant activity and phenolic content of raw and blanched Amaranthus species. *Food Chemistry, 94*, 47–52.

Amresh Reddy, G. D., Rao, C. V., & Shirwaikar, A. (2004). Ethnomedical value of *Cissampelos pareira* extract in experimentally induced diarrhea. *Acta Pharm, 54*, 27–35.

Ananthan, R., Baskar, C., NarmathaBai, V., Pari, L., Latha, M., & Ramkumar, K. M. (2003). Antidiabetic effect of *Gymnema montanum* leaves: Effect on lipid peroxidation induced oxidative stress in experimental diabetes. *Pharmacological Research, 48*, 551–556.

Anonymous, (1992). *Wealth of India: Raw materials* (3rd ed., Vol. 3. Council of Scientific and Industrial Research Publication, New Delhi (pp. 591–593).

Arteel, G. E. (2003). Oxidants and antioxidants in alcohol-induced liver disease. *Gastroenterology, 124*, 778–790.

Aruoma, A. M., Butler, M. J., & Halliwell, B. (1993). Evaluation of the antioxidant and prooxidant actions of gallic acid and its derivatives. *Journal of Agricultural and Food Chemistry, 41*, 1880–1885.

Aruoma, O. I. (1998). Free radicals, oxidative stress and antioxidants in human health and disease. *Journal of the American Oil Chemists Society, 75*, 199–212.

Asha, V. V., Akhila, S., Wills, P. J., & Subramoniam, A. (2004). Further studies on the antihepatotoxic activity of *Phyllanthus maderaspatensis* Linn. *Journal of Ethnopharmacology, 92*, 67–70.

Asolkar, L. V., Kakkar, K. K. & Chakre, O. I. (1992). Glossary of Indian medicinal plants with active principles. Publication and Information Directorate, Council of Scientific and Industrial Research, New Delhi.

Auddy, B., Ferreira, M., Blasina, F., Lafon, L., Arredondo, F., Dajas, F., et al. (2003). Screening of antioxidant activity of three Indian medicinal plants, traditionally used for the management of neurodegenerative disease. *Journal of Ethnopharmacology, 84*, 131–138.

Badami, S., Gupta, M. K., & Suresh, B. (2003). Antioxidant activity of the ethanolic extract of *Striga orobanchioides*. *Journal of Ethnopharmacology, 85*, 227–230.

Bagchi, D., Sen, C. K., Ray, S. D., Das, D. K., Bagchi, M., Preus, H. G., et al. (2003). Molecular mechanisms of cardioprotection by a novel grape seed proanthocyanidin extract. *Mutation Research, 9462*, 1–11.

Balasubashini, M. S., Rukkumani, R., Viswanathan, P., & Venugopal, M. (2004). Ferulic acid alleviates lipid peroxidation in diabetic rats. *Phytotherapy Research, 18*, 310–314.

Basharat, A. (1998). Medicinal properties of various species of *Phyllanthus*. *Hamdard-Medicus, 41*, 109–110.

Benzie, I. F. F., & Strain, J. J. (1999). Ferric reducing antioxidant power assay: Direct measure of total antioxidant activity of biological fluids and modified version for simultaneous measurement of total antioxidant power and ascorbic acid concentration. *Methods in Enzymology, 299*, 15–27.

Bhatia, A. L., & Jain, M. (2003). *Amaranthus paniculatus* (Linn.) improves learning after radiation stress. *Journal of Ethnopharmacology, 85*, 73–79.

Boily, Y., & Vanpuyvelde, L. (1986). Screening of medicinal plants of Rwanda (Central Africa) for antimicrobial activity. *Journal of Ethnopharmacology, 16*, 1–13.

Bolton, J. L., Trush, M. A., Penning, T. M., Dryhurst, G., & Monks, T. J. (2000). Role of quinones in toxicology. *Chemical Research in Toxicology, 13*, 135.

Brand-Williams, W., Cuvelier, M. E., & Berset, C. (1995). Use of a free radical method to evaluate antioxidant activity. *Food Science and Technology, 28*, 25–30.

Branen, A. L. (1975). Toxicology and biochemistry of butylated hydroxy anisole and butylated hydroxytoluene. *Journal of American Oil Chemists Society, 52*, 59–63.

Burton, G. W., & Ingold, K. U. (1981). Autoxidation of biological molecules. 1. The antioxidant activity of vitamin E and related chain-breaking phenolic antioxidants in vitro. *Journal of the American Chemical Society, 103*, 6472–6477.

Chandra, S., & Sastry, M. S. (1990). Chemical constituents of *Aerva lanata*. *Fitoterapia, 61*, 188.

Chatterjee, A. (1990). *Treaties of Indian medicinal plants* (Vol. 3). New Delhi: Council for Scientific and Industrial Research, p. 327.

Chatterjee, M., Sarkar, K., & Parames, C. (2006). Sil herbal (*Phyllanthus niruri*) protein isolate protects liver from nimesulide induced oxidative stress. *Pathophysiology, 13*, 95–102.

Chatterjee, S., Niaz, Z., Gautam, S., Adhikari, S., Variyar, P. S., & Sharma, A. (2007). Antioxidant activity of some phenolic constituents from green pepper (*Piper nigrum* L.) and fresh nutmeg mace (*Myristica fragrans*). *Food Chemistry, 101*, 515–523.

Chitra, V., & Leelamma, S. (1999). *Coriandrum sativum* changes the levels of lipid peroxides and activity of antioxidant enzymes in experimental animals. *Indian Journal of Biochemistry and Biophysics, 36*, 59–61.

Chopra, R. N., Chopra, I. C., Handa, K. L., & Kapur, L. D. (1958). Medicinal plants in diabetes. In P. Gupta (Ed.), *Indigenous drugs of India* (2nd ed.) (pp. 314–316). Calcutta, India: U.N. Dhar & Sons Ltd.

Chopra, R. N., Nayar, S. L., & Chopra, I. C. (1986). *Glossary of Indian Medicinal Plants*, 29.

Chua, M., Tung, Y., & Chang, S. (in press). Antioxidant activities of ethanolic extracts from the twigs of *Cinnamomum osmophloeum*. *Bioresource Technology*.

Dastmalchi, K., DamienDorman, H. J., Laakso, I., & Hiltunen, R. (2007). Chemical composition and antioxidative activity of Moldavian balm (*Dracocephalum moldavica* L.) extracts. *Food Science and Technology, 40*, 1655–1663.

Datta, S. C., Mathur, R. K., & Baruah, J. N. (1988). Minor alkaloids of *Coscinium fenestratum* root. *Indian Drugs*, 25–350.

Dufour, D., Pichette, A., Mshvildadze, V., Bradette-Hébert, M., Lavoie, S., Longtin, A., et al. (2007). Antioxidant, anti-inflammatory and anticancer activities of methanolic extracts from *Ledum groenlandicum Retzius*. *Journal of Ethnopharmacology, 111*, 22–28.

Dwivedi, S. (2007). *Terminalia arjuna* Wight & Arn – A useful drug for cardiovascular disorders. *Journal of Ethnopharmacology, 114*, 114–129.

Evans, D. A., Subramoniam, A., Rajasekharan, S., & Pushpangadan, P. (2002). Effect of *Trichopus zeylanicus* Gaertn, leaf extract on the energy metabolism in mice during exercise and at rest. *Indian Journal of Pharmacolology, 34*, 32–37.

Foo, L. Y. (1995). Amarinic acid and related ellagitannins from *Phyllanthns amarus*. *Phytochemistry, 39*, 217–224.

Fridovich, I. (1997). Superoxide anion radical (Obardot 2), superoxide dismutases, and related matters. *Journal of Biological Chemistry, 272*, 18515–18517.

Gérard Monnier, D., & Chaudiere, J. (1996). Metabolism and antioxidant function of glutathione. *Pathologie Biologie (Paris), 44*, 77–85.

Glazer, A. N. (1990). Phycoerythrin fluorescence-based assay for reactive oxygen species. *Methodes in Enzymology, 186*, 161–168.

Gopal, R., Gnanamani, A., Udayakumar, R., & Sadulla, S. (2004). *Enicostemma littorale* Blume – A potential hypolipidemic plant. *Natural Product Radiance, 3*, 401–405.

Govindachari, T. R., Sathe, S. S., & Vishwanathan, N. (1966). Gentianine, an artifact in *Enicostemma littorale*. *Indian Journal of Chemistry, 4*, 201–202.

Govindarajan, R., Rastogi, S., Vijayakumar, M., Rawat, A. K. S., Shirwaikar, A., Mehrotra, S., et al. (2003). Studies on the antioxidant activities of *Desmodium gangeticum*. *Biological and Pharmaceutical Bulletin, 26*, 1424–1427.

Greco, A., Minghetti, L., & Levi, G. (2000). Isoprostanes, novel markers of oxidative injury, help understanding the pathogenesis of neurodegenerative diseases. *Neurochemical Research, 25*, 1357.

Guerra, N. B., Melo, E. A., & Filho, J. (2005). Antioxidant compounds from coriander (*Coriandrum sativum* L) etheric extract. *Journal of Food Composition and Analysis, 18*, 193–199.

Guidi, I., Galimberti, D., Lonati, S., Novembrino, C., et al. (2006). Oxidative imbalance in patients with mild cognitive impairment and Alzheimer's disease. *Neurobiology of Aging, 27*, 262–269.

Gunasekera, S. P., Zuleta, I. A., Longley, R. E., Wright, A. E., & Pomponi, S. A. (2003). Discorhabdins S, T, and U, new cytotoxic pyrroloiminoquinones from a deep-water Caribbean sponge of the genus *Batzella*. *Journal of Natural Products, 66*, 1615–1617.

Gupta, M. B., Palit, T. K., Singh, N., & Bhargava, K. P. (1971). Pharmacological studies to isolate the active constituents from *C. rotundus* possessing anti-inflammatory, anti-pyretic and analgesic activities. *Indian Journal of Medical Research, 59*, 76–82.

Halliwell, B., & Gutteridge, J. M. C. (1999). *Free radicals in biology and medicine* (3rd ed.). Oxford University Press.

Handa, S. S., Sharma, A., & Chakraborti, K. K. (1986). Natural products and plants as liver protecting drugs. *Filetropia, 57*, 307–352.

Harikumar, K. B., & Kuttan, R. (2004). Protective effect of an extract of *Phyllanthus amarus* against radiation induced damage in mice. *Journal of Radiation Research, 45*, 133–139.

Harish, M. S., Nagur, M., & Badami, S. (2001). Antihistaminic and mast cell stabilizing activity of *Striga orobanchioides*. *Journal of Ethnopharmacology, 76*, 197–200.

Harish, R., & Shivanandappa, T. (2006). Antioxidant activity and hepatoprotective potential of *Phyllanthus niruri*. *Food Chemistry, 95*, 180–185.

Hashim, M. S., Lincy, S., Remya, V., Teena, M., & Anila, L. (2005). Effect of polyphenolic compounds from *Coriandrum sativum* on H_2O_2 induced oxidative stress in human lymphocytes. *Food Chemistry, 92*, 653–660.

Hiremath, S. P., Badami, S., Swamy, H. K. S., Patil, S. B., & Londonkar, R. L. (1997). Antiandrogenic activity of *Striga orobanchioides*. *Journal of Ethnopharmacology, 56*, 55–60.

Hiremath, S. P., Badami, S., Swamy, H. K. S., Patil, S. B., & Londonkar, R. L. (1994). Antifertility activity of *Striga orobanchioides*. *Biological and Pharmaceutical Bulletin, 17*, 1029–1031.

Hiremath, S. P., Swamy, H. K. S., Badami, S., & Meena, S. (1996a). Antibacterial and antifungal activity of *Striga orobanchioides*. *Indian Journal of Pharmaceutical Sciences, 58*, 174–178.

J. D. Hooker (1883). Asclepiadaceae. In J.D. Hooker (Ed.), *Flora of British India, Vol. 4.* (p. 31).

Hossain, M. Z., Shibib & Rahman, B. A. R. (1992). Hypoglycemic effects of *Coccinia indica*: Inhibition of key gluconeogenic enzyme, glucose-6-phosphatase. *Indian Journal of Experimental Biology, 30*, 418–420.

Ito, N., Fukushima, S., Hassegawa, A., Shibata, M., & Ogiso, T. (1983). Carcinogenicity of butylated hydroxyanisole in F344 rats. *Journal of National Cancer Institute, 70*, 343–347.

Jain, S. K. (1991). *Dictionary of Indian folk medicine and ethnobotany*. New Delhi: Deep Publications, p. 221.

Jayatilak, P. G., Pardanani, D. S., Murty, B. D., & Seth, A. P. (1976). Effect of indigenous drug (speman) on accessory reproductive functions in mice. *Journal of Experimental Biology, 14*, 170–173.

Jha, P., Flather, M., Lonn, E., Farkouh, M., & Yusuf, S. (1995). The antioxidant vitamins and cardiovascular disease. A critical review of epidemiologic and clinical trial data. *Annals of Internal Medicine, 123*, 860.

Kahkonen, M. P., Hopia, A. I., Vuorela, H. J., Raucha, J. P., Pihlaja, K., Kujala, T. S., et al. (1999). Antioxidant activity of plant extracts containing phenolic compounds. *Journal of Agricultural and Food Chemistry, 47*, 3954–3962.

Kapur, V., Pillai, K. K., Hussain, S. Z., & Balani, D. K. (1994). Hepatoprotective activity of jigrine on liver damage caused by alcohol, carbon tetrachloride and paracetamol in rats. *Indian Journal of Pharmacology, 26*, 35–40.

Kavimani, S., & Manisenthlkumar, K. T. (2000). Effect of methanolic extract of *Enicostemma littorale* on Dalton's ascitic lymphoma. *Journal of Ethnopharmacology, 71*, 349–352.

Khanna, A. K., Rizvi, F., & Chander, R. (2002). Lipid lowering activity of *Phyllanthus niruri* in hyperlipemic rats. *Journal of Ethnopharmacology, 82*, 19–22.

Kiemer, A. K., Hartung, T., Huber, C., & Vollmar, A. M. (2003). *Phyllanthus amarus* has anti-inflammatory potential by inhibition of iNOS, COX-2, and cytokines via the NF-kB pathway. *Journal of Hepatology, 38*, 289–297.

Kilani, S., Ammar, R. B., In'es, Bouhlel, Abdelwahed, A., Hayder, N., Mahmoud, A., et al. (2005). Investigation of extracts from (Tunisian) *Cyperus rotundus* as antimutagens and radical scavengers. *Environmental Toxicology and Pharmacology, 20*, 478–484.

Kilmartin, P. A., & Hsu, C. F. (2003). Characterisation of polyphenols in green, oolong, and black teas, and in coffee, using cyclic voltammetry. *Food Chemistry, 82*, 501–512.

Kirtikar, K. R., & Basu, B. D.(1933). In Lalit Mohan Basu (Ed.), *Indian medicinal plants, Vol. 1* (p. 96). Allahabad.

Kohen, R., Beit-Yannai, E., Berry, E. M., & Tirosh, O. (1999). Overall low molecular weight antioxidant activity of biological fluids and tissues by cyclic voltammetry. *Methodes in Enzymology, 300*, 285–296.

Kumaran, A., & Karunakaran, R. J. (2007). In vitro antioxidant activities of methanol extracts of five *Phyllanthus* species from India LWT. *Food Science and Technology, 40*, 344–352.

Kunzemann, J., & Herrmann, K. (1977). Isolation and identification of flavon (ol)-*O*-glycosides in caraway (*Carum carvi* L.), fennel (*Foeniculum vulgare* Mill.), anise (*Pimpinella anisum* L.), and coriander (*Coriandrum sativum* L.), and of flavon-C-glycosides in anise. I. Phenolics of spices. *Zeitschrift fü r Lebensmitteluntersuchung und forschung A, 164*, 194–200.

Lee, S. C., Kuan, C. Y., Yang, C. C., & Yang, S. D. (1998). Bioflavonoids commonly and potently induce tyrosine dephosphorylation/inactivation of oncogenic proline-directed protein kinase FA in human prostate carcinoma cells. *Anticancer Research, 1*, 1117–1121.

Levites, Y., Amit, T., Mandel, S., & Youdim, M. B. H. (2003). Neuroprotection and neurorescue against amyloid beta toxicity and PKCdependent release of non-amyloidogenic soluble precursor protein by green tea polyphenol (−)-epigallocatechin 3-gallate. *FASEB Journal, 17*, 952–954.

Levites, Y., Weinreb, O., Maor, G., Youdim, M. B. H., & Mandel, S. (2001). Green tea polyphenol (−)-epigallocatechin 3-gallate prevents *N*-methyl-4-phenyl-1,2,3,6-tetrahydropyridine-induced dopaminergic neurodegenration. *Journal of Neurochemistry, 78*, 1073–1082.

Li, G. X. (1992). Toxicity and clinic of traditional Chinese medicine. *Pharmacology*, 194–195.

Lim, Y. Y., & Murtijaya, J. (2007). Antioxidant properties of *Phyllanthus amarus* extracts as affected by different drying methods. *Food Science and Technology, 40*, 1664–1669.

MacLean, D. D., Murr, D. P., & DeEll, J. R. (2003). A modified total oxyradical scavenging capacity assay for antioxidants in plant tissues. *Postharvest Biology and Technology, 29*, 183–194.

Maroo, J., Ghosh, A., Mathur, R., Vasu, V. T., & Gupta, S. (2003a). Antidiabetic efficacy of *Enicostemma littorale* methanol extract in alloxaninduced diabetic rats. *Pharmaceutical Biology, 41*, 388–391.

Maroo, J., Vasu, V. T., & Gupta, S. (2003b). Dose dependent hypoglycemic effect of *Enicostemma littorale* Blume in alloxan induced diabetic rats. *Phytomedicine, 10*, 196–199.

Maroo, J., Vasu, V. T., Aalinkeel, R., & Gupta, S. (2002). Glucose lowering effect of aqueous extract of *Enicostemma littorale* Blume in diabetes: A possible mechanism of action. *Journal of Ethnopharmacology, 81*, 317–320.

Mazumdar, U. K., Gupta, M., Maiti, S., & Mukhejee, D. (1997). Antitumor activity of *Hygrophila spinosa* in Ehrlich ascites carcinoma and sarcoma-180 induced mice. *Indian Journal of Experimental Biology, 35*, 473–477.

Miller, N. J., Rice-Evans, C., Davies, M. J., Gopinathan, V., & Milner, A. (1993). A novel method for measuring antioxidant capacity and its application to monitoring the antioxidant status in premature neonates. *Clinical Science, 84*, 407–412.

Mukerjee, K., Ghosh, N. C., & Datta, T. (1972). *Coccinia indica*, As potential hypoglycaemic agent. *Indian Journal of Experimental Biology, 10*, 347–349.

Murakami, N., Murakami, T., Kadoya, M., Matsuda, H., Yamahara, J., & Yoshikawa, M. (1996). New hypoglycaemic constituents in "gymnemic acid" from *Gymnema sylvestere*. *Chemical and Pharmaceutical Bulletin, 44*, 469–471.

Murali, B., Upadhyaya, U. M., & Goyal, R. K. (2002). Effect of chronic treatment with *Enicostemma littorale* in non-insulin-dependent diabetic (NIDDM) rats. *Journal of Ethnopharmacology, 81*, 199–204.

Natarajan, K. S., Narasimhan, M., Shanmugasundaram, K. R., & Shanmugasundaram, E. R. B. (2006). Antioxidant activity of a salt-spice-herbal mixture against free radical induction. *Journal of Ethnopharmacology, 105*, 76–83.

Netzel, M., Netzel, G., Tian, Q., Schwartz, S., & Konczak, I. (2007). Native Australian fruits - A novel source of antioxidants for food. *Innovative Food Science and Emerging Technologies, 8*, 339–346.

Nevin, K. G., & Vijayammal, P. L. (2005). Effect of *Aerva lanata* against hepatotoxicity of carbon tetrachloride in rats. *Environmental Toxicology and Pharmacology, 20*, 471–477.

Popov, I. N., & Lewin, G. (1994). Photochemiluminescent detection of antiradical activity: II. Testing of nonenzymic water-soluble antioxidants. *Free Radical Biology and Medicine, 17*, 267–271.

Popov, I. N., & Lewin, G. (1996). Photochemiluminescent detection of antiradical activity; IV: Testing of lipid-soluble antioxidants. *Journal of Biochemical and Biophysical Methods, 31*, 1–8.

Popov, I., Lewin, G., & Baehr, R. (1987). Photochemiluminescent detection of antiradical activity. I. Assay of superoxide dismutase. *Biomed Biochim Acta, 46*, 775–779.

Punitha, I. S. R., Rajendran, K., Shirwaikar, A., & Shirwaikar, A. (2005). Alcoholic stem extract of *Coscinium fenestratum* regulates carbohy-

drate metabolism and improves antioxidant status in streptozotocin-nicotinamide induced diabetic rats. *Evidence-based Complementary and Alternative Medicine, 2*, 375–381.

Radisky, D. C., Radisky, E. S., Barrows, L. R., Copp, B. R., Kramer, R. A., & Ireland, C. M. (1993). Novel cytotoxic topoisomerase II inhibiting pyrroloiminoquinones from Fijian sponges of the genus *Zyzzya*. *Journal of American Chemical Society, 115*, 1632–1638.

Raj, K. J., & Shalini, K. (1999). Flavonoids – A review of biological activities. *Indian Drugs, 36*, 668–676.

Rajeshkumar, N. V., Joy, K. L., Kuttan, G., Ramsewak, R. S., Nair, M. G., & Kuttan, R. (2002). Antitumor and anticarcinogenic activity of *Phyllanthus amarus* extract. *Journal of Ethnopharmacology, 81*, 17–22.

Rajvaidya, S. G. (1935). Shankar Nighantu, Banousadhi Bhander, Jabalpur, MP, India.

Ramakrishna, B. S., Varghese, R., Jayakumar, S., Mathan, M., & Balasubramanian, K. A. (1997). Circulating antioxidants in ulcerative colitis and their relationship to disease severity and activity. *Journal of Gastroenterology and Hepatology, 12*, 490–494.

Rawal, A., Muddeshwar, M., & Biswas, S. (2004). Effect of *Rubia cordifolia*, *Fagonia cretica linn*, and *Tinospora cordifolia* on free radical generation and lipid peroxidation during oxygen–glucose deprivation in rat hippocampal slices. *Biochemical and Biophysical Research Communications, 324*, 588–596.

Raymundo, M. S., Paula, M. M. S., Franco, C., & Fett, R. (2007). Quantitative determination of the phenolic antioxidants using voltammetric techniques. *Food Science and Technology, 40*, 1133–1139.

Re, R., Pellegrini, N., Proteggente, A., Pannala, A., Yang, M., & Rice-Evans, C. (1999). Antioxidant activity applying an improved ABTS radical cation decolorization assay. *Free Radicle Biologyl and Medicine, 26*, 1231–1237.

Rice-Evans, C., & Miller, N. J. (1994). Total antioxidant status in plasma and body fluids. *Methodes in Enzymology, 234*, 279–293.

Rozenberg, O., Howell, A., & Aviram, M. (2006). Pomegranate juice sugar fraction reduces macrophage oxidative state, whereas white grape juice sugar fraction increases it. *Atherosclerosis, 188*, 68–76.

Sadique, J., Chandra, T., Thenmozhi, V., & Elango, V. (1987). The antiinflammatory activity of *Enicostemma littorale* and *Mollugo cerviana*. *Biochemical Medicine and Metabolic Biology, 37*, 167–176.

Sánchez-Moreno, J. A., Larrauri & Saura-Calixto, F. (1998). A procedure to measure the antiradical efficiency of polyphenols. *Journal of the Science of Food and Agriculture, 76*, 270–276.

Sane, R. T., Kuber, V. V., & Menon, S. (1995). Hepatoprotection: By *Phyllanthus amarus* and *Phyllanthus debilis* in CCl4 induced liver dysfunction. *Current Science, 20*, 1243–1246.

Scartezzini, P., & Speroni, E. (2000). Review of some plants of Indian traditional medicine with antioxidant activity. *Journal of Ethnopharmacology, 71*, 23–43.

Schlesier, K., Harwat, M., Böhm, V., & Bitsch, R. (2002). Assessment of antioxidant activity by using different in vitro methods. *Free Radical Research, 36*, 177–187.

Schonbaum G. R. & Chance B. (1976). Catalase. In P. D. Boyer (Ed.), *The enzymes, Vol. XIII* (2nd ed., pp. 363-408). New York Academy.

Seo, W. G., Pae, H. O., Oh, G. S., Chai, K. H., Kwon, T. A., Yun, Y. G., et al. (2001). Inhibitory effect of methanol extract of *Cyperus rotundus* rhizomes on nitric oxide and superoxide productions by murine macrophage cell line, RAW 264.7 cells. *Journal of Ethnopharmacology, 76*, 59–64.

Shamasundar, K. V., Singh, B., Thakur, R. S., Hussain, A., Kiso, Y., & Hikino, H. (1985). Antihepatoprotective principles of *Phyllanthus niruri* herbs. *Journal of Ethnopharmacology, 14*, 41–44.

Shanmugasundaram, K. R., Sujatha, R., & Shanmugasundaram, E. R. B. (1994). Amrita Bindu – A salt-spice-herbal health food supplement for the prevention of nitrosamine induced depletion of antioxidants. *Journal of Ethnopharmacology, 42*, 83–93.

Shanmugasundaram, P., & Venkataraman, S. (2006). Hepatoprotective and antioxidant effects of *Hygrophila auriculata* (K. Schum) Heine acanthaceae root extract. *Journal of Ethnopharmacology, 104*, 124–128.

Sharma, A. K., Pushpangandan, P., Chopra, C. L., Rajasekharan, S., & Amma, L. S. (1989). Adaptogenic activity of seeds of *Trichopus zeylanicus* Gaertn. The Ginseng of Kerala. *Ancient Science of Life, 8*, 212–219.

Shirwaikar, A., Issac, D., & Malini, S. (2004). Effect of *Aerva lanata* on cisplatin and gentamicin models of acute renal failure. *Journal of Ethnopharmacology, 90*, 81–86.

Shirwaikar, A., Rajendran, K., & Punitha, I. S. R. (2005). Antidiabetic activity of alcoholic stem extract of *C. fenestratum* in streptozotocin nicotinamide induced type 2 diabetic rats. *Journal of Ethnopharmacology, 97*, 369–374.

Shirwaikar, A., Somashekar, A. P., Udupa, A. L., Udupa, S. L., & Somashekar, S. (2003). Wound healing studies of *Aristolochia bracteolata* Lam. with supportive action of antioxidant enzymes. *Phytomedicine, 10*, 558–562.

Siems, W. G., Grune, T., & Esterbauer, H. (1995). 4-Hydroxynonenal formation during ischemia and reperfusion of rat small- intestine. *Life Science, 57*, 785–789.

Singh, A., & Handa, S. S. (1995). Hepatoprotective activity of *Apium graveolens* and *Hygrophila auriculata* against paracetamol and thioacetamide intoxication in rats. *Journal of Ethnopharmacology, 49*, 119–126.

Singh, B., Chandan, B. K., Sharma, N., Singh, S., Khajuria, A., & Gupta, D. K. (2005). Adaptogenic activity of glyco-peptido-lipid fraction from the alcoholic extract of *Trichopus zeylanicus* Gaerten (part II). *Phytomedicine, 12*, 468–481.

Singh, G. B., Singh, S., Bani, S., & Malhotra, S. (1990). Hypotensive action of a *Coscinium fenestratum* stem extract. *Journal of Ethnopharmacology, 38*, 151–155.

Sivarajan, V. V., & Balachandran, I. (1994). Ayurvedic drugs and their plant sources. In P. Mohan (Ed.). Oxford: IBH Publishing Co Pvt. Ltd..

Smith, M. A., Perry, G., Richey, P. L., Sayre, L. M., Anderson, V. E., Beal, M. F., et al. (1996). Oxidative damage in Alzheimer's [letter]. *Nature, 382*, 120.

Smith, M. A., Rottkamp, C. A., Nunomura, A., Raina, A. K., & Perry, G. (2000). Oxidative stress in Alzheimer's disease. *Biochimica et Biophysica Acta, 1502*, 139–144.

Soobrattee, M. A., Bahorun, T., Neergheen, V. S., Googoolye, K. & Aruoma, O. I. (in press). Assessment of the content of phenolics and antioxidant actions of the Rubiaceae, Ebanaceae, Celastraceae, Erythroxylaceae and Sterculaceae families of Mauritian endemic plants. *Toxicology in Vitro*.

Srinivasan, M., Padmanabhan, M., & Prince, P. S. (2005). Effect of *Enicostemma littorale* Blume extract on key carbohydrate metabolic enzymes, lipid peroxides and antioxidants in alloxan-induced diabetic rats. *Journal of Pharmacy and Pharmacology, 57*, 497–503.

Srinivasan, R., Chandrasekar, M. J. N., Nanjan, M. J., & Suresh, B. (2007). Antioxidant activity of *Caesalpinia digyna* root. *Journal of Ethnopharmacology, 113*, 284–291.

Srividya, N., & Periwal, S. (1995). Diuretic, hypotensive and hypoglycaemic effect of *Phyllanthus amarus*. *Indian Journal of Experimental Biology, 33*, 861–864.

Stadtman, E. R. (2004). Role of oxidant species in aging. *Current Medical Chemistry, 11*, 1105–1112.

Stanner, S. A., Hughes, J., Kelly, C. N., & Buttriss, J. A. (2004). Review of the epidemiological evidence for the 'antioxidant hypothesis'. *Public Health Nutrition, 7*, 407–422.

Sugie, S., Okanoto, K., Rahman, K. M. W., Tanaka, T., Kawai, K., Yamahara, J., et al. (1998). Inhibitory effects of plumbagin and juglone on azoxymethane induced intestinal carcinogenesis in rats. *Cancer Letters, 127*, 177–183.

Sundquist, E. A., Briviba, K., & Sies, H. (1994). Singlet oxygen quenching by carotenoids. *Methods in Enzymology, 234*, 354–366.

Tepe, B., & Sokmen, A. (2007). Screening of the antioxidative properties and total phenolic contents of three endemic Tanacetum subspecies from Turkish flora. *Bioresource Technology, 98*, 3076–3079.

Tharakan, B., Dhanasekaran, M., & Manyam, B. V. (2005). Antioxidant and DNA protecting properties of anti fatigue herb *Trichopus zeylanicus*. *Phytotherapy Research, 19*, 669–673.

Thyagarajan, S. P., Jayaram, S., & Valliammai, T. (1990). *Phyllanthus amarus* and hepatitis B. *Lancet, 336*, 949–950.

Ugochukwu, N. H., & Cobourne, M. K. (2003). Modification of renal oxidative stress and lipid peroxidation in streptozotocin-induced diabetic rats treated with extracts from Gongronema latifolium leaves. *Clinica Chimica Acta, 336*, 73–81.

Upadhyay, U. M., & Goyal, R. K. (2004). Efficacy of *Enicostemma littorale* in Type 2 diabetic patients. *Phytotherapy Research, 18*, 233–235.

Ursini, F., Maiorino, M., Brigelius-FloheÂ, R., Aumann, K. D., Roveri, A., Schomburg, D., et al. (1995). The diversity of glutathione peroxidase. *Methods in Enzymology, 252*, 38–53.

Vaidya, G. B. (1998). Nighantu Adarsa, 2 ed., Vol. 1, Chaukhambha Bharti Academy Publications,Varanasi 35, 44-45.

Valko, M., Leibfritz, D., Moncol, J., Cronin, M. T. D., Mazur, M., & Telser, J. (2007). Free radicals and antioxidants in normal physiological functions and human disease. *The International Journal of Biochemistry and Cell Biology, 39*, 44–84.

Valko, M., Rhodes, C. J., Moncol, J., Izakovic, M., & Mazur, M. (2006). Free radical metals and antioxidants in oxidative stress-induced cancer. *Chemico Biological Interaction, 160*, 1–40.

Valkonen, M., & Kuusi, T. (1997). Spectrophotometric assay for total peroxyl radical-trapping antioxidant potential in human serum. *Journal of Lipid Research, 38*, 823–833.

Varier, P. S. (1994a). *Coriandrum sativum* in Indian medicinal plants: A compendium of 500 species (2). Chennai: Orient Longman Ltd., pp. 416–417.

Varier, P. S. (1994b). *Coscinium fenestratum* in: Indian medicinal plants: A compendium of 500 species. Chennai: Orient Longman Ltd., Vol. 1, pp. 191–193.

Vasu, V. T., Modi, H., Thaikoottathil, J. V., & Gupta, S. (2005). Hypolipidaemic and antioxidant effect of *Enicostemma littorale* Blume aqueous extract in cholesterol fed rats. *Journal of Ethnopharmacology, 101*, 277–282.

Vedavathy, S., & Rao, K. N. (1991). Antipyretic activity of six indigenous medicinal plants of Tirumala hills. *Journal of Ethnopharmacology, 33*, 193–196.

Venkateswaran, S., & Pari, L. (2002). Effect of *Coccinia indica* on blood glucose, insulin and hepatic key enzymes in experimental diabetes. *Pharmaceutical Biology, 40*, 165–170.

Venkateswaran, S .P., Millman, I. & Blumberg, B. S. (1987). Effects of an extract from *Phyllanthus niruri* on hepatitis B and woodchuck hepatitis virus: In vitro and in vivo studies. In *Proceedings of the National Academy of Sciences USA, Vol. 84* (pp. 274-288).

Venukumar, M. R., & Latha, M. S. (2004). Effect of *Coscinium fenestratum* on hepatotoxicity in rats. *Indian Journal of Experimental Biology, 42*, 792–797.

Vijayvargia, R., Kumar, M., & Gupta, S. (2000). Hypoglycemic effect of aqueous extract of *Enicostemma littorale* Blume (*chhota chirayata*) on alloxan induced diabetes mellitus in rats. *Indian Journal of Experimental Biology, 38*, 781–784.

Vishwakarma, S. L., Rajani, M., Bagul, M. S., & Goyal, R. K. (2004). A rapid method for the isolation of swertiamarin from *Enicostemma littorale*. *Pharmaceutical Biology, 42*, 400–403.

Vlietinck, A. J., Vanhoof, L., Totte, J., Lasure, A., VandenBerghe, D., Rwangabo, P. C., et al. (1995). Screening of hundred Rwandese medicinal plants for antimicrobial and antiviral properties. *Journal of Ethnopharmacology, 46*, 31–47.

Vyas, D. S., Sharma, V. N., Sharma, H. K., & Khanna, N. K. (1979). Preliminary study of antidiabetic properties of *Aegle marmelos* and *Enicostemma littorale*. *Journal of Research in Indian Medicine, 14*, 2–4.

Wang, M. X., Cheng, H. W., Li, Y. J., Meng, L. M., & Malik (1994). Efficacy of *Phyllanthus species* in treating patients with chronic Hepatitis B. *Zhongguo Zhong Yaoza Zhi, 19*, 750–764.

Wang, M., Tsao, R., Zhang, S., Dong, Z., Yang, R., Gong, J., et al. (2006). Antioxidant activity, mutagenicity/anti-mutagenicity, and clastogenicity/anti-clastogenicity of lutein from marigold flowers. *Food and Chemical Toxicology, 44*, 1522–1529.

Wangensteen, H., Samuelsen, A. B., & Malterud, K. E. (2004). Antioxidant activity in extracts from coriander. *Food Chemistry, 88*, 293–297.

Wayner, D. D. M., Burton, G. W., Ingold, K. U., & Locke, S. (1985). Quantitative measurement of the total, peroxyl radical-trapping antioxidant capacity of human blood plasma by controlled peroxidation. *FEBS Letter, 187*, 33–37.

Winston, G. W., Regoli, F., Dugas, A. J., Fong, J. H., & Blanchard, K. A. (1998). A rapid gas chromatographic assay for determining oxyradical scavenging capacity of antioxidants and biological fluids. *Free Radical Biology Mededicin, 24*, 480–493.

Wolfe, K., Xianzhong, W. U., & Liu, R. H. (2003). Antioxidant activity of apple peels. *Journal of Agricultural Food Chemistry, 51*, 609–614.

Wollin, S. D., & Jones, P. J. H. (2001). Alcohol, red wine and cardiovascular disease. *Jornal of Nutrition, 131*, 1401–1404.

Wong, P. Y. Y., & Kitts, D. D. (2006). Studies on the dual antioxidant and antibacterial properties of parsley (*Petroselinum crispum*) and cilantro (*Coriandrum sativum*) extracts. *Food Chemistry, 97*, 505–515.

Zapesochnaya, G., Kurkin, V., Okhavov, V., & Hiroshnikov, A. (1992). Canthin-6-one and â-carboline alkaloids from *Aerva lanata*. *Planta Medica, 37*, 192–196.

Zhao, H., Fan, W., Dong, J., Lu, J., Chen, J., Shan, L. et al. (in press). Evaluation of antioxidant activities and total phenolic contents of typical malting barley varieties. *Food Chemistry*.

PHYTOTHERAPY RESEARCH
Phytother. Res. **21**, 800–804 (2007)
Published online 29 May 2007 in Wiley InterScience
(www.interscience.wiley.com) **DOI**: 10.1002/ptr.2178

SHORT COMMUNICATION

Medicinal Plants used by the People of Northeast India for Curing Malaria

Utpal Bora*, Abhishek Sahu, Abinash Pratim Saikia, Venkat Kishore Ryakala and Pranab Goswami

Department of Biotechnology, Indian Institute of Technology, Guwahati-781039, India

The present study showed that the people of the Northeastern region of India use at least 65 plants belonging to 38 families to treat malaria. Different plant parts such as the leaf, root, bark and fruit and in some cases the whole plant were used for making the herbal preparations. All crude preparations were made using water as the medium. The preparations were orally administered either as a plant crude extract, juice and decoction or leaf infusion. Of the 65 plants, 21 were found to be used in the form of a decoction. The hard parts of the herbs such as the root and bark were taken in the form of a decoction. In some cases the ingredients of the herbal preparation also included honey or sugar. The present investigation also indicated that most of the preparations made for curing malaria were derived from single plant sources.

Keywords: medicinal plants; malaria; Northeast India.

INTRODUCTION

Malaria is one of the most severe diseases in the world that kills over 1 million each year with some 3.2 billion people living in 107 countries or territories currently at risk (Korenromp, 2004). The development of resistance in the malarial parasites to the existing antimalarial drugs and the difficulties in controlling the mosquito vector has further increased the risk. According to the World Health Report 2003 malaria alone contributes to 10.7% of all children's deaths in developing countries.

Malaria causes high morbidity in Assam (Dev *et al.*, 2001). Very recently the Center Of Excellence in Disaster Management and Humanitarian Assistance (COEDMHA) Pacific Disaster Management Information Network (PDMIN) team survey report 2005 described India's northeast as a 'malaria zone' with the disease claiming an estimated 500 lives annually. WHO classifies the region as a highly endemic area for malaria (Korenromp, 2004). Recent studies have demonstrated the emergence of multiple drug resistant malaria vectors in Assam (Dua *et al.*, 2003), which is very alarming. Therefore it has become necessary to find efficient, cheap and easily available cures to tackle the nemesis of malaria. Medicinal plants provide a promising bargain since they are easily accessible and affordable. Many communities worldwide use traditional herbal medicines for controlling the disease, some of which are reported to be effective and promising. In fact the origin of the commercially available antimalarial drugs such as quinine and artemisinin can be sourced to plants (Waynoka *et al.*, 2004). Quinine isolated from *Cinchona* sp. bark and artimisinin from the Chinese plant *Artimesia annua* are established drugs against malaria (Agtmael *et al.*, 1999; Perez *et al.*, 1994). Apart from this currently cryptolepine derived from *Cryptolepis sanguinolenta* and tazospine purified from Madagascarian plant *Strychnopsis thouarsii* are potential antimalarial lead compounds (Cimanga *et al.*, 1997; 8, Carraz *et al.*, 2006).

This laboratory has been focusing on the ethnobotanical and ethnopharmacological knowledge of the people of Northeast India. Earlier it was reported that the people of Assam use unique herbal remedies for curing skin diseases (Saikia *et al.*, 2006). Here we report the use of medicinal plants by the people of Northeast India against malaria.

EXPERIMENTAL

Description of study area. The study area comprised the states of Assam, Nagaland, Meghalaya, Arunachal Pradesh, Manipur and Mizoram located in the Northeast part of India (21.57 °N–29.30 °N latitude and 88 °E–97.30 °E longitude). The climate is characterized by heavy rainfall, much of which occurs during the monsoon season from July to September. The relative humidity and temperature are between 60–80% and 10–36 °C, respectively. The torrential forest covers approximately 1.37 million hectares of land in this area. The heavy rains frequently lead to floods, stagnation of water and disruption of sanitation, which creates an environment favourable for the growth and multiplication of the malaria vectors in this region.

* Correspondence to: Utpal Bora, Department of Biotechnology, Indian Institute of Technology Guwahati, North Guwahati-781039, Assam, India.
E-mail: ubora@iitg.ernet.in, ubora@rediffmail.com
Contract/grant sponsor: Indian Institute of Technology.

Received 12 September 2006
Revised 15 March 2007
Accepted 20 March 2007

Table 1. Medicinal plants used for curing malaria in Northeast India

Botanical name	Local name	Family	Parts of plant used	Place	Mode of use
Acacia concina DC.	Khangthur	Mimosaceae	Leaf	Mizoram	The leaf infusion is taken orally
Acacia farnesiana (L.) Willd.	Tarua Kadam	Mimosaceae	Bark, leaves	Assam	Bark and leaves are crushed, boiled and inhaled by the patient
Acorus calamus L.	U-bet	Acoraceae	Roots	Meghalaya	Root decoction is taken orally
Adhatoda vasica Nees.	Kawldawi	Acanthaceae	Leaf and root	Mizoram	Decoction of the leaves and roots is taken orally
Aegle marmelos (L.) Correa ex Roxb.	Bael	Rutaceae	Fruit	Assam	Equal amounts of juice from these leaves and the leaves of *Ocimum sanctum* L. are mixed along with honey and the mixture is taken orally
Allium cepa L.	Piyaj	Liliaceae	Roots	Assam	Taken orally along with *Piper nigrum* L.
Alstonia scholaris (L.) R.Br.	Satiyana	Apocynaceae	Bark	Assam/ Mizoram/ Arunachal Pradesh	The barks are powdered and taken orally
Andrographis paniculata Nees.	Hnahkhapui	Acanthaceae	Leaf	Mizoram	The leaf infusion is taken orally
Artemisia nilagirika Clarke	Sai	Asteraceae	Leaf	Mizoram	Decoction of the leaves is taken orally
Begonia inflata Clarke	Sekhupthur	Begoniaceae	Root	Mizoram	Decoction of rhizome is taken orally
Begonia roxburghii A.DC.	Babarai, Baya	Begoniaceae	Root, petiole and leaves	Arunachal Pradesh	Roots, petioles and leaves are eaten raw
Berberis asiatica Roxb. ex .D.C	Naksari	Berberidaceae	Fruit, root, bark	Assam	Root bark infusion is given orally
Carica papaya L.	Amita	Carcaceae	Leaves	Assam	Leaves are crushed and taken orally
Chenopodium ambrosioides L.	Chisik bol	Chenopodiaceae	Leaf	Assam/ Arunachal Pradesh/ Mizoram/ Meghalaya/ Manipur/ Nagalad	Oil from the seeds is given orally
Cinchona officinalis L.	Chincona	Rubiaceae	Bark	Assam	The juice from the crushed bark is given orally
Cinnamomum bejolghota (Buch.-Hum.) Sweet.	Thakthingsuak	Lauraceae	Bark, leaves and wood	Mizoram	The bark and the leaves are boiled with the leaves of *Anacolosa crassipes*. The steam is inhaled and the decoction is taken orally
Cissampelos pareira L.	Tubukilota	Menispermaceae	Roots	Assam	Roots are crushed and taken orally
Citrus medica L.	Jora tenga	Rutaceae	Fruits	Assam	Fruit juice is given to patient
Clausena excavata Burm. f.	Norohinga	Rutaceae	Leaf	Assam/ Arunachal Pradesh/ Mizoram/ Meghalaya/ Manipur/ Nagalad	The leaves are chewed with beetle nut leaves
Clerodendrum L.	Kinchang	Verbenaceae	Leaf, bark, root	Assam/ Arunachal Pradesh/ Mizoram/ Meghalaya/ Manipur/ Nagalad	The decoction is given orally

DOI: 10.1002/ptr

Table 1. (*Continued*)

Botanical name	Local name	Family	Parts of plant used	Place	Mode of use
Coptis teeta Wall	Rinko	Renunculaceae	Seeds, dried root, rhizomes	Assam and Arunachal Pradesh	Small quantity of rhizome taken with water
Costus speciosus Sm.	Sambul	Costaceae	Rhizome and seeds.	Mizoram	The powdered seeds mixed with local liquor and given to patient
Croton caudatus Geisel	Lotamahudi	Euphorbiaceae	Roots	Assam	The roots are crushed and taken orally
Dendrocnide sinuate (Blume) Chew	Pudrangta	Urticaceae	Roots and leaves	Arunachal Pradesh	Leaves are mixed with leaves of *Stephania glabra* (2:1) and boiled in water. The water is administered orally
Dichroa febrifuga Lour.	Lab-Tohtih	Hydrangeaceae	Bark	Meghalaya	Decoction of the bark is orally taken
Dioscorea belophylla Voight	Yazeng pep	Dioscoreaceae	Tubers	Arunachal Pradesh	Tubers are crushed and mixed with hot water for oral administration
Gomophostemma parviflora Wall	Bhedaitita	Lamiaceae	Leaves	Assam	The leaves decoction is used orally
Helianthus annuus L.	Beliphul	Asteraceae	Flowers	Assam	The flowers are crushed and given orally
Hyptis suaveolens (L). Poit.	Narutami	Lamiaceae	Leaves and young twigs	Arunachal Pradesh	Steam from hot decoction of shoot is used
Impatiens tripetala Roxb.	Demdewka	Balsaminaceae	Stem, leaves, flowers	Assam	Stem, leaves and flowers are used
Impatients angustifolia Stud.	Yule-gon	Balsaminaceae	Root and leaf	Arunachal Pradesh	Leaf paste is given orally
Indofevillea khasiana	Yazang pipr	Cucurbitaceae	Root and stem	Arunachal Pradesh	Roots and stems are powdered together and are taken with hot water
Justica Neck.	Kawldai	Acanthaceae	Leaves	Mizoram	The leaves are boiled in water and used for bathing. The leaf paste is applied on the whole body and leaf decoction taken orally
Lantana camara L.	Shillongpar	Verbenaceae	Whole plant	Mizoram	Decoction of the bark of stems and roots is given orally
Maesa macrophylla Wall	Tak sangne	Myrsinaceae	Berries	Arunachal Pradesh	Fresh berries are eaten
Melia azedarach L.	Mahaneem	Meliaceae	Leaf	Assam	The juice from the crushed leaves is taken orally
Melothria L.	Kabomako	Cucurbitaceae	Tubers, roots and fruits.	Arunachal Pradesh	Pounded tubers are taken with hot water
Mikania micrantha H.B.K	Japan-hlo	Asteraceae	Leaf	Mizoram	The leaf juice is taken orally
Ocimum sanctum L.	Tulasi	Lamiaceae	Leaf	Assam	The juice from the crushed leaves is taken orally. Equal amounts of juice from these leaves and the leaves of *Aegle marmelos* (L.) Correa ex Roxb. are mixed to which honey is added and taken orally
Passiflora nepalensis Wall.	Nau-awimu	Passifloraceae	Root	Mizoram	Root decoction is taken orally
Picrasma javanica Blume	Thingdamdawi	Simaroubaceae.	Bark	Mizoram	Decoction of the inner coat of bark is taken orally
Piper longum L.	Voko-hrui	Piperaceae	Fruit	Mizoram	Decoction of the fruit with ginger and sugar is taken orally
Piper nigrum L.	Jhaluk	Piperaceae	Seeds	Assam	It is orally taken along with *Allium cepa* L.
Plantago erosa Wall.	Lahuriya	Plantaginaceae	Seeds	Assam	Powder is given orally
Plantago major L.	Kelbe-an	Plantaginaceae	Root	Mizoram	Root decoction is taken orally
Polygala persicariaefolia DC.	Sherita	Polygalaceae	Whole plant	Assam/ Arunachal Pradesh/ Mizoram/ Meghalaya/ Manipur/ Nagalad	Whole plant is boiled and decoction taken orally

Table 1. (*Continued*)

Botanical name	Local name	Family	Parts of plant used	Place	Mode of use
Pongamia pinnata (L.) Pierre	Karas	Fabaceae	Leaves	Assam	The juice from the crushed leaves is mixed with honey and the mixture is taken orally
Prunus cerasoides D. Don.	Tlaizang	Rosaceae	Bark	Mizoram	Decoction of the bark is taken orally
Roscoea purpurea Sm.	Yu-wa-ngon	Zingiberaceae	Root	Meghalaya	The decoction is given orally
Satyrium Sw.	Yu-wa	Orchidaceae	Tuber	Arunachal Pradesh, Manipur	Tuber is eaten raw
Smilacina fusca Wall.	Ping-non	Liliaceae	Root	Assam/ Arunachal Pradesh/ Mizoram/ Meghalaya/ Manipur/ Nagalad	Powder is administered orally
Solanum myriacanthum Dun.	Byako	Solanaceae	Roots and seeds	Arunachal Pradesh	Decoction of roots administered orally
Solanum torvum Sw.	Hati bhekuri	Solanaceae	Roots	Assam	Powdered roots are given orally
Solanum torvum Sw.	Byakta	Solanaceae	Fruits and root	Arunachal Pradesh	Root extract taken orally
Stephania glandulifera Miers.	Teplar.	Menispermaceae	Corms and leaves	Arunachal Pradesh	A few pieces of corm along with 3 to 4 leaves are mixed with 3–4 leaves of *Dendrocnide sinulata* 'Pudrangta' (N) and boiled with water. The decoction is administered orally
Swertia chirata Buch.-Ham. ex Wall.	Chiretta	Gentianaceae	Leaf, root	Assam	Leaves and roots are crushed and taken orally
Swertia dilatata Wall.	Yu-thok-won	Gentianaceae	Root	Meghalaya	Powdered roots are administered
Swertia nervosa Wall.	Shyon-lang-monto	Gentianaceae	Whole plant	Assam	The decoction of the plant is given
Taraxacum Wigg.	Ish	Asteraceae	Whole plant, Root	Assam	Powder is given orally
Tinospora cordifolia Miers	Gulanch	Menispermaceae	Leaf, bark	Assam	The juice is mixed with honey and orally taken
Verbena officinalis L.	Shunutamtsu	Verbenaceae	Whole plant	Nagaland	Fresh herb is crushed and mixed with water and the strained extract is given orally
Viola biflora L.	Lahi-chi	Violaceae	Whole plant	Meghalaya	The decoction of whole plant is given orally
Vitex peduncularis Wall.	Thingkhawilu	Lamiaceae.	Root, leaf, bark and wood	Mizoram	The coat of inner bark is boiled in water and the decoction is administered as follows: (i) The water taken orally. (ii) The patient is bathed with the water; (iii) The steam is deeply inhaled while the patient is covered with a cloth
Xanthium strumarium L.	Agora	Asteraceae	Leaves, fruits	Assam	Leaf decoction is given orally
Zanthoxylum hamiltonianum Wall	Honyor	Rutaceae	Tender leaves, roots and bark	Arunachal Pradesh	Roots and bark decoction are given orally

DOI: 10.1002/ptr

Method of database preparation. The study was carried out by interviewing the various traditional healers and village elders in different locations of the study area. The age, experience and reputation were taken into consideration when selecting the interviewers. Structured forms in local languages were prepared and filled in with the information received from the respondent (both healer and patients). The information was crosschecked and a database was generated. Botanical identification of the reported species was done with the help of taxonomists in Assam State Zoo cum Botanical Garden, Guwahati. The data were tabulated to include the botanical name, local name, family name, plant part(s) used and the mode of preparation.

RESULTS AND DISCUSSION

The present study showed that the people of many states in Northeast India use at least 65 plants belonging to 38 families for treating malaria. These plants are documented in Table 1 indicating the botanical name, family name, plant part used and the mode of administration. The people use different plant parts for making the herbal preparations, namely leaf, root, bark and fruit and in some cases the whole plant. It was observed that all the crude preparations were made using water as the medium. The preparations were orally administered either as a plant crude extract, juice and decoction or leaf infusion. Generally the hard parts of the herbs such as the root and bark were taken in the form of a decoction, as they cannot be eaten easily. As many as 30% of the preparations were found to be used in the form of a decoction. In some cases the ingredients of the herbal preparation also included honey or sugar. The purpose of these supplements is not yet known but they may be used for taste enhancement to the otherwise bitter plant preparations as well as making the preparation palatable. In the present investigation it was observed that most of the preparations made for curing malaria were derived from single plant sources. We anticipate the isolation of potential antimalarial compounds from these, as the therapeutically active ingredient from a single plant source would be easier than from mixed herbal preparations.

Acknowledgements

AS is thankful to IITG for providing financial help in the form of a fellowship. APS, undergraduate student from IIT Madras, thanks Dr U. Bora, for providing a placement for him as a trainee student to carry out this work with him. We thank Mr N.C. Das, Botanist, Assam State Zoo cum Botanical Garden, Guwahati for the Botanical identification.

The study was performed according to the international, national and institutional rules considering biodiversity rights. The consent of the volunteers was taken prior to the interviews and information was collected in the vernacular local language.

REFERENCES

Agtmael MA, Eggelte TA, Boxtel CJ. 1999. Artemisinin drugs in the treatment of malaria: from medicinal herb to registered medication. *Trends Pharm Sci* **20**: 199–205.

Carraz M, Jossang A, Franetich JF *et al.* 2006. A plant-derived morphinan as a novel lead compound active against malaria liver stages. *PLoS Med* **3**: 2392–2402.

Cimanga K, DeBruyne T, Pieters L, Vlietinck AJ. 1997. *In vitro* and *in vivo* antiplasmodial activity of cryptolepine and related alkaloids from *Cryptolepis sanguinolenta*. *J Nat Prod* **60**: 688–691.

Dev V, Hira CR, Rajkhowa MK. 2001. Malaria-attributable morbidity in Assam, north-eastern India. *Ann Trop Med Parasitol* **95**: 789–796.

Dua VK, Dev V, Phookan S, Gupta NC, Sharma VP, Subbarao SK. 2003. Multi-drug resistant *Plasmodium falciparum* malaria in Assam, India: timing of recurrence and antimalarial drug concentrations in whole blood. *Am J Trop Med Hyg* **69**: 555–557.

Korenromp E. 2004. *World Malaria Report: Roll Back Malaria*. World Health Organization: Geneva.

Perez HA, Rosa M, Apitz R. 1994. *In vivo* activity of ajoene against rodent malaria. *Antimicrob Agents Chemother* **38**: 337–339.

Saikia AP, Ryakala VK, Sharma P, Goswami P, Bora U. 2006. Ethnobotany of medicinal plants used by Assamese people for various skin ailments and cosmetics. *J Ethnopharmacol* **106**: 149–157.

Waynoka GN, Chhabra SC, Lang'at-Thoruwa CC, Omar SA. 2004. Brine shrimp toxicity and antiplasmodial activity of five Kenyan medicinal plants. *J Ethnopharmacol* **90**: 129–133.

DOI: 10.1002/ptr